DOCTORAL THESIS

2014

UNDERSTANDING THE REGULATION OF LEAF AND PLANT GAS EXCHANGE UNDER WATER STRESS WITH A PROCESS-BASED MODEL OF STOMATAL CONDUCTANCE

Sebastià Martorell Lliteras

DOCTORAL THESIS

2014

Doctoral Programme of Biology of the plants

UNDERSTANDING THE REGULATION OF LEAF AND PLANT GAS EXCHANGE UNDER WATER STRESS WITH A PROCESS-BASED MODEL OF STOMATAL CONDUCTANCE

Sebastià Martorell Lliteras

Thesis supervisor: Dr. Antonio Diaz Espejo
Thesis supervisor: Dr. Hipólito Medrano Gil

Doctor by the Universitat de les Illes Balears

Nosotros,

DR. ANTONIO DIAZ ESPEJO, Científico Titular del Consejo Superior de Investigaciones Científicas del Intituto de Recursos Naturales y Agrobiología de Sevilla, y

DR. HIPÓLITO MEDRANO GIL, Catedratico de Fisiologia Vegetal del Departmento de Biología de la Facultat de Ciències de la Universitat de les Illes Balears

CERTIFICAMOS:

Que el presente trabajo titulado *"Understanding the regulation of leaf and plant gas Exchange under water stress with a process-based model of stomatal conductance"* presentado por Sebastià Martorell Lliteras para optar al TÍTULO univesitario oficial de DOCTOR por la Universitat de les Illes Balears dentro del programa de doctorado de Biología de las Plantas en Condicions Mediterráneas, se ha realizado bajo nuestra dirección.

Revisado el presente trabajo, autorizamos su presentación para que pueda ser juzgada por el tribunal correpondiente.

Palma de Mallorca, 4 de noviembre del 2014

Director   Director   Autor

Antonio Diaz Espejo   Hipólito Medrano Gil   Sebastià Martorell Lliteras

Als meus pares,

AGRAÏMENTS-ACKNOWLEDGMENTS

I qui ho havia de dir fa un grapat d'anys que faria una tesis doctoral... Arribat aquest moment són moltes les coses que he aprés durant aquests anys gràcies a tots vosaltres i per això vos ho vull agrair a tots

En primer lloc a la tasca feta pels meus directors el Dr. Antonio Diaz-Espejo y el Dr. Hipólito. Gracias Hipólito por apostar por mí y abrirme las puertas a la ciencia. Tus consejos y tu sabiduria han sido claves en esta tesis siendo para mí una experiencia única. Además, te tengo que decir que te veo como un jovencito de 20 años con mucha guerra para dar a los próximos becarios. Gracias Antonio, la distancia entre Sevilla y Palma parece mucha, pero ha sido como si estuvieras en Mallorca. Gracias por toda la atención que has tenido conmigo. Esta tesis sin tí no habría sido lo mismo. Mil gracias.

Als doctors Miquel Ribas i Jeroni Galmés. Miquel, si no fos per tu et puc assegurar que no tendría la possibilitat de presentar un doctorat. Gràcies per ajudar-me sempre que t'ho he demanat i sobretot gràcies per transmetre els teus coneixements. No canviïs. Gràcies Jeroni per deixar-me entrar al laboratori quan encara només era estudiant de Biologia. El teu rigor al laboratori i les teves bones pràctiques han estat claus per arribar aquí.

També vull agraïr als doctors Pepe Escalona i Jaume Flexas la seva disponibilitat per ajudarme en qualsevol moment a la Dra. Josefina Bota per haverme ajudat i animat, així com a la resta de companys Miquel Angel Conesa, Josep Cifre, Joan Rosselló, Àlex, Igor, Xurxo, Enrico pel vostre recolzament i bons consells al llarg de la tesis.

Agraïr de manera molt especial a les doctores Magdalena i Alicia (les meves primeres "jefes") la seva tasca. M'ho he passa molt bé amb vosaltres i espero poder repetir! Sense vosaltres no hagués estat possible. I molt especialment a na Belén que sempre m'ha ajudat en tot lo que ha pogut! Gràcies.

També a tots els becaris i precaris que han passat per can "Boom", na Perla, na Cristina, n'Ocho, en Pere, n'Alejandro (Vamos Alejandro! Esto ya lo tienes!!!!), na Aranatxa, na Hanan , n'Amani, na Carmen, na Veriozca, na Pati, en JJ, en Rafa, n'Antònia, en Néstor, n'Esther, en Marcel y en Marc. Gràcies a tots per els compartir

les vostres històries i per fer que el dia a dia durant aquesta tesis hagi estat com si viure en una gran família.

També agrair a nen Pep Sastre Jr. i el vell la seva disponibilitat per ajudar en qualsevol moment i en Miquel Truyols "l'amo de s'hivernacle" (menos mal que hi ets per posar un poc d'ordre per que sinó seria un desastre).

I would also like to state my gratitude to Dr Brendan Choat, Dra Marilyn Ball and Dr. Lawren Sack and their respectives research groups in Australia and United States. Thank you for allowing me to be part of your laboratories. I'm also very grateful to Jack Eggerton, Stephanie, Christine, Megan, Grace, Rodrigo, Alica Fornés and Celia, for being so nice outside the laboratory making funny my stages abroad. And finally I would like state my gratitude to Dr Thomas Buckley for his work and help during this PhD thesis. Thanks Tom! You are a big one!

Ja per acabar vull donar les gràcies a la meva família i als meus amics el qualts tots aquests anys m'han ajudat a seguir i m'han donat suport amb tot el que he fet. Especialment al meu germà el qual sempre m'ha fet costat durant aquests anys i m'ha aconsellat i ajudat. I finalment donar les gràcies a na Bel, la qual ha patit de ben aprop les conseqüències de la tesis, sempre fent-me costat i ajudantme a desconnectar i a seguir endavant.

Gràcies a tots

SYMBOLS AND ABBREVIATIONS LIST

Symbols	Meaning
$\partial^2 A/\partial E^2$	curvature of A vs E relationship
$\partial A/\partial E$	marginal carbon product of water
A, A_N	net CO_2 assimilation rate
ABA	abcisic acid
A_d, A_s	demand or supply limited value of A
ATP	adenosine triphosphate
A_v, A_j	RuBP-carboxylation or regeneration limited value of A_d
BMF	Buckley, Mott & Faquhar (2003) model of stomatal conductance
BWB	Ball, Woodrow & Berry (1987) model of stomatal conductance
BWB-L	Leuning (1995) model of stomatal conductance
C_a	atmospheric CO_2 concentration
C_{bulk}	Leaf capacitance
C_c	chloroplastic CO_2 concentration
C_i	sub-stomatal CO_2 concentration
C_i*	apparent CO_2 photocompensation point
c_p	molar heat capacity of air
C_s	leaf surface CO_2 concentration
D_a	saturation vapour pressure deficit of air
d_{leaf}	leaf characteristic dimension
E	leaf transpiration rate
E_{plant}	Plant transpiration
ET_0	Evapotranspiration
ETR (J_{flu})	electron transport rate
F	curvature correction factor
f	fraction of absorbed photons that do not contribute to photochemistry
F'_m	maximum fluorescence in light-adapted state
F_0	basal fluorescence of a dark adapted leaf
f_{ir}	fraction of infrared radiation that comes from the sky
F_o	basal fluorescence of the dark adapted leaf
F_v/F_m	maximum quantum efficiency of PSII photochemistry
FvCB	Farquhar, von Caemmerer & Berry (1980) model of photosynthesis
g_{bh}, g_{bw}, g_{bc}	leaf boundary layer conductance to heat, water or CO_2
GCM	Global circulation models
g_m	mesophyll conductance to CO_2
g_{Rn}	radiation conductance
g_s, g_{sc}	stomatal conductance to water or CO_2
g_{smax}	maximum stomatal conductance
g_{so}	optimal stomatal conductance
g_{tw}, g_{tc}	total leaf conductance to water or CO_2
J	potential electron transport rate
J_a	linear electron transport rate by gas exchange
J_f	linear electron transport rate by chlorophyll fluorescence
J_i	light-limited (capacity-saturated) value of J
J_m (J_{m25})	capacity-limited (light-saturated) value of J (at 25°C)
K_c, K_o	Michaelis constant for RuBP carboxylation or oxygenation

Symbols	Meaning
K_{cat}	in vivo specific activity of Rubisco per active sites
k_d	canopy extinction coefficient for diffuse irradiance
K_h	Hydraulic conductance
K_{leaf}	Leaf hydraulic conductance
K_{Li}	Stem hydraulic conductivity
L	cumulative leaf area index
m, a	Empirical parameters of the BWB model
n	Parameter related to ABA in the BMF model
O	mole fraction of oxygen
P_{50}	Leaf water potential at 50% loss of hydraulic conductance
PAR	photosynthetic active radiation
P_{atm}	atmospheric pressure
PLC	Percentage loss of conductance
PPFD	photosynthetic photon flux density
R_d (R_{d25})	non-photorespiratory CO_2 release (at 25°C)
R_n^*	net isothermal radiation
RWC_{TLP}	Relative water content at turgor loss point
SWC	soil water content
T_{air} ($T_{air,K}$)	air temperature (in Kelvins)
T_{leaf} ($T_{leaf,K}$)	leaf temperature
TPU	triose phosphate
v_c	velocities of carboxylation of Rubisco
V_m (V_{m25})	carboxylation capacity (at 25°C)
v_o	velocities of oxygenation of Rubisco
$V_{o,max}$	maximum rates for the oxygenation activity of Rubisco
VPD	vapour pressure deficit
v_{wind}	wind speed
w_i, w_a	water vapour mole fraction of intercellular spaces or air
WUE	water use efficiency
WUE_i (A_N/g_s)	intrinsic water use efficiency
WUE_l	leaf water use efficiency
α	leaf absorptance
Ψ_{md}	midday leaf water potential
Ψ_{pd}	predawn leaf water potential
Φ_{CO2}	apparent quantum efficiency of CO_2 fixation
Φ_{PSII}	maximum quantum efficiency of the PSII photochemistry
Δw	effective leaf-air water vapour mole fraction gradient
$\Delta\Psi$	difference between predawn and midday water potentials
Φ	absorbed shortwave radiation
Γ_* (Γ_{*25})	photorespiratory CO_2 compensation point (at 25°C)
Ψ_{leaf}	Leaf water potential
$\Psi_{\pi FT}$	Osmotic potential at full turgor
$\Psi_{\pi TLP}$	Osmotic potential at turgor loss point
β, χ	Proportionality factor
ε	Modulus of elasticity
ε_{leaf}	leaf emissivity to IR
γ	psychrometric constant
μ	target value for $\partial A/\partial E$
θ_A	curvature parameter for relationship of A_d to A_v and A_j

Symbols	Meaning
θ_J	curvature parameter for relationship of J to J_m and J_i
σ	Stefan-Boltzmann constant
τ	ATP concentration in the photosynthesizing cells

LIST OF PUBLICATIONS DERIVED FROM THIS THESIS

1. Martorell S., Diaz-Espejo A., Medrano H., Ball M. C. & Choat B. (2014). Rapid hydraulic recovery in Eucalyptus pauciflora after drought: linkages between stem hydraulics and leaf gas exchange. *Plant, Cell & Environment*, **37**, 617-626.

2. Martorell S., Medrano H., Tomàs M., Escalona J.M., Flexas J. & Diaz-Espejo A. (2014) Plasticity of vulnerability to leaf hydraulic dysfunction during acclimation to drought in grapevines: an osmotic-mediated process. *Physiologia Plantarum* Doi: 10.1111/ppl.12253

3. Martorell S., Díaz-Espejo A., Tomàs M., Pou A., El Aou-ouad H., Escalona J.M., Vadell J., Ribas-Carbó M., Flexas J. & Medrano H. Differences in water-use-efficiency between two vitis vinifera cultivars (Grenache and Tempranillo) explained by the combined response of stomata to hydraulic and chemical signals during water stress. *Agricultural Water Management.* (Submitted)

4. Martorell S., Tomàs M., Pou A., Ribas-Carbó M., Galmés J., Escalona J.M., Flexas J., Medrano H. & Diaz-Espejo A. The temperature response of mesophyll conductance is the main determinant of the differences in optimal temperature for photosynthesis between two grapevine cultivars. (to be submitted)

5. Martorell S., Buckley TN., Tomàs M., Flexas J., Escalona JM., Ribas-Carbó M., Medrano H. & Diaz-Espejo A. On the quest of a mechanistic model of stomatal response to water stress (to be submitted)

6. Martorell S., Buckley TN., Tomàs M., Flexas J., Escalona JM., Ribas-Carbó M., Medrano H., Diaz-Espejo A. Hydraulic constraints can explain the sub-optimal distribution of photosynthetic capacity in plant canopies de to diffusional limitations (to be submitted)

7. Buckley, T. N.,* Martorell, S.,* Diaz-Espejo, A., Tomàs, M., & Medrano, H. (2014). Is stomatal conductance optimized over both time and space in plant crowns? A field test in grapevine (Vitis vinifera). *Plant, Cell & Environment* doi: 10.1111/pce.12343

*Both authors contributed equally to the authorship of this work**.**

CONTENTS

ABSTRACT

Water availability is one of the biggest constraints limiting the plant growth and species distribution around the world. This is the case in the Mediterranean region where, moreover, the frequency and amount of rainfall will decrease due to global warming. This will provoke longer periods of drought and a general decrease of water availability. In this context, one of the most vulnerable crops is grapevine. This crop has been traditionally rain-feed, although in recent years it's becoming an irrigated crop. This increases the demand to regulate the water use by more precise irrigation techniques based on the plant water status. A good physiological indicator that allows knowing the plant water status is stomatal conductance. Although it is widely known the importance of the stoma, there is not an accurate model to predict their behavior as many physiological and environmental parameters co-regulate it.

The aims of this thesis are to: a) study the physiological mechanisms regulating stomatal conductance, b) apply a process-based model to predict the behavior of stomatal conductance c) use this model as tool to better understand the physiological stomatal regulation along the canopy.

Results show that stoma has a strong regulation by hydraulic conductance being a key physiological parameter regulating water use. In addition, abscisic acid and osmotic adjustment are also playing an important role in their regulation. On the other hand, the mechanistic model of stomatal conductance has been validated predicting with a good accuracy the variations throughout the day and season in well water and water stress conditions. At time, because this model is based on physiological parameters permits to infer about the relevance of those physiological parameters under water stress, predicting that hydraulic conductance has a main role on the regulation of stomatal conductance in different parts of the canopy.

RESUM

La disponibilitat d'aigua és un dels majors obstacles que limiten el creixement de les plantes i la distribució a tot el món. Aquest és el cas de la regió Mediterrània, on s'espera que la freqüència i la quantitat de precipitacions disminuiran a causa de l'escalfament global. Aquest fet provocarà períodes més llargs de sequera i una disminució general de la disponibilitat d'aigua. En aquest context, un dels cultius més vulnerables és el de la vinya. El cultiu de la vinya ha estat tradicionalment un cultiu se secà, encara que en els darrers anys s'està convertint en un cultiu de regadiu. Aquest fet augmenta la demanda d'aigua i la necessitat de regular el seu ús amb tècniques de reg més precises basades amb l'estat hídric de la planta. Un dels millors indicadors fisiològics que permeten conèixer l'estat hídric de la planta és la conductància estomàtica. Encara que és àmpliament coneguda la seva importància, no existeix un model precís per prediure el seu comportament. Aquest fet es deu sobretot a que són molts els paràmetres fisiològics i ambientals que co-regulen alhora l'obertura estomàtica.

Els objectius d'aquesta tesi doctoral són: a) l'estudi dels mecanismes fisiològics que regulen la conductància estomàtica, b) aplicar un model mecanicista per preveure els valors de la conductancia estomàtica c) i utilitzar aquest model com a eina per comprendre millor la regulació fisiològica dels estomes al llarg de la "canopy".

Els resultats mostren que l'estoma té una forta regulació per part de la conductància hidràulica sent aquest un paràmetre fisiològic clau. A més, l'àcid abscísic i l'ajust osmòtic també estan jugant un paper important en la seva regulació. D'altra banda, el model mecanicista ha estat validat i s'ha observat com ha estat capaç de predir les variacions de g_s al llarg del dia i l'estació en condicions d'estrès hídric i de regadiu. Al ser un model mecanicista aquest es pot utilitzar com a eina de predicció dels paràmetres fisiològics. Sent així s'ha estudiat la la regulació de l'estoma a diferents parts de la "canopy" observant que la conductància hidràulica té un paper principal en la regulació de la conductància estomàtica en les diferents localitzacions estudiades.

1. INTRODUCTION

1.1. Global interest for water optimisation by plants and crops from the climate change perspective.

1.1.1. Water and Plants

Water availability is one of the main limitations for plant's growth as well as an important environmental factor to understand the distribution of species around the world. Daily water flux throughout plants is about ten-fold higher than their water content but it is essential to maintain CO_2 uptake for plant growth. Water is also very important for its role in the physiology of plants given its physical and chemical properties. Most plant physiological processes are dependent on water supply while being their main constituent (80-90% of fresh weight in herbaceous plants and more than 50% in woody plants). Moreover, water is the solvent in which gases, minerals and other solutes enter in the plant cells and move across them and through organs. Water is also a reactant or substrate in many important physiological processes, (ie: photosynthesis, respiration, hydrolytic processes) while being responsible of the maintaing cell turgor, which is an essential function for cell enlargement and standing of the herbaceous plants (Kramer & Boyer 1995).

Water stress limits plant growth and crop production more than any other single environmental factor (Boyer, 1982). Water scarcity has been classified as one of the main problems to be faced by the world's population in the next century given its importance and finite source. In addition, agriculture account for 70-80% of global freshwater withdrawals and more than 90% of its consumptive use (Hightower & Pierce, 2008). Consequently in the near future, plants are likely to suffer more episodes of drought stress which reinforces the need for profound research on water savings in agriculture, or, in other words how to optimise water use by plants. In fact, there is an explicit mandatory by the United Nations asking for a general effort for this optimization defined as "more crop per drop" (FAO, 2005) reinforcing the necessity for a broad effort in research and development to optimise water use for food production.

1.1.2. Mediterranean climate

Mediterranean climate region is a convenient scenario to study drought events as it is characterized by a hot and drought period in summer and a cool and wet period in winter (Nahal, 1981). Aschmann (1973) defined the Mediterranean climate areas as the

places where at least 65% of the precipitation occurs in autum-winter even though the annual precipitation values range from 200 to 1400 mm (Guijarro, 1986). The monthly winter average temperature are below 15ºC, although annual hours below 0ºC comprise less than 3% of the total. The length of the dry season of this climate can be from one to eight months although it can vary between regions (north or south) and years. From plant life perspective the most important characteristic is that the period of high soil water availability (autumn-spring) never coincides with the period of high irradiance and temperature, leading plants to acclimate to survive througha period of water scarcy under higher temperature and evaporative demand.

1.1.3. Climate change in the Mediterranean region and effects on crops.

According to IPCC predictions (2013), climate change will impact severely the Mediterranean regions with important consequences on socio-economy, agriculture and conservation biology. According to these predictions there will be a more frequent hot and fewer cold temperature extremes over most land areas on daily and seasonal time scales as global mean temperature increases. Heat waves are predicted to occur with higher frequency although occasional cold winter extremes will continue to occur (IPCC 2013). Moreover changes in water cycle are projected to occur with contrasting results depending on the region. In general fewer precipitations are predicted increasing drought episodes in the Mediterranean region (IPCC 2013). Consequently, drought events are expected to strengthen in terms of intensity, frequency and extension in the near future (IPCC 2013). Drought events will become increasingly important as demand for food and water for irrigation will rise together with human population (Somerville and Briscoe, 2001). Therefore, research efforts point to increase plant Water Use Efficiency (WUE) and particularly to identify and select those physiological traits that increase plant WUE and production under water-limited conditions. In consequence, there is special interest not only to improve our understanding of plant physiological responses to water stress but also to apply such knowledge to find new solutions to the forthcoming water scarcity increase.

1.1.4. Grapevine water requirements as a limitation for crop sustainability in the next century

Grapevine is a Mediterranean crop nowadays growing in different climates between latitudes of 4º and 51º in the Northern Hemisphere and between 6º and 45º in the Southern Hemisphere. It is widely established that individual climate factors such as solar radiation, temperature extremes, wind, heat accumulation and precipitation can affect grape growth and wine quality.

Water availability is clearly a determinant factor for crop load (yield) and fruit quality in grapevines with water shortage being probably the most dominant environmental constraint (Medrano et al., 2003; Cifre et al., 2005; Chaves et al., 2007; Flexas et al., 2010). To overcome this limitation, irrigation is becoming a common practice in the new viticulture world but also in most Mediterranean areas where historically it had been a rain fed crop. Therefore, there would be an increasing need to irrigate grapevines in the future which will significantly increase water consumption (Hannah et al., 2013). Some studies have predicted that grapevine regions would have to adapt to those new climatic conditions or would be displaced to new scenarios moving towards traditional areas (Hannah et al., 2013). Fortunately, there are different agronomic practices which can improve crop performance under climate change conditions and there is also an impressive grapevine genetic variability (Mullins et al., 1992) which can help to choose more adapted cultivars to drought and water stress (Van Leeuven et al., 2013).

1.1.5. Grapevine drought stress response

Grapevine crop always suffer some degree of drought stress during their growing season as it is located in Mediterranean or temperate climates (Van Leeuwen and Seguin, 1994; Gaudillère et al., 2002). It is well established that the combination of drought stress, high temperatures and high evaporative demand affects grapevine yield and berry quality (Chaves et al., 2010; Flexas et al., 201) being this stress reflected in its grape quality. In response to water stress, a reduction of plant carbon assimilation and partial loss of canopy leaf area ocurred after a severe drought stress (Flexas et al., 1998; 2002; Chaves et al., 2003, 2007; Souza et al., 2003).

There are several responses of grapevine to water stress being the efficient control of transpiration by stomata the most common (Medrano et al., 2003; Shultz, 2003; Pou et al., 2012; Tomàs et al., 2012; 2013;). Moreover, the control of xylem embolism

(Lovisolo et al., 2002; Pou et al., 2012; 2013;) or the ability of osmotic adjustment (Rodrigues et al., 1993; Patakas and Noitsakis, 1999, 2001) have also been shown to contribute to the general responses improving grapevine performance under water stress conditions. Stomatal closure leads to important reductions in transpiration corresponding to moderate decreases of photosynthesis (Medrano el al, 2003; Flexas et al, 2010). The high response of g_s to soil water available content (SWC) permits to improve the WUE by controlling irrigation dosage, irrigation scheduling or irrigation methodology (Chaves et al., 2007; Romero et al.,2012). In any case, there is a wide amount of evidence under controlled and field conditions of a large response capacity of g_s against SWC in grapevines which has been suggested as the main path to improve its WUE and thus improving also its environmental sustainability (Chaves et al 2007; Flexas et al., 2010; Shultz and Stoll 2010). Fortunately, suboptimal water availability conditions which correspond to higher WUE are, in general, the best conditions for fruit quality in the highest expression, thus yield reduction by water saving could correspond to fruit quality improvement.

There is genetic variability between cultivars of grapevine for water use efficiency. Some ranges of differential control of g_s and A_N among cultivars have been observed under well watered plants and water stress (Bota et al., 2001; Flexas et al., 2010; Tomàs et al., 2012; Tomàs et al., 2014). This variability can be observed as a consequence of a differentiated regulation of g_s and g_m between cultivars with their corresponding effects on A_N and WUE. The demonstration of genetic variability among cultivars open an interesting field of research for both the identification of the main water stress response characteristics involved in this differential behavior and also to explore the interest of higher WUE cultivars for new climatic change conditions.

On the basis of the demonstrated importance of stomatal control in the general response to water stress in grapevines and the existence of genetic variability for this response, this thesis will focus on stomatal physiology and their regulation mechanisms.

1.2. Regulation of water stress responses: The role of water relations (WR), hydraulic conductivity (K_h), and Abscisic Acid (ABA) in the control of stomatal aperture.

1.2.1 Stomata

Undoubtedly plant stomata is most the vital gate to control water losses (transpiration) and CO_2 uptake between plants and the atmosphere. Stomata play a central role in plant responses to water stress, as reported at different levels from the molecular to the whole plant perspectives (Nilson and Assmann, 2007). Its capacity to control water losses is also widely recognized as crucial to understand the ability of plants to growth in terrestrial ecosystems consequently; one of the most important steps in the early colonization of the terrestrial environment by plants was the emergence of stomata. Stomatal pores can occupy between 0.5 and 5% of the total leaf surface with all the CO_2 absorbed and water transpired passing across them. Their frequency and size can vary depending on growth conditions and the position of the leaves (Xu and Zou, 2008). Stomata movements are dependent on changes of the turgor pressure of their guard cells and their adjacent epidermal cells. The balance between pressures of both cells is critical for the determination of the stomatal aperture. Changes can be driven by supply or loss of water varying the total water potential of the guard cells (hydropassive mechanism), or with changes of their osmotic potential produced by active changes (hydroactive mechanism) (for rev. Buckley, 2005)

1.2.2 Understanding the control of stomatal aperture: The role of water relations

Stomatal aperture is the result of changes in turgor of guard and adjacent cells, thus leaf water relations play a key role controlling it. Leaf water status is measured in terms of water potential with two main components: pressure (turgor) and osmotic potentials. Their dynamics play an important role in the regulation of the cells' water flow. Moreover both components can change their values due to aquaporins, a small protein channels located in the membranes, that actively transport water between the semipermeable membranes of the cells (Tyerman et al., 1999; Katsuhara et al., 2008; Maurel et al., 2008). Aquaporins can accelerate the diffusion of water across the membrane more than ten-fold. Additionally there is a genetic regulation of them being differently expressed depending on the water status of the plant and other conditions.

Another important characteristic of plant cells is that they are embedded into a rigid cell wall built to resist expansion, thus contributing to generate an inner hydrostatic pressure when positive water flows into the cell. This pressure is the principal driving force of the pressure potential component in the cell, commonly called turgor pressure. On the other hand, when water flows out of a cell, both volume and turgor pressure decrease linearly as a consequence of the loss of pressure against to the cell wall. When turgor pressure approaches values near zero, cells would enter into plasmolysis, although this does not occur because capillary forces at the air-water interface in the cell wall microcapillarities prevent them from draining, so that tension is supported by the wall rather than the membrane. Although not presenting plasmolysis, a visible wilting of leaves is observed when values of turgor pressure approach zero (Acock & Grange, 1981; Jones, 2013)

Plant cells present plenty of sugars, amino acids and other compounds (osmolites) in the cytoplasm with a certain osmotic potential which always results in a much more negative osmotic potential than the surrounding cell wall water. This situation creates a gradient force which drives water into the cytoplasm until turgor pressure compensates this force. The variations in osmolite concentration will therefore correspond to turgor variations (Kramer 1980; Boyer 1982). This mechanism, termed osmotic adjustment involve an actively increase/decrease of solutes content in cells modifying the concentration of proline, sugars, salts or other solutes in the vacuoles. It is necessary to increase the concentration of solutes in the cytoplasm with the so called compatible solutes (e.g. sugars, polyols or proline) to avoid potential damage effects of high solute concentration. This process would permit cells to maintain turgor in a less negative water potential. There are other processes described to induce a modification of the turgor loss point such as apoplastic adjustment, which consist on the reduction of symplastic water content by redistributing more water outside the cell walls, and the so called elastic adjustment, which leads to increased cell wall flexibility (decreasing ε). Both processes have been suggested to have an influence on the turgor loss point although there are controversy in the literature finding increases and decreases of their respective contribution to acclimation in the response to drought stress (Bartlett et al., 2012; 2014).

Osmotic adjustment maintains cell turgor and water absorption under drought stress conditions (more negative water potential), and enable plants to sustain stomatal

conductance, hydraulic conductance, CO_2 uptake, and growth at lower soil water availability (Abrams and Kubiske 1990; Sack et al., 2003; Baltzer et al., 2008; Mitchell et al., 2008; Blackman et al., 2010). The turgor loss point has been recognized as the best recognized classical indicator of plant water stress, having impacts on cellular structural integrity, metabolism and whole-plant performance (Kramer and Boyer 1995; McDowell 2011). Also it has been considered as the higher-level trait that quantifies leaf and plants drought tolerance (Sack et al,. 2003). Turgor loss point defines the soil water potential below which the plant cannot take up sufficient water to recover from wilting and it has been described as a functional trait clarifying the species-level drought responses and biogeographic trends (Barlett et al., 2012).

Although stomatal conductance and maintenance of leaf turgor by osmotic adjustment are considered to be coupled, their connection is not universal (Munns 1988; Saliendra and Meinzer 1991). Guard cell turgor pressure is being regulated by leaf water status, light, CO_2 and also by chemical signaling (Nilsen and Orcutt 1996; Chaves et al., 2003) could change the regulation of stomatal conductance which regardless of their osmotic adjustment. Stomata closure has been observed when a decrease of soil or leaf water potential. This closure can be produced along a wide range of water potential. However, depending on the stress level and the previously suffered conditions (i.e. a large period of water stress), stomata can close in a different range of leaf water potentials (Jones and Rawson, 1979; Jones, 2013). On the basis of the relationship between leaf water potential and stomatal conductance it has been termed two types of plant behaviors have been termed. When the plant water potential is sustained when soil dries, plants have been termed isohydric, while if plants water potential decreases alongside with soil water potential, they are termed anisohydric (Tardieu and Simonneau, 1998). These types of responses have been observed in many plants as well as an intermediate response termed as "isohydrodinamic" (Franks et al 2007). In grapevine those behaviours have been reported in two different cultivars (Shultz 2003, Pou et al., 2008., Pou et al., 2013; Tramontini et al., 2014) with contrasting results depending on the environmental conditions so that this classification can be considered a simplification of stomatal conductance behavior in response to water status conditions (Domec and Johnson, 2012; Pou et al., 2012).

1.2.2.1 Water transport across the plant

Water moves through the plant via xylem vessels creating a continuous system from the roots to the evaporation sites, thus creating the so called soil-plant-air-continuum. How plants are able to transport water from roots to the distal leaves is a subject of large controversies. Dixon and Joly (1894) proposed that water is able to be transported following the Cohesion-Tension theory. This theory highlights that the pulling force coming from the evaporative surfaces is able to move water under tension through the xylem water columns. This theory supposes adhesion of water to conduit walls and the cohesion of water molecules to each other. With the grounds of this theory, water flow in the xylem can be measured and the ability to this flux is estimated as the hydraulic conductance of a determined plant, branch or leaf.

1.2.2.2 Leaf hydraulic conductance

Leaf hydraulic conductance (K_{leaf}) is the measure of how efficiently water is transported through a leaf from the petioles to the evaporative surfaces divided by the driving force caused by the difference in water potential. Most of carbon assimilation and water loss takes place in leaves which are an important limitation for the hydraulic system with an average resistance of the total plant of 30%, although in some case it can account for 80% (Sack and Holbrook, 2006). Water is transported across veins and can be transported from major to minor veins or directly to surrounding tissues. Water exits from xylem to the bundle sheaths and moves across cells or around them to go out as water vapour across the stomata. Leaf hydraulic conductance (K_{leaf}) across these paths, from veins to the stomatal cavity, is considered a hydraulic bottleneck, and is now understood to play a pivotal role in the control of transpiration (Nardini and Salleo 2000, Brodribb *et al.*, 2005, Sack and Tyree 2005).This has accelerated much research on acclimation of K_{leaf} to changing environmental conditions, including temperature (Sellin and Kupper 2007), light (Sack *et al.,* 2002, Voicu *et al.,* 2008) and dehydration (Brodribb and Holbrook 2003; Guyot *et al.,* 2012, Scoffoni *et al.,* 2012).

K_{leaf} has been reported to be seriously limited under drought stress conditions and represents a very vulnerable point of the water transport system (Salleo et al., 2001; Johnson et al., 2011; Bucci et al., 2012). The reduction of K_{leaf} due to dehydration can be due to: a) cavitation of xylem conduits (Johnson et al., 2009; 2012), b) reduction in the permeability of the extra-xylary tissues (Sack and Holbrook, 2006; Pou et al., 2013) or c) collapse of xylem cells (Brodribb and Holbrook, 2005). Which of these

components is more important to determine the limitation of water flow is dependent on the species and still a matter of debate (Sack et al., 2004; Nardini et al., 2005; Charra-Vaskou et al., 2012). Some results showed that leaf xylem may have similar values than extra-xylary pathway (Sack and Holbrook 2006), but, recently Scoffoni et al. (2014) reported that extra-xylary pathways may be more vulnerable than xylem, delaying the embolism formation or collapse of leaf veins. Nevertheless, there is a clear reduction of K_{leaf} under water stress fully related to stomata closure (Salleo et al., 2001; Brodribb and Holbrook 2004; Sack and Holbrook, 2006; Brodribb and Cochard 2009; Scoffoni et al., 2011). This represents an important limitation of water flow and consequently of plant productivity worldwide, impacting species distribution (Engelbrecht et al. 2007, Choat et al. 2012) and agriculture productivity (McElrone et al. 2012). Knowledge about K_{leaf} regulation and its expected vulnerability is particularly important for improving crop water use efficiency in the future scenarios of climate change (Fereres and Soriano, 2007; Chaves et al., 2007).

Grapevine leaf hydraulic conductance has been matter of seldom studies (Choat et al., 2009; Pou et al. 2008; Pou et al. 2012; Pou et al., 2013). Due to the lack of information, there is a special need to know how leaf hydraulic conductance is regulated under water stress, across the growing season and how it respond to dehydration. This information will improve the present knowledge on the depedndece of water pathways regulation and stomata opening on K_h.

1.2.2.3. Xylem hydraulic conductance

K_h reduction by cavitation or embolism of the xylem conduits is a common consequence of water stress. Cavitation and embolism events have been largely reported in response to water stress (Tyree and Dixon, 1986; Sperry et al., 2002; Torres-Ruiz et al., 2013) and overall impacts have been measured with different methods (acoustically, loss of conductance, or X-ray tomography). Cavitation events are characteristic of each species depending on xylem anatomy and hydraulic properties (Tyree et al., 1994; McElrone et al., 2014).

Water under negative tension is in a metastable status because is liquid and under pressure would be water vapor. The large negative pressure generated into xylem water vessels by drought stress conditions make vessels prone to cavitation due to their "lower

partial pressure" and the possibility of air seeding coming from the pit pores. Reduced soil water availability increases xylem sap tension leading to higher probabilities of cavitation (Zimmerman 1983; Tyree & Sperry 1989). Gas created by embolism becomes trapped in the xylem conduits. This gas can spread across vessels with air seeding at pit membranes, cavitating more vessels and causing a progressive decrease of xylem hydraulic conductance (Sperry et al., 1988; Choat et al., 2008; Brodersen et al. 2013). Pit membranes are interconnections between vessels that present nanometer-sized pores that prevent the spread of gas through the xylem vessels. When critical pressure values are reached in vessels exceeding the capillary sealing capacity of pit membranes the embolism is spread to other vessels causing dramatic falls of hydraulic conductivity which could become irreversible (Choat, 2013; Lens et al., 2013). Plants need to maintain xylem water potential within a range that prevents extensive embolism in the xylem vessels in order to survive to drought stress. One method to control the spread of embolism is stomatal closure which limits water loss and delay the spread of gas embolism across the xylem network.

The capacity to resist cavitation-induced embolism between plants species is measured by "vulnerability curves" which compare the response of xylem sap to increasing hydraulic tensions. These curves measure the percentage loss of hydraulic conductance of an organ plotted versus the pressure reached in the xylem conduits (Sperry et al., 1987). These curves can be performed in stems, roots, leaves and petioles. Descriptive and quantitative parameters are derived from vulnerability curves. Among them, P_{50} corresponds to the xylem pressure inducing 50% loss of hydraulic conductance and P_e determines the water potential at which cavitation starts. Plant species show large variation in P_{50} values in stems reaching values between -0.5 to -14MPa (Maherali et al., 2004). Recently, Choat et al., 2012 defined drought-induced embolism resistance of woody plants as a key physiological trait to survive and recover from drought stress. This highlights the importance of the xylem hydraulic conductance variations in the adaption of species to different habitats. Variations between species to drought induced-embolism are a consequence of the anatomical differences between species. The diameter and length of vessel, the inter-vessels pit membranes structures, vessels grouping and wood density differentiate between speciesand are responsible for the degree of resistance to cavitation (Choat et al,. 2008; Nardini et al., 2014; Lens et al., 2013).

Xylem embolism is directly related to stomatal behavior (Hubbard et al., 2001). Nevertheless, the links between them are poorly understood and need to be elucidated to understand water stress regulation. There are several studies reporting the decrease of stomatal conductance is related to the induction of embolism in xylem vessels (Sparks & Black 1999; Salleo et al., 2001; Brodribb et al., 2003; Choat et al., 2007). The mechanisms of the relationship between xylem embolism and stomatal conductance are not clear although those seem to be two possibilities; either stomata can respond directly to the decrease of stem hydraulic conductance or stomata can close due to a lower leaf water status caused by the decline of xylem hydraulic conductance (Tyree & Sperry 1989; Jones & Sutherland 1991; Nardini & Salleo, 2000; Sperry et al., 2002). Both options are possible in the regulation of stomatal conductance but the information that we have until now don't let us to elucidate the effective signal for the stomatal closure yet. Nevertheless, stomata is going to limit photosynthesis and make leaves more vulnerable to heat and light stress. If drought persists for a long period of time, stomata cannot stop runoff of water from leaves and prevent the spread of embolism across the xylem network. This situation can trigger a complete failure of the hydraulic system leading to episodes of branch or whole plant death (Brodribb and Cochard 2009; Kursar et al., 2009; Urli et al., 2013; Choat, 2013)

1.2.2.4 Recovery of hydraulic conductance after a period of drought.

Plants are able to refill embolized vessels after drought period when there is an increase in soil water availability (Salleo et al. 1996; Zwieniecki & Holbrook 1998; Brodersen et al., 2010). The recovery can be fast in hours (Holbrook et al., 2001; Kaufmann et al., 2009; Brodersen et al., 2010) or slow (weeks or months) requiring the growth of new xylem vessels (Brodribb et al., 2010). Positive root pressure would be one of the solutions to refill embolized conduits in some species (Sperry et al 1987; Cochard et al., 1994). However root pressure is not an intrinsic characteristic of each plant species and can vary according to the period of the year. Also, sometimes the value of root pressure measured is not sufficient refill embolized conduits (Salleo et al., 1996; Ameglio et al., 2002). Nevertheless, refilling is observed in numerous plant species being able to recover vessels without root pressure. Other theories postulate that the refilling process seem to be associated with the chemical properties of the vessel walls and their pit geometry allowing the confinement of positive pressures to refill conduits (Zwieniecki

and Holbrook, 2000). These positive forces can be generated by osmotic processes (Secchi and Zwieniecki, 2012) that are facilitated by living cells adjacent to the vessel walls. These cells would increase the concentration of osmotic solutes into the vessels and facilitate the refilling of the vessels.

Moreover, there are measurements that demonstrate that refilling can be produced while xylem vessels are subjected to negative pressures. Brodersen et al., 2010 demonstrated that grapevines were able to refill embolized vessels under xylem tension. Although the process needs further research to be solved, there are evidences that refilling occurs and is able to restore its hydraulic system (Brodersen et al., 2010; Zwieniecki et al., 2013).

The relationship between stomatal conductance and the process of refilling is dependent on the regulation of hydraulic conductance and chemical signals (Broddrib and Cochard, 2009). In general a good agreement is found between the restoration of A_N and the xylem hydraulic conductance (Lovisolo et al. 2008; Resco et al. 2009;Brodribb et al. 2010; Chen et al. 2010). This coordination between the restoration of the hydraulic conductance flow and photosynthesis is very interesting in terms of the potential net primary production attainable by different ecosystems types. Furthermore, the stomatal conductance recovery seems to be different depending on water stress and sometimes it is not coupled with the recovery of A_N (Lovisolo et al., 2008, Pou et al., 2012). Especial attention has been paid to chemical signals, which could be a possible regulator of stomatal conductance in the process of recovery (Lovisolo et al., 2008). Also hydraulic constraints seem to play a role in the recovery of g_s although some sections of the hydraulic path flow can be fully recovered (Brodribb and Cochard 2009).

1.2.3. ABA as a regulator of gas exchange.

It is widely demonstrated that an important part of the down-regulation of g_s under water stress is due to changes in ABA concentration in xylem sap or leaf (Davies and Zhang, rev. Dodd, 2005). Plants under drought stress are able to produce abscisic acid (ABA) in the shoot (Crhristmann et al., 2005; 2007) or roots (Loveys et al 1985). ABA is able to produce an osmotic efflux on guard cells reducing their turgor and closing stomata (Zhang & Davies 1990; Assmann & Shimazaki, 1999; Blatt, 2000)

Grapevines were one of the first plant species in which ABA was postulated to play a direct role on stomatal clousure (Loveys and Kriedemann 1974; Liu et al., 1978; Loveys 1984a, 1984b). In general, a negative relationship has been reported between g_s and

ABA xylem (Pou et al., 2008; Rodrigues et al., 2008; Romero et al., 2012; Speirs et al., 2013) or ABA in leaf tissue (Loveys and Kriedemann 1974; Liu *et al*. 1978; Lovisolo *et al*. 2002*a;* Speirs et al., 2013). Presently it is unclear if the clousure of stomatal is initiated by a) the signal from the roots, the leaf water potential (Rodrigues et al., 2008), b) the synthesis of new ABA in leaves (Zeevaart, 1980; Pierce and Raschke, 1981; Tan et al., 1997; Soar et al., 2006), c) by alliberation of sequestered leaf ABA in response to changes in pH (Stoll et al., 2000; Rodrigues et al., 2008) d) by changes in xylem sap pH (Sauter and Hartung, 2005; Else et al., 2006) or e) by re-activation of esterified ABA (Lee et al., 2006). All of them are possible situations that can be the responsible for the signal transduction.

1.3. Modeling as a tool to understand stomatal conductance and photosynthesis in plants

Mathematical modelling is a powerful tool to formulate hypotheses and to describe plant function and growth, although it is widely accepted that the inherent complexity of biological systems makes near impossible to find simple mathematical functions to describe their functionalism. Therefore, it is necessary to assume certain simplifications of the biological systems and their relevant components. In general, two types of models are used. Empirical models, which do not attempt to describe the mechanisms controlling a phenomenon and use very little information a priori for their development and, mechanistic models which are developed using knowledge of previous work and aim to explain a phenomenon at a more detailed level of organisation being useful for a generalised application. The present PhD thesis is based on the use of such mechanistic models to better understand stomatal conductance and photosynthesis in grapevine plants.

1.3.1. Models of stomatal conductance

There are many models aiming to describe stomatal conductance with three major approaches: empirical (data-based), mechanistic (process-based) and economic (optimization-based). The first two approaches are related because is really difficult to avoid some assumptions about factors which control stomata response and in some cases some assumptions have to be taken although the process-based models are more detailed than empiricals. The latter models are characteristic of being simpler and more mathematically tractable than mechanistic models. Consequently, empirical models are

more used given their simplicity and applicability. Mechanistic models are mathematically harder and are better suited to study at the cellular and subcellular processes involved in environmental sensing, signal transduction or ion movements. These characteristics make mechanistic models a really good tool to generate knowledge about regulation processes although they harder to work with.

The third approach, related to optimization, is philosophically closer to empirical modelling in the sense that both approaches assume that certain emergent properties of stomatal functioning are conservative and are therefore useful for prediction. They are based on the premise that plants tend to optimize the use of limiting resources in a quantifiably optimal process. The statement is that stomata pores are regulated by genomes that have been favored by natural selection to better enhanced behaviour at different ambients. This approach has the potential to be more robust than empirical approaches, but they rely on fundamental assumptions which can emerge from a consensus but not from a contrasted knowledge (Mäkelä et al., 2002).

1.3.1.1. Empirical models

Empirical models of stomatal conductance were focused to predict rather than to explore the mechanisms by which stomata respond to the environmental variables. Jarvis (1976) presented the first model of this type for stomatal conductance including the interacting response to multiple environmental factors. These variables were: light, temperature, CO_2, humidity and leaf water status. The Jarvis model present a response of each function fitted to each parameter, normalizing the maximums to a value of 1. Then, all response curves were multiplied and predicted the value of g_s with a good accuracy when the measurement ranges covered all the situations encountered during the period of measurements. This model is still used, specially integrated into large models such as general circulation models (GCM) (Egea et al.,2011). The main disadvantage of this model is that it requires large amount of data to cover the wide range of environmental conditions and that values can change with leaf age (Whitehead et al., 2011). Also this type of models doesn't attempt to know which is the mechanism involved in the regulation of stomatal conductance and there is only the intention of being a predictive tool.

Another empirical model of stomatal conductance is the Ball-Berry model (Ball, Woodrow & Berry, 1987) and variations made with it. The original version of this

model described g_s as a function of net photosynthesis (A_N), CO_2 concentration at the leaf surface (C_s), the relative humidity at the leaf surface (h_s) and the residual stomatal conductance when photosynthesis is zero (g_{s0}). The parameter *m* in the equation is an empirical constant that varies among leaves and time.

$$g_s = g_{s0} + m \frac{A\,h_s}{C_s}$$

This model has been widely used for its simplicity with only two free parameters and its ability to accurately predict g_s over wide ranges of environmental conditions. It is used in canopy models and GCMs being a good predictive tool to predict water loss (Egea et al., 2011). Although it is easy to test the model against empirical measurements of A_N and g_s it requires a separate model for A_N. This feature is typically done using a biochemical model of photosynthesis (Farquhar, Caemmerer & Berry 1980), which combined with values for boundary layer and mesophyll conductance yields a closed system that can be solved either iteratively or analytically (Baldocchi 1994). Several modifications of this model have been proposed. Leuning (1990) suggested replace C_s with (C_s-Γ), where Γ is the CO_2 compensation point, to prevent A_N becoming negative at low C_s which could lead to negative g_s values. After that the equation $1/(1+Ds/D_0)$ was added to the Ball-Berry model, where D_0 is an empirical parameter (Leuning 1995). The revised version of the Ball-Berry model share some features with mechanistic models such as the hyperbolic relationship between g_s and D_s which also arises in mechanistic models from the effect of transpiration on turgor pressures of cells in the stomatal complex (e.g. Dewar 1995; Gao *et al*. 2002; Buckley, Mott & Farquhar 2003). Similarly, the responses to A_N and $1/(C_s - Γ)$ can be interpreted as the effect of mesophyll *ATP* or *NADPH* on ion pumping by guard cells (Dewar 1995). Regardless of the good proxy, it fails to predict water stress and a function of the empirical parameters response to water stress is needed to model under water stress conditions.

1.3.1.2. Mechanistic (process-based) models

The mechanistic/empirical models are those which their main purpose is generate testable predictions from hypotheses regarding to the mechanisms of stomatal control. Mechanistic models have been crucial in developing our understanding of how stomata work. However, they are often not useful for predicting g_s as a function of environmental conditions in part because their parameters represent biophysical

properties that are experimentally difficult to measure. Recent attempts to produce a detailed mechanistic model of guard cell ion transport and osmolyte synthesis (Chen *et al.* 2012; Hills *et al.* 2012; Wang *et al.* 2012) show the strengths and weaknesses of detailed mechanistic modeling of stomatal conductance. The Buckley model, hearafter "BMF model" (Buckley et al. 2003) is one of the best mechanistic models that actually predict g_s with accuracy. This model is based on five assertions relating stomatal conductance: 1-Stomatal conductance is proportional to stomatal aperture; 2- Aperture is controlled by guard cell turgor pressure; 3- Turgor is the sum of water potential and osmotic pressure; 4- Water potential is "drawn down" to guard cells from a source and through a resistance by transpiration and 5- Transpiration rate is the product of conductance and evaporative gradient. The BMF model assumes that guard cell osmotic pressure is actively regulated to seek a value that is proportional to both epidermal turgor pressure and the concentration of ATP in the photosynthesizing cells (τ), which is a function of irradiance, intercellular CO_2 concentration and photosynthesis. Additional parameters in the model include soil water potential, leaf osmotic pressure, plant hydraulic resistance, VPD and a *"na"* parameter that describes the sensitivity to epidermal turgor and ATP concentration. The present PhD thesis uses a simplification of the BMF model with the following formula:

$$g_s = \frac{naK(\Psi_s + \pi)}{K + na\text{VPD}}$$

where *K* is the leaf-specific hydraulic conductance, Ψ_s is soil water potential, π is bulk leaf osmotic pressure and VPD is leaf to air water vapour mole fraction gradient. *N* and *a* capture non-hydraulic effects: *a* is mesophyll ATP concentration expressed relative to its maximum value and *n* is a lumped parameter representing other non-hydraulic factors:

$n \equiv \chi\beta\tau_m$, and

$a \equiv \tau/\tau_m$,

Where τ is ATP concentration in photosynthesizing cells, χ is a proportionlality factor that scales the guard and epidermal cell turgor pressures to g_s, β is a proportionality

factor that scales the product of τ and the epidermal turgor to changes in guard cell osmotic pressure and $τ_m$ is the the maximum τ (the total pool of adenylates, ADP+ATP).

1.3.1.3. Optimization models

Cowan and Faquhar 1977 developed a model to quantify the optimal behavior for stomata in a changing environment. The model suggest that plants must optimize instantaneous water use efficiency with an optimal stomatal conductance. The model inted to explain stomatal behaviour by computing the theoretically optimal pattern of g_s and compares this pattern to observations in the field. They theory behind is that a leaf has a finite daily total supply of transpirable water and that g_s should vary over time and in relation to unpredictable variations in environmental conditions so that daily total carbon gain will be maximum for the water used. The abstract solution to this problem was that g_s should vary such that a particular property of the gas exchange equations – the marginal carbon product of water ($∂A/∂E$) – remains invariant over the day. This predicts qualitative trends in g_s quite well, including the short-term responses to irradiance and humidity, and the mid-day depression of photosynthesis under moderately water stressed conditions (e.g. Cowan & Farquhar 1977; Ball & Farquhar 1984). Nevertheless, in practice, it has been difficult to implement optimality as a predictive tool. This is partly because the 'target' value of $∂A/∂E$, often denoted 1/λ, must be specified arbitrarily, and partly because it can be mathematically and computationally difficult to compute the value of g_s that produces this target $∂A/∂E$ at each point during the day. The optimal solution depends rather sensitively on fine details of the model of photosynthesis and gas exchange used to compute $∂A/∂E$ (Buckley et al., 2002; Buckley, Cescatti & Farquhar 2013). Nevertheless, several recent studies have had some success in advancing this approach for predicting g_s (Schymanski*et al.* 2008; Katul*et al.*, 2009; Manzoni *et al.* 2011; Medlyn *et al.* 2011).

1.3.2. Modeling photosynthesis*:*

The major input of free energy into the biosphere is provided by photosynthesis. Globally the effect is the removal of one mole of water and the formation of one mole of oxygen for every mole of CO_2 reduced to sugars. Photosynthesis has been modelled using the mechanistic model proposed by Farquhar et al., (1980). This model is based on the knowledge of the biochemistry of the enzyme Ribulose-1,5-biphosphate (RuBisCo). They proposed that leaf net photosynthesis could be modelled as the

minimum of two limiting rates: A_v the limitation due to its carboxylation rate and A_j when the RuBisCo regeneration is limited.

$A_n = min\ (A_v, A_j) - R_d$

The following are the equations describing the limitations encountered:

$$A_v = V_m \frac{c_c - \Gamma_*}{c_c + K_c(1 + O/K_o)} - R_d \text{, and}$$

$$A_j = \tfrac{1}{4} J \frac{c_c - \Gamma_*}{c_c + 2\Gamma_*} - R_d \text{,}$$

where V_m is carboxylation capacity, J is potential electron transport rate, c_c is chloroplastic CO_2 concentration, Γ_* is photorespiratory CO_2 compensation point, K_c and K_o are the Michaelis constants for RuBisCo carboxylation and oxygenation, respectively, O is oxygen concentration and R_d is the rate of non-photorespiratory CO_2 release. Assimilation rate is calculated as the minimum of A_v and A_j.

As photosynthesis process is mediated by RuBisCo, temperature is one of the main environmental variables affecting photosynthesis (Medlyn *et al.,* 2002). Temperature responses of the photosynthetic parameters of the Faquhar's model are important to be use since along the temperature gradient is important, affecting the kinetics of the enzyme RuBisCo.

Another important factor to take in the modeling process is CO_2 supply. Diffusion of CO_2 from the atmosphere to the sub-stomatal internal cavities is through stomata, and from there to the carboxylation sites located inside the stroma is through the leaf mesophyll. Those diffusions are really important to determine with accuracy the CO_2 concentration at the carboxylation site and to estimate net photosynthesis.

Using the Fick's law of diffusion, A_N can be expressed as:

$A_N = g_s\ (C_a - C_i) = g_m\ (C_i - C_c)$;

Where g_s and g_m are the stomatal and mesophyll conductance to CO_2 diffusion respectively, and C_a, C_i and C_c are the CO_2 concentrations in the atmosphere, in the sub-stomatal internal cavity and in the chloroplast stroma, respectively (Long & Bernacchi,

2003). Then, decreases of CO_2 diffusion through the leaf depend on stomatal and mesophyll conductance.

In Gaastra's (1959) pioneer work on leaf photosynthesis, mesophyll conductance was defined as a diffusion component of the photosynthesis pathway, and it was confirmed by later works showing that g_m could be variable and could respond to environmental factors (Jones & Slatyer, 1972; Samsuddin & Impens, 1979). Thereafter, for decades, gas exchange studies assumed that $C_i=C_c$ and therefore, g_m was constant and infinite. However, evidences that C_c was lower than C_i were repeatedly demonstrated. There were several confirmations by comparing online carbon isotope discrimination studies (Evans et al., 1986), comparing the initial slope of A_N-C_i curves with the activity of ribulose 1-5-bisphosphate carboxylase/oxygenase (Rubisco) determined in vitro (Evans & Terashima, 1988) and by comparison of chlorophyll fluorescence with gas exchange measurements (Bongi & Loreto, 1989; Di Marco et al., 1990). In summary, there is now convincing evidence that g_m is finite and not constant, C_c is significantly less than C_i, and g_m is a significant limitation to photosynthesis. That reinforces the need to have in account g_m to model photosynthesis to have a better estimation.

Many environmental effects have been described to affect g_m (for review: Flexas *et al.*, 2008; Flexas *et al.*, 2012) but one of the most important for modeling photosynthesis is the g_m response of g_m to temperature. Walker *et al.*, (2013) recently showed that it is important to estimate the response of g_m to temperature for the species for which photosynthesis has to be modelled. In several studies the effect of temperature on g_m has been reported (Bernacchi et al., 2002; Warren and Dreyer 2006, Yamori 2006, Diaz-Espejo et al., 2007; Flexas et al 2008; Warren 2008; Egea et al., 2011; Evans & von Caemmerer 2013) and it can be concluded that for every species g_m presents a different response temperature (Diaz-Espejo, 2013; Flexas and Diaz-Espejo, 2014).

1.4. Scaling up to whole plant

Plant canopies are characterized by extensive and interacting gradients of environmental conditions (light, temperature, humidity and wind). Each leaf in the canopy is exposed to a unique combination of these environmental conditions being difficult to accurately predict the whole canopy carbon gain and water flux. Along the environmental variables affecting canopy resources distribution, light is considered the key environmental driver of photosynthesis in plant canopies (Kull and Kruijt, 1999; Niinemmets and Anten

2009). All leaves receive a limited amount of light which can vary according to the position occupied in the crown. Although light is important, nitrogen is considered a limiting element. Its concentration in soil and its uptake and assimilation by plants is limited due to the energy cost requirement in the assimilation process (Gutschick, 1981; Field and Mooney, 1986; Chapin et al., 1987) being a limiting element. Nitrogen is used in the construction of the photosynthetic apparatus of leaves (Evans, 1989) and the vast majority of the nitrogen in the leaf is used for that purpose having good relationships between the amount of nitrogen and A_N. Taking in consideration the last statements, both (light and nitrogen), have been postulated as the most limiting factors around the canopy limiting photosynthesis rate (Field and Mooney, 1986; Evans, 1989) and widely used to scale up photosynthesis from a simple leaf to the whole canopy.

There are approaches to scale up carbon and water fluxes from the leaf to the canopy: predictive integration models and optimization models. Scaling up photosynthesis with predictive models requires understanding of the distribution of foliage and photosynthetic potential within the canopy and information of temporal and spatial variation of environmental conditions within the canopy (Niinemts and Antem 2009). There has been a large evolution in all modeling processes improving the detail where the description of the processes along the canopy occur with detailed improvement of the prediction of carbon gain and water loss. Nevertheless, an alternative to further complicate models can be the use of optimization principles assuming that the canopy is constructed so that it maximizes its carbon gain in a given environment (Cowan and Faquhar 1977). As nitrogen and light are a limited resource it can be inferred that all elements involved in the regulation process of photosynthesis are optimized to maximize carbon gain.

Thus, if nitrogen is optimally distributed along the canopy, then total photosynthesis could be calculated analytically, using a "big-leaf" model (Sands 1995). This approximation is used in current models to investigate Earth sytem responses to climate change (Sellers et al., 1997; Friedlingstein et al., 2006). However, measurements indicate that nitrogen is not optimally distributed along the canopy (Ellsworth and Reich 1993; Dang et al., 1997; Carswell et al., 2000; Meir et al., 2002; Lloyd et al., 2010). Therefore, it is not unreasonable to think that other constrains along the canopy are playing a role in the determination of photosynthesis. Thus light and nitrogen content are not the only factor well related to explain crown photosynthesis. CO_2 and H_2O supply can constitute an important constrain during the day being both important in the

process of regulation of photosynthesis along the canopy (Buckley and Warren, 2013; Peltomieni et al., 2012; Niinemets 2012).

One of the physiological factors that has a special influence on photosynthesis is stomatal conductance. Cowan and Farquhar 1977 suggested that stomatal conductance optimize water loss to maximize carbon gain (optimization theory). Under this hypothesis, stomatal conductance and photosynthesis are well related and both are taken into account to estimate whole canopy photosynthesis. However, this theory fails to predict photosynthesis at the canopy scale with clear having overestimations of the rates of canopy photosynthesis (Anten et al., 2000). Its limitations could be environmental variables such as temperature, humidity and windiness. These environmental variables have been reported to affect leaf photosynthesis and could explain the deviation between optimal profiles and real values (Niinemets and Valladares, 2004). Recently, several studies have reported other possibilities to explain the disjunction between theory and real data. They concluded that H_2O and CO_2 pathways are possible limitations within the optimization models. Buckley and Warren, (2014) introduced g_m variations in the crown profile and concluded that it can limit photosynthesis and may be the responsible for the suboptimal photosynthesis rates. On the other hand, Peltoniemi et al., 2012 suggested that hydraulic conductance could be a major factor responsible of some of the observed variations of the optimization theory. They concluded the need to have an optimized hydraulic conductance in order to obtain an optimized carbon gain. In general; more realistic models are needed to scale up photosynthesis from leaves to a total canopy (Buckley et al., 2002; Ninemets, 2012; Peltoniemi et al., 2012; Buckley et al., 2013). This has led to think that environmental variables, such as water and CO_2 pathways play an important role when photosynthesis is scaled up to the canopy level (Diaz-Espejo et al., 2007; Peltoniemi et al., 2013; Buckley et al., 2013; Buckley et al., 2014).

1.4.1 Modeling Grapevine A_N and g_s.

Grapevine is an economically important crop, widely cultivated around the world. The importance of modeling grapevine g_s and A_N in grapevines is the use of the model as a predictive tool to study their water use and also to optimize their water use efficiency. Some studies have worked at the leaf level modeling photosynthesis and stomatal conductance (Shultz 2003, Hendrickson et al., 2004; Greer and Weedon, 2012). These

studies worked the response of Farquhar's parameters to temperature without taking in account g_m limitation. There is also a recently developed model predicting total canopy photosynthesis and transpiration in well watered conditions (Prieto et al., 2012). Regardless of its importance, the knowledge on modeling of photosynthesis and stomatal conductance in grapevine is really poor. This reinforces the need to try or develop other models to include g_m limitation and also to investigate the regulation of stomatal conductance to better understand the process around stomatal regulation. If we are able to understand the regulation of stomatal conductance then, managing grapevines is going to be easier and water use optimized.

2. OBJECTIVES AND OUTLINE

2.1. Objectives of the Thesis

The **general hypothesis** of the present work is that the application of processes-based models will improve understanding of plant responses to water stress, particularly stomatal conductance control. The present Thesis is focused on providing much of the necessary data to feed those models, particularly with experimental data under realistic crop conditions.

In consequence, **the objectives of the present thesis are:**

1. To improve the present knowledge on the role of water relations, leaf gas exchange, ABA and hydraulic conductance of stem and leaves on the regulation of stomatal conductance and photosynthesis.

2. To introduce the use of mechanistic models to better understand the responses of grapevine leaves to water stress, particularly for stomatal conductance and photosynthesis.

3. To explore the usefulness of modeling to scale up from leaf to whole plant, gaining a new perspective for whole grapevine behavior.

2.2. Outline of the Thesis

The present Thesis is organised in 7 Chapters. Across these chapters, the water relations related to the control of stomatal conductance, the modeling approach of stomatal conductance as well as the up scaling from leaves to canopy are presented and studied.

Chapter 1: INTRODUCTION

This Chapter introduces the background and sets the contexts for this Thesis. It includes a general overview of stomata regulation, modeling approaches and whole plant physiological parameters.

Chapter 2: OBJECTIVES AND OUTLINE

In the present Chapter the general objectives are presented as well as a brief outline of the Thesis.

Chapter 3: THE PLANTS RESPONSE TO WATER STRESS: WATER RELATIONS ADJUSTMENT AND STOMATAL CONDUCTANCE

This chapter covers the mechanism regulating stomatal conductance in relation to 3.1) stem hydraulic conductance and the role of stomatal clousure 5.2) the variation of leaf hydraulic conductance along the season and their relation with the osmotic adjustment 5.3) the differential behavior of two grapevines cultivars in response to water stress.

Chapter 4: MODLEING THE GRAPEVINE RESPONSE TO WATER STRESS: PROCESS-BASED MODELS OF STOMATAL CONDUCTANCE (g_s) AND PHOTOSYNTHESIS (A_N)

In this chapter gs and photosynthesis are modeled with process based models obtaining good results on their application.

Chapter 5: UP SCALING FROM LEAF TO WHOLE CANOPY PROCESSES: CHARACTERIZING THE LEAF POSITION AND MICROCLIMATE EFFECTS OF GRAPEVINE CANOPIES

In this chapter 5.1)the role of hydraulic conductance and ABA is predicted using the mechanistic model of stomatal conductance and 5.2) the optimization theory is tested in a field study in the grapevine canopy

Chapter 6: GENERAL DISCUSION

This Chapter contains a general discussion and overview of all the results presented in Chapters 3,4 and 5.

Chapter 7: CONCLUSIONS

The last Chapter presents a list of the main conclusions derived from the present Thesis in relation to the general objectives described in Chapter 2

3. THE PLANTS RESPONSE TO WATER STRESS: WATER RELATIONS ADJUSTMENT AND STOMATAL CONDUCTANCE

3.1. Rapid hydraulic recovery in *Eucalyptus pauciflora* after drought: linkages between stem hydraulics and leaf gas exchange

Sebastià Martorell[1, 3], Antonio Diaz-Espejo[2], Hipólito Medrano[1], Marilyn C. Ball[3], Brendan Choat[3, 4]

[1] Grup de Biologia de les Plantes en Condicions Mediterrànees. Universitat de les Illes Balears, UIB, Crta. Valldemossa km, 7.5 Palma de Mallorca, Spain

[2] Irrigation and Crop Ecophysiology Group, Instituto de Recursos Naturales y Agrobiología, IRNAS-CSIC, Apartado 1052, 41080, Sevilla, Spain

[3] Plant Science Division, Research School of Biology, The Australian National University, Canberra, ACT 0200, Australia.

[4] University of Western Sydney, Hawkesbury Institute for the Environment, Richmond, 2753, NSW, Australia

ABSTRACT

In woody plants photosynthetic capacity is closely linked to rates at which the plant hydraulic system can supply water to the leaf surface. Drought induced embolism can cause sharp declines in xylem hydraulic conductivity that coincide with stomatal closure and reduced photosynthesis. Recovery of photosynthetic capacity after drought is dependent on restored xylem function, although few data exist to elucidate this coordination. We examined the dynamics of leaf gas exchange and xylem function in *Eucalyptus pauciflora* seedlings exposed to a cycle of severe water stress and recovery after re-watering. Stomatal closure and leaf turgor loss occurred at water potentials that delayed the extensive spread of embolism through the stem xylem. Stem hydraulic conductance recovered to control levels within 6 h after re-watering despite a severe drought treatment, suggesting an active mechanism embolism repair. However, stomatal conductance did not recover after 10 d of rewatering, effecting tighter control of transpiration post drought. The dynamics of recovery suggest that a combination of hydraulic and non-hydraulic factors influenced stomatal behaviour post drought.

INTRODUCTION

Water availability is one of the principal factors controlling the productivity of ecosystems and shaping the distribution of plant species. Periods of severe drought cause major declines in the net primary productivity of tropical and temperate forests (Ciais *et al.* 2005; Phillips *et al.* 2009; Zhao & Running 2010), and drive large scale forest mortality events (Allen *et al.* 2010). The drought sensitivity of woody plants is also a major factor shaping community composition and the distribution of species across moisture gradients (Engelbrecht *et al.* 2007; Kursar *et al.* 2009). A key physiological trait influencing the ability of woody plants to survive and recover from drought is their resistance to drought-induced embolism (Choat *et al.* 2012).

As the soil dries, tension in the xylem sap increases leading to a higher probability of cavitation, a sudden phase change from liquid water to vapour (Zimmermann 1983; Tyree & Sperry 1989). This process creates gas emboli that become trapped within xylem conduits. Embolism spreads through the vascular network by air seeding at pit membranes with gas blockages causing a progressive decrease in xylem hydraulic

33

conductance (Sperry, Donnelly & Tyree 1988a; Choat, Cobb & Jansen 2008; Brodersen *et al.* 2013). Because stomatal opening and photosynthesis are contingent on the efficiency with which water can be delivered to the leaves, xylem embolism represents a primary constraint on plant productivity and survival during drought. Plants must therefore maintain xylem water potentials within a range that will prevent extensive embolism in the xylem.

Stomatal closure is the primary mechanism by which plants limit water loss and delay decreases in xylem water potential during drought. However, the links between stomatal behaviour and xylem embolism remain poorly understood. Several studies provide evidence of tight correlations between stomatal closure and the induction of embolism in the stem xylem (Sparks & Black 1999; Salleo *et al.* 2001; Brodribb *et al.* 2003; Choat, Sack & Holbrook 2007). It remains unclear if stomata respond directly to cavitation via the effects of decreasing stem hydraulic conductance on leaf water status, or if declines in leaf water status are driven by loss of conductance in other parts of the hydraulic pathway (Tyree & Sperry 1989; Jones & Sutherland 1991; Nardini & Salleo 2000; Sperry *et al.* 2002). In any case, it is obvious that while stomatal closure limits plant water loss, it will also reduce photosynthesis and render leaves more vulnerable to damage via heat and light stress. In periods of extended drought, stomatal closure cannot restrict water loss sufficiently to prevent the formation of extensive embolism in the xylem. This results in the almost complete loss of xylem flows and can lead to branch die back or whole plant death (Brodribb & Cochard 2009, Kursar *et al.* 2009; Urli *et al.* 2013; Choat *et al.* 2013).

However, there is evidence that plants can refill embolized vessels if periods of drought are followed by sufficient increases in soil water availability (Salleo *et al.* 1996; Zwieniecki & Holbrook 1998; Brodersen *et al.* 2010). This recovery can be rapid, taking place on a timescale of hours (Holbrook *et al.* 2001; Kaufmann *et al.* 2009; Brodersen *et al.* 2010), compared with the longer time intervals (weeksmonths) required to grow new active xylem (Brodribb *et al.* 2010). In fact, a number of studies suggest that refilling occurs in periods of active transpiration during the day (Canny 1997; McCully, Huang & Ling 1998), with some demonstrating that refilling can occur while the bulk xylem water potential is negative (Salleo *et al.* 1996; Holbrook & Zwieniecki 1999; Tyree *et al.* 1999; Stiller, Sperry & Lafitte, 2005). This suggests an active refilling mechanism which is hypothesized to depend on the pumping of solutes into refilling vessels by adjacent parenchyma (Zwieniecki & Holbrook 2009; Nardini, Lo

Gullo & Salleo 2011). Although this refilling mechanism is yet to be elucidated, it evidently offers a means by which plants can rapidly restore hydraulic capacity after drought.

Despite the established links between hydraulic and photosynthetic capacity, few studies have examined the coordination between hydraulic conductance and photosynthesis during recovery from drought (Lovisolo *et al.* 2008; Resco *et al.* 2009; Brodribb *et al.* 2010; Chen *et al.* 2010). The available evidence suggests that recovery of photosynthesis in woody plants is strongly linked to hydraulic recovery, regardless of the timing and mechanism of restoration. The timing of recovery has important implications to how ecosystem level net primary productivity will respond to cycles of drought and re-wetting.

In this study we examined the dynamics of drought and recovery in *Eucalyptus pauciflora* seedlings. We investigated the hypothesis that recovery from drought can occur rapidly upon re-watering and is facilitated by refilling of embolized xylem conduits. The dependence of recovery of photosynthetic capacity upon hydraulic recovery was also addressed.

MATERIALS AND METHODS

Plant material and conditions

Experiments were conducted on 2 years-old potted *E. pauciflora* Sieber ex Sprengel seedlings in a greenhouse polytunnel at the Australian National University (Canberra, Australia) during March and April 2011. Average maximum and minimum temperatures for the period of experimentation were 21.3 and 8.6 ℃ respectively. Mean relative humidity was 73% for the period of experimentation. The polyethylene tunnel cover reduced photosynthetic photon flux density by 50% and average irradiance measured at midday on a sunny day was 550 μmol photon m^{-2} s^{-1}.

One month before the start of the experiment, plants were transplanted from 1 L pots to 4 L pots. The soil used for the experiment was a soil organic mixture containing four parts aged mushroom compost, three parts washed river sand, two parts shredded peat, and one part course grade perlite.

Plants were 60 – 80 cm tall, 4-6 mm in diameter at the stem base, and had 478.32 ± 110.37 cm^2 (mean ± SD) of total leaf area at the beginning of the experiment. A total of 130 potted *E. pauciflora* seedlings were used for the experiment with 100 plants randomly assigned to a *water stress* treatment and 30 plants maintained as the *control*

treatment. Water stressed plants had water withheld after the initial baseline physiological measurements had been conducted. Control plants were maintained under well water conditions throughout the experiment. After the water stress treatment commenced, it took approximately 20 d to observe variations in predawn leaf water potential of the seedlings. Predawn leaf water potential was highly variable after this point as plants with greater leaf area exhibited more rapid decline in water potential. For this reason measurements were performed every 3-4 d to assess the variability of hydraulic and photosynthetic traits during the dry down period. The water stress treatment was applied for 38 d. After this, a subset of water stressed plants was re watered to investigate rates of recovery from drought. All of the rewatered treatment plants had reached a predawn water potential between -2.5 and -3 MPa before re watering occurred. This target water potential was based on preliminary measurements and previous work indicating that death of above ground biomass occurred at water potentials of -3.6 MPa in potted *E. pauciflora* seedling exposed to drought (Kirschbaum 1987).

Re watering occurred at 0900h in the greenhouse polytunnel with the entire volume of the soil soaked during re watering. Plants in the re watered treatment were measured at 6 h, 1 d, and 10 d after re-watering to establish post drought levels of gas exchange and hydraulic parameters. At each measurement point during the cycle of drought and recovery five replicate plants were measured. There were a total of 12 measurement days over the course of the experiment.

Control plants were measured at three time points during the experiment: at the beginning of the experiment, at the initial stage of the recovery, and at the end of the recovery period. Five replicates were measured per sampling time.

Gas exchange measurements

Leaf gas exchange was measured using a portable open gas exchange system (Li-6400; Li-Cor, Inc., Lincoln, NE, USA) equipped with a light source (Li-6200-02B LED, Li-Cor). Light-saturated net CO_2 assimilation rate (A_N), stomatal conductance (g_s) and transpiration rate (E) were measured in mature leaves between 0900 and 1100. Environmental conditions in the leaf chamber consisted of a photosynthetic photon flux density of 1500 µmol m^{-2} s^{-1}, an air temperature of 25 ºC and an ambient CO_2 concentration of 400 µmol mol^{-1}.

Water relations

Predawn water potential (Ψ_{PD}), leaf water potential (Ψ_L), and stem water potential (Ψ_x) were measured at each sampling point. Leaves were collected just after gas exchange measurements were completed. For stem water potential measurements, leaves were bagged with a sealed and foiled plastic bag for at least 30 min before to collection (Begg & Turner, 1970). Samples were all double bagged in a plastic bag saturated with water vapour and carried to the laboratory in an insulated box. Water potentials were measured with a Scholander pressure chamber (Soil Moisture Equipment Corp 3005, Santa Barbara Corp; Santa Barabara CA, USA). Additionally, one leaf was collected to measure the relative water content (RWC) from the same plant. Leaves were carried in the insulated, double bagged box. Fresh weight was determined with an analytical balance and the leaf was the allowed to rehydrate during 24 h at 4 °C. After that period, saturated weight was measured and the leaf was placed at drying oven at 70 °C for 48 h. Dry weight was determined and RWC was calculated as follows:

$$RWC = (FW-DW)/(TW-DW), \quad (1)$$

where FW corresponds to a fresh weight, DW is dry weight and TW is turgid weight. Turgor loss point (Ψ_{tlp}) was located at the inflection point of the $1/\Psi_L$ versus RWC values for the values obtained respectively.

Hydraulic conductivity

Plants were harvested for measurement of stem hydraulic conductivity after leaf gas exchange measurements were completed. At each measurement point, the shoots of five replicate seedlings were harvested. Stems were cut underwater close to the soil to relieve tension in the xylem (Wheeler et al. 2013), wrapped with parafilm, and sealed in a plastic bag with moist paper towel to prevent evaporation. They were carried to the laboratory and hydraulic conductivity was measured using the methods of Sperry, Donelly & Tyree (1988b).

Stems were re-cut underwater to a length of 20 cm. Initial tests indicated that few xylem vessels were cut open at both ends in 20 cm lengths of stem. Lateral branches and leaves were removed with the cut surfaces sealed using superglue (Loctite 409; Henkel North America, Rocky Hill, CT, USA) to prevent leaks. The two ends of the stem were shaved with a fresh razor to ensure that xylem conduits were not occluded at

the cut surface. Flow was estimated using a 10^{-5} g resolution balance (AX205; Mettler Toledo, Giessen, Germany). The initial hydraulic conductance (k_i) was measured under an applied pressure of 3-4 kPa using an artificial sap solution containing 2 mM KCl, 0.5 mM NaCl, 0.3 mM $CaCl_2$, filtered to 0.2 µm. After k_i was determined, segments were flushed with the same solution for 5 min at a pressure of 150 kPa. Hydraulic conductivity was re-measured and maximum hydraulic conductance (k_{max}) estimated after the flushing. The percentage loss of conductivity (PLC) was calculated as:

$$PLC = 100 \times (1 - k_i/k_{max}) \quad (2)$$

The length, cross sectional area of conductive xylem, and the leaf area supported by each stem were measured and used to calculate specific hydraulic conductivity (K_S) and leaf specific hydraulic conductivity (K_L) respectively. The initial values of conductivity before flushing were designated as K_{Si} and K_{Li} for sapwood and leaf specific conductivities, respectively. The conductive section was measured at the apical end of the sample after perfusing the stem with a staining solution (safranin 0.01%). After staining, a freehand section was taken with a razor from the apical end, viewed under a compound microscope and imaged with a digital camera. Analysis of the conductive section was performed using the software Image J (http://imagej.nih.gov/ij/). Leaf area was determined using a leaf area meter (Li-Cor Li-3100).

Leaf hydraulic conductivity (K_{Leaf}) was estimated using transpiration rates measured with the Li-Cor 6400 and the difference in water potential between adjacent bagged and unbagged leaves. Leaves used in water potential measurements were collected immediately after gas exchange measurements were completed on each plant. K_{Leaf} was then calculated according to Ohm's Law as:

$$K_{Leaf} = E / (\Psi_L - \Psi_x), \quad (3)$$

where $\Psi_L - \Psi_x$ represents the pressure gradient between leaf and stem in MPa and E is the transpiration rate measured from leaf gas exchange in mmol s^{-1} m^{-2}.

Statistical analysis:

Differences between means were assessed by an analysis of variance (anova). When differences were significant we applied a multiple comparison of means post hoc Tukey

(P<0.05), performed with SPSS 19.0 (IBM Corp., Armonk, NY, USA). A Dixon test was applied to identify possible outliers and remove them from K_{Leaf} data. Comparison between regressions was performed with a Student's t test (P<0.05) between residuals using SPSS 19.0. Regression coefficients and correlations were calculated with the 8.0 Sigma Plot software package (Systat Software, Chicago, IL, USA).

RESULTS

Dry-down experiment

No significant changes in Ψ_{PD} were observed during the first 20d after irrigation was withheld (Fig. 1a). Minimum values of Ψ_x and Ψ_L were close to -1.3 MPa during this period, $\Delta\Psi$ (Ψ_{PD}-Ψ_L) varied between -0.5 and -1.2 MPa (Fig. 1b). The observed variation in $\Delta\Psi$ during this period was presumably driven by differences in whole plant transpiration. After that, Ψ_x and Ψ_L decreased linearly with Ψ_{PD} although the slope of this relationship was different to 1 (p<0.05), resulting in a reduction of $\Delta\Psi$ as Ψ_{PD} decreased further (Fig. 1b). The maximum $\Delta\Psi$ occurred at Ψ_L = -1.5 MPa, while the minimum $\Delta\Psi$ (= 0.2 MPa) occurred at Ψ_L between -2 and -3 MPa.

The PV curve obtained from the Ψ_L and RWC data (Fig. 2) indicated that leaf turgor loss (Ψ_{tlp}) occurred at -1.6 MPa and at a RWC of 0.9. This Ψ_{tlp} corresponds closely with the minimum Ψ_L observed in well-watered, transpiring plants (Fig. 1a).
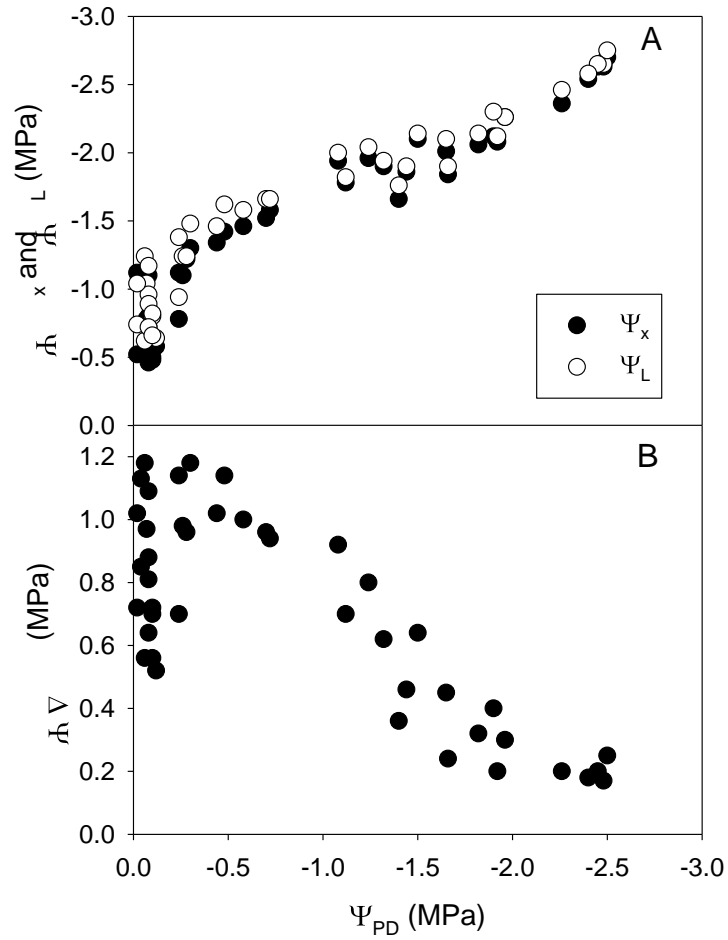
Figure 1: A) Response of xylem (Ψ_x) and leaf water potential (Ψ_L) to predawn leaf water potential to the drought treatment. B) Evolution of plant water potential gradient ($\Delta\Psi = \Psi_{PD} - \Psi_L$) vs. Ψ_{PD}.
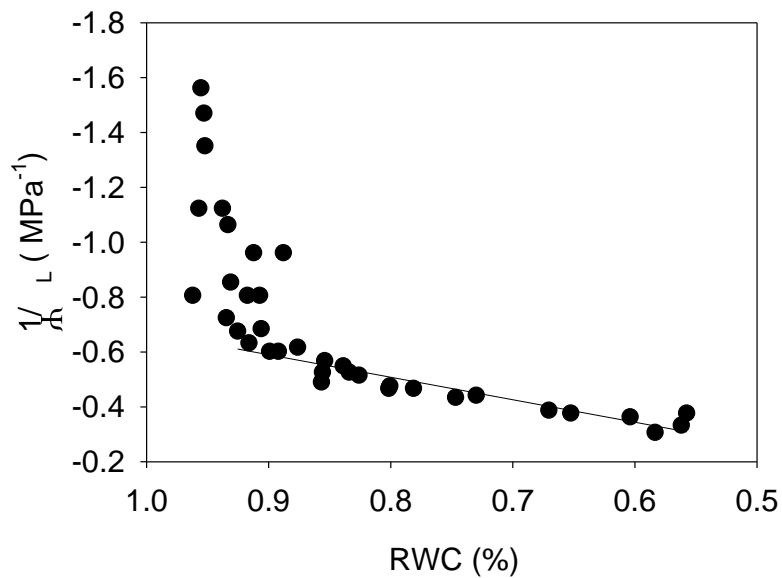

Figure 2: Pressure-volume curve generated from leaf water potential (Ψ_L) and leaf relative water content (RWC) during the dry-down experiment.

During the dry-down process, g_s and A_N declined rapidly as Ψ_L decreased from -0.5 MPa to -1.5 MPa (Fig. 3). Maximum A_N values of 30 μmol m^{-2} s^{-1} corresponded to E above 5 mmol m^{-2} s^{-1} and g_s of 0.95 mol m^{-2} s^{-1}. Stomatal closure occurred at Ψ_L of -1.6 MPa, at which point g_s was around 5% of maximum values (Fig. 3a inset).
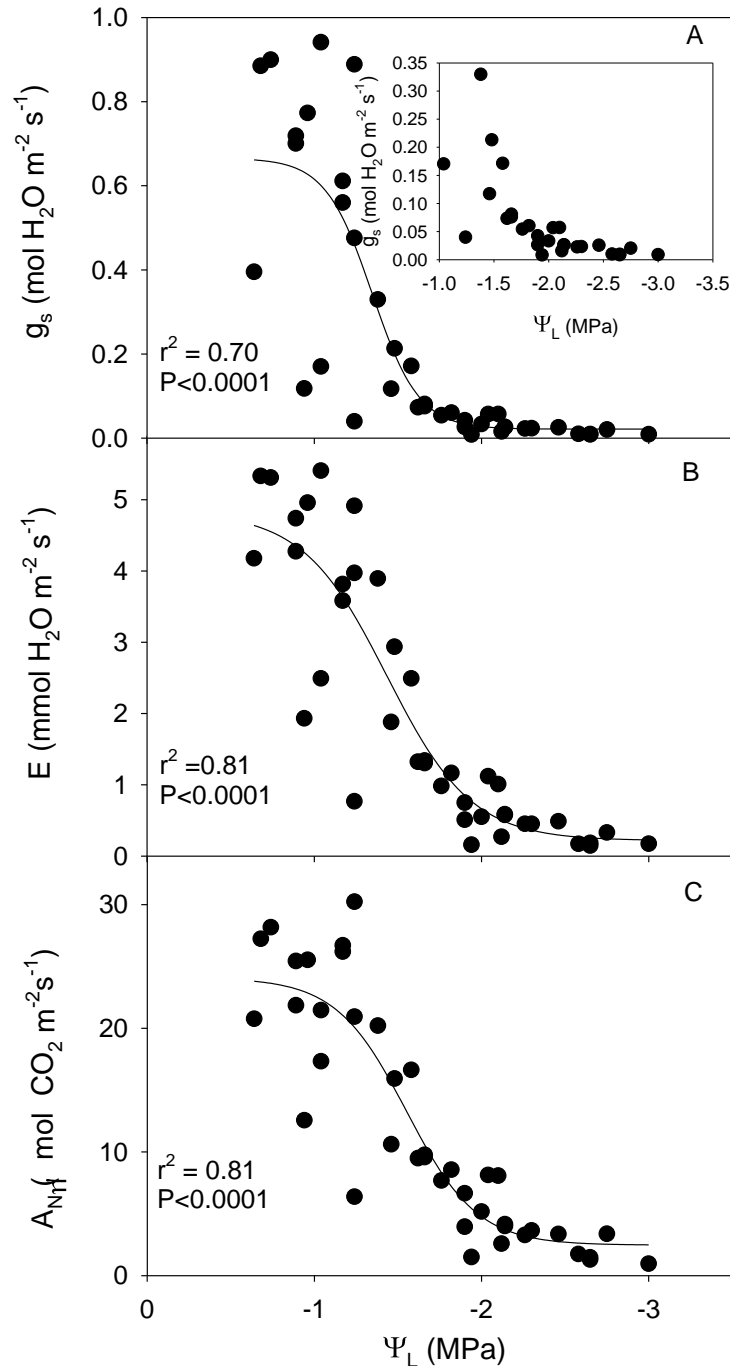

Figure 3: A) Stomatal conductance (g_s), B) leaf transpiration (E) and C) net CO_2 assimilation rates (A_N) vs Ψ_x measured during the drought treatment. Each point corresponds to an individual measurement. The function fitted to data points was $y = y_0 + \dfrac{a}{1+e^{-\left(\frac{x-x_0}{b}\right)}}$

K_{Li} measured in the main stem declined in a linear fashion with Ψ_x (Fig. 4) with a fivefold decrease in K_{Li} measured between the maximum and minimum values determined.
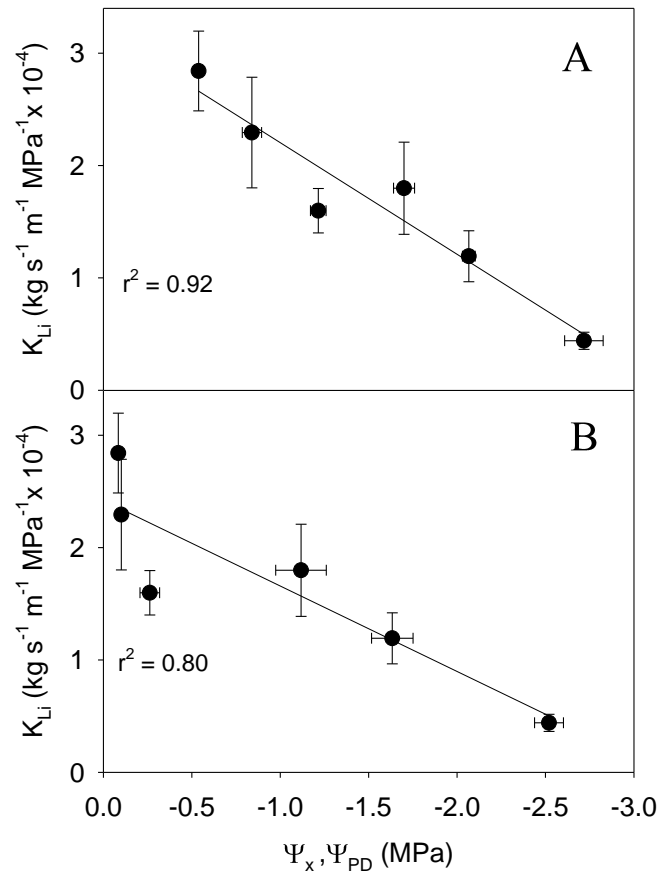

Figure 4: Specific leaf hydraulic conductivity (K_{Li}) *vs.* A) xylem water potential (Ψ_x) and B) pre-dawn water potential (Ψ_{PD}) measured during the drought treatment. Each point is a mean of 7 measurements $\pm$ SE. Function fitted to data is y = mx + n

From these data, cavitation, calculated as percentage of loss of conductivity (PLC) was estimated according to Sperry *et al.* (1988b). When PLC of the stem was plotted *vs.* Ψ_x (Fig. 5a), 50% loss of conductivity (P_{50}) occurred at a Ψ_x of -1.61 MPa and 88% loss of conductivity (P_{88}) occurred at Ψ_x = -2.9 MPa.

High values of K_{Leaf} were observed during the first stages of the experiment (Fig 5b) when Ψ_L was high. This high K_{Leaf} corresponded with high A_N values observed in the first measurement period before plants had been exposed to drought stress. P_{50} of leaves and stems was similar (Fig. 5b), taking into account the differences between stem and leaf water potential which were usually between 0.2 and 0.3 MPa. Although, at values lower than -1.5 MPa leaves experienced a larger PLC with leaf P_{88} equal to -2.19 MPa.
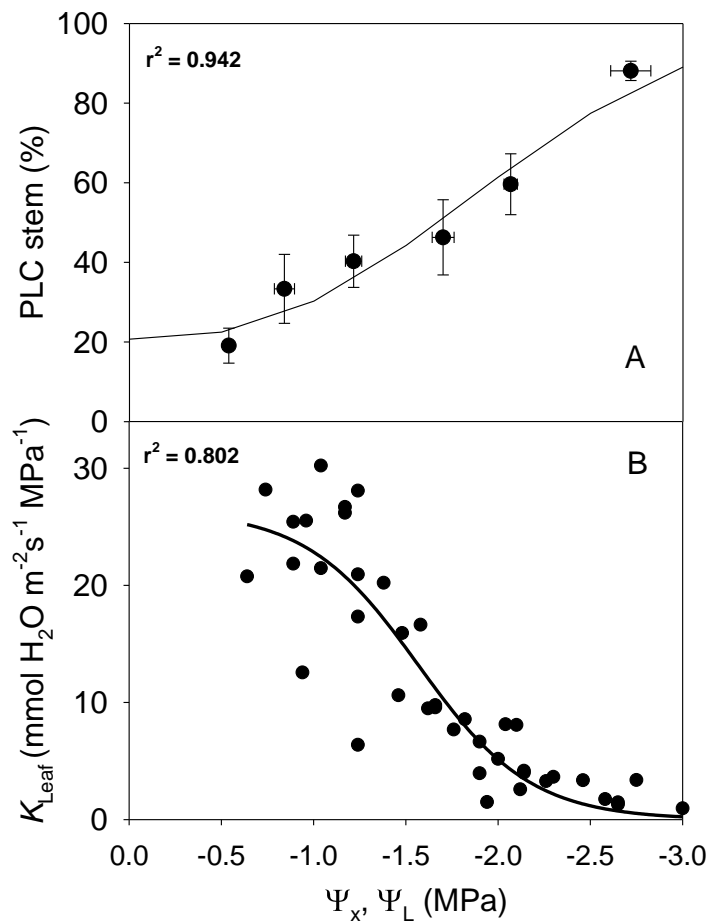

Figure 5: A) percentage of loss of hydraulic conductivity (PLC) as a function of xylem water potential (Ψ_x). Constructed from points shown in Fig. 4. B) Leaf hydraulic conductance as a function of leaf water potential (Ψ_L).

Recovery after irrigation

As a consequence of the 12-fold reduction in g_s, E was significantly depressed in stressed plants relative to controls just prior to re-watering of stressed plants (Fig. 6a and 6b). A_N was also affected by stomatal closure being reduced sevenfold in stressed plants (Fig. 6c), while Ψ_x declined to -2.7 MPa (Fig. 7a). Similarly, K_{Li} had eightfold

lower conductivity (Fig. 7b), corresponding to a PLC of more than 90% (Fig. 7c) and K_{Leaf} have a threefold lower conductivity than control plants.
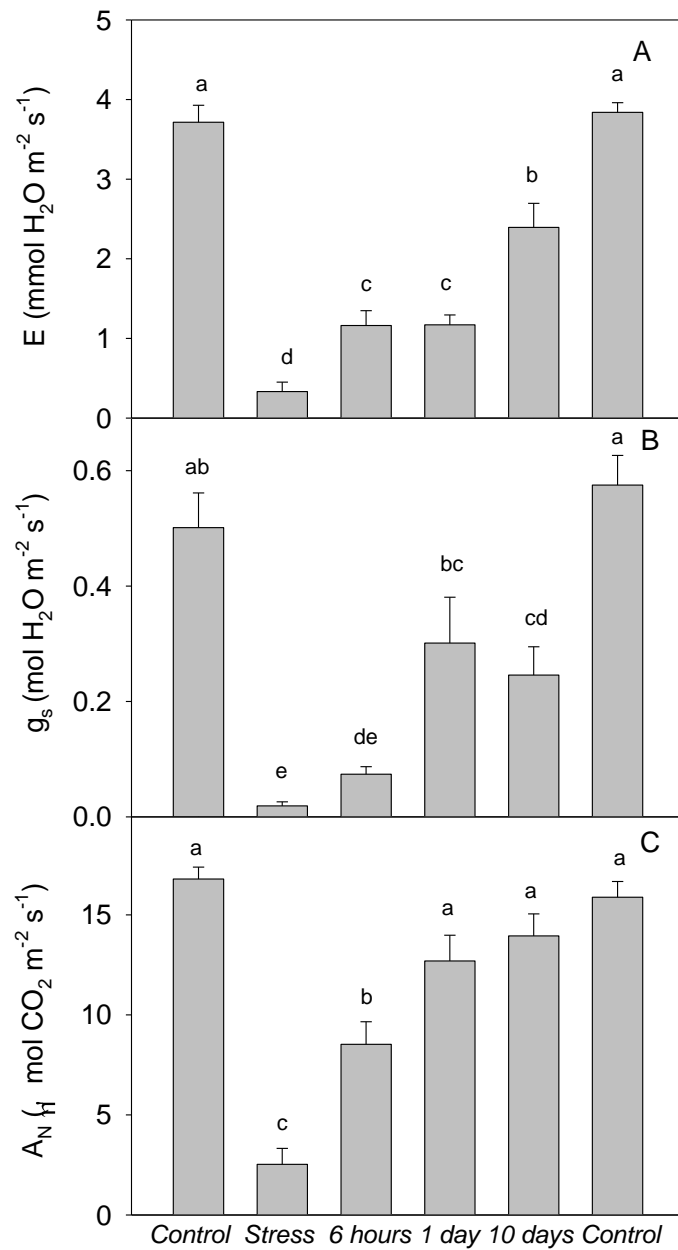

Figure 6: A) Leaf transpiration *(E)*, B) stomatal conductance (g_s) and C) net CO_2 assimilation rate (A_N) at different times after irrigation. Values for control plants are provided for the beginning and end of experiment. Bars are means of 5 samples ± SE.
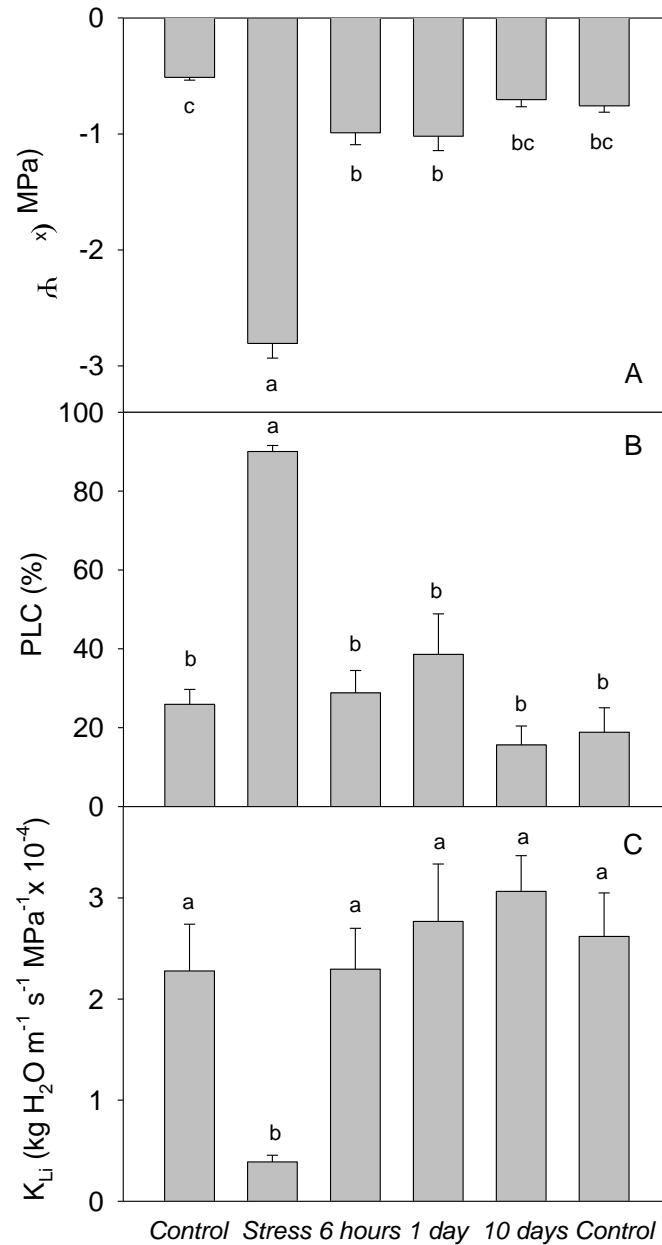
Figure 7: A) Xylem water potential (Ψ_x), B) percentage of loss of hydraulic conductivity (PLC) and C) specific hydraulic conductivity (K_{Li}) at different times after irrigation during water stress recovery experiment. Values for control plants are provided for the beginning and end of experiment. Bars are means of 5 samples ± SE.

Ψ_x recovered to levels close to control values 6 h after applying irrigation, although it was 10 d after irrigation before Ψ_x was equal to control values (Fig. 7a). However, K_{Li} and PLC were fully recovered just six hours after irrigation (Figs. 7a, 7b). That was not the case of E and g_s (Figs. 6a, 6b), which did not reach control values even after 10 d following irrigation. In contrast, A_N of stressed plants was not significantly different from that of control plants 10 d after re-watering.

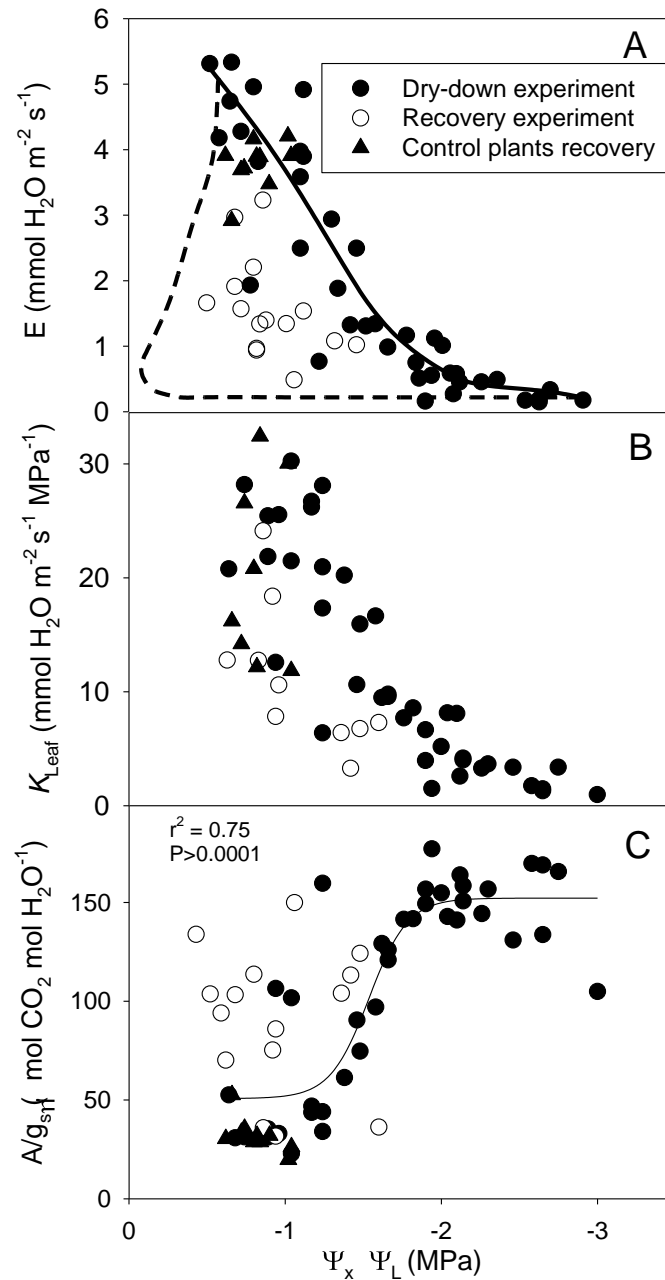**Figure 8**: A) Relationship between leaf transpiration rate (E) and xylem water potential (Ψ_x) during the dry-down (black circles) recovery (white circles) and control plants at recovery (black triangle). Continuous line represents the decrease in E as Ψ_x declined and the dashed line represents the theoretical non-hydraulic limited recovery following the model proposed by Broddrib and Cochard (2009). B) Relationship between leaf hydraulic conductance (K_{Leaf}) and leaf water potential (Ψ_L) during the dry-down (black circles) recovery (white circles) and control plants at recovery. C) Relationship between instantaneous water use efficiency (A_N/g_s) and leaf water potential (Ψ_L) during dry-down (black circles) recovery (white circles) and control plants at recovery (black triangles). A curve was fitted to the dry down data using a sigmoidal function: $y = y_0 + \dfrac{a}{1+e^{-\left(\frac{x-x_0}{b}\right)}}$

During the dry-down experiment E decreased linearly as Ψ_x decreased down to values below -2 MPa (Fig. 8a, black circles). However, during the recovery process a

lower E was measured than previously at each Ψ_x. During these two stages K_{Leaf} exhibited a similar behaviour with lower values during the recovery period than in the dry-down phase for a given Ψ_L (Fig. 8b). No significant differences were found between control and re watered plants after 1 d of rewatering ($P < 0.05$).

Instantaneous water use efficiency (Fig.8c) showed a higher water use efficiency for a given Ψ_L in re watered plants than in control/dry down plants. When A_N was plotted against g_s (Fig.9), it was clear that plants had lower maximum A_N at the end of the experiment and recovery plants were able to maintain the same A_N with a lower water consumption.
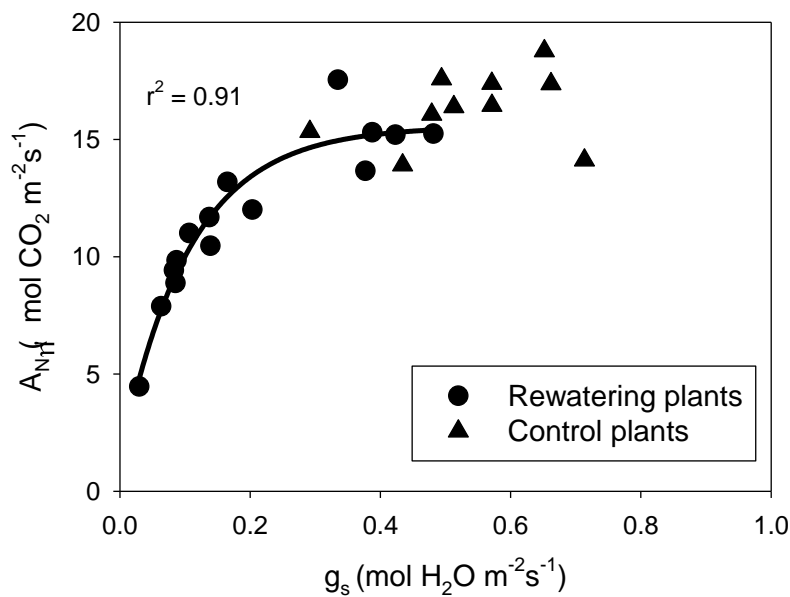
Fig 9. Relationship between net photosynthesis (A_N) and stomatal conductance (g_s) during recovery (black circles) and control plants at recovery stage (black triangles). A curve was fitted to the recovery data using an exponential function: $y = y_0 + a\,(1 - e^{-bx})$

DISCUSSION

We observed close coordination among leaf gas exchange, leaf tissue water relations and the hydraulic capacity of the stem during a dry down of *E. pauciflora* seedlings. Although almost complete hydraulic failure occurred at a Ψ_x of -3.0 MPa, stem hydraulic capacity was rapidly restored upon re-watering. The speed and timing of recovery suggests that xylem vessels were refilled via an active process similar to that suggested by observations of embolism repair in other angiosperm species (Salleo *et al.* 1996; McCully *et al.* 1998; Holbrook *et al.* 2001; Domec *et al.* 2006; Brodersen *et al.*

2010). Recovery of leaf gas exchange lagged behind hydraulic recovery, indicating that stomatal behaviour was influenced by factors other than the supply of water to the stem xylem. These results provide crucial information for understanding how linkages between stem and leaf traits influence the recovery of woody plants from drought.

Stomatal response to drought induced embolism

Leaf turgor loss and stomatal closure thresholds occurred at leaf water potentials just above P_{50} stem water potential, suggesting a protective role for stomatal closure in delaying the occurrence of extensive embolism in the stem (Jones & Sutherland 1991; Sparks & Black 1999). Given that the normal range of water potentials for *E. pauciflora* seedlings growing in the field is between -1.0 and -2.0 MPa (Körner & Cochrane 1985; Cochrane & Slatyer 1988), this species appears to operate close to P_{50} safety margin, as observed for the majority of angiosperm species worldwide (Choat *et al.* 2012). This tight coordination of leaf gas exchange and stem hydraulic traits is thought to be the product of a tradeoff between growth and the risk of extensive xylem cavitation (Tyree & Sperry, 1988; Sperry *et al.* 2002).

Initial rates of g_s and A_N in *E. pauciflora* seedlings were higher than those measured for mature, field grown *Eucalyptus* trees (White, Turner & Galbraith 2000; Merchant *et al.* 2007; Szóta *et al.* 2011), but in line with previous measurements of well watered *Eucalyptus* seedlings (Whitehead & Beadle 2004). As the soil dried, declines in Ψ_{PD} and Ψ_L precipitated a rapid decrease in g_s (Fig. 3A). Stomatal closure and turgor loss points were close to P_{50}, (-1.6 MPa) indicating a high degree of coordination between leaf and stem traits in *E. pauciflora*. In this case, stomatal closure delayed Ψ_x falling below the stem P_{50} threshold, after which there was a steep drop in hydraulic conductivity and a greatly increased risk of hydraulic failure in the main stem. This regulation of Ψ_L and Ψ_x could be described as an isohydric strategy although it is unlikely *Eucalyptus* or other woody species operate in a purely isohydric fashion in the field (Drake & Froend *et al.* 2007; Domec & Johnson 2012).

Previous work on angiosperms suggests that stomatal closure is more closely related to the Ψ_x causing incipient cavitation (P_{12} or P_{25}) than to P_{50} (Sparks & Black, 1999; Cochard *et al.* 2002; Brodribb *et al.* 2003; Meinzer *et al.* 2009). However, the exact PLC at which stomata close is often difficult to determine because many species exhibit native embolism of 10-30% even under well water conditions in the field (Sperry *et al.* 1988a; Pockman & Sperry 2000; Cobb, Choat & Holbrook 2007). It is

likely that these low levels of embolism represent a population of vulnerable vessels that are not easily recoverable via embolism repair mechanisms but do not strongly influence gas exchange on a day to day basis. With this in mind, it is difficult to determine whether stomata are responding directly to cavitation events based on PLC data, which contain some 'memory' of previous water stress. Data from non-destructive techniques such as ultrasonic acoustic emissions (UAE) probes support the theory that stomatal closure begins close to the point of incipient cavitation in the stem (Salleo *et al.* 2000, 2001). Further experiments using non-invasive techniques are required to fully elucidate the relationship between stem cavitation and leaf gas exchange.

Over longer timescales, stomatal closure cannot prevent the decline of xylem water potential to levels that cause extensive embolism in the stem. At xylem water potentials of

 -3.0 MPa, *E. pauciflora* seedlings suffered close to 90% PLC.

Recovery of hydraulic capacity by embolism repair

E. pauciflora seedlings recovered hydraulic capacity rapidly, with K_{Li} returning to control levels within 6 h of re watering. The speed of hydraulic recovery eliminates the possibility that it was achieved by growth of new xylem tissue. Other possibilities include root pressure (Sperry *et al.* 1987; Cobb *et al.* 2007), refilling driven by an active mechanism local to the stem xylem (Salleo *et al.* 1996; McCully *et al*. 1998; Holbrook *et al.* 2001; Domec *et al.* 2006; Brodersen *et al.* 2010) or by passive refilling if the stem xylem reaches water potentials close to zero (Yang & Tyree 1992). No evidence of root pressure was observed in detopped seedling of *E. pauciflora,* consistent with previous studies in which

E. pauciflora plants were detopped after soil flooding (Atwell, Henery & Ball 2009). 'Novel' embolism repair mechanisms that are able to drive vessel refilling while bulk xylem water potential is negative have been observed in a range of angiosperm species (Salleo *et al.* 1996; Hacke & Sperry 2003; Brodersen *et al.* 2010).). It is possible that xylem water potential reached pressures at which dissolution of gas would take place according to Henry's Law. However, the time required for Recent observations suggest that refilling of vessels by this mechanism is delayed in moderately and severely water stressed plants and this delay presumably occurs because of the time necessary to rehydrate living cells involved in the refilling process (Salleo *et al.* 2009; Brodersen *et al.* 2010). It is possible that xylem water potential reached pressures at which

dissolution of gas would take place according to Henry's Law. However, the time required for this mode of refilling is much longer (tens of hours) than the 6 h observed for full recovery in this case.

We observed that around 30% PLC was unrecoverable, similar to the level observed in control plants (Fig. 7b). A residual PLC of 10-30% has been also reported in other studies (Sperry *et al.* 1988a, Pockman & Sperry 2000, Alsina *et al.* 2007) and could be attributed to conduits that the plant is not able to refill. Why these conduits do not refill is an open question but may relate to the structural integrity of these conduits (e. g. permanent damage to pit membranes or secondary cell walls).

Recovery of leaf gas exchange after re-watering

While stem hydraulic capacity was restored within 6 h, g_s and E did not fully recover even after 10 d at favourable water status. Some hysteresis was apparent in the recovery of E as a function of Ψ_x (Fig 8a). If recovery of transpiration was constrained purely by a hydraulic component of the system, no hysteresis would be expected between dry down and recovery segments of the E versus. Ψ_x curve (solid line, Fig 8a) as suggested by Brodribb & Cochard, (2009). The occurrence of hysteresis suggests that both hydraulic and non-hydraulic limitations were involved since K_{Li} and K_{Leaf} recovered within 24 h of re watering (Fig. 7a and 8b) and it is likely that root xylem vessels were also refilled by this point. The other possibility is that non-hydraulic factors continued to limit leaf gas exchange after hydraulic recovery was complete. Lovisolo *et al.* (2008) observed that stomatal conductance was limited after drought in grapevines despite a full recovery of hydraulic conductivity in petioles, stems and roots. These authors suggested that a residual abscisic acid (ABA) signal in the leaf played an important role in the regulation of transpiration during recovery from drought stress. More recently, Brodribb and McAdam (2013) described a similar role for ABA limiting stomatal aperture in *Pinus radiata* during recovery from drought. In this way, recovery of hydraulic conductivity and leaf water potential are promoted by limited stomatal opening after drought.

Although post drought g_s did not reach control values it was close to values observed for eucalypts in field experiments after dry periods (White *et al.* 2000; Merchant *et al.* 2007; Szóta *et al.* 2011). Net assimilation rates had recovered to control values 1 d after re watering. This is consistent with the findings of Kirschbaum (1987, 1988), who observed that mesophyll capacity for photosynthesis in drought *E.*

pauciflora leaves recovered to control levels 24 h after re watering. In the present study, re watered plants had higher intrinsic water-use efficiency than control plants and were thus able to maintain similar A_N as controls for a given g_s (Fig.9). An increase in water use efficiency is often seen in drought acclimated plants (Miyashita *et al.* 2005; Pou *et al.* 2008, 2012). In this case it appears that A_N was saturated with respect to stomatal conductance during the initial phase of the experiment when plants were in a well water condition and had not previously been exposed to drought. The post drought water use efficiency moved stomatal conductance closer to an 'optimum' level relative to photosynthesis.

ACKNOWLEDGMENTS

REFERENCES

Allen, C.D., Macalady, A.K., Chenchouni, H., *et al.* (2010) A global overview of drought and heat-induced tree mortality reveals emerging climate change risks for forests. *Forest ecology and management* **259**, 660-684

Alsina M.M., De Herralde F., Aranda X., Savé R. & Biel C. (2007) Water relations and vulnerability to embolism are not related: experiments with eight grapevine cultivars. *Vitis* **46**, 1-6.

Atwell B.J., Henery M.L. & Ball M.C. (2009) Does soil nitrogen influence growth, water transport and survival of snow gum (Eucalyptus pauciflora Sieber ex Sprengel.) under CO2 enrichment? Plant, Cell & Environment **32**, 553–566.

Begg J.E. & Turner N.C. (1970) Water potential gradients in field tobacco. *Plant Physiology* **46**, 343-346.

Brodersen C., McElrone A.J., Choat B., Lee E.F., Shackel K.A. & Matthews M.A. (2013) In vivo visualizations of drought-induced embolism spread in Vitis vinifera. Plant Physiology **162**, 1–10.

Brodersen C. R., McElrone A. J., Choat B., Matthews M. A. & Shackel K. A. (2010) The dynamics of embolism repair in xylem: in vivo visualizations using high-resolution computed tomography. *Plant Physiology* **154**, 1088-1095.

Brodribb T. J. & Cochard H. (2009) Hydraulic failure defines the recovery and point of death in water-stressed conifers. *Plant Physiology* **149**, 575-584.

Brodribb T.J. & McAdam S.A.M. (2013) ABA mediates a divergence in the drought response of two conifers. Plant Physiology **162**, 1370-1377.

Brodribb T.J., Holbrook N.M., Edwards E.J. & Gutierrez M.V. (2003) Relations between stomatal closure, leaf turgor and xylem vulnerability in eight tropical dry forest trees. Plant, Cell & Environment **26**, 443–450.

Brodribb T. J., Bowman D. J. M. S., Nichols S., Delzon S. & Burlett R. (2010) Xylem function and growth rate interact to determine recovery rates after exposure to extreme water deficit. *New Phytologist* **188**, 533-542.

Canny M.J. (1997) Vessel contents during transpiration: embolisms and refilling. *American Journal of Botany* **84**, 1223-1230.

Chen J. W., Zhang Q., Li X. S. & Cao K. F. (2010) Gas exchange and hydraulics in seedlings of *Hevea brasiliensis* during water stress and recovery. *Tree Physiology* **30**, 876-885

Choat, B. (2013). Predicting thresholds of drought-induced mortality in woody plant species. *Tree physiology* **33**, 669-671

Choat B., Sack L. & Holbrook N. M. (2007) Diversity of hydraulic traits in nine Cordia species growing in tropical forests with contrasting precipitation. *New Phytologist* **175**, 686-698

Choat B., Cobb A.R. & Jansen S. (2008) Structure and function of bordered pits: new discoveries and impacts on whole-plant hydraulic function. *New Phytologist* **177**, 608-626

Choat B., Jansen S., Brodribb T. J., *et al*. (2012) Global convergence in the vulnerability of forests to drought. *Nature* **491**, 752–755

Ciais P., M. Reichstein N., Viovy A., *et al*. (2005) Europe-wide reduction in primary productivity caused by the heat and drought in 2003. *Nature* **472**, 529-533

Cobb A. R., Choat B. & Holbrook, N. M. (2007) Dynamics of freeze-thaw embolism in *Smilax rotundifolia* (Smilacaceae). *American Journal of Botany* **94**, 640-649

Cochard H., Coll L., Le Roux X. & Améglio T. (2002) Unraveling the effects of plant hydraulics on stomatal closure during water stress in walnut. *Plant Physiology* **128**, 282-290.

Cochrane P. M. & Slatyer R. O. (1988) Water relations of *Eucalyptus pauciflora* near the alpine tree line in winter. *Tree Physiology* **4**, 45-52.

Domec J.C. & Johnson D. (2012) Does homeostasis or disturbance of homeostasis in minimum leaf water potential explain the isohydric vs. anisohydric behavior of *Vitis vinifera* L. cultivars? *Tree Physiology* **32**, 245-248

Domec J.C., Scholz F.G., Bucci S.J., Meinzer F.C., Goldstein G. & Villalobos-Vega R. (2006) Diurnal and seasonal variation in root xylem embolism in neotropical savanna woody species: impact on stomatal control of plant water status. *Plant, Cell & Environment* **29**, 26-35.

Engelbrecht B.M.J., Comita L.S., Condit R., Kursar T.A., Tyree M.T., Turner B.L. & Hubbell S.P. (2007) Drought sensitivity shapes species distribution patterns in tropical forests. *Nature* **447**, 80-82.

Franks P.J., Drake P.L. & Froend R.H. (2007) Anisohydric but isohydrodynamic: seasonally constant plant water potential gradient explained by a stomatal control mechanism incorporating variable plant hydraulic conductance. *Plant, Cell & Environment* **30**, 19-30

Hacke U.G. & Sperry J.S. 2003. Limits to xylem refilling under negative pressure in *Laurus nobilis* and *Acer negundo*. *Plant, Cell & Environment* 26, 303-311.

Holbrook N. M. & Zwieniecki M. A. (1999) Embolism repair and xylem tension: do we need a miracle? *Plant Physiology* **120**, 7-10.

Holbrook N.M., Ahrens E.T., Burns M.J. & Zwieniecki M.A. (2001) In vivo observation of cavitation and embolism repair using magnetic resonance imaging. *Plant Physiology* **126**, 27-31

Jones H.G. & Sutherland R.A. (1991) Stomatal control of xylem embolism. *Plant, Cell & Environment* **14**, 607-612.

Kaufmann I., Schulze-Till T., Schneider H.U., Zimmermann U., Jakob P. & Wegner, L.H. (2009) Functional repair of embolized vessels in maize roots after temporal drought stress, as demonstrated by magnetic resonance imaging. *New Phytologist* **184**, 245-256

Kirschbaum, M. U. F. (1987) Water stress in *Eucalyptus pauciflora*: comparison of effects on stomatal conductance with effects on the mesophyll capacity for photosynthesis, and investigation of a possible involvement of photoinhibition. *Planta* **171**, 466-473.

Kirschbaum, M. U. F. (1988) Recovery of photosynthesis from water stress in Eucalyptus pauciflora—a process in two stages. *Plant, Cell & Environment* **11**, 685-694.

Körner, C. & Cochrane, P.M. (1985) Stomatal responses and water relations of *Eucalyptus pauciflora* in summer along an elevation gradient. *Oecologia* **66**, 443-455.

Kursar T.A., Engelbrecht B.M.J., Burke A., Tyree M.T., EI Omari B. & Giraldo J.P. (2009) Tolerance to low leaf water status of tropical tree seedlings is related to drought performance and distribution. *Functional Ecology* **23**, 93-102.

Lovisolo C., Perrone I., Hartung W. & Schubert A. (2008) An abscisic acid-related reduced transpiration promotes gradual embolism repair when grapevines are rehydrated after drought. *New Phytologist* **180**, 642-651

McCully M.E., Huang C.X. & Ling L.E.C. (1998) Daily embolism and refilling of xylem vessels in the roots of field-grown maize. *New Phytologist* **138**, 327-342.

Meinzer F.C., Johnson D.M., Lachenbruch B., McCulloh K.A. & Woodruff D.R. (2009) Xylem hydraulic safety margins in woody plants: coordination of stomatal control of xylem tension with hydraulic capacitance. *Functional Ecology* **23**, 922-930.

Merchant A., Callister S.K., Arndt M., Tausz M., & Adams M.A. (2007). Contrasting physiological responses of six Eucalyptus species to water deficit. *Annals of Botany* **100**, 1507-1515.

Miyashita K., Tanakamaru S., Maitani T., & Kimura K. (2005) Recovery responses of photosynthesis, transpiration, and stomatal conductance in kidney bean following drought stress. *Environmental and Experimental Botany* **53**, 205-214

Nardini A. & Salleo S. (2000) Limitation of stomatal conductance by hydraulic traits: sensing or preventing xylem cavitation? Trees, Structure and Function **15**, 14-24

Nardini A., Lo Gullo M.A. & Salleo S. (2011) Refilling embolised xylem conduits: is it a matter of phloem unloading? *New Phytologist* **138**, 327-342.

Phillips, O. L., Aragao L.E.O.C., Lewis S.L., *et al.* (2009) Drought sensitivity of the Amazon rainforest. *Science* **323**, 1344-1347

Pockman W.T. & Sperry J.S. (2000) Vulnerability to cavitation and the distribution of Sonoran desert vegetation. *American Journal of Botany* **87**, 1287-1299

Pou A., Flexas J., Alsina M.M., *et al.* (2008) Adjustments of water-use efficiency by stomatal regulation during drought and recovery in the drought-adapted *Vitis* hybrid Richter-110 (*V. berlandieri V. rupestris*). *Physiologia Plantarum* **134**, 313-323.

Pou A., Medrano H., Tomàs M., Martorell S., Ribas-Carbó M. & Flexas J. (2012) Anisohydric behaviour in grapevines results in better performance under moderate water stress and recovery than isohydric behavior. *Plant and Soil* **359**, 335-349

Resco V., Ewers B.E., Sun W., Huxman T.E., Weltzin J.F. & Williams D.G. (2009) Drought induced hydraulic limitations constrain leaf gas exchange recovery from drought after precipitation pulses in the C3 woody legume, *Prosopis velutina*. *New Phytologist* **181**, 672-682.

Salleo S., Lo Gullo M. A., De Paoli D. & Zippo M. (1996) Xylem recovery from cavitation-induced embolism in young plants of *Laurus nobilis*: a possible mechanism. *New Phytologist* **132**, 47-56

Salleo S., Nardini A., Pitt F. & Lo Gullo M.A. (2000) Xylem cavitation and hydraulic control of stomatal conductance in Laurel (*Laurus nobilis* L.) *Plant, Cell & Environment* **23**, 71-79

Salleo S., Lo Gullo M.A., Raimondo F. & Nardini A. (2001) Vulnerability to cavitation of leaf minor veins: any impact on leaf gas exchange? *Plant, Cell and Environment* **24**, 851-859.

Salleo S., Trifilo P., Esposito S., Nardini A., Lo Gullo M.A. (2009) Starch to sugar conversion in wood parenchyma of field-growing *Laurus nobilis* plants: a component of the signal pathway for embolism repair? *Functional Plant Biology* **36**, 815-825

Sparks, J.P. & Black R.A. (1999) Regulation of water loss in populations of *Populus trichocarpa*: the role of stomatal control in preventing xylem cavitation. *Tree Physiology* **19**, 453-459.

Sperry J.S., Holbrook N.M., Zimmermann M.H. & Tyree M.T. (1987) Spring filling of xylem vessels in wild grapevine. *Plant Physiology* **83**, 414-417.

Sperry J.S., Donnelly J.R. & Tyree M.T. (1988a) Seasonal occurrence of xylem embolism in sugar maple (*Acer saccharum*). *American Journal of Botany* **75**, 1212-1218.

Sperry J.S., Donnelly J.R. & Tyree M.T. (1988b) A method for measuring hydraulic conductivity and embolism in xylem. *Plant, Cell & Environment* **11**, 35-40

Sperry J.S., Hacke U.G., Oren R. & Comstock J.C. (2002) Water deficits and hydraulic limits to leaf water supply. *Plant, Cell and Environment* **25**, 251-263

Stiller V., Sperry J.S. & Lafitte R. (2005) Embolized conduits of rice (*Oryza sativa*, Poaceae) refill despite negative xylem pressure. *American Journal of Botany* **92**, 1970-1974.

Szóta C., Farrell C., Koch J. M., Lambers H. & Veneklaas E. J. (2011) Contrasting physiological responses of two co-occurring eucalypts to seasonal drought at restored bauxite mine sites. *Tree Physiology* **31**, 1052-1066

Tyree M.T. & Sperry J.S. (1988) Do woody plants operate near the point of catastrophic xylem dysfunction caused by dynamic water stress? Answers from a model. *Plant Physiology* **88**, 574-580.

Tyree M.T. & Sperry J.S. (1989) Characterization and propagation of acoustic emission signals in woody plants: towards an improved acoustic emission counter. *Plant, Cell & Environment* **12**, 371-382.

Tyree M.T., Salleo S., Nardini A., Lo Gullo M.A. & Mosca R. (1999) Refilling of embolized vessels in young stems of laurel. Do we need a new paradigm? *Plant Physiology* **120**, 11-22

Urli, M., Porte A., Cochard H., Guengant Y., Burlett R. & Delzon S. (2013) Xylem embolism threshold for catastrophic hydraulic failure in angiosperm trees. *Tree Physiology* **33**, 672-683.

Wheeler J. K., Huggett B.A., Tofte A.N., Rockwell F.E. & Holbrook M. (2013) Cutting xylem under tension or supersaturated with gas can generate PLC and the appearance of rapid recovery from embolism. *Plant, Cell & Environment* **36**, 1938-1949

White D.A., Turner N.C. & Galbraith, J.H. (2000) Leaf water relations and stomatal behaviour of four allopatric Eucalyptus species in Mediterranean south-western Australia. *Tree Physiology* **20**, 1157-1165.

Whitehead D. & Beadle C.L. (2004) Physiological regulation of productivity and water use in *Eucalyptus*: a review. *Forest Ecology and Management* **193**, 113-140

Yang S. & Tyree M.T. (1992) A theoretical model of hydraulic conductivity recovery from embolism with comparison to experimental data on Acer saccharum. Plant, Cell & Environment **15**, 633–643.

Zhao M. & Running S. W. (2010) Drought-induced reduction in global terrestrial net primary production from 2000 through 2009. *Science* **329**, 940-943

Zimmermann M.H. (1983) Xylem Structure and the Ascent of Sap. Springer-Verlag, New York, NY,USA.

Zwieniecki M.A. & Holbrook N.M. (1998) Diurnal variation in xylem hydraulic conductivity in white ash (*Fraxinus americana L.*), red maple (*Acer rubrum L.*) and red spruce (*Picea rubens Sarg.*). *Plant, Cell & Environment* **21**, 1173-1180.

Zwieniecki M.A. & Holbrook N.M. (2009) Confronting Maxwell's demon: biophysics of xylem embolism repair. *Trends in Plant Science* **14**, 530-534

3.2. Plasticity of vulnerability to leaf hydraulic dysfunction during acclimation to drought in grapevines: an osmotic-mediated process

Martorell S[1], Medrano H[1], Tomàs M[1], Escalona J.M[1], Flexas J[1], Díaz-Espejo A[2,*]

[1]Research Group on Plant Biology under Mediterranean Conditions, Departament de Biologia, Universitat de les Illes Balears, Carretera de Valldemossa Km 7.5, 07122 Palma de Mallorca, Illes Balears, Spain;

[2]Irrigation and Crop Ecophysiology Group, Instituto de Recursos Naturales y Agrobiología de Sevilla (IRNAS, CSIC). Avenida Reina Mercedes 10, 41012 Sevilla, Spain

ABSTRACT

Previous studies have reported correlation of leaf hydraulic vulnerability with pressure-volume parameters related to cell turgor. This link has been explained on the basis of the effects of turgor on connectivity among cells and tissue structural integrity, which affect leaf water transport. In this study, we tested the hypothesis that osmotic adjustment to water stress would shift the leaf vulnerability curve towards more negative water potential ($\mathit{\Psi}_{\text{leaf}}$) by increasing turgor at low $\mathit{\Psi}_{\text{leaf}}$. We measured leaf hydraulic conductance (K_{leaf}), K_{leaf} vulnerability (P_{50} and P_{80}; $|\mathit{\Psi}_{\text{leaf}}|$ at 50 and 80% loss of K_{leaf}, respectively) bulk leaf water relations, leaf gas exchange and sap flow in two *Vitis vinifera* cultivars (Tempranillo and Grenache), under two water treatments. We found that P_{50}, P_{80}, and maximum K_{leaf} decreased seasonally by more than 20% in both cultivars and watering treatments. However, K_{leaf} at -2 MPa increased 3-fold, while osmotic potential at full turgor and turgor loss point decreased. Our results indicate that leaf resistance to hydraulic dysfunction is seasonally plastic, and this plasticity may be mediated by osmotic adjustment.

Key words:

Abbreviations:

g_s, stomatal conductance; K_{leaf}, leaf hydraulic conductance; $K_{\text{leaf,max}}$, maximum leaf hydraulic conductance; P_{50}, 50% loss of hydraulic conductance; P_{80}, 80% loss of hydraulic conductance;

RWC_{TLP}, relative water content at turgor loss point; $\Delta\Psi$, difference between predawn and midday water potentials; $\mathit{\Psi}_{\text{md}}$, midday leaf water potential; $\mathit{\Psi}_{\text{pd}}$, predawn water potential; $\mathit{\Psi}_{\pi,\text{FT}}$, osmotic potential at full turgor; $\mathit{\Psi}_{\pi,\text{TLP}}$, osmotic potential at turgor loss point; ε, modulus of elasticity.

INTRODUCTION

The ability of plants to draw water from soil to leaves depends on hydraulic conductance, which is therefore an important limitation to leaf gas exchange (Meinzer and Grantz 1990, Hubbard *et al.* 2001, Sperry *et al.* 2002, Martorell *et al.* 2014). A significant part of whole-plant hydraulic resistance occurs in leaves, commonly up to 30% (Sack *et al.* 2003; Sack and Holbrook 2006), and perhaps as high as 80% (Sack

and Holbrook 2006). As a consequence, leaf hydraulic conductance (K_{leaf}) is considered a hydraulic bottleneck, and is now understood to play a pivotal role in the control of transpiration (Nardini and Salleo 2000, Brodribb *et al.* 2005, Sack and Tyree 2005). This has stimulated much research on acclimation of K_{leaf} to changing environmental conditions, including temperature (Sellin and Kupper 2007), light (Sack *et al.* 2002, Voicu *et al.* 2008) and dehydration (Brodribb and Holbrook 2003, Guyot *et al.* 2012, Scoffoni *et al.* 2012).

One important aspect of K_{leaf} responses to environment is the decline of K_{leaf} with leaf water status during dehydration, which can result from either cavitation or collapse of xylem conduits (Johnson *et al.* 2009, 2012, Brodribb and Holbrook 2005) or a reduction in the permeability of extra-xylary tissues (Sack and Holbrook 2006, Pou *et al.* 2013). Which of these components is more limiting to water flow is a matter of debate, and the answer varies among species (Sack *et al.* 2004, Nardini *et al.* 2005, Charra-Vaskou *et al.* 2012). There is some consensus that the hydraulic resistance of leaf xylem might be similar in magnitude to the resistance of the extra-xylary pathways (Sack and Holbrook 2006). However, recently Scoffoni *et al.* (2014) reported that the extra-xylary pathway may be more vulnerable than the xylem pathway, thereby delaying the onset of xylem embolism or collapse in leaf veins. Whatever the cause, reduced K_{leaf} under water stress represents an important limitation to plant productivity worldwide, impacting both species distribution (Engelbrecht *et al.* 2007, Choat *et al.* 2012) and agriculture (McElrone *et al.* 2012). Understanding what controls K_{leaf} vulnerability is particularly important for improving crop water use efficiency in the face of climate change (Fereres and Soriano 2007, Ruiz-Sánchez *et al.* 2010).

Grapevine is one of the most extensively cultivated and economically important crops in the world. However, most studies on hydraulic conductance of grapevine have focused on stems (Shultz 2003, Alsina *et al.* 2007, Lovisolo *et al.* 2008, Choat *et al.* 2010, Brodersen *et al.* 2010, 2013) and fewer studies have focused on petioles (Lovisolo *et al.* 2008, Zufferey *et al.* 2011) or leaves (Choat *et al.* 2009, Pou *et al.* 2012, 2013). As a result, the impact of water stress on K_{leaf} in grapevine – and particularly the extra-xylary component – is not well understood. Extra-xylar water flow in grapevine may involve either of two routes in parallel: an apoplastic route through cell walls or a symplastic cell-to-cell route across one or more cell membranes, involving PIP aquaporins (Cochard *et al.* 2007). Both pathways have been reported to depend on

turgor pressure. One mechanism for this dependence is the loss of hydraulic connectivity between cells that occurs when cells shrink during dehydration (Sancho-Knapik *et al.* 2011, Scoffoni *et al.* 2012, Scoffoni *et al.* 2014). Another is the putative regulation of aquaporin activity in relation to cell turgor pressure (Kim and Steudle 2007, Cochard *et al*. 2007). Active osmotic adjustment during acclimation to drought could ameliorate either of these effects by reducing the turgor loss point to more negative water potentials.

The objective of this study was to test the hypothesis that osmotic adjustment during drought reduces K_{leaf} vulnerability in grapevine. We examined K_{leaf} variations along the growing season in well watered and water-stressed vines of two cultivars with contrasting drought tolerance.

MATERIAL AND METHODS

Plant material and experimental conditions

The experiment was conducted in the experimental field of the University of Balearic Islands during summer 2012 on two cultivars of grapevine (*Vitis vinifera* L.) var. Tempranillo and Grenache (the last reputed to be more drought tolerant). Climatic conditions were typical of the Mediterranean area and consisted of an average temperature of 25.2 ºC for the experimental period (June 1th to 30th August), ranging from a maximum of 37.3ºC in August to a minimum 13.4ºC in June. During this period mean relative humidity was 58% and average PPFD at noon 1700 μmol m^{-2} s^{-1}. Soil was a clay loam type 1.5 m deep. Plants were 3-year-old grafted on rootstock Richter-110 and planted in rows (distance between rows was 2.5 m and plants 1 m). They were conducted in a bilateral double cordon having between 10-12 canes per plant. Two treatments were applied: well watered (WW), in which enough water was supplied to replenish average daily water loss, as described in Medrano *et al*. (2012), and water stressed (WS), in which irrigation was withheld for the entire summer. The total rainfall over the three months of the experiment was 0.4 mm.

Leaf water relations

Midday leaf water potential (Ψ_{md}, measured at noon) and predawn water potential (Ψ_{pd}, measured just before sunrise) were measured monthly (on 26 June, 26 July and 27

August) with a pressure chamber (Soil Moisture Equipment Corp. Santa Barbara, CA, USA). Four replicates per treatment and cultivar were measured.

Leaf hydraulic conductance

Leaf hydraulic conductance (K_{leaf}) was measured using the leaf rehydration kinetics method described by Brodribb and Holbrook (2003):

$$K_{leaf} = C_{bulk} \ln[\Psi_o/\Psi_f]/t \quad (1),$$

where C_{bulk} is the leaf capacitance, Ψ_o is initial water potential, Ψ_f is final water potential after rehydration and t is time since rehydration began. Leaf vulnerability curves and pressure-volume curves were measured monthly, in conjunction with water potential measurements described above. Sunlit exposed shoots 1.5 to 2.5 meters long were collected in the afternoon, cut under water and wrapped with parafilm at the cut surface. Once in the laboratory, samples were re-cut under water (Wheeler *et al.* 2013) and left to rehydrate overnight. On the following morning stems were cut in portions containing three leaves and were allowed to desiccate slowly at light intensities sufficient to ensure light-induced hydraulic function (ca 50 μmol quanta m^{-2}s^{-1}). The stem portions were dehydrated to varying degrees, including low enough Ψ_{leaf} to cause 100% loss of K_{leaf}. Stem sections with leaves were equilibrates in sealed plastic bags for two hours before measurement, after which two leaves of the same branch were measured for initial Ψ_{leaf} (Ψ_o). If the difference between those two leaves was more than 0.1 MPa the sample was discarded. The remaining leaf was rehydrated for 30 seconds and final water potential (Ψ_f) was measured. A rehydration time of 30 seconds was chosen based on preliminary rehydration curves on different leaves attached at the same plant stem. Measurements were performed in different ranges of water stress and showed that 30 seconds of leaf rehydration was enough. Curves were constructed with a number of replicates between 31 and 59.

Pressure volume (P-V) curves

Pressure volume curves were measured simultaneously with vulnerability curves, to obtain leaf turgor loss point, osmotic adjustment and leaf capacitance using five replicates per treatment (Tyree and Hammel 1972). Leaves were collected the evening before measurements and rehydrated overnight before P-V determination. During the

dehydration of leaves in the laboratory, leaf water potential was periodically measured with a pressure chamber (Soil moisture Equipment. Corp. Santa Barbara, CA, USA) and leaf weight was measured with an analytical balance (Kern ABT320-4M, 10^{-4} g resolution). The turgor loss point was identified as the inflection point of the $1/\Psi_{leaf}$ versus relative water content (RWC) curve. Mean cell modulus of elasticity (ε) was estimated as the slope of turgor potential (Ψ_p) versus RWC through the phase from full turgor to turgor loss point. The fitting method proposed by Sack and Pasquet-Kok (2011) was used to fit the P-V curves. This method fits lines by the standard major axis (Model II regression) so that either variable can be predicted from the other and the parameter calculation is more robust.

Bulk leaf capacitance (C_{bulk}, mol m^{-2} MPa^{-1}) was estimated according to Blackman and Brodribb (2011) as follows:

$$C_{bulk}= \delta RWC/\delta \Psi_{leaf} * (DW/LA)*(WWL/DW)/M \quad (2),$$

Where DW is leaf dry weight (g), LA is leaf area (m^2), WWL is mass of leaf water at RWC = 1.0 (g) and M is the molar mass of water. C_{bulk} was determined from the slopes of linear regressions fitted to data on either side of the inflection point in $1/\Psi_{leaf}$ vs RWC from P-V curves data. These pre-and post-turgor loss slopes were averaged for each treatment and sampling time to get a representative value for each treatment and cultivar. Ratios of DW/LA and WWL/DW were measured for each cultivar and treatment at the different sampling times mentioned above in ten replicates per cultivar and treatment. The average value of capacitance on either side of the inflection point in $1/\Psi_{leaf}$ vs RWC was used in the estimation of K_{leaf} data.

Leaf gas exchange measurements

Leaf gas exchange was measured using a portable open flow gas exchange system (Li-6400; Li-Cor, Inc. Nebraska, USA) equipped with a clear chamber (Li-6400-08). Measurements were made at ambient air temperature and PPFD and CO_2 concentration of 400 µmol mol^{-1}. Diurnal time courses of stomatal conductance (g_s) were measured in June, July and August in mature leaves. Five replicates per treatment were measured hourly.

Sap flow measurements

Sap flow was measured by the stem heat balance method using the standard Sap Flow meter P 4.1 from Environmental Measuring Systems (EMS, Brno, Czech Republic), with the same protocol as described in Escalona *et al.* (2002). The mass flow of sap was estimated from the balance of heat fluxes into and out of the heated section of the stem (Sakuratani 1981, Baker and Bavel 1987). Sensors were insulated with 2 cm thick open-porous polyurethane foam and protected from radiation with aluminum foil. Four stem gauges were installed for each treatment and cultivar. Leaf area of each stem was measured at the end of the experiment using a digital camera (Olympus digital camera, SP800UZ) and the images analyzed using Image J (http://imagej.nih.gov/ij/). Sap flow measurements were expressed on a leaf area basis.

Statistical analysis

Statistical differences between treatment means were calculated using analysis of variance (ANOVA), and significant effects were followed up using post hoc multiple comparison tests of Duncan ($p<0.05$). Dixon tests were applied to K_{leaf} data to identify possible outliers. Statistical analyses were performed in SPSS 19.0 (IBM Corp. Armonk, NY, USA). To clarify the differences between sampling dates, K_{leaf} data were grouped into bins by water potential, each with a range of 0.3 to 0.5 MPa and 3 to 8 measurements. For statistical prediction, sigmoidal curves ($y = y_0 + \frac{a}{1+e^{-\left(\frac{x-x_0}{b}\right)}}$) were fitted through non-grouped K_{leaf} vs Ψ_{leaf} data using SigmaPlot 8.0 (Systat Software, Chicago, IL, USA) as has been reported in other studies (Johnson et al., 2012; Scoffoni et al., 2012) .

RESULTS

Seasonal changes in K_{leaf}

Maximum K_{leaf} ($K_{leaf,max}$) declined over the summer, and the water potential causing 50% and 80% loss of K_{leaf} (P_{50} and P_{80}, respectively) became more negative as the summer progressed, indicating a progressive decrease in hydraulic vulnerability to dysfunction (Fig. 1, Table 1).
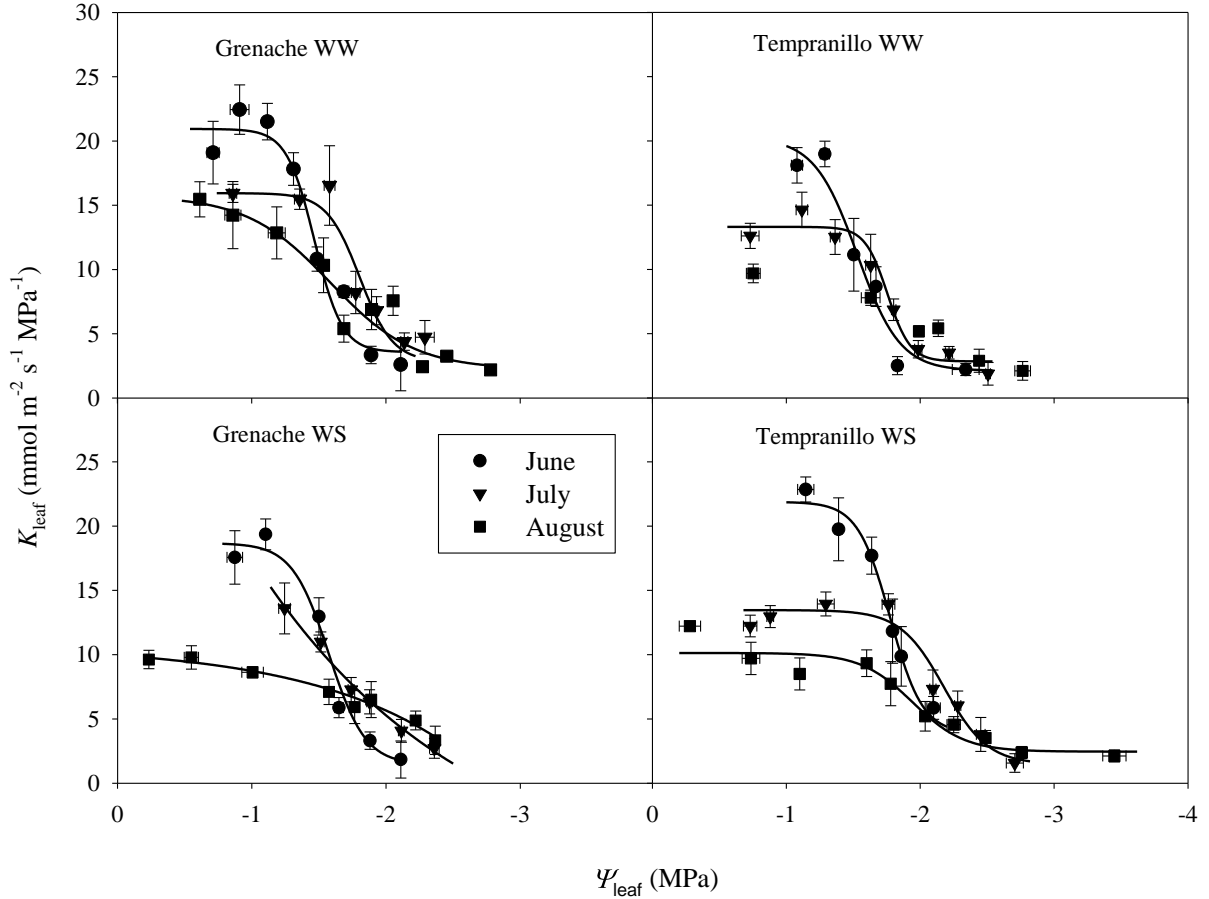
Figure 1. Vulnerability curves for both cultivars and water treatments in June, July and August. Lines correspond to the sigmoidal curve: $y = y_0 + \dfrac{a}{1+e^{-\left(\frac{x-x_0}{b}\right)}}$ fitted to individual measurements of K_{leaf}. Data were binned in this case to clarify the differences between different months. Each point represents the average of at least 3 measurements. Vertical bars represent $\pm$ SE.

$K_{\text{leaf,max}}$ declined in both cultivars and watering treatments, with the exception of Grenache WW, in which $K_{\text{leaf,max}}$ was similar in July and August. $K_{\text{leaf,max}}$ was similar between cultivars. As the percentage loss of conductance at a given Ψ_{leaf} can be misinterpreted when $K_{\text{leaf,max}}$ does not remain constant, we also analyzed the seasonal progression of K_{leaf} at a reference Ψ_{leaf} of -2 MPa (Fig. 2). K_{leaf} at -2 MPa increased as summer progressed in both cultivars and water treatments, by up to 200% (Fig. 2). This trend in K_{leaf} at -2 MPa was also found at other reference Ψ_{leaf} values like -1.8 MPa or -2.3 MPa. However, only at -2 MPa we were able to get enough points of both cultivars and water treatments and all three dates to make a reliable and robust comparison among them.

Table 1: Seasonal progression of leaf water potential inducing 50% loss of leaf hydraulic conductance (P_{50}, MPa) and 80% (P_{80}, MPa), and maximum leaf hydraulic conductance ($K_{leaf,max}$, mmol m^{-2} s^{-1}MPa^{-1}). The coefficient of regression (r^2) from the sigmoidal fits is also shown. WW= well water treatment and WS= water stress treatment. Regular letters indicate seasonal differences and capital letters differences between cultivars in $K_{leaf,max}$ data (P<0.05).

	June				July				August			
	r^2	P_{50}	P_{80}	$K_{leaf,max}$	r^2	P_{50}	P_{80}	$K_{leaf,max}$	r^2	P_{50}	P_{80}	$K_{leaf,max}$
Grenache WW	0.77	-1.51	-1.81	20.93[a,A]	0.77	-1.86	-2.22	15.94[b,B]	0.65	-1.71	-2.43	15.35[b,B]
Grenache WS	0.62	-1.60	-1.83	18.62[a,A]	0.64	-1.75	-2.28	15.26[b,B]	0.53	-2.15	-2.59	9.78[c,C]
Tempranillo WW	0.49	-1.58	-1.87	19.60[a,A]	0.76	-1.81	-2.54	13.31[b,B]	0.79	-2.09	-2.86	9.82[c,C]
Tempranillo WS	0.54	-1.83	-2.20	21.85[a,A]	0.65	-2.22	-2.53	13.47[b,B]	0.69	-2.07	-3.07	10.13[b,C]

K_{leaf} and leaf water relations

Leaf water potential at mid-day (Ψ_{md}) and pre-dawn (Ψ_{pd}) declined along the summer (Table 2). Water stress reduced Ψ_{pd} in August to a minimum of -0.85 MPa in Grenache and -0.53 MPa in Tempranillo. A similar pattern was observed in Ψ_{md}, which reached -1.88 MPa in Grenache and -1.64 MPa in Tempranillo. As a result, $\Delta\Psi (= \Psi_{pd} - \Psi_{md})$ was relatively constant along the season for both cultivars and treatments, with slightly larger values in Tempranillo.
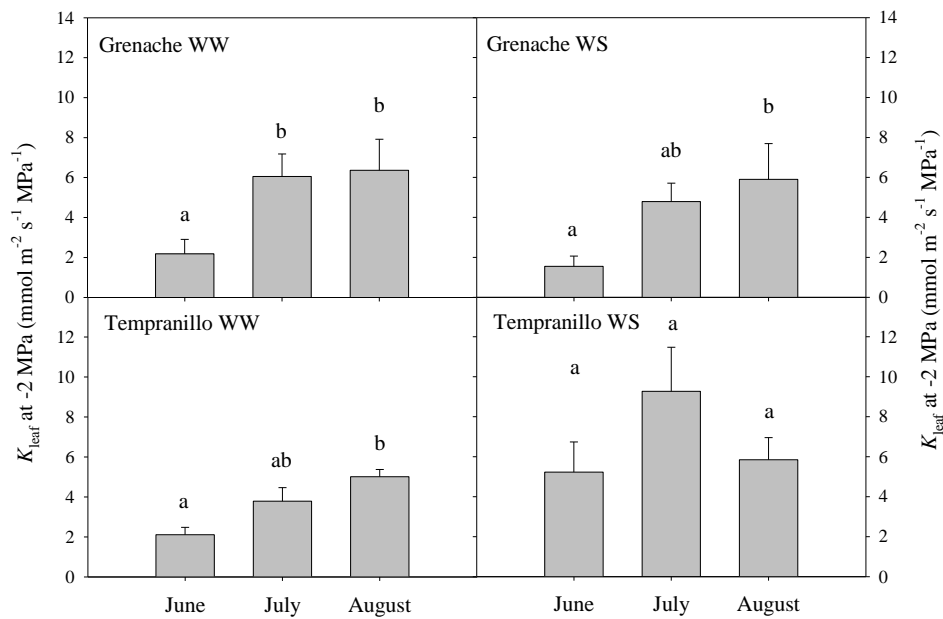
Figure 2: Seasonal progression of leaf hydraulic conductance measured between -1.9 to -2.1 MPa in both Tempranillo and Grenache cultivars in well watered (WW) and water stressed (WS) plants. Letters above columns indicate significant differences between columns (P < 0.05) different. n=5. Vertical bars represent ± SE.

	June	July	August
Ψ_{pd}			
Grenache WW	- 0.16 ± 0.02^a	- 0.27 ± 0.02^a	- 0.24 ± 0.06^a
Grenache WS	- 0.31 ± 0.02^a	- 0.55 ± 0.02^b	- 0.85 ± 0.07^c
Tempranillo WW	- 0.16 ± 0.02^a	- 0.33 ± 0.02^b	- 0.30 ± 0.04^b
Tempranillo WS	- 0.28 ± 0.01^a	- 0.48 ± 0.02^b	- 0.53 ± 0.02^c
Ψ_{md}			
Grenache WW	- 1.07 ± 0.03^a	- 1.05 ± 0.06^a	- 1.00 ± 0.04^a
Grenache WS	- 1.13 ± 0.05^a	- 1.60 ± 0.01^b	- 1.88 ± 0.04^c
Tempranillo WW	- 1.09 ± 0.01^a	- 1.28 ± 0.05^b	- 1.11 ± 0.06^{ab}
Tempranillo WS	- 1.27 ± 0.04^a	- 1.59 ± 0.03^b	- 1.64 ± 0.11^b
$\Delta\Psi$			
Grenache WW	0.91 ± 0.05^a	0.78 ± 0.08^a	0.76 ± 0.08^a
Grenache WS	0.82 ± 0.04^a	1.06 ± 0.03^b	1.04 ± 0.04^b
Tempranillo WW	0.94 ± 0.02^a	0.95 ± 0.06^a	0.80 ± 0.08^a
Tempranillo WS	0.99 ± 0.04^a	1.12 ± 0.04^a	1.11 ± 0.11^a

Table 2: Predawn leaf water potential (Ψ_{pd}, MPa) midday water potential (Ψ_{md}, MPa and soil to leaf water potential gradient ($\Delta\Psi = \Psi_{md} - \Psi_{pd}$, MPa) measured at both treatments in June, July and August. Letters indicate for significant differences (P<0.05) among the different dates on the same treatment.

Osmotic potential at full turgor ($\Psi_{\pi,FT)}$ and at the turgor loss point ($\Psi_{\pi,TLP}$) were also lower (more negative) in July and August than in June (Table 3), which allowed leaves to maintain turgor at lower Ψ_{leaf} later in summer and in the WS treatments. Cell modulus of elasticity (ε) varied between 10 and 16 MPa during season and between cultivars (Table 3). Furthermore, the combination of $\Psi_{\pi,FT}$ and ε allowed the plant to keep relative water content at turgor loss point (RWC$_{TLP}$) at relatively high values (between 88-92%) along the season. The minimum Ψ_{leaf} (Table 2) reached by each cultivar seasonally was correlated with $\Psi_{\pi,TLP}$, and it was always higher than $\Psi_{\pi,TLP}$ (Table 3).

		June	July	August
Grenache WW				
	$\Psi_{\pi,FT}$	-0.98 ± 0.02[b]	-1.10 ± 0.03[ab]	-1.17 ± 0.06[a]
	$\Psi_{\pi,TLP}$	-1.30 ±0.02[b]	-1.56 ± 0.03[a]	-1.63 ± 0.07[a]
	RWC$_{TLP}$	92.52 ± 0.33[a]	89.85 ± 0.56[b]	90.28 ± 0.66[ab]
	ε	12.46 ± 0.60[ab]	10.85 ± 0.67[b]	13.59 ± 0.50[a]
Grenache WS				
	$\Psi_{\pi,FT}$	-0.85 ± 0.05[b]	-1.29 ± 0.07[a]	-1.27 ± 0.05[a]
	$\Psi_{\pi,TLP}$	-1.18 ± 0.05[b]	-1.80 ± 0.07[a]	-1.76 ± 0.08[a]
	RWC$_{TLP}$	92.56 ± 0.59[b]	88.53 ± 0.92[a]	88.26 ± 0.91[a]
	ε	11.23 ± 0.73[a]	12.14 ± 0.96[a]	9.98 ± 0.50[a]
Tempranillo WW				
	$\Psi_{\pi,FT}$	-0.95 ± 0.02[b]	-1.25 ± 0.06[a]	-1.32 ± 0.05[a]
	$\Psi_{\pi,TLP}$	-1.33 ± 0.05[b]	-1.77 ± 0.07[a]	-1.76 ± 0.06[a]
	RWC$_{TLP}$	91.37 ± 0.90[a]	89.99 ± 0.74[a]	91.74 ± 0.64[a]
	ε	10.53 ± 1.35[a]	12.74 ± 1.45[ab]	16.45 ± 1.05[b]
Tempranillo WS				
	$\Psi_{\pi,FT}$	-1.13 ± 0.09[b]	-1.42 ± 0.04[a]	-1.44 ± 0.04[a]
	$\Psi_{\pi,TLP}$	-1.46 ± 0.07[b]	-1.92 ± 0.06[a]	-2.01 ± 0.07[a]
	RWC$_{TLP}$	90.57 ± 0.73[a]	88.79 ± 1.25[a]	89.16 ± 0.70[a]
	ε	12.95 ± 0.99[a]	13.49 ± 1.16[a]	13.09 ± 0.54[a]

Table 3: Leaf water relation parameters obtained by pressure volume curves at June, July and August in both cultivars and water treatments. Osmotic potential at full turgor ($\Psi_{\pi,FT}$, MPa), turgor loss point ($\Psi_{\pi,TLP}$, MPa), relative water content at turgor loss point (RWC$_{TLP}$, %) and mean bulk modulus of elasticity (ε, MPa).WW= well water treatment and WS= water stress treatment. Values are means of 5 samples ± SE. Letters indicate for differences between dates in the same treatment and cultivar (P<0.05).

We observed strong and positive linear relationships between P_{80} and both $\Psi_{\pi,TLP}$ and $\Psi_{\pi,FT}$ (Figs. 3A,B; P<0.001, r^2= 0.81), indicating a decrease in hydraulic vulnerability to dysfunction concurrent with osmotic adjustment. K_{leaf} at -2 MPa was also correlated with $\Psi_{\pi,TLP}$ and $\Psi_{\pi,FT}$ (Fig. 4A,B; P<0.005, r^2= 0.57; P<0.003, r^2= 0.61 respectively) demonstrating that K_{leaf} at -2 MPa increased over summer despite the decline in its maximum ($K_{leaf,max}$).
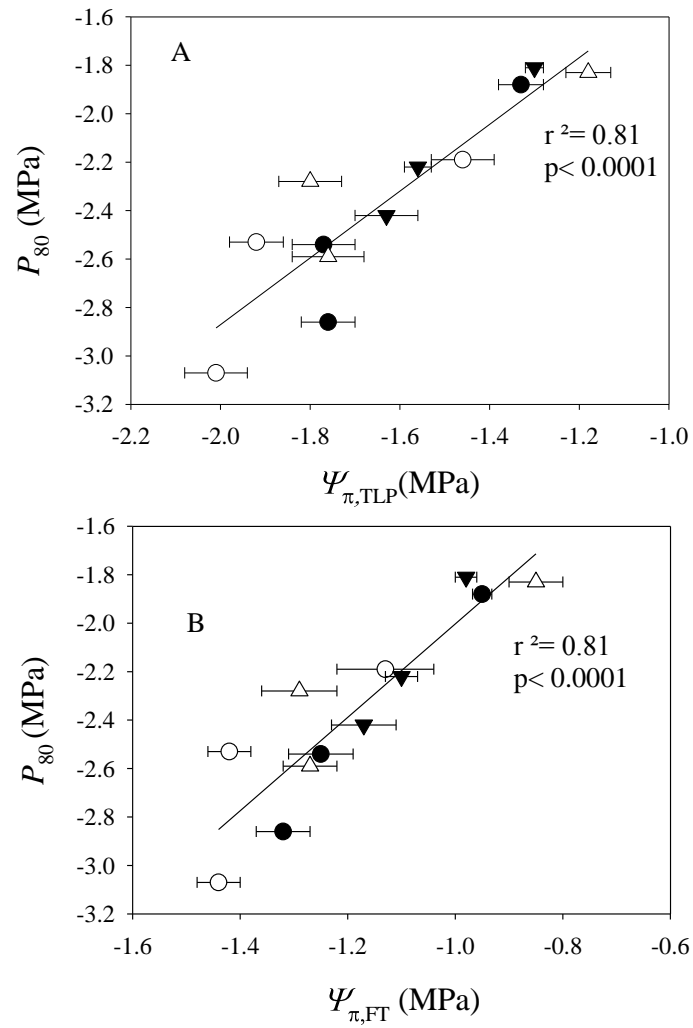
Figure 3: Relationship between the leaf water potential inducing 80% loss of leaf hydraulic conductance (P_{80}) and A) the turgor loss point ($\Psi_{\pi,TLP}$), and B) at full turgor ($\Psi_{\pi,FT}$). Circles correspond to Tempranillo and triangles to Grenache cultivars. Open symbols to well watered plants (WW) and closed symbols to water stressed plants (WS). The regression line for all points is plotted together with the r^2 and P values.
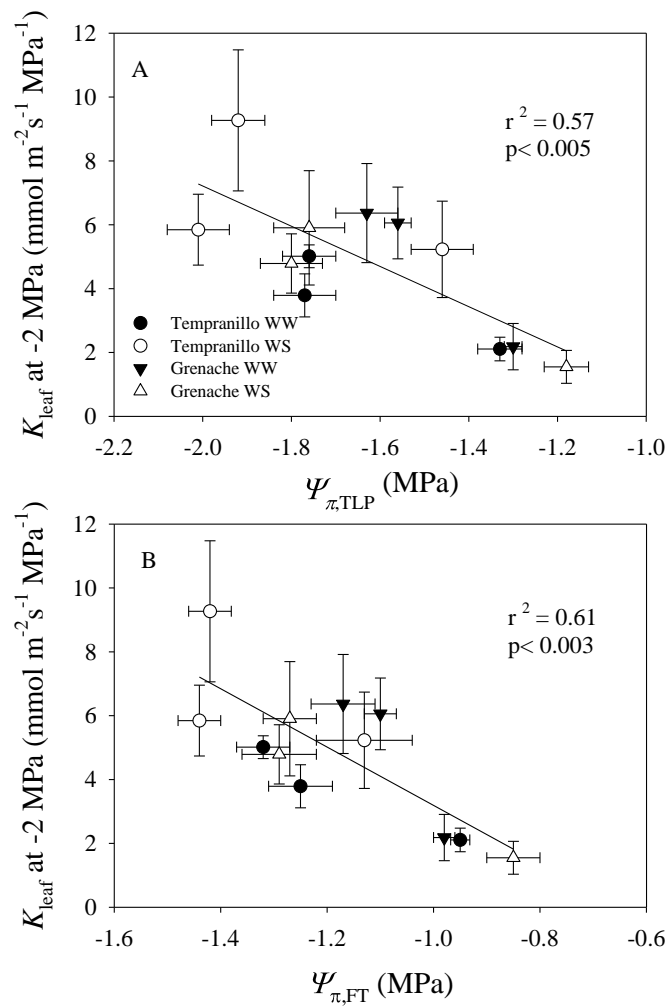
Figure 4: Relationship between osmotic potential and leaf hydraulic conductance (K_{leaf}) at -2 MPa A) at the turgor loss point ($\Psi_{\pi,TLP}$) and B) at full turgor ($\Psi_{\pi,FT}$).Circles correspond to Tempranillo and triangles to Grenache cultivars. Closed symbols to well watered plants (WW) and open symbols to water stressed plants (WS).

Seasonal water use

Water use was greater in WW than WS at both the leaf level (Fig 5A-C) and the canopy level (Fig 5D-F). The canopy-level difference was greater in Grenache than in Tempranillo in June and July, but leaf- and canopy-level water loss declined strongly in both treatments and cultivars during August.
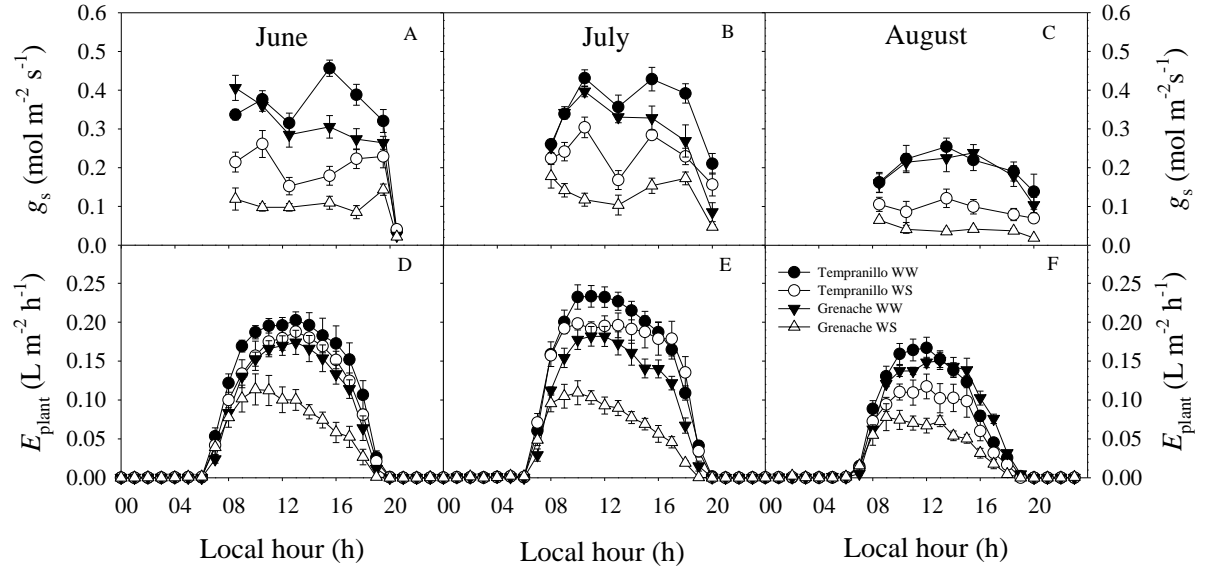
Figure 5: Diurnal progression along the season of A) stomatal conductance (g_s), B) transpiration measured by sap flow. Circles correspond to Tempranillo and triangles to Grenache cultivars. Closed symbols to well watered plants (WW) and open symbols to water stressed plants (WS).

DISCUSSION

We found that leaf hydraulic vulnerability to dysfunction (measured by P_{80}, the water potential causing 80% loss of conductivity) decreased over the summer in grapevine, and that P_{80} was strongly correlated with turgor loss point, as we hypothesized. These results show the first clear evidence that leaf vulnerability to hydraulic dysfunction can acclimate to seasonal drought within a single species. Previous studies have shown P_{50} and P_{80} to be lower in species from arid and semiarid environments than in species from moist climates (Blackman *et al.* 2010, Scoffoni *et al.* 2012, Nardini *et al.* 2012). This has been interpreted as an evolutionary adaptation: lower P_{50} and P_{80} allow arid species to maintain a lower minimum Ψ_{leaf} without much hydraulic dysfunction, which provides a competitive advantage in arid regions (Nardini *et al.* 2012). Our results demonstrate that a similar relationship between P_{50} or P_{80} and water availability can also occur for a single species as an acclimatory response to water stress.

This study also provides circumstantial evidence that the observed acclimation of leaf hydraulic vulnerability to drought was caused, at least in part, by osmotic adjustment. Acclimation of osmotic pressure at full turgor ($\Psi_{\pi,FT}$) and bulk modulus of elasticity (ε) to water stress within a single species has been well documented for decades (Kramer and Boyer 1995), and these aspects of leaf acclimation to water stress may help to

70

maintain the conductivity of the extra-xylary pathway for water flow in two ways. First, maintaining turgor may prevent excessive cell shrinkage during water stress (Sancho-Knapik *et al.* 2011, Scoffoni *et al.* 2012, Scoffoni *et al.* 2014), thereby maintaining cell to cell pathways (symplastic and transcellular paths) and preventing a reduction in evaporative surface in the intercellular spaces (Scoffoni *et al.* 2014). Second, turgor may directly modulate aquaporin function, so maintenance of turgor may be required to sustain high conductivity of the symplastic pathway (Kim and Steudle 2007, Cochard *et al.* 2007). This hypothesis is supported by the strong relationship that we found between $\Psi_{\pi,TLP}$ and P_{80}. Furthermore, these changes in P_{80} were not caused by changes in maximum K_{leaf} (which also declined over the summer), as demonstrated by the fact that K_{leaf} at a reference water potential of -2.0 MPa actually *increased* over the summer, and still maintained the correlation with $\Psi_{\pi,TLP}$ and $\Psi_{\pi,FT}$ (Fig. 4).

Although it is widely interpreted that concomitant changes in ε have an effect on $\Psi_{\pi,TLP}$, Bartlett *et al.* (2012) recently demonstrated that ε changes vary widely between studies of drought stress and play a secondary role in driving drought tolerance as some times values can increment or decrease in water stress conditions. That reinforce the hypothesis that changes in $\Psi_{\pi,TLP}$ are driven primarily by osmotic adjustment (which is reflected by changes in $\Psi_{\pi,FT}$) (Barlett et al., 2012). However, ε could play a role in preventing loss of K_{leaf} at low Ψ_{leaf}, because the decline in K_{leaf} caused by shrinkage during dehydration (Scoffoni *et al.* 2014) is likely caused by reduced cell volume rather than turgor pressure *per se*. This secondary role of ε in the response to drought of leaves, i.e. facilitation of K_{leaf} at lower Ψ_{leaf} by the maintenance of higher RWC and preventing cell dehydration, might has gone unnoticed by Bartlett *et al.* (2012) when interpreting their results on the acclimation to drought. In any case, the role of cell volume on K_{leaf} deserves further experimental support.

Although we did not partition K_{leaf} into xylem and extra-xylary components in this study, changes in the xylem of petioles or minor leaf veins are unlikely to explain the changes in P_{80} and in K_{leaf} at -2.0 MPa observed between June and August. All leaves were of similar age, and acclimation during ontogeny, which could have allowed for the construction of a vein network of different vulnerability, cannot be involved. Although it has been reported that changes in the ionic composition of the sap might enhance the hydraulic conductivity of xylem vessels (Nardini *et al.* 2011), it has not never been

reported and increase as high as the one observed in this study (Fig. 2). The most parsimonious explanation to both the decrease of P_{80} and the increase of K_{leaf} at -2 MPa is the shift of the vulnerability curve towards more negative Ψ_{leaf} values, in line with our initial hypothesis. On the other hand, the decline in $K_{leaf,max}$ over the summer could be due to the loss of hydraulic capacity in the xylem by fatigue, as proposed by Hacke *et al.* (2001), or due to an accumulation of tyloses associated with senescence (Salleo *et al.* 2002). Tylose secretion in grapevines (Sun *et al.* 2006, 2008, Fritschi *et al.* 2007) has been proposed to be related to the loss of hydraulic capacity (McElrone *et al.* 2012).

A second option to explain the reduction of $K_{leaf,max}$ is related to the regulation of cell permeability by aquaporins. There are numerous studies showing the reduction of the genetic expression of PIPs and their putative effect on all components of plant hydraulics, including leaves (Cochard *et al.* 2007, Heinen *et al.* 2009, Pou *et al.* 2013). This regulation is mainly achieved in response to leaf water status (Heinen *et al.* 2009), but recently ABA has been suggested as an important effector of this response (Pantin *et al.* 2012). According to this view, elevated ABA levels in late summer would reduce the maximum capacity of the symplastic pathway, but would not affect its vulnerability to short term changes in Ψ_{leaf} as gauged by P_{80}.

Difference in K_{leaf} plasticity along leaf lifespan between cultivars

Although water availability was larger in WW than in WS plants, the higher atmospheric demand in August compared to June, and leaf age would have made the differences between water treatments smaller than expected. Tempranillo achieved similar or even higher Ψ_{pd} and Ψ_{md} than Grenache in June and July and had lower $\Psi_{\pi,FT}$ than Grenache, even in the WW treatments. Furthermore, Tempranillo WS showed an increase of K_{leaf} at -2 MPa (Fig. 2) in June and July. Both aspects, lower $\Psi_{\pi,FT}$ and increased K_{leaf} at -2MPa, were not observed in Grenache cultivar being a characteristic difference between them. Both the enhancement of K_{leaf} at low Ψ_{leaf}, and the larger osmotic adjustment of Tempranillo in comparison with Grenache fit well with the reputation of Tempranillo of being a stronger water consumer than Grenache (Flexas *et al.* 2010, Tomás *et al.* 2012). This can be graphically observed in Fig. 2 were it is seen how Tempranillo WS reached the highest K_{leaf} at -2 MPa, even higher than its own value in June. Our data show how Tempranillo WS maintained higher g_s (Fig. 5A-C) and larger transpiration rates (Fig. 5D-F) than Grenache WS during the entire season

and similar to Grenache WW in June and July. This behavior in a short period of time would be advantageous for Tempranillo allowing plants of this cultivar to maintain higher CO_2 assimilation rates and to be more competitive. However, if drought persists this strategy could endanger their performance, for which Grenache would perform better under severe stress as could be expected according to their reputation as drought adapted cultivar (Shultz 2003, Flexas *et al.* 2010).

The plasticity in the hydraulic vulnerability dysfunction of leaves reported in this study contrasts to the relatively low plasticity observed in shoots (Maherali and de Lucia 2000, Cornwell *et al*. 2007). When plasticity of stem vulnerability to cavitation has been found, it has generally been attributed to genetic differentiation (Kolb and Sperry 1999) or ecotypes in contrasting climatic conditions (Beikircher and Mayr 2009, Corcuera *et al.* 2011, Wortemann *et al.* 2011, Rico *et al.* 2013). It is perhaps not surprising that leaves would exhibit greater plasticity of hydraulic function than stems, due to the role of living tissues in the extra-xylary pathway of leaves. Our results suggest that a complete understanding of how leaf gas exchange acclimates to drought awaits a better understanding the extra-xylary pathway and its regulation.

CONCLUSIONS

Our data show for the first time that the vulnerability of leaf conductance can acclimate to water stress within a single species. The maintenance of K_{leaf} at more negative values of Ψ_{leaf} was strongly correlated to osmotic adjustment, suggesting that maintenance of turgor pressure may be involved in the plastic acclimation of leaf hydraulic vulnerability to dysfunction. This result highlights the importance of the extra-xylary component of K_{leaf}. Future work is needed to fully understand the regulation of K_{leaf} by cell turgor, and to determine which is the role of aquaporins and anatomical or structural changes during dehydration. Finally, the capacity of osmotic adjustment observed in these two cultivars of grapevine seems to have an impact in plant performance beyond its effect of cell water relations. The enhancement of K_{leaf} at lower water potentials, which might help to explain established contrasting reputation for these two cultivars, points out to the extra-xylary component of K_{leaf} as one of the most plastic components in the hydraulic acclimation of the plant to the changing environment.

REFERENCES

Alsina M.M, De Herralde F., Aranda X., Save R. & Biel CC (2007) Water relations and vulnerability to embolism are not related: experiments with eight grapevine cultivars. *Vitis,* **46**, 1-7

Baker J.M. & Van Bavel C.H.M. (1987) Measurement of mass flow of water in the stems of herbaceous plants. *Plant Cell & Environment*, **10**, 777-782

Bartlett M.K., Scoffoni C. & Sack L. (2012) The determinants of leaf turgor loss point and prediction of drought tolerance of species and biomes: a global meta-analysis. *Ecology Letters*, **15**, 393-405

Beikircher B. & Mayr S. (2009) Intraspecific differences in drought tolerance and acclimation in hydraulics of *Ligustrum vulgare* and *Viburnum lantana*. *Tree Physiology,* **29,** 765-775.

Blackman C.J., Brodribb T.J. & Jordan G.J. (2010) Leaf hydraulic vulnerability is related to conduit dimensions and drought resistance across a diverse range of woody angiosperms. *New Phytologist*, **188,** 1113-1123

Blackman C.J. & Brodribb T.J. (2011) Two measures of leaf capacitance: insights into the water transport pathway and hydraulic conductance in leaves. *Functional Plant Biology*, **38**, 118-126

Brodersen C.R., McElrone A.J., Choat B., Matthews M.A. & Shackel K.A. (2010) The dynamics of embolism repair in xylem: in vivo visualizations using high-resolution computed tomography. *Plant Physiology* **154,** 1088-1095

Brodersen C.R., Choat B., Chatelet D.S., Shackel K.A., Matthews M.A. & McElrone A.J. (2013) Xylem vessel relays contribute to radial connectivity in grapevine stems (*Vitis vinifera* and *V. arizonica; Vitaceae*). *American Journal of Botany,* **100**, 314-321

Brodribb T.J. & Holbrook N.M. (2003) Stomatal closure during leaf dehydration, correlation with other leaf physiological traits. *Plant Physiology*, **132**, 2166-2173

Brodribb T.J., Holbrook N.M., Zwieniecki M.A. & Palma B. (2005) Leaf hydraulic capacity in ferns, conifers and angiosperms: impacts on photosynthetic maxima. *New Phytologist*, **165,** 839-846

Charra-Vaskou K., Badel E., Burlett R., Cochard H., Delzon S. & Mayr S. (2012) Hydraulic efficiency and safety of vascular and non-vascular components in *Pinus pinaster* leaves. *Tree Physiology*, **32**, 1161-1170

Choat B., Gambetta G.A., Wada H., Shackel K.A. & Matthews M.A. (2009) The effects of Pierce's disease on leaf and petiole hydraulic conductance in *Vitis vinifera* cv. Chardonnay. *Physiologia Plantarum*, **136**, 384-394

Choat B., Drayton W.M., Brodersen C., Matthews M.A., Shackel K.A., Wada H. & McElrone A.J. (2010) Measurement of vulnerability to water stress-induced cavitation in

grapevine: a comparison of four techniques applied to a long-vesseled species. *Plant Cell & Environment*, **33**, 1502-1512

Choat B., Jansen S., Brodribb T.J., *et al.* (2012) Global convergence in the vulnerability of forests to drought. *Nature*, **491**, 752-756

Cochard H., Venisse J.S., Barigah T.S., Brunel N., Herbette S., Guilliot A., Tyree M.T. & Sakr S. (2007) Putative role of aquaporins in variable hydraulic conductance of leaves in response to light. *Plant Physiology*, **143**, 122-133

Corcuera L., Cochard H., Gil-Pelegrin E. & Notivol E. (2011) Phenotypic plasticity in mesic populations of *Pinus pinaster* improves resistance to xylem embolism (P_{50}) under severe drought. *Trees*, **25**, 1033-1042

Cornwell W.K., Bhaskar R., Sack L. & Cordell S. (2007) Adjustment of structure and function of Hawaiian *Metrosideros polymorpha* at high vs. low precipitation. *Functional Ecology*, **21**, 1063-1071

Engelbrecht B.M., Comita L.S., Condit R., Kursar T.A., Tyree M.T., Turner B.L. & Hubbell S.P. (2007) Drought sensitivity shapes species distribution patterns in tropical forests. *Nature*, **447**, 80-82

Escalona J., Flexas J. & Medrano H. (2002) Drought effects on water flow, photosynthesis and growth of potted grapevines. *Vitis*, **41**: 57-62

Fereres E. & Soriano M.A. (2007) Deficit irrigation for reducing agricultural water use. *Journal of Experimental Botany*, **58**, 147-159

Flexas J., Galmés J., Gallé A., Gulias J., Pou A., Ribas-Carbó M., Tomàs M. & Medrano H. (2010) Improving water use efficiency in grapevines: potential physiological targets for biotechnological improvement. *Australian Journal of Grape Wine Research*, **16,** 106-121

Fritschi F.B., Lin H. & Walker M.A. (2008) Scanning electron microscopy reveals different response pattern of four *Vitis* genotypes to *Xylella fastidiosa* infection. *Plant Disease*, **92**, 276-286

Guyot G., Scoffoni C. & Sack L. (2012) Combined impacts of irradiance and dehydration on leaf hydraulic conductance: insights into vulnerability and stomatal control. *Plant Cell & Environment*, **35**, 857-871

Hacke U.G., Stiller V., Sperry J.S., Pittermann J. & McCulloh K.A. (2001) Cavitation fatigue. Embolism and cycles can weaken cavitation resistance of xylem. *Plant Physiology*, **125**, 779-786

Heinen R.B., Ye Q. & Chaumont F. (2009) Role of aquaporins in leaf physiology. *Journal of Experimental Botany*, **60**, 2971-2985

Hubbard R.M., Ryan M.G., Stiller V. & Sperry J.S. (2001) Stomatal conductance and photosynthesis vary linearly with plant hydraulic conductance in Ponderosa pine. *Plant Cell & Environment*, **24**, 113-121

Johnson D.M., Meinzer F.C., Woodruff D.R. & McCulloh K.A. (2009) Leaf xylem embolism, detected acoustically and by cryo-SEM, corresponds to decreases in leaf hydraulic conductance in four evergreen species. *Plant Cell & Environment*, **32**, 828-836

Johnson D.M., McCulloh K.A., Woodruff D.R. & Meinzer F.C. (2012) Evidence for xylem embolism as a primary factor in dehydration-induced declines in leaf hydraulic conductance. *Plant Cell & Environment*, **35**, 760-769

Kim Y.X. & Steudle E. (2007) Light and turgor affect the water permeability (aquaporins) of parenchyma cells in the midrib of leaves of *Zea mays*. *Journal of Experimental Botany*, **58**, 4119-4129

Kolb K.J. & Sperry J.S. (1999) Differences in drought adaptation between subspecies of sagebrush (*Artemisia tridentata*). *Ecology*, **80**, 2373-2384

Kramer P.J. & Boyer J.S. (1995) Water relations of plants and soils. Elservier Science.

Lovisolo C., Perrone I., Hartung W. & Schubert A. (2008) An abscisic acid-related reduced transpiration promotes gradual embolism repair when grapevines are rehydrated after drought. *New Phytologist*, **180**, 642-651

Maherali H. & De Lucia E.H. (2000) Xylem conductivity and vulnerability to cavitation of ponderosa pine growing in contrasting climates. *Tree Physiology*, **20**, 859-867

Martorell S., Díaz-Espejo A., Medrano H., Ball M.C. & Choat B. (2014) Rapid hydraulic recovery in *Eucalyptus pauciflora* after drought: linkages between stem hydraulics and leaf gas exchange. *Plant Cell & Environment*, **37**, 617-626

McElrone A.J., Brodersen C.R., Alsina M.M., Drayton W.M., Matthews M.A., Shackel K.A., Wada H., Zufferey V. & Choat B. (2012) Centrifuge technique consistently overestimates vulnerability to water stress-induced cavitation in grapevines as confirmed with high-resolution computed tomography. *New Phytologist*, **196**, 661-665

Medrano H., Pou A., Tomás M., Martorell S., Gulias J., Flexas J. & Escalona J.M. (2012) Average daily light interception determines leaf water use efficiency among different canopy locations in grapevine. *Agricultural Water Management*, **114**, 4-10

Meinzer F.C. & Grantz D.A. (1990) Stomatal and hydraulic conductance in growing sugarcane: stomatal adjustment to water transport capacity. *Plant Cell & Environment*, **13**, 383-388

Nardini A. & Salleo S. (2000) Limitation of stomatal conductance by hydraulic traits: sensing or preventing xylem cavitation? *Trees*, **15**, 14-24

Nardini A., Salleo S. & Andri S. (2005) Circadian regulation of leaf hydraulic conductance in sunflower (*Helianthus annuus* L. cv Margot). *Plant Cell & Environment*, **28**, 750-759

Nardini A., Salleo S. & Jansen S. (2011) More than just a vulnerable pipeline: xylem physiology in the light of ion-mediated regulation of plant water transport. *Journal of Experimental Botany*, **62**, 4701-4718.

Nardini A., Pedà G. & Rocca N.L. (2012) Trade-offs between leaf hydraulic capacity and drought vulnerability: morpho-anatomical bases, carbon costs and ecological consequences. *New Phytologist*, **196**, 788-798

Pantin F., Monnet F., Jannaud D., Costa J.M., Renaud J., Muller B. & Genty B. (2013) The dual effect of abscisic acid on stomata. *New Phytologist*, **197**, 65-72

Pou A., Medrano H., Tomàs M., Martorell S., Ribas-Carbó M. & Flexas J. (2012) Anisohydric behaviour in grapevines results in better performance under moderate water stress and recovery than isohydric behaviour. *Plant & soil*, **359**, 335-349

Pou A., Medrano H., Flexas J. & Tyerman S.D. (2013) A putative role for TIP and PIP aquaporins in dynamics of leaf hydraulic and stomatal conductances in grapevine under water stress and re-watering. *Plant Cell & Environment*, **36**, 828-843

Rico C., Pittermann J., Polley H.W., Aspinwall M.J. & Fay P.A. (2013) The effect of subambient to elevated atmospheric CO_2 concentration on vascular function in *Helianthus annuus*: implications for plant response to climate change. *New Phytologist*, **199**, 956-965

Ruiz-Sánchez M.C., Domingo-Miguel R. & Castel J.R. (2010) Deficit irrigation in fruit trees and vines in Spain. *Spanish Journal of Agricultural Research*, **8**, 5-20

Sack L., Melcher P.J., Zwieniecki M.A. & Holbrook N.M. (2002) The hydraulic conductance of the angiosperm leaf lamina: a comparison of three measurement methods. *Journal of Experimental Botany*, **53**, 2177-2184

Sack L., Cowan P.D., Jaikumar N. & Holbrook N.M. (2003) The 'hydrology' of leaves: co-ordination of structure and function in temperate woody species. *Plant Cell & Environment*, **26**, 1343-1356

Sack L., Streeter C.M. & Holbrook N.M. (2004) Hydraulic analysis of water flow through leaves of sugar maple and red oak. *Plant Physiology*, **134**, 1824-1833.

Sack L. & Tyree M.T. (2005) Leaf hydraulics and its implications in plant structure and function. *In Vascular Transport in Plants. Eds* NM Holbrook, MA Zwieniecki. Elsevier New York

Sack L. & Holbrook N.M. (2006) Leaf hydraulics. *Annual Reviews of Plant Biology*, **57**, 361-381

Sack L., Pasquet-Kok J. & PrometheusWiki contributors. (2011) "Leaf pressure-volume curve parameters." *PrometheusWiki*. 05 Apr. 2011 prometheuswiki.publish.csiro.au/ tiki-citation.php?page=Leaf%20pressure-volume%20curve%20parameters#sthash. 0GHJnhGz.dpuf

Sakuratani T. (1981) A heat balance method for measuring water flux in the stem of intact plants. *Journal of Agricultural Metheorology,* **37**, 9-17

Salleo S., Nardini A., Lo Gullo M.A. & Ghirardelli L.A. (2002) Changes in stem and leaf hydraulics preceding leaf shedding in *Castanea sativa L. Biologia Plantarum*, **45**, 227-34

Sancho-Knapik D., Álvarez-Arenas T.G., Peguero-Pina J.J., Fernández V. & Gil-Pelegrín E. (2011) Relationship between ultrasonic properties and structural changes in the mesophyll during leaf dehydration. *Journal of Experimental Botany*, **62**, 3637-3645

Schultz H.R. (2003) Differences in hydraulic architecture account for near-isohydric and anisohydric behaviour of two field-grown *Vitis vinifera L.* cultivars during drought. *Plant Cell & Environment* **26**, 1393-1405

Scoffoni C., McKown A.D., Rawls M. & Sack L. (2012) Dynamics of leaf hydraulic conductance with water status: quantification and analysis of species differences under steady state. *Journal of Experimental Botany* **63**, 643-658

Scoffoni C., Vuong C., Diep S., Cochard H. & Sack L. (2014) Leaf shrinkage with dehydration: coordination with hydraulic vulnerability and drought tolerance. *Plant Physiology*, **164**,1772-1788.

Sellin A. & Kupper P. (2007) Temperature, light and leaf hydraulic conductance of little-leaf linden (Tiliacordata) in a mixed forest canopy. *Tree Physiology*, **27**, 679-688

Sperry J.S., Hacke U.G., Oren R. & Comstock J.P. (2002) Water deficit and hydraulic limits to leaf water supply. *Plant Cell & Environment*, **25**, 251-263

Sun Q., Rost T.L. & Matthews M.A. (2006) Pruning-induced tylose development in stems of current-year shoots of *Vitis vinifera* (Vitaceae). *Americal Journal of Botany*, **93**, 1567-1576

Sun Q., Rost T.L. & Matthews M.A. (2008) Wound-induced vascular occlusions in *Vitis vinifera* (Vitaceae): tyloses in summer and gels in winter. *Americal Journal of Botany*, **95**, 1498-1505

Tomás M., Medrano H., Pou A., Escalona J.M., Martorell S., Ribas-Carbó M. & Flexas J. (2012) Water-use efficiency in grapevine cultivars grown under controlled conditions: effects of water stress at the leaf and whole-plant level. *Australian Journal of Grape & Wine Research* **18**, 164-172

Tyree M.T. & Hammel H.T. (1972) Measurement of turgor pressure and water relations of plants by pressure bomb technique. *Journal of Experimental Botany*, **23**, 267-282

Voicu M.C., Zwiazek J.J. & Tyree M.T. (2008) Light response of hydraulic conductance in bur oak (*Quercus macrocarpa*) leaves. *Tree Physiology* **28**, 1007-1015

Wheeler J.K., Huggett B.A., Tofte A.N., Rockwell F.E. & Holbrook N.M. (2013) Cutting xylem under tension or supersaturated with gas can generate PLC and the appearance of rapid recovery from embolism. *Plant Cell & Environment*, **36**, 1938-1949

Wortemann R., Herbette S., Barigah T.S., Fumanal B., Alia R., Ducousso A., Comory D., Roeckel-Drevet P. & Cochard H. (2011). Genotypic variability and phenotypic plasticity of cavitation resistance in *Fagus sylvatica* L. across Europe. *Tree Physiology*, **31**, 1175-1182

Zufferey V., Cochard H., Ameglio T., Spring J.L. & Viret O. (2011) Diurnal cycles of embolism formation and repair in petioles of grapevine (*Vitis vinifera* cv. Chasselas). *Journal of Experimental Botany*, **62**, 3885-3894

3.3. Differences in water-use-efficiency between two Vitis vinifera cultivars (Grenache and Tempranillo) explained by the combined response of stomata to hydraulic and chemical signals during water stress.

Martorell S [a], Díaz-Espejo A [b], Tomàs M [a], Pou, A [c], El Aou-ouad, H [a], Escalona, J.M [a], Vadell, J [a], Ribas-Carbó, M [a], Flexas, J [a], Medrano H [a]

[a] Research Group on Plant Biology under Mediterranean Conditions, Departament de Biologia, Universitat de les Illes Balears, Carretera de Valldemossa Km 7.5, 07122. Palma de Mallorca, Illes Balears, Spain;

[b] Irrigation and Crop Ecophysiology Group, Instituto de Recursos Naturales y Agrobiología de Sevilla (IRNAS, CSIC). Avenida Reina Mercedes 10, 41012 Sevilla, Spain.

[c] Institute des Sciences de la Vie (ISV), Université Catholique de Louvain, Croix de Sud, 4-5 bte 1348 Louvaine-la-Neuve, Belgium.

ABSTRACT

Knowledge about regulation of stomatal conductance is necessary to improve grapevine water use efficiency. The vast range of grapevine cultivars may allow choosing the best-performing ones to global changing conditions provided the understanding and characterization of their physiological responses. In this study, a comparison between two cultivars (Tempranillo and Grenache) with different reputation in water use efficiency was performed during two experimental years in field-conditions. Water relations, leaf gas exchange and abscisic acid (ABA) dynamics were measured at different phenological stages along the growing seasons. A clear difference in the regulation of leaf water relations was observed between cultivars under water stress conditions. Specifically, results showed that there is a clear relationship between hydraulic conductance (K_h) and stomatal regulation. However, ABA can exert a differentiating role on stomatal control during different stages within the grapevine growth period. Furthermore, the combination of both signals, ABA and K_h, resulted in differential water use efficiency among cultivars.

Keywords: Grapevine, water relations, water use efficiency, absicic acid, hydraulic conductance.

INTRODUCTION

Water availability for plants is one of the most limiting factors in agriculture (Araus 2004; Morison *et al.* 2008). Grapevines are predominantly located in the Mediterranean region with semi-arid climate where the growing season coincides with the highest annual temperatures and drought months (Flexas *et al.* 2010). This particular climatic conditions and their exacerbation predicted by global warming (Chaves *et al.* 2007; Fraga *et al.* 2012; Hannah *et al.* 2013; IPCC 2013) demand an advance on the knowledge about the ecophysiological response to water stress in grapevine cultivars. This knowledge will allow improving crop water use efficiency (WUE) (Flexas *et al.* 2010; Medrano *et al.* 2010; Tomàs *et al.* 2012).

Grapevines are among the most genetically heterogeneous plant species (Mullins *et al.* 1992). Such large genetic variability should allow the opportunity to choose the cultivars with the highest WUE, to counteract potential negative effects of global warming. Many works have compared cultivars in terms of WUE, resulting in contrasting results depending on environmental conditions, level of water stress and its

duration and intensity, as well as the diversity of grapevine cultivars (Bota *et al.* 2001; Shultz, 2003; Tomàs *et al.* 2012, 2014; Rogiers *et al.* 2012, Zhang *et al.* 2012; Pou *et al.* 2012; Tramontini *et al.* 2014). Differences in the water economy among cultivars are well illustrated by the relationships between water availability and water losses, estimated by the leaf water potential (Ψ_l) and stomatal conductance (g_s), respectively. On the basis of this relationship two contrasting behaviors have been described (Shultz, 2003): one reflecting a low control of Ψ_l by g_s (*anisohydric response*) which allow plants to maintain a lower water potential under water stress having a non-tightly control of g_s; and *isohydric* for the cultivars showing a strong control of transpiration by stomata leading to slight Ψ_l reductions (Stocker, 1956; Tardieu and Simonneau 1998). However, such contrasting behaviors, which have been ascribed to specific cultivars in some studies (Shultz, 2003; Pou *et al.* 2012; Zhang *et al.* 2012) is not unequivocal. Contrasting or contrary results have been found and published, possibly depending on the experimental conditions from each study (Collins *et al.* 2010; Pou *et al.* 2012; Tramontini *et al.* 2014). Therefore, the classification of cultivars based on this criterion is vague and, moreover, the physiological characteristics of any cultivar are more complex and highly conditioned by the strong interaction between cultivar and environment, especially in the control of stomatal function by soil water deficit (Domec and Johnson, 2012).

In fact, different regulatory mechanisms have been identified in the control of turgor on guard cells and accordingly g_s, but it is still complex to know exactly how they act, since the response could be mediated by various processes at the same time. Chemical messengers like abscisic acid (ABA) (Dood, 2005), xylem sap pH (Wilkinson and Davies, 2008), electrical signals (Grams *et al.* 2007) or hydraulic signals (Hubbard *et al.* 2001) have been postulated and demonstrated to exert a control on g_s being all of them significant in their regulation. Despite the large list of candidates to regulate guard cells only two of them, ABA and hydraulic conductance, have gained most of the attention during the last years.

ABA is a phytohormone that has been associated to decreases of stomatal conductance in response to water stress (rev. Dodd, 2005). It has been documented that ABA induce an osmotic efflux from guard cells reducing their turgor and, consequently, closing stoma (Zhang and Davies 1990; Assmann and Shimazaki, 1999; Blatt, 2000). Also it

has been proven recently that ABA might exert a control on leaf hydraulic conductance having an indirect effect on stomatal conductance (Pantin *et al.* 2013). In grapevines, there is wide and convincing evidence on the relationship between g_s and ABA (Correia *et al.* 1995; Lovisolo *et al.* 2008; Pou *et al.* 2008; Romero *et al.* 2012; Speirs *et al.* 2013; Tramontini *et al*. 2014). On the other hand, hydraulic conductance has been also documented as an important physiological parameter for g_s (Hubbard *et al.* 2001). In some cases it has been found a close coordination between stomatal closure and the loss of hydraulic conductance (Lovisolo *et al.* 2008; Martorell *et al.* 2014). Under water stress, stomata closure prevents cavitation events to widely spread along the vascular system of the plant. Reductions on hydraulic conductance trigger reductions on water supply to the leaves, therefore affecting guard cells water relations. There are also wide experimental evidences of hydraulic control of g_s in grapevines (Shultz, 2003; Lovisolo *et al.* 2008; Pou *et al.* 2008; Pou *et al.* 2012; Pou *et al.* 2013). In conclusion, it has been largely demonstrated that both, ABA and hydraulic conductance play an important role in the regulation of stomatal aperture, even though there are few studies analyzing the value of each one of those players on the stomatal control of grapevine cultivars with contrasting behavior under water stress.

In this study, a field trial was conducted with two cultivars with contrasting reputation in their adaptation to drought. The Grenache cultivar is reputed as more adapted to hot and dry areas than Tempranillo (Shultz 2003; Medrano et al. 2003), and usually presents higher WUE (Tomàs *et al.* 2012; Pou *et al.* 2012). A deeper knowledge on how these two cultivars regulate g_s and water relations in response to water stress is of paramount importance if we intend to understand the fundamental processes of stomatal control on WUE.

In consequence, we examined in this study, which were the physiological characteristics that differentiate Tempranillo and Grenache cultivars responses to water stress. The main objective was to unravel the role played by hydraulic and chemical signals in the regulation of transpiration by stomata in both cultivars.

MATERIALS AND METHODS

Plant material and treatments:

The experiment was conducted in the experimental field of the University of Balearic Islands on grapevine plants of Tempranillo and Grenache cultivars during summer 2011 and 2012. Plants were two years old (planted in 2011) grafted on Richter-110 and planted in rows (distance between rows was 2.5 m and plants 1 m). They were trained in a bilateral double cordon having between 6-8 canes per plant in 2011 and 10-12 canes per plant in 2012. Two irrigation treatments were applied: well watered plants (WW) which received around 3 liters per plant and day (K_c around 0.3) by 2011 and around 9 liters per day per plant in 2012 (K_c around 0,75). The dosage increase was adjusted because the much higher vegetative growth in 2012 than in 2011 (approximately 50% of difference in total leaf area between both years). The Water Stress (WS) treatment consisted on withholding irrigation during the whole summer in both years.

Climatic conditions

Climatic conditions were recorded by a meteorological station located in the same field (Meteodata 3000, Geonica). In general 2012 was drier than 2011; however, in general, both years were comparable (Table 1). Rainfall was no significant during the experimental period and mean temperature ranged similar values between months. Mean relative humidity was maintained around 60% in both years having slightly differences between months. Accumulated evapotranspiration (ETP_{accum}) was similar for both years having only a certain decrease due to more frequent cloudy days in August 2012.

Year	Month	Tº mean (ºC)	Tº max (ºC)	Tº min (ºC)	HR mean (%)	ETP accum (mm)	Rainfall (mm)
2011	May	19.40 ± 0.29^a	25.34 ± 0.44^a	12.91 ± 0.37^a	63.28 ± 1.29^b	135.59	5.40
2011	June	21.46 ± 0.57^b	26.83 ± 0.76^b	15.70 ± 0.45^b	65.18 ± 1.61^b	133.32	23.10
2011	July	24.31 ± 0.30^c	28.99 ± 0.41^c	19.05 ± 0.36^d	63.90 ± 1.20^b	145.81	11.60
2011	August	25.67 ± 0.29^d	31.46 ± 0.50^d	19.51 ± 0.32^{de}	60.15 ± 1.89^{ab}	151.08	0.00
2012	May	18.67 ± 0.41^a	24.40 ± 0.39^a	12.30 ± 0.39^a	60.47 ± 1.76^{ab}	132.69	12.10
2012	June	23.96 ± 0.37^c	30.07 ± 0.50^{cd}	17.43 ± 0.41^c	56.61 ± 1.54^a	138.50	0.20
2012	July	24.90 ± 0.27^{cd}	30.31 ± 0.39^{cd}	18.81 ± 0.38^d	60.18 ± 1.68^{ab}	146.84	0.10
2012	August	26.69 ± 0.24^e	33.15 ± 0.46^e	20.17 ± 0.23^e	57.34 ± 2.01^a	100.39	0.10

Table 1: Climatic conditions measured during experimental periods in 2011 and 2012. Values represented are mean temperature (Tº mean), mean minimum Temperature (Tmin), Relative Humidity (HR), evapotranspiration accumulated (ETPaccum) and Rainfall per month. Letters denote statistical differences between month (p<0.05).

Soil characteristics*:*

Soil characteristics were assessed for the regions were Grenache and Tempranillo were planted. Both soils were similar in composition being classified in a clay loam soil but differ in depth. Tempranillo's soil presented a deeper soil (2.5 meters) than Grenache's soil (1.1 meters). Calculated total available water for Tempranillo resulted to be 390 liters contrasting with the 180 liters that could hold Grenache soil, differences being due to different soil depth in the sampling positions.

Leaf water relations

Midday leaf water potential (Ψ_{md}), and predawn water potential (Ψ_{pd}) were measured every week from May to September. Water potentials were measured with a pressure chamber (Soil moisture Equipment, Corp., Santa Barbara, CA, USA). Measurements of Ψ_{pd} were before sunrise and Ψ_{md} was measured at noon. Four replicates per treatment and cultivar were measured. The gradient between Ψ_{md} and Ψ_{pd} was calculated as: (Ψ_{md} - $\Psi_{pd} = \Delta\Psi$).

Pressure volume curves were measured to obtain leaf turgor loss point ($\Psi_{\pi,TLP}$), osmotic potential at full turgor ($\Psi_{\pi,FT}$), relative water content at turgor loss point (RWC_{TLP}) and bulk leaf modulus of elasticity (ε) in five replicates per treatment (Tyree and Hamel 1972). Curves were measured at the initial phase of water stress treatments (later June dates for each season). Leaves were collected the day before at the evening and were left to rehydrate overnight before P-V determination. Leaf water potential was measured using a pressure chamber (Soil moisture Equipment. Corp., Santa Barbara, CA, USA) and leaf weight were measured with an analytical balance (Kern ABT320-4M, precision of 0.0001 g) during a slow dehydration process in the laboratory. Turgor loss point was located at the inflection point of the $1/\Psi_{leaf}$ versus RWC curve. The fitting method proposed by Sack & Pasquet-Kok (2011) was used to fit the P-V curves.

Gas exchange measurements

Leaf gas exchange was measured using a portable open gas exchange system (Li-6400; Li-Cor, Inc., Nebraska, USA) equipped with a light source (Li-6400-02B LED, Li-Cor). Environmental conditions in the chamber were of 1500 µmol m^{-2} s^{-1} of photosynthetic photon flux density, ambient air temperature and a CO_2 concentration of 400 µmol mol^{-}

[1]. Stomatal conductance (g_s), photosynthesis (A_N) and transpiration (E) were measured monthly at mid- morning around 11-13 am (local time) in younger fully expanded leaves of five plants per treatment.

Kh measurements

Whole plant hydraulic conductance (K_{hplant}) was calculated considering K_{hplant} from the Ohm's law analogy for the soil–plant–atmosphere continuum (Lovisolo *et al.* 2002):

$E = K_{hplant}$ x ($\Psi_{soil} - \Psi_{leaf}$); (1)

where E, Ψ_{leaf} and Ψ_{soil}, were transpiration rate, leaf water potential and soil water potential, respectively. Ψ_{md} was taken as Ψ_{leaf} and Ψ_{pd} was taken as a proxy for $\Psi_{soil.}$

ABA extraction, purification and quantification

ABA was determined by liquid chromatography–tandem mass spectrometry (UHPLC-MS-MS, Agilent 1290 Infinity, Waldbronn, Germany) following the method described by Gomez-Cadenas *et al.* (2002). Xylem leaf sap was extracted in the field with a Scholander chamber at 10th July 2012 and 23rd and 27th of August 2011 and 2012 respectively at 9 o'clock (local hour). A maximum overpressure of 0.2 MPa was applied until 10-15 µL of sap was obtained, which occur typically after 2-3-min. The sap was collected in 0.5 mL vials and immediately frozen in liquid nitrogen in the field. Once in the lab samples were stored until use in a -80 ℃ freezer. Prior determination, sap was thawed at room temperature and 1 µL of deutered-ABA (δ-ABA), as an internal standard, was added to 10 µL of each sample. δ-ABA was prepared following (Gomez-Cadenas *et al.* 2002). Samples with the internal standard were then centrifuge at 15000 *g* for 15 min at 4℃, prior to UHPLC-MS-MS analysis.

Statistical analysis

Statistical differences between means were assessed by an analysis of variance (ANOVA). When differences were significant a multiple comparison of means post hoc Duncan ($P<0.05$) was performed with SPSS 19.0 (IBM Corp., Armonk, NY, USA). Regression coefficients and correlations were calculated with the 11.0 Sigma Plot software package (Systat Software, Chicago, IL, USA).

RESULTS

Under Well Watered (WW) conditions, Tempranillo and Grenache plants showed predawn water potential (Ψ_{pd}) values equal or higher than -0.4 MPa and -0.3 MPa in 2011 and 2012, respectively (Fig. 1AB) and no differences were found between cultivars. Under water stress treatments (WS) a clear reduction of Ψ_{pd} was found between cultivars and Tempranillo WS showed a larger Ψ_{pd} than Grenache WS. However, in both years, the gradient of water potential between soil and leaf ($\Delta\Psi = \Psi_{md} - \Psi_{pd}$) tended to increase throughout the season (Fig 1C D) from values around 0.6 - 0.7 MPa in May to values around -1 to -1.2 MPa in August at the end of the experiment for both WW and WS, with significant differences between treatments and cultivars.
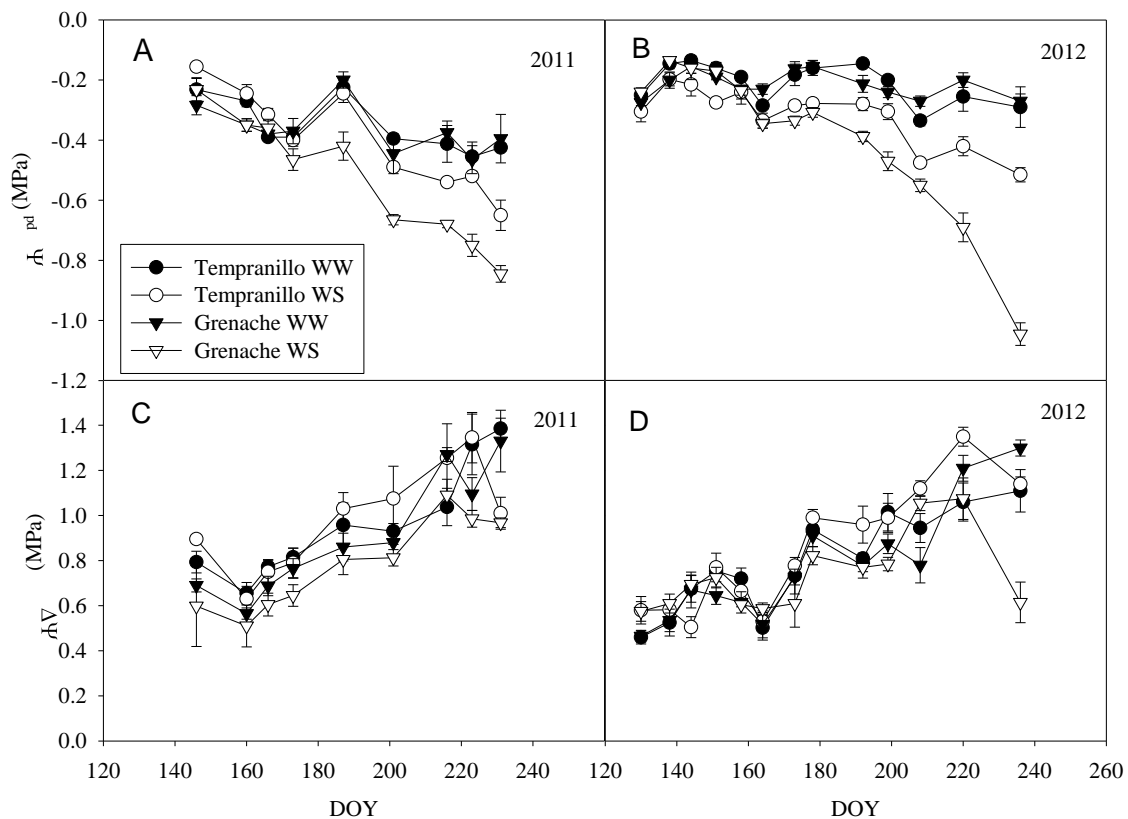

Figure 1: Predawn leaf water potential (Ψ_{pd}) and gradient between predawn and midday water potential ($\Delta\Psi$) during the two years of experiment. Values are four replicates ± standard errors. Letters denote significant differences between treatments and cultivars each day (P<0.05)

In relation to leaf water relations, $\Psi_{\pi,FT}$ and $\Psi_{\pi,TLP}$ were similar in both years. There were significant differences (P<0.05) between cultivars in their osmotic adjustments, with Tempranillo having in general higher osmotic adjustment (Table 2). Regarding

86

treatments, Tempranillo WS presented higher osmotic adjustment than Grenache WS, which shows a significant difference in the osmotic regulation. There were differences in RWC_{TLP} between cultivars, with Tempranillo having smaller values than Grenache. In contrast, ε was not significantly different between cultivars, although Tempranillo tended to present higher values indicating more rigidity in their cell wall.

	GWW 2011	GWW 2012	GWS 2011	GWS 2012	TWW 2011	TWW 2012	TWS 2011	TWS 2012
$\Psi_{\pi,FT}$ (MPa)	-0.88 ± 0.07[b]	-0.98 ± 0.02[ab]	- 0.81 ±0.03[b]	-0.85 ± 0.05[b]	-0.83 ± 0.04[b]	-0.95 ± 0.02[ab]	-1.09 ±0.11[a]	-1.13 ±0.09[a]
$\Psi_{\pi,TLP}$ (MPa)	-1.33 ± 0.08[abc]	-1.30 ±0.02[abc]	-1.27 ± 0.04[bc]	-1.18 ± 0.05[c]	-1.23 ± 0.06[c]	-1.33 ± 0.05[abc]	-1.51 ±0.10[ab]	-1.46 ±0.07[a]
RWC_{TLP} (%)	92.41 ± 0.33[bc]	92.52 ± 0.33[bc]	93.06 ±0.40[bc]	92.56 ±0.59[bc]	93.80 ± 0.41[c]	91.37 ± 0.90[ab]	90.45 ±0.51[a]	90.57 ±0.73[a]
ε (MPa)	10.88 ± 0.74[a]	12.46 ± 0.60[a]	10.92 ±0.23[a]	11.23 ±0.73[a]	12.37 ± 0.81[a]	10.53 ± 1.35[a]	12.30 ±1.14[a]	12.95 ±0.99[a]

Table 2: Leaf water relations parameters of Tempranillo and Grenache in last June dates. Osmostic potential at full turgor ($\Psi_{\pi,FT}$), osmotic potential at turgor loss point ($\Psi_{\pi,TLP}$), relative water content at turgor loss point (RWC_{TLP}) and modulus of elasticity (ε) are represented for each year and treatment. Where G corresponds to Grenache and T to Tempranillo both treatments are presented as WW (Well Watered) and WS (Water stress). Values are 5 means ± standard error. Different letters indicate significant differences between treatments and cultivars.

Leaf gas exchange parameters decreased throughout the season (Fig 2) in both years. For example, g_s gradually decreased achieving in August a reduction to 25% of initial values in WW conditions (Fig 2 C, D). However, the decline in A_N was only evident in August (Fig 2 A, B). This gradual decrease was more pronounced in the case of K_{hplant} being around a 50% of the initial value measured in May in well-watered conditions (Fig 2 E, F).

As expected, WS treatments induced strong reductions of leaf gas exchange parameters throughout the season. However, Tempranillo WS maintained values similar to well watered plants for most of the experimental period having a clear reduction only at the end of the experiment. Grenache WS showed a more severe water stress decreasing A_N, and g_s progressively throughout the season. Even though both cultivars had no significantly difference for A_N, and g_s rates throughout the season, intrinsic water use

efficiency (WUE$_i$) was higher for Grenache cultivar in well watered and more clearly in water stressed treatments (Fig 2 G, H).
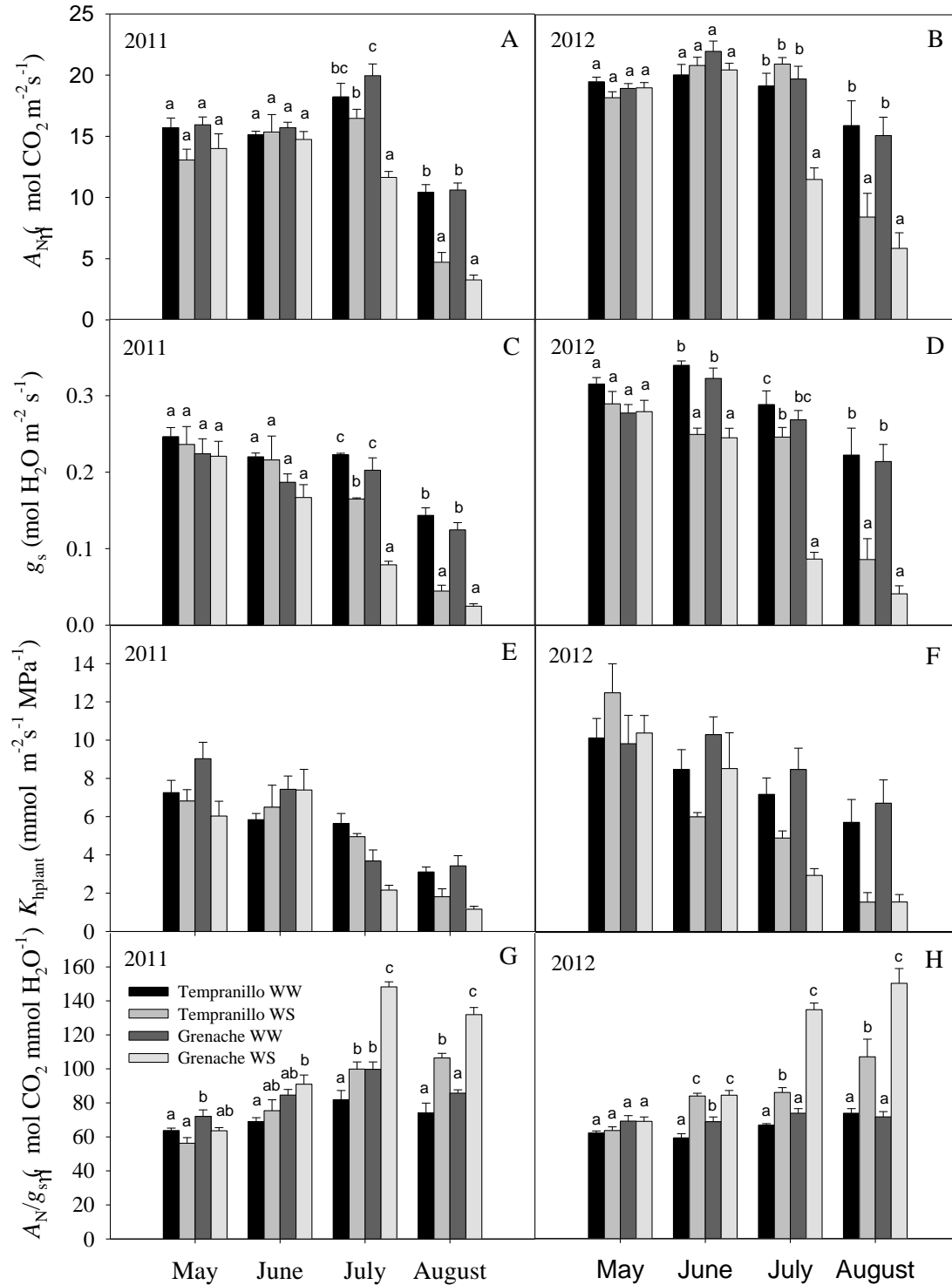

Figure 2: Evolution of photosynthesis (A_N), stomatal conductance (g_s), plant hydraulic conductance (K_{hplant}) and intrinsic water use efficiency (A_N/g_s) for a representative day of each month during 2011 and 2012. Values are five replicates ± standard errors. Letters denote statistic significant differences between treatments and cultivars at each date (P<0.05).

For a better comparison between (WUE$_i$) in response to water stress, Ψ_{pd}, both variables were plotted together (Fig 3). The relationship was calculated separately for each cultivar, showing in both cases to be highly significant and with a high and significant regression coefficient values. As it is clearly showed in Figure 3, for all the different soil water content values corresponding from mild to severe water stress reflected as Ψ_{pd}, Grenache maintained higher WUE$_i$ than Tempranillo.
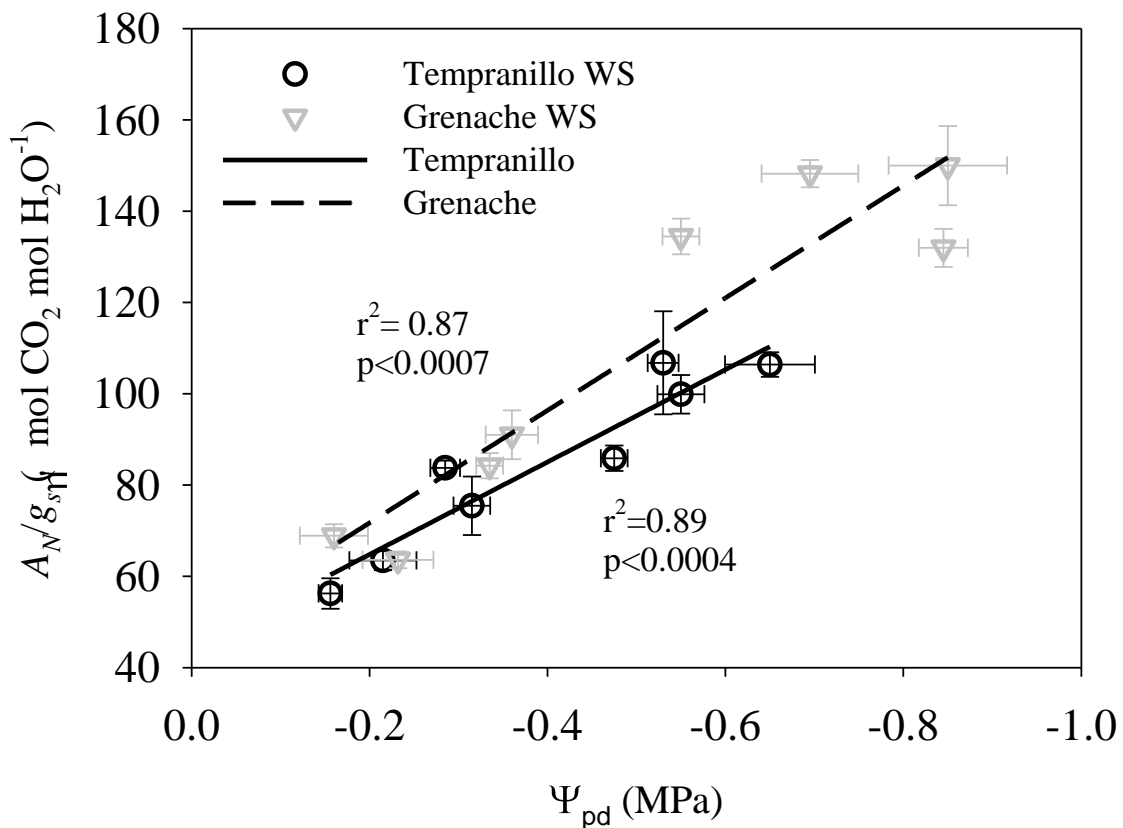

Figure 3: Relationship between predawn water potentital (Ψ_{pd}) and leaf intrinsic water use efficiency (A_N/g_s). Data for water stress treatments was plotted. Values are five replicates ± standard errors.

Despite differences observed in WUE$_i$, the relationship g_s/Ψ_{pd} (Fig 4A) showed that the response curves were very similar for both genotypes. In contrast, when g_s was plotted against Ψ_{md} (Fig 4B) only small differences were observed between cultivars. Moreover the small differences observed indicate that for similar Ψ_{md} Grenache usually maintained lower g_s values.
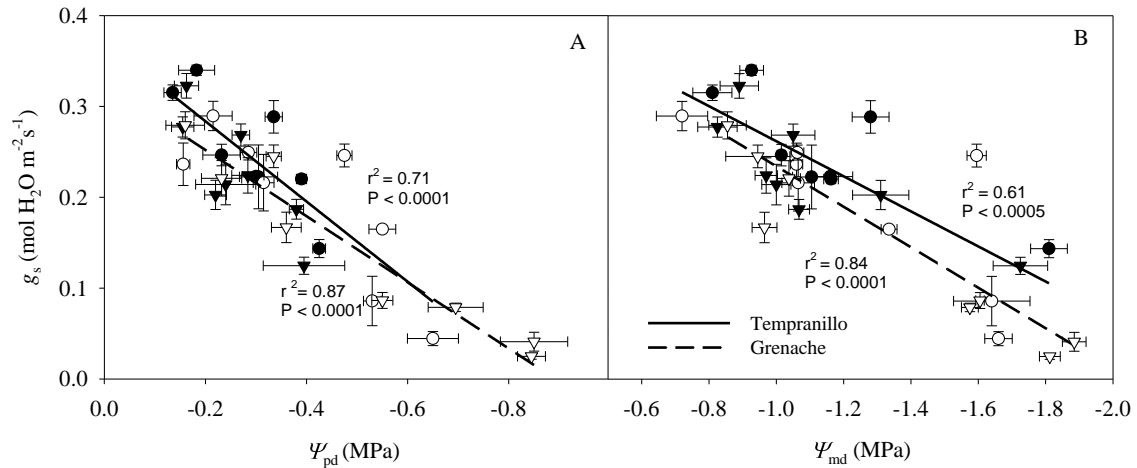
Figure 4: Relationship between stomatal conductance (g_s) with predawn water potential (Ψ_{pd}) (A) and midday water potential (Ψ_{md}) (B). Triangles correspond to Grenache and circles to Tempranillo. Filled symbols represent Well Water treatments and blank symbols represent Water Stress treatments. Values are five replicates ± standard errors.

Variations in Ψ_{pd} were more closely correlated with ABA concentration in xylem sap ([ABA]) (Fig 5). Interestingly, this relationship was clearly dependent on the sampling time showing two significant and clearly different relationships between July and August dates (Fig 5). Well-Watered treatments presented values of [ABA] below 200 μg mL^{-1} and the maximum values of [ABA] were found around 300 μg mL^{-1} and both in July and August observed for Grenache cultivar. Interestingly, July and August presented similar range of [ABA] although in August plants had a larger soil water deficit, as reflected by Ψ_{pd}. In general, Grenache WS presented higher [ABA] than Tempranillo WS showing a clear difference between these two cultivars in the production of [ABA].
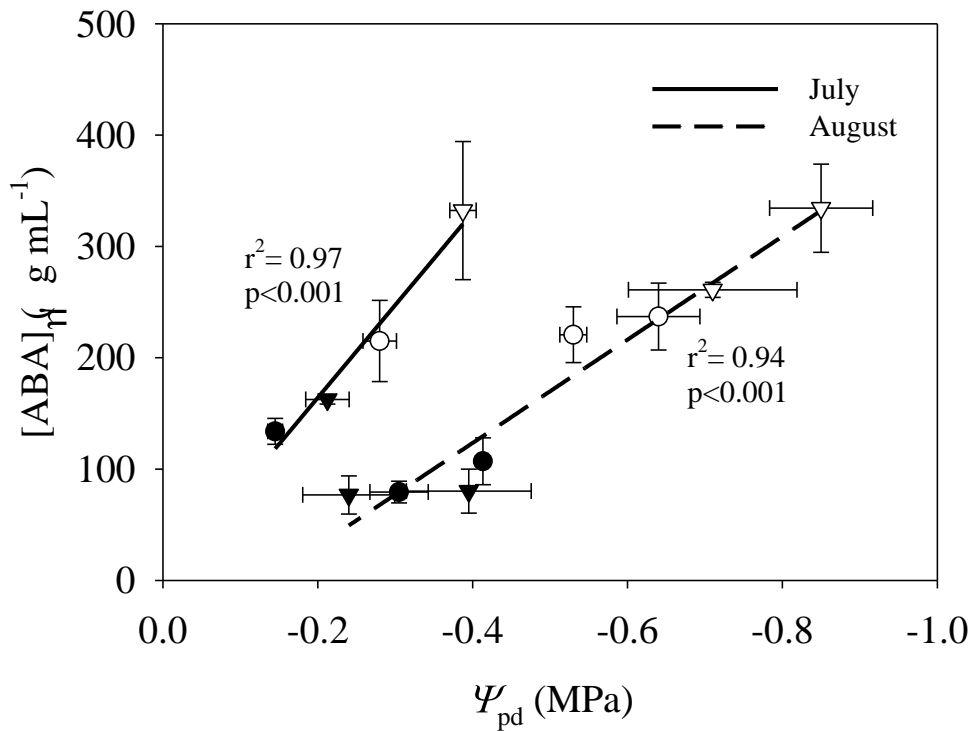
Figure 5: Predawn water potential (Ψ_{pd}) versus Abscisic acid xylem sap concentration ([ABA]) under well water conditions (full symbols) and water stress (blank symbols) between both cultivars. Grenache (triangles) and Tempranillo (circles) were plotted both together in the same graph. Two sampling dates were differentiated, July continuous line and August discontinuous line. Values are five replicates ± standard errors.

Similarly, two different regressions lines were observed when [ABA] was plotted against g_s (Fig 6). These relationships were noticed even though both treatments and cultivars were taken into account, and clearly showed a possible change of sensitivity of g_s to [ABA] with leaf age. Again, although the sensitivity of cultivars were similar, Grenache showed the highest [ABA], which corresponded to the lowest g_s ones.
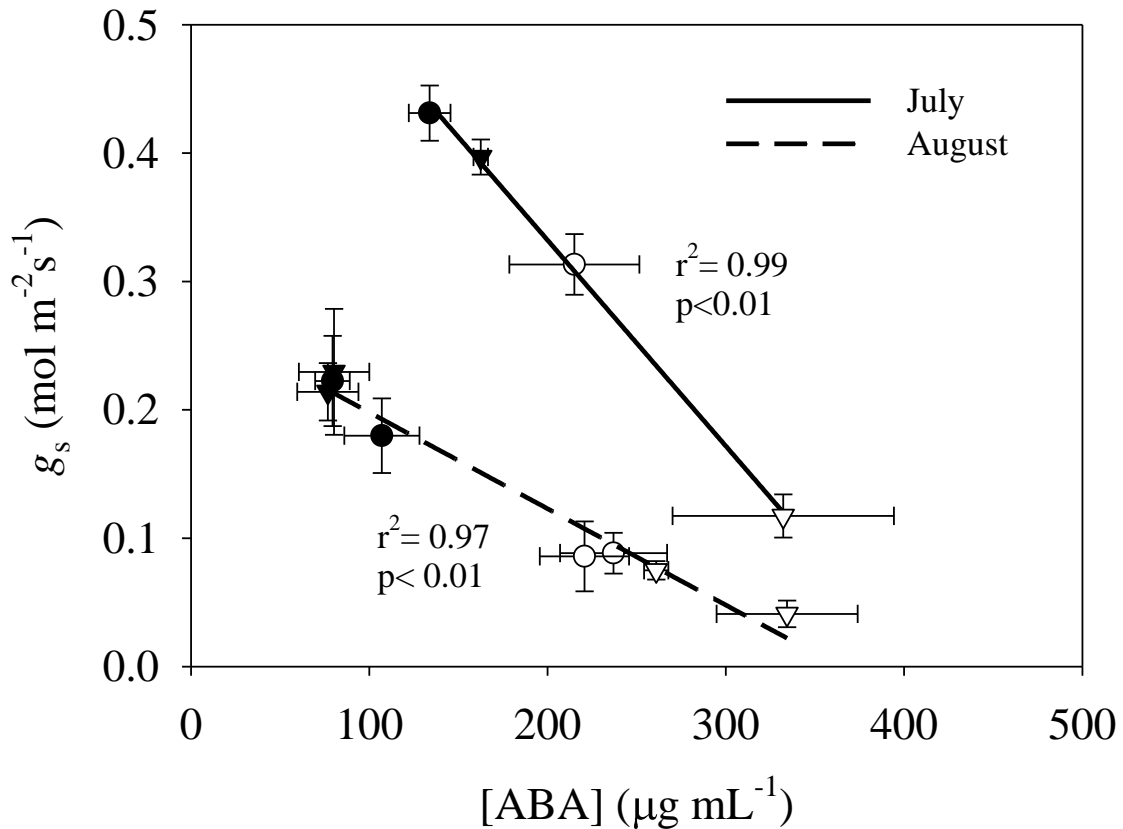
Figure 6: Stomatal conductance (g_s) versus Abscisic acid xylem sap concentration ([ABA]) under well watered conditions (full symbols) and water stress (blank symbols) between both cultivars. Grenache is represented by triangles and Tempranillo by circles. Two sampling dates were differentiated, July continuous line and August discontinuous line. Values are five replicates ± standard errors.

Analyzing the K_h control of g_s, results showed a clear dependence of g_s from K_{hplant}, with significant high regression coefficients, and similar range of K_h values between both cultivars. However, for this character, the g_s dependency from K_{hplant} was not different between dates but differed between cultivars (Fig 7). Consistently, for the same values of K_{hplant}, Tempranillo had higher stomatal conductance (around a 30% higher) all along the K_{hplant} range. This dependency was maintained even though the data from both treatments and seasons were plotted together. In this case, the range of variation of g_s was almost similar for both cultivars, showing a clear difference between them in the K_{hplant} regulation of g_s.
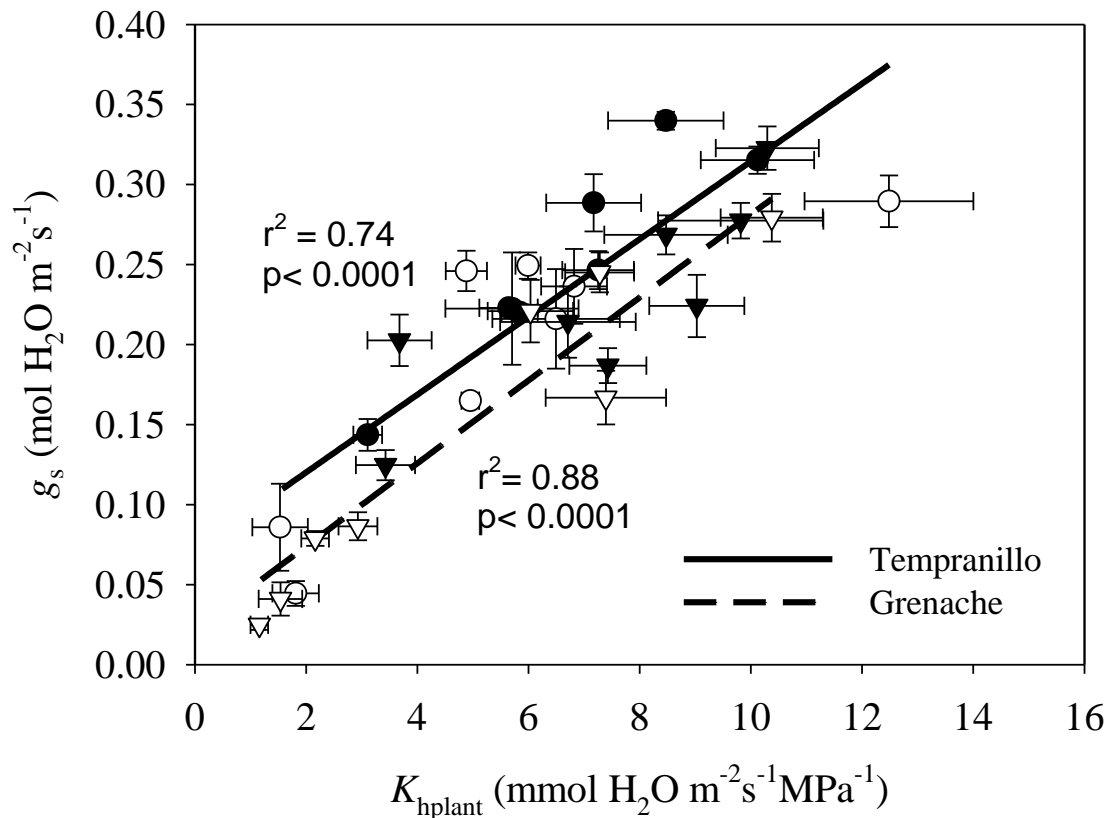
Figure 7: Relationship between plant hydraulic conductance (K_{hplant}) and stomatal conductance (g_s) between cultivars Tempranillo (circles) and Grenache (triangles) under two water treatments Well Watered (full symbols) and Water Stress (blank symbols). Values are five replicates ± standard errors.

Finally, plotting WUE_i against the K_{hplant}, a general increase of A_N/g_s was evident, as expected, but the relationship showed to be also cultivar dependent (Fig 8). The slope of the relationship was higher for Grenache than Tempranillo showing a higher sensitivity of the water use efficiency in respect to the variations in K_{hplant} for this cultivar.
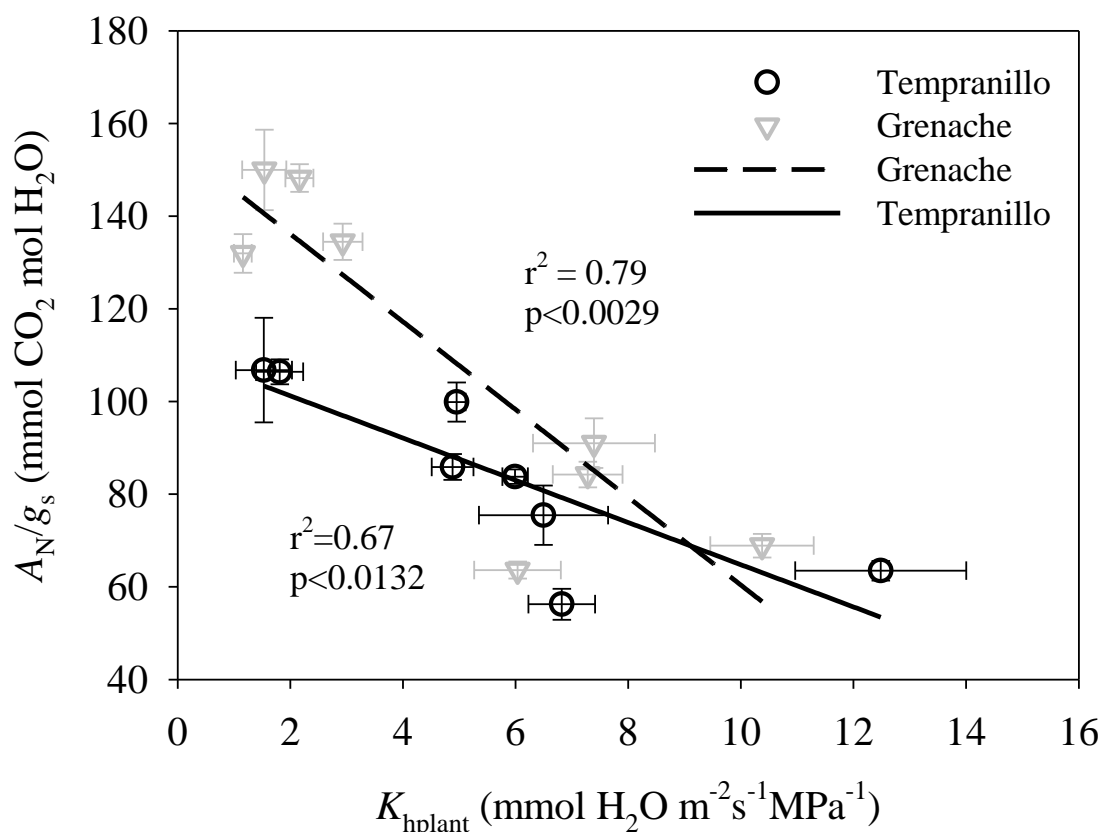
Figure 8: Relationship between plant hydraulic conductance (K_{hplant}) and water use efficiency (A_N/g_s) only for water stress treatments. Circles represent Tempranillo variety and triangles Grenache. Each regression line represents a different variety including data from 2011 and 2012. Regression coefficients are shown on the graphic and values are five replicates ± standard errors.

DISCUSSION

Consistent with previous reports in potted plants, Grenache showed slightly higher water use efficiency (WUE) than Tempranillo (Flexas *et al.* 2010; Tomàs *et al.* 2012;). The data presented in this study for field growing plants during two consecutive years confirmed the reputation of Grenache as more recommendable for drought prone areas (Jones, 2006; Van Leeuwen *et al.* 2013) and of increasing interest for foreseeing climatic change conditions. Higher WUE was more evident under water stress even though under irrigation or mild water stress the differences were also present (Figure 2).

The identification of the physiological basis of this difference was attempted by measuring water relations, leaf gas exchange rates, plant hydraulic conductance and ABA in xylem sap. Grenache and Tempranillo showed differential regulation of water

relations and ABA. Tempranillo plants were able to modify osmotic water potential at full turgor and turgor loss point enabling to maintain turgor at lower water potentials. Also, a lower ABA concentration was found constitutively in Tempranillo. In contrast, Grenache showed more constant water relations and displayed higher levels of ABA. Both cultivars were different in terms of WUE and the combination of ABA, K_{hplant} and leaf water relations were the responsible of this behavior between both cultivars.

Leaf water relations differences

Although soil water availability characteristics were more favorable in Tempranillo plot, Ψ_{pd} was maintained in WW treatments with similar values for both cultivars (Figure 1) and within values typically observed for well-irrigated grapevines (Rodrigues et al. 2008; Rogiers et al. 2012). In WS conditions both cultivars decreased their respective value of Ψ_{pd}. However, Grenache was able to reach more negative values significantly below the Tempranillo ones for both years studied. The gradient between Ψ_{pd} and Ψ_{md} ($\Delta\Psi$) showed a sustained increase with growth season during both years for both cultivars. The later was consistent with findings by Patakas and Noitsakis (1999) and Patakas *et al.* (2001) in Victoria and Savatiano cultivars respectively. This increase was somehow higher in Tempranillo, reflecting an adjustment of their osmotic water potential. This osmotic adjustment seems to be the responsible of the sustained higher values of $\Delta\Psi$ in Tempranillo WS compared to Grenache WS in both years. Similarly, with that higher osmotic adjustment Tempranillo also showed a significant $\Psi_{\pi,TLP}$ (table 1) under water stress conditions. Osmotic adjustment could also contribute to delay the effects of water stress in this cultivar enabling to maintain turgor at lower water potential (Kubiske and Abrams 1990; Sack et al. 2003; Bartlett et al. 2012; Martorell et al. 2014b). In consequence, this effect contributes to maintain stomata opened at lower water potentials. Also, RWC_{TLP}, was maintained constant for both cultivars between 92-90%, being Tempranillo WS able to maintain the turgor at lower RWC. In contrast with the differences observed in osmotic adjustment, no differences were found in leaf ε between cultivars and treatments indicating that adjustment in ε was not an important character driving the acclimation to drought stress (Bartlett *et al.* 2012).

Leaf water use efficiency differences between cultivars

95

A clear decay throughout the summer was observed in gas exchange parameters in WW treatments that could be consequence of leaf age (Wilson et $al.$ 2000). In general, both cultivars showed similar results throughout the season although Grenache clearly maintained non-significant but lower stomatal conductance (g_s) values than Tempranillo and similar values of net photosynthesis (A_N) in Well Watered treatments, which showed more pronounced differences under Water Stress. This behavior results in higher WUE_i (Fig. 2) as was previously reported (Flexas et $al.$ 2010; Tomàs et $al.$ 2012). This sustained reduction of g_s corresponded with a clear decay of K_{hplant}, which along the season was lowered by half of the initial value for WW treatments. The reduction was even bigger for WS plants, but no clear differences were shown between cultivars. That reduction of K_{hplant} with leaf age could be consequence of the formation of tyloses by grapevine under process of senescence (Sun et $al.$ 2008; McElrone et $al.$ 2012) or hydraulic fatigue of the system (Hacke et $al.$ 2001) leading to reduce water availability to leaves and therefore g_s. The water stress decay for leaf gas exchange parameters showed contrasting results depending on the variety being less pronounced for Tempranillo than for Grenache.

The presumably higher soil water availability in Tempranillo plots could affect these results but, when WUE_i was compared against Ψ_{pd} (figure 3) for both cultivars and years the figure showed highly significant determination of Ψ_{pd} on the leaf WUE_i values, but with two differentiated correspondence lines. From this correspondences, Grenache WUE_i values were consistently 15-20% higher than Tempranillo ones for the whole range of Ψ_{pd}. For lower values of Grenache Ψ_{pd}, not found in Tempranillo, the WUE_i values were much higher, but following the same correspondence line. These results confirmed the reputed higher WUE_i of Grenache and their interest as a variety recommendable for drought prone areas (Jones, 2006; Van Leeuwen et $al.$ 2013).

Comparing the regulation of g_s between cultivars

There is abundant literature on the contrasting iso/anyso-hidric behavior of different grapevine cultivars in some way explained by a differential regulation of g_s under water stress, being Grenache reported as isohydric (Shultz 2003). In some recent results the isohydric and anisohydric behavior seemed not constitutive for a characteristic variety and more environmentally dependent (Collins et $al.$ 2010; Domec and Johnson, 2012; Pou et $al.$ 2012). In this field experiment, the typical relationship between g_s and Ψ_{pd}

showed that contrasting cultivars in terms of WUE did not have any clear difference in the response of g_s to Ψ_{pd} (Fig. 3 A). Even though the ranges of water stress measured weren't coincident with the reported by Shultz (2003) (which started to found clear differences around values of Ψ_{pd} of -0.6 MPa). The data presented in this study does not allow marking a differential behavior between both cultivars for the g_s dependency of Ψ_{pd}. It seems, in coincidence with Domec and Johnson, (2012) and Pou *et al.* (2012) that the terms *isohydric* and *anisohydric*, can be not so "constitutive" of a certain variety but with a clear dependency on the environmental conditions.

However, when maximum stomatal conductance was plotted against Ψ_{md}, a particular relationship was found for each cultivar. In general, for the same Ψ_{md} the corresponding g_s was somehow higher for Tempranillo than Grenache. This correspondence of g_s against Ψ_{md} was also reported comparing different roostocks response to water stress by Tramontini *et al.* (2013) but from our results did not show enough consistency to qualify as iso or anysohydric behavior the performance of those cultivars.

ABA and hydraulic conductance

There are an abundance of assessments on the Abscisic Acid (ABA) regulation of the g_s in a wide number of plants (Davies and Zang 1991, Tardieu and Simonneau 1998, Lovisolo *et al.* 2002). For grapevines, the relationship between xylem ABA and g_s is also widely established both in pots and field growing plants (Chaves, *et al.* 2007; Pou *et al.* 2008; Rodrigues *et al.* 2008; Lovisolo *et al.* 2008; Lovisolo *et al.* 2010; Speirs *et al.* 2013). The experiment presented here showed that xylem ABA was well correlated with Ψ_{pd} and the relationship was coincident for both cultivars. However, it was remarkable that this relationship was clearly dependent on the sampling time with a dramatic change between July and August leading to two clearly differentiated regression lines. Tempranillo and Grenache under WW treatments had values of ABA xylem sap lower than 200 μg mL^{-1} (Fig. 4) being similar to the observed in other studies (Speirs *et al.* 2013). Interestingly, Grenache showed higher values of ABA than Tempranillo in the same water stress levels adding a differential characteristic between both cultivars in the dependence of ABA from Ψ_{pd}.

Independent of the sampling time (July and August) Tempranillo WS reached values up to 200 μg mL^{-1} and Grenache up to 300 μg mL^{-1}. Interestingly, for both cultivars as

water stress increased, and Ψ_{pd} was more negative (in correspondence with osmotic adjustment) the highest [ABA] concentration was not changed pointing out that important reductions of Ψ_{pd} between July and August were not corresponded with higher [ABA] in xylem sap.

Such maximum [ABA] seems to be limited by a certain roof likely reflecting the limited capacity to produce it independent of the root water status. The possible effect of variations in transpiration rates could be claimed, but in this case transpiration (as g_s) was lower in August in WS plants so that the calculated total amount of ABA would be lower. That behavior showed a fine-tuning to the water flow, or a limit to the concentration of the ABA in Xylem sap.

The [ABA] versus g_s regression lines were in coincidence with the [ABA] vs water potential relationships, also showing two different regression lines for both cultivars. A steeper regression was observed in July and a less pronounced one for August. For similar [ABA] in xylem sap, g_s lowered in August to around 30% of the July one. That differential response could be due to a change of sensitivity of [ABA] on guard cells or mesophyll cells since [ABA] concentration in xylem sap was the same in July and August, or, maybe was reflecting the important contribution of the fall in the leaf Ψ_{md} values (Fig 1). In consequence, the [ABA] control of g_s seems to be mediated by the Ψ_{pd} which even represents the whole plant water status can be depleted without an extra increase of the [ABA] synthesis or concentration. This could be explained by the same production of [ABA] by the root fraction even though having lower water potentials.

Another important player in the control of stomatal aperture is the K_{hplant} which also showed important variations throughout the season. However, the g_s dependency from K_{hplant} presented a common relationship for both growing seasons studied. Interestingly, this relationship was cultivar dependent so that the regression line for Tempranillo showed for similar K_{hplant} higher g_s values thus showing that Tempranillo and Grenache had different sensibility against hydraulic restrictions being both with similar sensitivity (slope) but showing in Tempranillo higher g_s for similar K_h. Again, the higher osmotic adjustment component of Tempranillo could be playing some role to explain these results. Although of that, deeper analysis of g_s regulation is necessary to justify this assessment.

When WUE$_i$ was plotted against hydraulic conductance a nice differentiation between both cultivars was shown. Tempranillo showed lower WUE$_i$ than Grenache for the same hydraulic conductance. In contrast Grenache kept more closed the stoma for similar K_{hplant} leading to overcome drought stress with presumably lower water expenses as it has been reputed in different studies (Shultz, 2003; Pou *et al.* 2012, Tomàs *et al.* 2012).

Summarizing, the present results confirms the reputation of Grenache as a cultivar with higher leaf WUE, also showing interesting insights to explore the possible role of the differential weight of water relations, [ABA] and K_h on the g_s regulation. This is evidence to consider the osmotic adjustment characteristics and concomitantly leaf turgor as another player in the regulation of g_s under water stress. Furthermore, this study showed that differences in this adjustment could lead to substantial differentiation in the stomatal regulation and the leaf water use efficiency.

ACKNOWLEDGMENTS

REFERENCES

Araus J.L. (2004) The problems of sustainable water use in the Mediterranean and research requirements for agriculture. *Annals of Applied Biology*, **144**, 259-272.

Assmann S.M., & Shimazaki K.I. (1999) The multisensory guard cell. Stomatal responses to blue light and abscisic acid. *Plant Physiology*, **119**, 809-816.

Bartlett M. K., Scoffoni C. & Sack L. (2012) The determinants of leaf turgor loss point and prediction of drought tolerance of species and biomes: a global meta-analysis. *Ecology Letters*, **15**, 393-405.

Beis A., & Patakas A. (2010) Differences in stomatal responses and root to shoot signalling between two grapevine varieties subjected to drought. *Functional Plant Biology,* **37**, 139-146.

Blatt M.R. (2000) Cellular signaling and volume control in stomatal movements in plants. *Annual Review of Cell Development Biology,* **16**, 221-241.

Bota B.J., Flexas J., & Medrano H. (2001). Genetic variability of photosynthesis and water use in Balearic grapevine cultivars. *Annals of Applied Biology*, **138**, 353-361.

Chaves M.M., Santos T.P., Souza C.R., Ortuño M.F., Rodrigues M.L., Lopes C.M., Maroco J.P. & Pereira, J.S. (2007) Deficit irrigation in grapevine improves water-use-efficiency without controlling vigour and production quality. *Annals of Applied Biology,* **150**, 237-252.

Collins M.J., Fuentes S., & Barlow E. W. (2010) Partial rootzone drying and deficit irrigation increase stomatal sensitivity to vapour pressure deficit in anisohydric grapevines. *Functional Plant Biology*, **37**, 128-138.

Correia M.J., Pereira J.S., Chaves M.M., Rodrigues M.L. & Pacheco C.A. (1995) ABA xylem concentrations determine maximum daily leaf conductance of field‐grown *Vitis vinifera L.* plants. *Plant Cell & Environment,* **18**, 511-521.

Davies W.J. & Zhang J. (1991) Root signals and the regulation of growth and development of plants in drying soil. *Annual Review of Plant Biology,* **42**, 55-76.

Dodd I. C. (2005) Root-to-shoot signalling: assessing the roles of 'up'in the up and down world of long-distance signalling in planta. In *Root Physiology: from Gene to Function*. Springer Netherlands.

Domec J.C. & Johnson D. M. (2012) Does homeostasis or disturbance of homeostasis in minimum leaf water potential explain the isohydric versus anisohydric behavior of Vitis vinifera L. cultivars? *Tree Physiology*, **32**, 245-248.

Flexas J., Galmés J., Gallé A., Gulias J., Pou A., Ribas-Carbó M., Tomàs M. & Medrano H. (2010) Improving water use efficiency in grapevines: potential physiological targets for biotechnological improvement. *Australian Journal of Grape & Wine Research* **16**, 106-121

Fraga H., Malheiro A.C., Moutinho-Pereira J. & Santos J.A. (2013) Future scenarios for viticultural zoning in Europe: ensemble projections and uncertainties. *International Journal of Biometeorology*, **57**, 909-925.

Gómez-Cadenas A., Pozo O.J., García‐Augustín P., & Sancho J.V. (2002) Direct analysis of abscisic acid in crude plant extracts by liquid chromatography-electrospray/tandem mass spectrometry. *Phytochemistry Analysis*, **13**, 228-234.

Grams T.E., Koziolek C., Lautner S., Matyssek R. & Fromm J. (2007) Distinct roles of electric and hydraulic signals on the reaction of leaf gas exchange upon re‐irrigation in *Zea mays L. Plant Cell & Environment,* **30**, 79-84.

Hacke U.G., Stiller V., Sperry J.S., Pittermann J. & McCulloh K.A. (2001) Cavitation fatigue. Embolism and refilling cycles can weaken the cavitation resistance of xylem. *Plant Physiology*, **125**, 779-786.

Hannah L., Roehrdanz P.R., Ikegami M., Shepard A.V., Shaw M.R., Tabor G., Zhi L., Marquet P.A. & Hijmans R.J. (2013) Climate change, wine, and conservation. *Procedings of the National Academy of Sciences*, **110**, 6907-6912.

Hubbard R.M., Ryan M.G., Stiller V. & Sperry J.S. (2001) Stomatal conductance and photosynthesis vary linearly with plant hydraulic conductance in ponderosa pine. *Plant Cell & Environment*, **24**:113–121

Jones G., 2006. Climate and terroir: Impacts of climate variability and change on wine. Fine Wine and Terroir—The Geoscience Perspective. Geoscience Canada, eds Macqueen RW, Meinert LD (Geological Association of Canada, St John's, Newfoundland), pp 1–14.

Kubiske M.E. & Abrams M.D. (1990) Pressure‐volume relationships in non‐rehydrated tissue at various water deficits. *Plant Cell & Environment*, **13**, 995-1000.

Lovisolo C., Hartung W. & Schubert A. (2002) Whole-plant hydraulic conductance and root-to-shoot flow of abscisic acid are independently affected by water stress in grapevines. *Functional Plant Biology*, **29**, 1349-1356.

Lovisolo C., Perrone I., Carra A., Ferrandino A., Flexas J., Medrano H. & Schubert A. (2010) Drought-induced changes in development and function of grapevine (Vitis spp.) organs and in their hydraulic and non-hydraulic interactions at the whole-plant level: a physiological and molecular update. *Functional Plant Biology*, **37**, 98-116.

Lovisolo C., Perrone I., Hartung W. & Schubert A. (2008). An abscisic acid-related reduced transpiration promotes gradual embolism repair when grapevines are rehydrated after drought. *New Phytologist.* **180**, 642-651.

Martorell S., Diaz-Espejo A., Medrano H., Ball M.C. & Choat, B. (2014) Rapid hydraulic recovery in *Eucalyptus pauciflora* after drought: linkages between stem hydraulics and leaf gas exchange. *Plant Cell & Environment*, **37**, 617-626.

Martorell S., Medrano H., Tomàs M., Escalona J.M., Flexas J. & Díaz-Espejo A., (2014b). Plasticity of vulnerability to leaf hydraulic dysfunction during acclimation to drought in grapevines: an osmotic-mediated process. *Physiologia Plantarum.* DOI: 10.1111/ppl.12253

McElrone A.J., Brodersen C.R., Alsina M.M., Drayton W.M., Matthews M.A., Shackel K.A., Wada H., Zufferey V. & Choat B. (2012) Centrifuge technique consistently overestimates vulnerability to water stress-induced cavitation in grapevines as confirmed with high-resolution computed tomography. *New Phytologist*, **196**, 661-665.

Medrano H., Escalona J.M., Cifre J., Bota J. & Flexas J. (2003) A ten-year study on the physiology of two Spanish grapevine cultivars under field conditions: effects of water availability from leaf photosynthesis to grape yield and quality. *Functional Plant Biology*, **30**, 607-619.

Medrano H., Pou A., Tomàs M., Martorell S., Escalona J.M., Gulias J. & Flexas J. (2010) Improving water Use Efficiency in Grapevines: Agronomic and Biotechnological Approaches. XXVIII International Horticultural Congress on Science and Horticulture for People (IHC2010): International Symposium on the 931 (pp. 97-107).

Morison J.I.L., Baker N.R., Mullineaux P.M. & Davies, W.J. (2008) Improving water use in crop production. *Philosophical Transactions of the Royal Society of London*, **363**, 639–658.

Mullins M.G., Bouquet A. & Williams L.E. (1992) *Biology of the grapevine*. Cambridge University Press.

Pantin F., Monnet F., Jannaud D., Costa J.M., Renaud J., Muller B., Simonneau T. & Genty B. (2013) The dual effect of abscisic acid on stomata. *New Phytologist*, **197**, 65-72.

Patakas A. & Noitsakis B. (2001) Leaf age effects on solute accumulation in water-stressed grapevines. *Journal of Plant Physiology*, **158**, 63-69.

Patakas A. & Nortsakis B. (1999) Mechanisms involved in diurnal changes of osmotic potential in grapevines under drought conditions. *Journal of Plant Physiology*, **154**, 767-774.

Pou A., Flexas J., Alsina M.M. *et al.* (2008) Adjustments of water use efficiency by stomatal regulation during drought and recovery in the drought-adapted Vitis hybrid Richter-110 (V. berlandieri× V. rupestris). *Physiologia Plantarum*, **134**, 313-323.

Pou A., Medrano H., Flexas J. & Tyerman S. D. (2013) A putative role for TIP and PIP aquaporins in dynamics of leaf hydraulic and stomatal conductances in grapevine under water stress and re-watering. *Plant Cell & Environment*, **36**, 828-843.

Pou A., Medrano H., Tomàs M., Martorell S., Ribas-Carbó M. & Flexas J. (2012) Anisohydric behaviour in grapevines results in better performance under moderate water stress and recovery than isohydric behaviour. *Plant & Soil*, **359**, 335-349.

Rodrigues M.L., Santos T.P., Rodrigues A.P., de Souza C. R., Lopes C. M., Maroco J. P., Pereira J.S. & Chaves M.M. (2008) Hydraulic and chemical signaling in the regulation of stomatal conductance and plant water use in field grapevines growing under deficit irrigation. *Functional Plant Biology*, **35**, 565-579.

Rogiers S.Y., Greer D.H., Hatfield J.M., Hutton R.J., Clarke S.J., Hutchinson P.A. & Somers A. (2012). Stomatal response of an anisohydric grapevine cultivar to evaporative demand, available soil moisture and abscisic acid. *Tree Physiology*, **32**, 249-261.

Romero P., Dodd I. C. & Martinez-Cutillas A. (2012) Contrasting physiological effects of partial root zone drying in field-grown grapevine (*Vitis vinifera L. cv. Monastrell*) according to total soil water availability. *Journal of Experimental Botany*, **63**, 4071-4083.

Sack L., Pasquet-Kok J. & PrometheusWiki contributors. (2011) Leaf pressure-volume curve parameters. *PrometheusWiki.* prometheuswiki.publish.csiro.au/ tiki-

citation.php?page=Leaf%20pressure-volume%20curve%20parameters#sthash. 0GHJnhGz.dpuf

Sack L., Cowan P.D. Jaikumar N. & Holbrook N. M. (2003) The 'hydrology'of leaves: co-ordination of structure and function in temperate woody species. *Plant Cell & Environment*, **26**, 1343-1356.

Schultz H.R. (2003) Differences in hydraulic architecture account for near-isohydric and anisohydric behaviour of two field-grown *Vitis vinifera L.* cultivars during drought. *Plant Cell & Environment*, **26**, 1393-1405.

Speirs J., Binney A., Collins M., Edwards E. & Loveys B. (2013) Expression of ABA synthesis and metabolism genes under different irrigation strategies and atmospheric VPDs is associated with stomatal conductance in grapevine (*Vitis vinifera L. cv Cabernet Sauvignon*). *Journal of Experimetnal Botany*, **64**, 1907-1916.

Stocker O. (1956) Die Abhängigkeit des transpiration von den umweltfaktoren. *In* Encyclopedia of Plant Physiology. Vol. 3. Ed. W. Ruhland. Springer, Berlin, pp 436–488.

IPCC, 2013. Stocker, T. F., Dahe, Q., Plattner, G. K., 2013. Climate Change 2013: The Physical Science Basis. Working Group I Contribution to the Fifth Assessment Report of the Intergovernmental Panel on Climate Change. Summary for Policymakers

Sun Q., Rost T.L. & Matthews M. A. (2008) Wound-induced vascular occlusions in *Vitis vinifera* (Vitaceae): Tyloses in summer and gels in winter. *American Journal of Botany*, **95**, 1498-1505.

Tardieu F. & Simonneau T. (1998) Variability among species of stomatal control under fluctuating soil water status and evaporative demand: modelling isohydric and anisohydric behaviours. *Journal of Experimental Botany*, **49**, 419-432.

Tomás M., Medrano H., Pou A., Escalona J.M., Martorell S., Ribas-Carbó M. & Flexas J. (2012) Water-use efficiency in grapevine cultivars grown under controlled conditions: effects of water stress at the leaf and whole-plant level. *Australian Journal of Grape & Wine Research*, **18**, 164-172.

Tramontini S., Vitali M., Centioni L., Schubert A. & Lovisolo C. (2013) Rootstock control of scion response to water stress in grapevine. *Environmental Experimetal Botany*, **93**, 20-26.

Tramontini S., Döring J., Vitali M., Ferrandino A., Stoll M. & Lovisolo C. (2014) Soil water-holding capacity mediates hydraulic and hormonal signals of near-isohydric and near-anisohydric *Vitis* cultivars in potted grapevines. *Functional Plant Biology,* doi.org/10.1071/FP13263

Tyree M.T. & Hammel H.T. (1972) Measurement of turgor pressure and water relations of plants by pressure bomb technique. *Journal of Experimental Botany*, **23**, 267-282

Van Leeuwen C., Schultz H.R., de Cortazar-Atauri I.G., *et al.* (2013) Why climate change will not dramatically decrease viticultural suitability in main wine-producing areas by 2050. *Procedings of the National Academy of Sciences* **110**, E3051-E3052.

Wilkinson S. & Davies W.J. (2008) Manipulation of the apoplastic pH of intact plants mimics stomatal and growth responses to water availability and microclimatic variation. *Journal of Experimental Botany* **59**, 619-631.

Wilson K.B., Baldocchi D.D. & Hanson P.J. (2000) Quantifying stomatal and non-stomatal limitations to carbon assimilation resulting from leaf ageing and drought in mature deciduous tree species. *Tree Physiology*, **20**, 787-797.

Zhang J. & Davies W.J. (1990) Does ABA in the xylem control the rate of leaf growth in soil-dried maize and sunflower plants? *Journal of Experimental Botany*, **41**, 1125-1132.

Zhang Y., Oren R. & Kang S. (2012) Spatiotemporal variation of crown-scale stomatal conductance in an arid *Vitis vinifera L. cv. Merlot* vineyard: direct effects of hydraulic properties and indirect effects of canopy leaf area. *Tree Physiology*, **32**, 262-279.

4. MODELING THE GRAPEVINE RESPONSE TO WATER STRESS: PROCESS-BASED MODELS OF STOMATAL CONDUCTANCE AND PHOTOSYNTHESIS

4.1. The temperature response of mesophyll conductance is the main determinant of the differences in optimal temperature for photosynthesis between two grapevine cultivars.

Martorell S, Tomàs M, Pou A., Ribas-Carbó M, Galmés J, Escalona JM, Flexas J, Medrano H, Diaz-Espejo A.

[1]Research Group on Plant Biology under Mediterranean Conditions, Departament de Biologia, Universitat de les Illes Balears, Carretera de Valldemossa Km 7.5, 07122 Palma de Mallorca, Illes Balears, Spain;

[2]Irrigation and Crop Ecophysiology Group, Instituto de Recursos Naturales y Agrobiología de Sevilla (IRNAS, CSIC). Avenida Reina Mercedes 10, 41012 Sevilla, Spain

ABSTRACT

Photosynthesis is one of the most important physiological processes taking place in plants. In this study we parameterized the photosynthesis model of Faquhar et al., (1980). Temperature response of the photosynthetic parameters and mesophyll conductance to CO_2 (g_m) were obtained for grape vine Grenache *cvar* and compared with the published ones for Semillon *cvar*. Results showed a differential g_m response between cultivars in the response to temperature. Contrarily, the same response curve of the photosynthetic parameters was obtained for both cultivars. The application of a new contribution analysis (Buckley and Diaz-Espejo 2014) differentiates them as different adapted to climates being differently regulated by diffusional components and equally by biochemical regulation. We suggest that this kind of studies can help to elucidate the best adapted cultivars to climate change conditions.

INTRODUCTION

Global warming conditions will impact severely the Mediterranean regions with important consequences on socio-economy, agriculture and conservation biology. According to predictions, in the near future there will be more frequent extreme temperature events joined with a general mean temperature increase (IPCC 2013). In fact, heat waves will be striking more often and for longer periods in different regions worldwide (Teskey et al., 2014). Grapevine (mostly located in the Mediterranean climate) is a clearly a vulnerable crop in this future climate change scenarios since its growth period coincides with the lowest water availability and highest temperatures (Flexas et al., 2010; Shultz and Stoll, 2010; Hannah et al., 2013). Consequently, there is a need to improve our capacity to assess what is going to happen in the near future and how grapevine will respond to these new scenarios. Plant physiology process-based models developed using knowledge of previous studies could be an important tool to understand and predict which constraints can affect the future of vineyards.

Photosynthesis (A_N) is a physiological process intimately related to growth and production in plants. Farquhar et al., (1980) proposed a process-based model for A_N (hereafter "FvCB model") based on the biochemistry process of the ribulose-1-5-biphosphate (RuBisCo) fixing CO_2. RuBisCo can be limited by the carboxylation rate or

by the electron transport rate. Those limitations are variables dependent on the temperature and it has been shown to be specie-specific (Diaz-Espejo 2013).

On the other hand, CO_2 supply constitutes another limitation for A_N (Flexas *et al.,* 2008; Flexas et al., 2012; Flexas and Diaz-Espejo 2014). CO_2 must overcome two resistances on the diffusion pathway to the carboxylation sites. Those resistances are stomatal conductance (g_s), which has been always taken in account, and g_m, that has not been always took in account and its inclusion improve the estimation of FvCB photosynthetic parameters (Warren and Dreyer, 2006; Flexas et al., 2006; Flexas et al., 2008; Flexas et al., 2012). g_m has been largely ignored modeling grapevine photosynthetic parameters response to temperature (Shultz, 2003; Greer and Weedon, 2012; Prieto et al., 2012) being necessary its inclusion to understand better the mechanistic basis of the photosynthetic machinery.

On the other hand, g_m is able to vary according to different environmental variables (for review: Flexas *et al.,* 2008; Flexas *et al.,* 2012) being also variable in response to temperature. In the last years, several studies highlighted the diversity response of g_m to temperature of different species (Bernacchi et al., 2002; Warren and Dreyer 2006, Yamori et al., 2006, Diaz-Espejo et al., 2007; Flexas et al., 2008; Warren 2008; Egea et al., 2011; Evans & von Caemmerer 2013; Walker *et al.,* 2013; von Caemmerer and Evans, 2014) and it can be concluded that g_m response to temperature is specie-specific (Flexas and Diaz-Espejo 2014). In that sense, the recent work by von Caemmerer and Evans (2014) confirmed this idea measuring under similar experimental and methodological conditions nine species. However, it has never been tested if there are differences in the kinetic of response to temperature between cultivars of the same species.

Grapevine is cropped from cold areas in North Europe to the hottest South ones, showing a wide inter-cultivar variety with cultivars more adapted to high and low environmental average temperatures (Mullins et al., 1992). Recently, the leaf temperature response was deeply characterized in a cold adapted cultivar (Semillon blanc) by Greer and Weedon (2012), but (1) the fact that these authors did not considered g_m in their study; (2) that new photosynthesis limitation response models that have recently been developed (Buckley and Diaz-Espejo, 2014), and (3) the interest of comparing these previous results with more heat adapted cultivars; altogether

provides an interesting scenario to explore the interest of photosynthetic models to contrast the temperature responses of cold adapted and heat adapted cultivars.

In consequence, the goals of this study are: i) to estimate the response of the parameters of the FvCB model of photosynthesis to temperature in Cc-basis; ii) to compare two grapevine cultivars considered to be adapted to different temperatures; iii) and to identify and quantify the contributions to the reduction in photosynthesis of the different variables that determine the photosynthesis rate at several temperatures.

MATERIALS AND METHODS

Plant material and treatments

The experiment was performed at the University of Balearic Islands during summer 2010 (from 16th June to 19th July). Grenache plants were obtained by direct hard wood shoots rooting. Cuttings were soaked in 0.3% Captan solution for 3h and hydrated for 24 h and left in a rooting bench. When cuttings had 4-5 leaves, plants were transplanted to pots of 15 L containing a mixture of organic substrate and perlite mixture (3:1). After that, they grew outdoors (1 month). Until the start of the experiment plants were irrigated every day and were supplemented with an organic mineral fertilizer NPK (Nitrogen, Phosporous and Potassium). Plants were irrigated at field capacity every day during the experiment.

Photosynthesis model

Photosynthesis has been modelled using the mechanistic model proposed by Farquhar et al., (1980). This model is based on the knowledge of the biochemistry of the enzyme Ribulose-1,5-biphosphate (RuBP). They proposed that leaf net photosynthesis could be modelled as the minimum of two limiting rates: A_v the limitation due to carboxylation rate and A_j when the Ribulose-1,5-biphosphate (RuBP) regeneration is limited.

$A_n = min\ (A_v, A_j) - R_d$

The following are the equations describing the limitations encountered:

$$A_v = V_m \frac{c_c - \Gamma_*}{c_c + K_c\left(1 + O/K_o\right)} - R_d \text{, and}$$

$$A_j = \tfrac{1}{4} J \frac{c_c - \Gamma_*}{c_c + 2\Gamma_*} - R_d,$$

where V_m is maximum carboxylation capacity, J is potential electron transport rate, C_c is chloroplastic CO_2 concentration, Γ^* is photorespiratory CO_2 compensation point, K_c and K_o are the Michaelis constants for RuBP carboxylation and oxygenation, respectively, O is oxygen concentration and R_d is the rate of non-photorespiratory CO_2 release. Assimilation rate is calculated as the minimum of A_v and A_j.

A_N-c_i curves, photosynthetic parameters and gas exchange.

A_N-c_i curves response were performed to determine the photosynthetic parameters of carboxilation rate (V_c), electron transport rate (J_m) and mesophyll conductance (g_m). An open gas exchange system (Li-6400; Li-Cor, Inc., Lincoln, Nebraska, USA) equipped with an integrated leaf chamber fluorometer (Li-6400-40; Li-Cor Inc., Nebraska, USA) and with the expanded temperature control kit (Li-6400-88) was used. A_N-c_i curves on potted plants were performed at 15, 20, 25, 30, 35 and 40 ºC at a saturating light intensity of 1500 µmol mol^{-1} and ranging CO_2 concentrations (c_a) steeply between 50 and 1800 µmol mol^{-1}. For the measurements at 15, 20 and 25 ºC, plants were placed into a growth chamber with ambient temperature controlled to the corresponding temperature. For 30, 35 and 40ºC, plants were maintained outdoors and leaf temperature was controlled into the leaf chamber. Curves were corrected for gaskets leaks as described by Flexas *et al.,* (2007)

Estimation of V_c, J_m and g_m estimation

V_c, J_m and g_m was estimated using the method proposed by Ethier and Livingston (2004) using it to fit the parameters by nonlinear least square regression. Also a temperature response of V_c, J_m and g_m from Semillon cultivar (Greer and Weedon, 2012) was recalculated using the same approach to estimate their parameters in Cc base.

Additionally g_m was also estimated in Grenache cultivar using Hartley et al., (1992).

where the photochemical efficiency of photosystem II (Φ_{PSII}) was determined according to Genty, Briantais & Baker (1989)

$\Phi_{PSII} = (F_m' - F_s)/F_m'$,

where F_s is the steady-state fluorescence yield and F_m' the maximum fluorescence yield obtained with a light-saturating pulse of 8000 µmol m^{-2} s^{-1}.

Then the electron transport rate (J_{Flu}) was calculated as follows:

$$J_F = \Phi_{PSII} \cdot PPFD \cdot \alpha \cdot \beta$$

where PPFD is the photosynthetically active photon flux density, α is leaf absorptance and β reflects the partitioning of absorbed quanta between photosystems II and I. The product of $\alpha \cdot \beta$ was determined following Valentini *et al.,* (1995) using the relationship obtained between Φ_{PSII} and Φ_{CO2} varying light intensity under non photo respiratory conditions (less than 1% of O_2 in the atmosphere).

After that, mesophyll conductance (g_m) to CO_2 was estimated according to Harley et al., (1992).

$$g_m = \frac{A_N}{C_i - \dfrac{\Gamma *\left(J_F + 8(A_N + R_d)\right)}{J_F - 4(A_N + R_d)}}$$

where A_N and C_i were taken from gas exchange measurements at saturating light. Dark respiration (R_d) was determined by gas exchange measurements after plants had been dark adapted for 2 h during the afternoon, at 30ºC and estimated for the different temperature using the temperature dependencies of Bernacchi *et al.,* (2001). The chloroplastic CO_2 photocompensation point ($\Gamma*$) and their temperature dependency was extracted from Bernacchi et al., (2002).

Values obtained from g_m were used to transform A_N-c_i curves responses into a A_N vs choloroplastic CO_2 concentration (C_c) curve responses as $C_c = C_i - A_N/g_m$

The resulting response curves of V_c, J_m, and g_m to temperature were modeled according to the equations proposed by Warren and Dreyer (2006) for a non-peaked function responses:

$$P_{(T)} = P_{(T_{ref})} e^{\left[\frac{E_a}{RT_{ref}}\left(1 - \frac{T_{ref}}{T}\right)\right]}$$

where $P(_{T_{ref}})$ is the parameter value at a reference temperature, T_{ref} is the reference temperature (25ºC, 298 ºK), E_a (J mol^{-1}) is the activation energy, R (8.3143 J K^{-1} mol^{-1}) is the gas constant, and T (ºK) is the leaf temperature.

And as follows for the peaked function responses:

$$P_{(T)} = \frac{P_{(T_{ref})} e^{\left[\frac{E_a}{RT_{ref}}\left(1-\frac{T_{ref}}{T}\right)\right]}}{1 + e^{\left[\frac{\Delta ST - E_d}{RT}\right]}} \left(1 + e^{\left(\frac{\Delta ST_{ref} - E_d}{RT_{ref}}\right)}\right)$$

where ΔS (J K^{-1} mol^{-1}) is an entropy term, E_d (J mol^{-1}) is the deactivation energy, and $P_{(T_{ref})}$ is the potential value that the parameter would have at the reference temperature (T_{ref}).

Contributions analysis

The contributions analysis proposed by Buckley and Diaz-Espejo (2014) were used to partition changes in photosynthesis into contributions from the underlying variables. This new approach uses numerical integration having the advantage to avoid the bias caused by the discrete approximations and avoiding the need to compute partial derivatives for each variable and relying instead on substitution in the photosynthesis model. This approach is easily extended to encompass effects of changes in any photosynthetic variable, under any conditions.

This approach integrates changes produced in A across the interval between reference value (in this case the optimum temperature for photosynthesis) and comparison points (each temperature of measurement) and the resulting contributions are expressed as percentages of the value of A at a reference point (A_{ref}). The contribution from a variable x_j to a change in A is defined as:

$$\rho_{xj} \equiv \frac{100}{A_{ref}} \cdot \sum_{k=0}^{n-1} \left[\delta A \middle| \delta x_j\right]_k^{k+1}$$

Similarly, it can be calculated the total contribution from diffusional conductances (g_{sc}, g_m and g_{bc});

$$\rho_{diff} \equiv \frac{100}{A_{ref}} \cdot \sum_{k=0}^{n-1} \left[\delta A \middle| \delta g_{sc}, \delta g_{bc}, \delta g_m\right]_k^{k+1}$$

and the total contribution from variables that involve the biochemistry of photosynthesis;

$$\rho_{bio} \equiv \frac{100}{A_{ref}} \cdot \sum_{k=0}^{n-1} \left[\begin{array}{c} \delta A \middle| \delta V_{cmax}, \delta J_{max}, \delta V_{tpu}, \delta R_d, \\ \delta K_c, \delta K_o, \delta \Gamma_*, \delta \phi, \delta \theta_j, \delta i \end{array}\right]_k^{k+1}$$

111

RESULTS

A_N-C_i curves at six different temperatures were analyzed following the curve-fitting method proposed by Ethier and Livingston (2004) and results are shown in Fig. 1. Previously, g_m was estimated independently by the variable-J method (Harley et al., 1992) obtaining a good agreement with the g_m obtained by the curve fitting method ((P<0.05; r^2= 0.75). An exponential response and a peaked function curve were obtained for maximum carboxylation rate (V_c) and maximum electron transport rate (J_m) in response to temperature, respectively (Fig 1a, 1b) expressed in a C_c-basis.

Photosynthetic Parameters	Value at 25ºC (μmol mol^{-1})	E_a (KJ mol^{-1})	ΔS (J K^{-1} mol^{-1})	E_d (KJ mol^{-1})
V_c	88.04	67.23	-	-
J_m	92.11	44.10	469.86	150.00
g_m	0.248	84.79	348.80	101.17

Table 1: Photosynthetic parameters obtained by the fit of the equations of Warren and Dreyer, (2006) in response to temperature for Grenache cultivar.

The estimated values calculated this way, taking into account a finite mesophyll conductance (g_m), were higher for V_c and J_m than when they were estimated in a C_i-basis. In a previous study, the response curves to temperature of V_c and J_m were studied for a cold adapted cultivar, *Semillon cvar* on C_i basis (Greer and Weedon, 2012). Data obtained in that study was plotted, recalculated and included in Figures 1 and 2 to be compared with our results of a reputed heat resistant *Grenache cvar*. In C_i-basis data showed absolute differences in V_c between cultivars which clearly increased with temperature (Fig 1 a), but more importantly, it showed a difference in the shape of the response. Semillon presented a peak response to temperature, meanwhile Grenache kept an exponential rise at high temperatures. On the other hand, no difference was evident for J_m when both cultivars were compared.
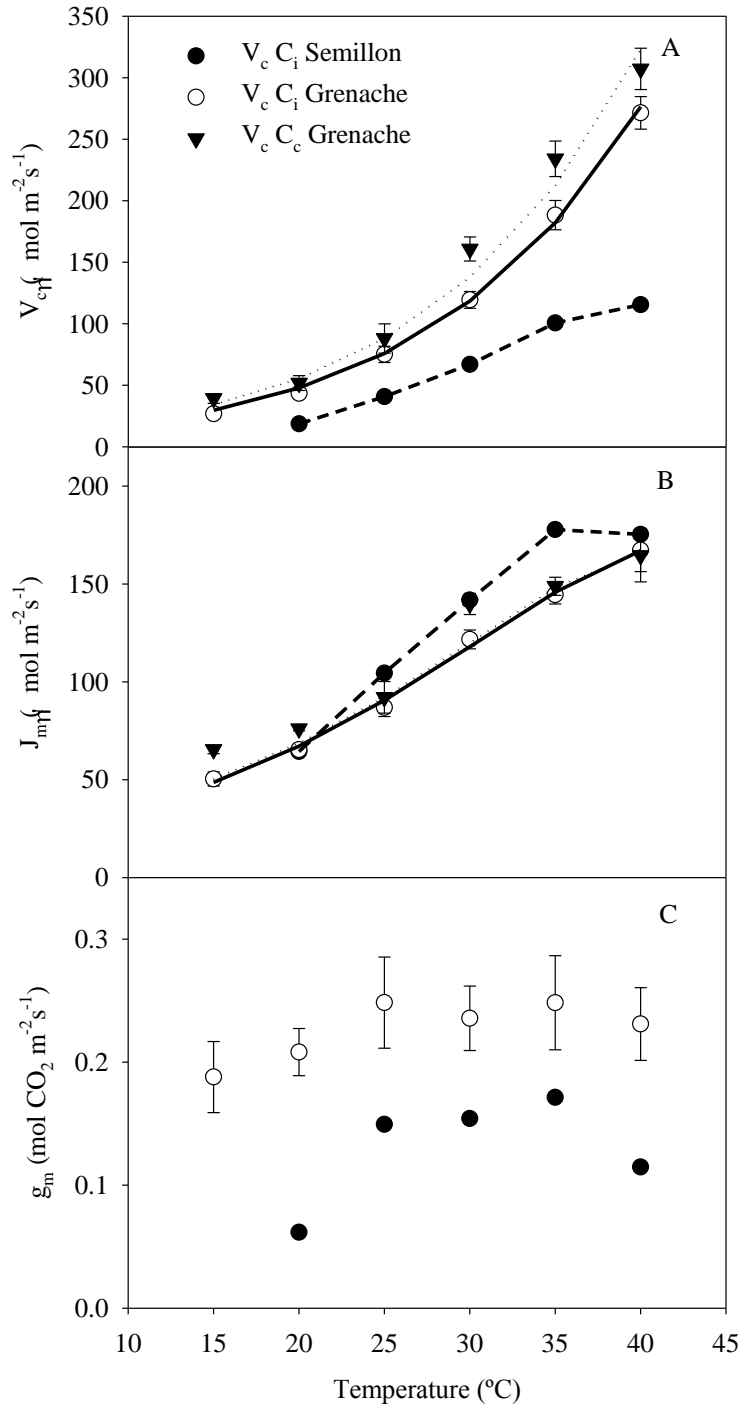
Figure 1: A and B) V_c and J_m versus temperature based on c_i and c_c basis from for Grenache cultivar. There is represented in discontinuos line the Vc and Jm of Semillon variety from the study of Greer and Weedon, 2012. C) mesophyll conductance versus temperature. Black dots corresponds to Semillon and blank dots to Grenache. All data represent the curve obtained for each temperature.

As we are interested in the shape of the response to temperature when comparing cultivars, we decided to normalize the C_c-based V_c, J_m, and g_m by their values at 25 ºC. Thereby, the confounding effects of different absolute values, (which could be related to

differences in nitrogen content), were canceled out. No differences in V_c and J_m response at any temperature were observed between cultivars when they were plotted in C_c-basis (Fig. 2a,b), suggesting a critical impact of g_m in the response to temperature shown in Fig. 1a,b. Figure 2c confirms that the response to temperature of g_m differed between both cultivars. From 25ºC to 35ºC both cultivars presented a similar kinetics of response to temperature. But Semillon decreased g_m in relation to Grenache at both low (15ºC) and high (40ºC) temperatures.
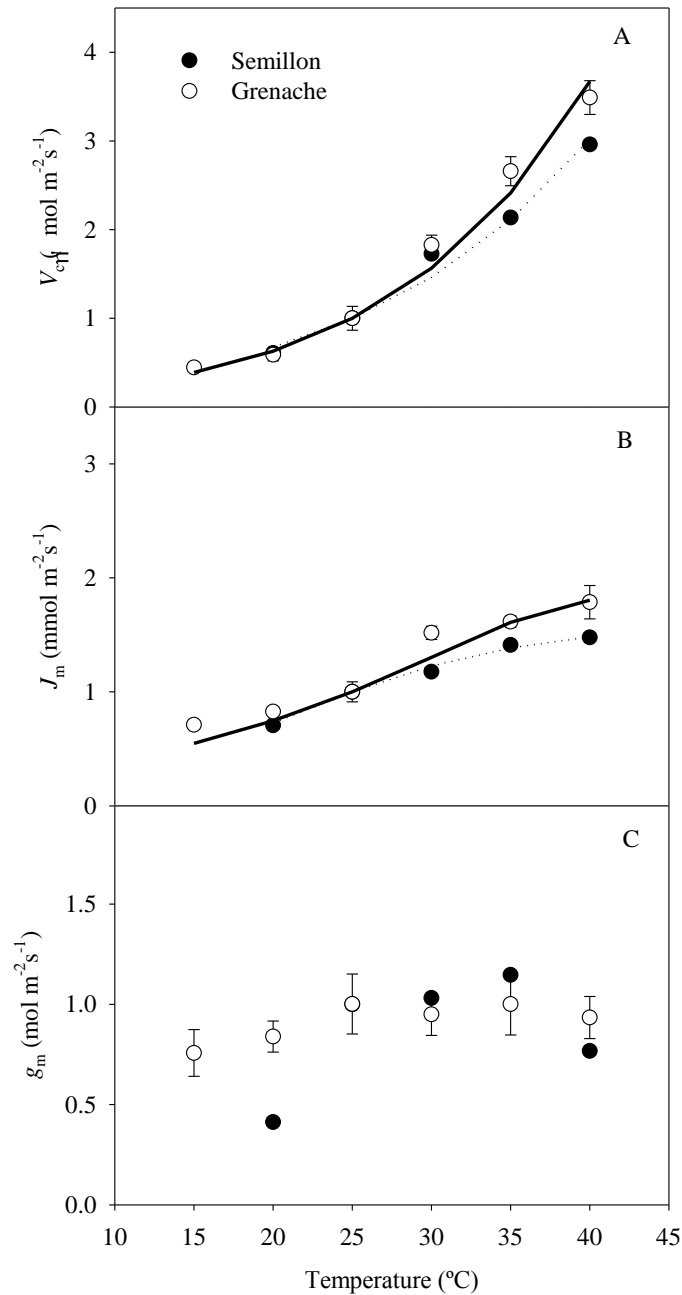
Figure 2: V_c, J_m, and g_m response on C_c basis for Grenache and Semillon cultivars normalized to 1 at 25ºC.

Both varieties differed on the optimum temperature for photosynthesis (A_N) (Figure 3). Grenache showed the optimum at around 35 ºC and Semillon at around 30 ºC.
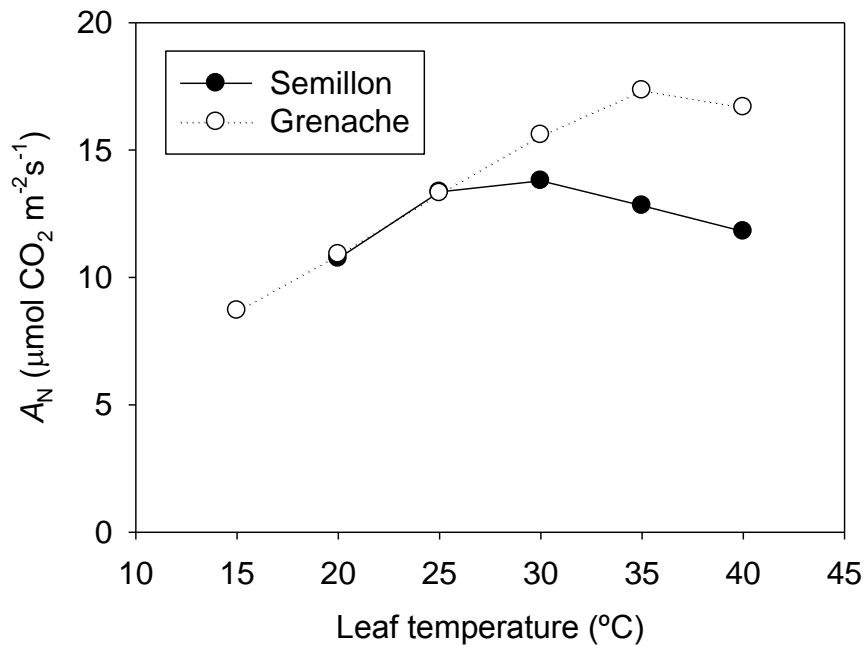

Figure 3: Photosynthesis modelled with the temperature response of V_c and J_m response to temperature vs temperature. Grenache are black dots and Semillon blank dots.

The finite changes in A_N at the different temperatures studied were partitioned into contributions from the changes in the different variables that determine A_N (Fig. 4) by using the approach recently suggested by Buckley and Diaz-Espejo (2014). Firstly, the total relative change in A_N did not differ greatly between both cultivars if we do consider the shift of the optimal toward lower temperature in Semillon, i.e. if we compare for example the total relative change of Grenache at 30 and 25 ºC with Semillon at 25 and 20ºC. At the minimum temperature that we can compare both cultivars, 20ºC, Grenache appears clearly as more sensitive to low temperatures than Semillon (37% vs 23% respectively). At 15 ºC Grenache had a reduction of 49% of its A_N. The relative change in A_N at each individual temperature was partitioned into biochemical and diffusional contributions.
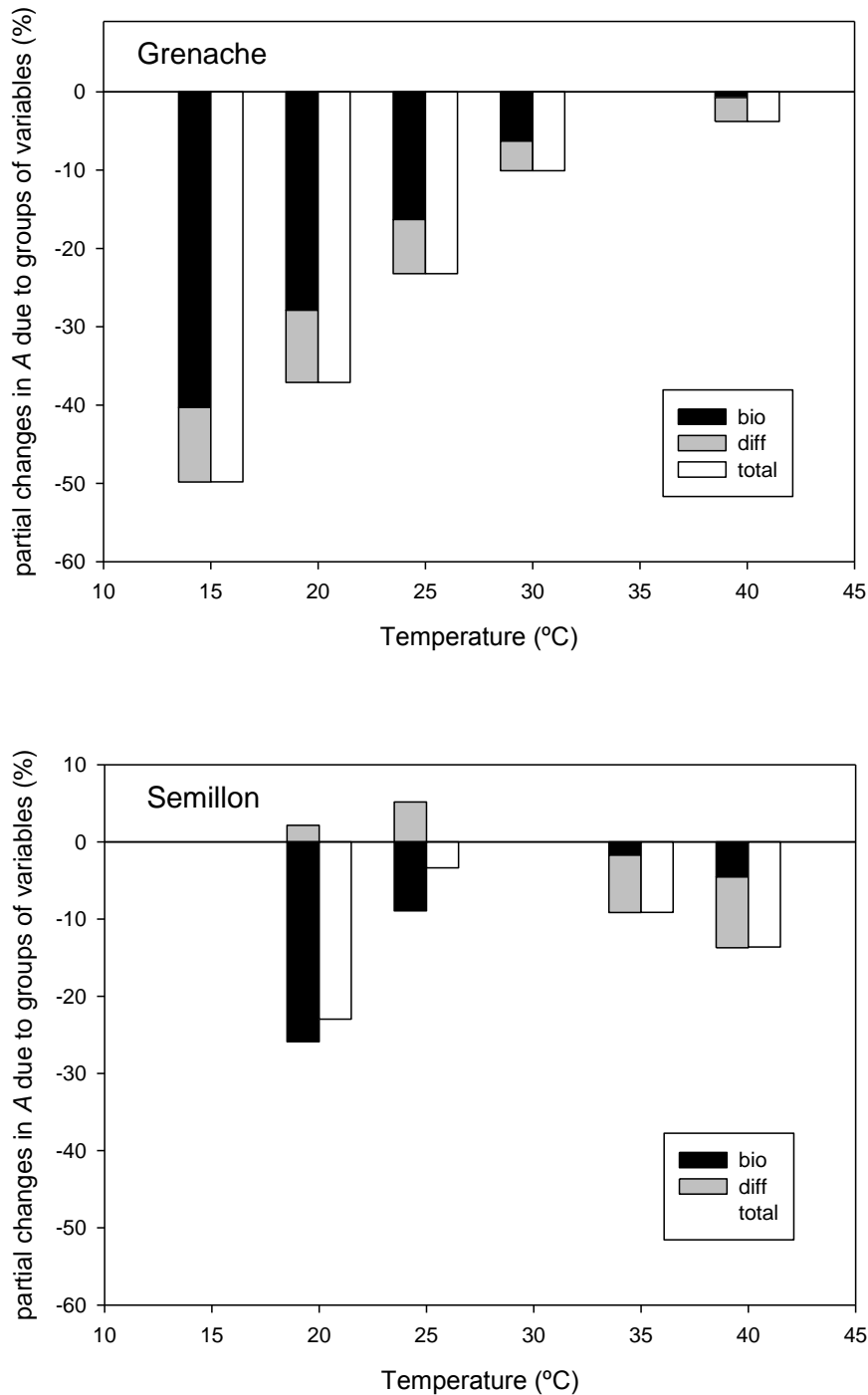
Figure 4: Biochemical, diffusional and total limitations at the whole range of temperatures measured A) corresponds to Grenache data and B) to Semillon data. Color black corresponds to biochemical limitations, grey to diffusional limitations and blank to total limitation.

Our results suggest that below optimal temperature the biochemical contribution largely exceeded that of diffusional one for both cultivars (Fig. 4). The diffusional contributions showed a different pattern at each cultivar. In the case of Grenache this was always negative, meanwhile in Semillon was positive at temperatures below optimum and negative at temperature above optimum. This seemed to suggest that the different

response to temperature of g_m in both cultivars might be involved in this result. However, when we focus on the diffusional contribution and we partitioned it further into the g_s and g_m components, we can observe that g_s is the main factor driving the diffusional contribution (Fig. 5). Meanwhile, the contribution of g_s to A_N was negative at all temperatures in Grenache, in the case of Semillon it was positive at temperatures below optimum, and only negative at higher temperatures.
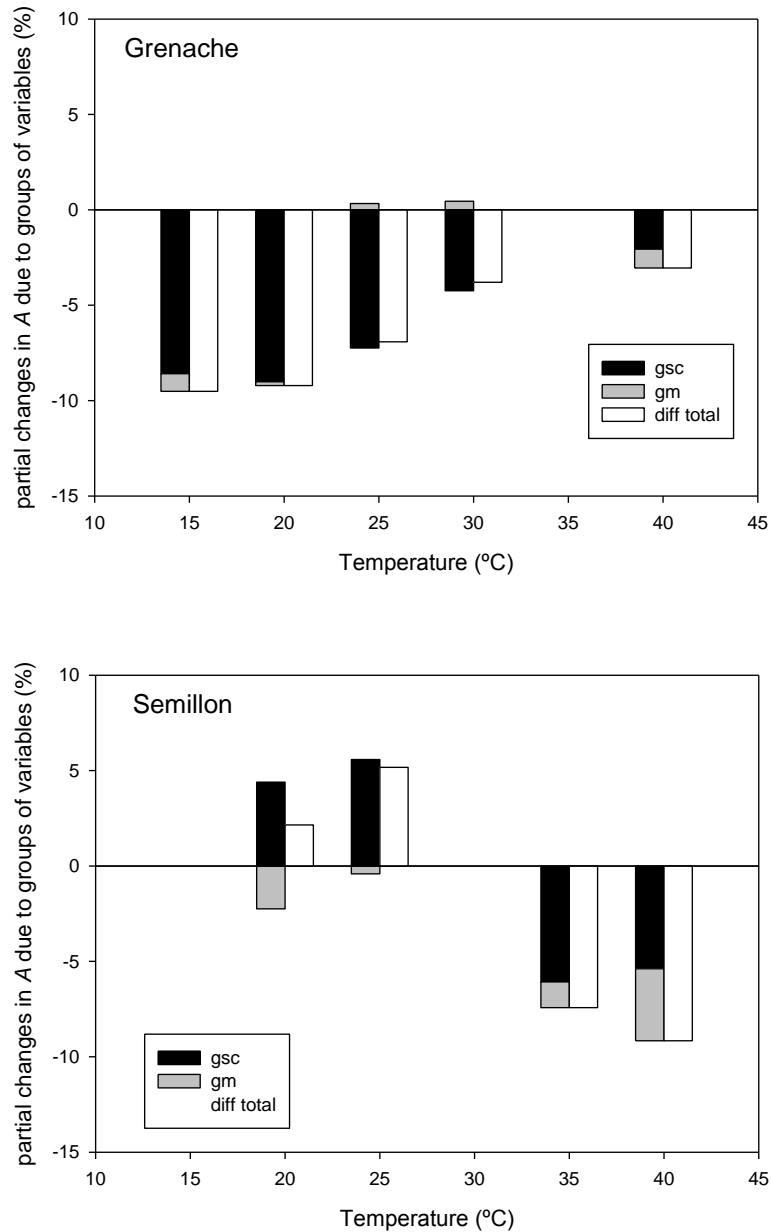

Figure 5: Contributions analysis using the method proposed by Buckley and Diaz-Espejo (2014) showing diffusional contributions. Black bars corresponded to stomatal conductance contributions, grey bars to mesophyll conductance contributions and also blank spaces were total difussional contributions.

The partitioning of the components of the biochemical contribution shows that most of the change was driven by J_m (Fig. 6) at temperatures below optimum for both varieties. It is also interesting to note that the contribution of K_c is counterbalanced by V_c at all tempeartures, even when the contribution shift at the optimum value from of sign to other (negative to positive or viceversa) in the case of Semillon variety.
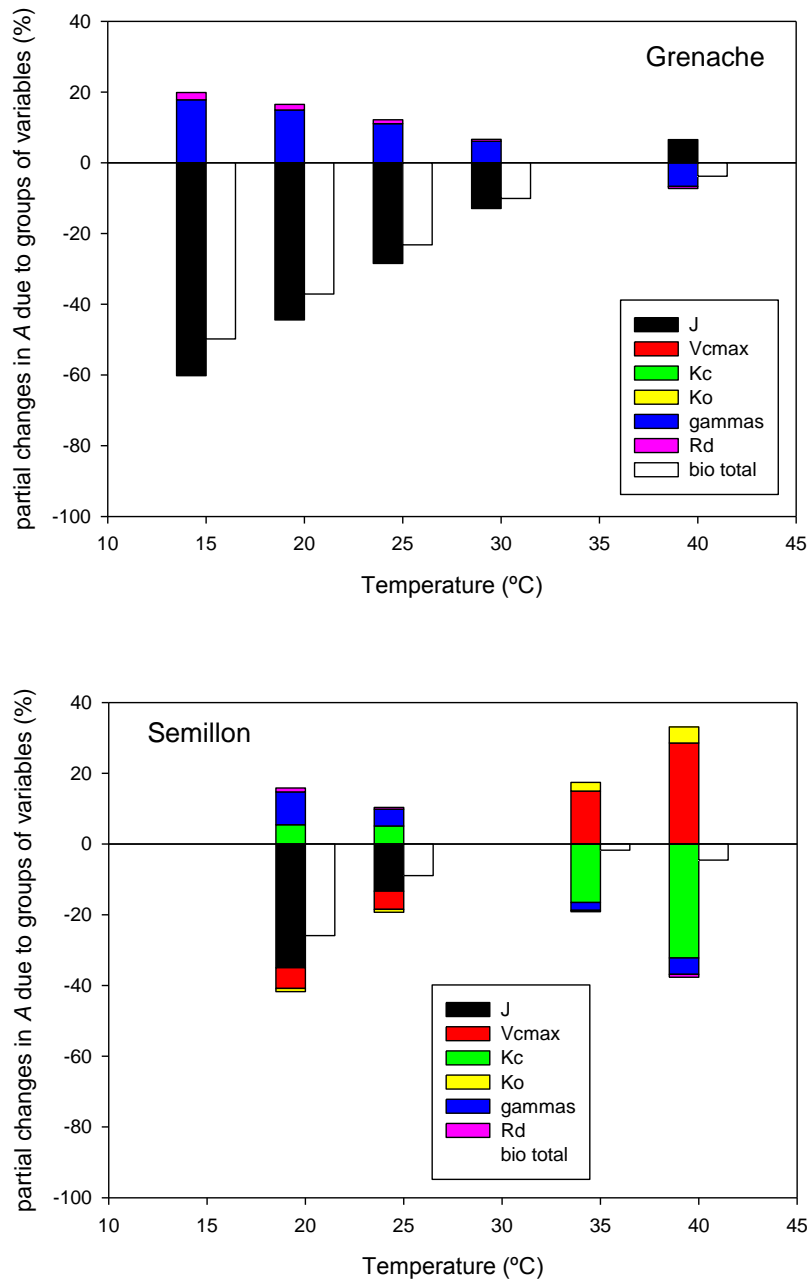

Figure 6: Contributions from different variables from the biochemical model of photosynthesis (Farquhar et al., 1980). Each color represent a variable as it is explained in the legend of the figure. A) graph showed Grenache data and B) Semillon.

DISCUSSION

Our study shows for the first time, how the temperature response of g_m can differ among cultivars within a single species. This feature enhances the role of g_m in the modelling of A_N under a given environmental conditions, and it moves the focus from the prominence of RuBisCO properties to explain the differences in optimum temperature of Grenache and Semillon to diffusional aspects. Von Caemmerer and Evans (2014) have measured the temperature response of g_m in nine species, including both trees and herbs, under similar experimental and methodological conditions confirming the species-specific difference suggested in previous works. However, our work gives a step forward suggesting that not only species of contrasting habitats or growing forms are prone to show a differential response to temperature of g_m, but also varieties or cultivars within a single species.

Despite of grapevine being a widely studied species, we could not find any work in literature in which the parameters of the FvCB model in response to temperature had been estimated on a C_c-basis. We found only two works where the specific parameters for the temperature response were estimated, although in a C_i-basis: Schultz (2003) and Greer and Weedon (2012). In some cases, photosynthesis has been modelled in grapevine not only neglecting the role of g_m, but also using parameters from other species, not even phylogenetically related like tobacco (Prieto et al., 2012). When the response to temperature of V_c or J_m in a C_i-basis of two different cultivars, like Grenache and Semillon are compared, clear differences are observed especially for V_c (Fig. 1a,b). V_c and J_m have been reported to vary by two orders of magnitude among species as well as their response to temperature and, therefore, they have to be specified for different species and plant growth conditions (Wullschleger 1993, Kattge and Knorr, 2007). This had been explained in terms of species-specific differences in their capacity to acclimate to higher temperatures (Yamori et al., 2006), to the decrease in RuBisCO activation state at moderately high temperatures attributed to suppressed RuBisCo activase activity (Salvucci & Crafts-Brandner 2004), or to the limitation of the ribulose 1,5- bisphosphate (RuBP) regeneration capacity (Schrader et al . 2004; Wise et al . 2004). As parallel change in the activation of RuBisCO and down-regulation in the electron transport have been reported at moderately high temperatures (Cen & Sage, 2005), it has been proposed that the RuBisCO activation state may be a regulatory response to the limitation of one of the processes contributing to RuBP regeneration,

including the damage to thylakoid reactions (Sharkey, 2005). Any of these mechanisms might have explained the difference in the response observed between Grenache and Semillon, since the kinetics of RuBisCo is not expected to vary much within a species. However, the differences in the kinetics response to temperature of V_c and J_m disappeared when a finite g_m was included in the analysis (Fig. 2), and then their temperature responses became indistinguishable.

The response of g_m to temperature seems at a first glance the responsible for the shift in the optimum temperature of A_N between cultivars. The drop of g_m at 40ºC in Semillon as compared to Grenache suggests this variable is behind the drop in V_c in a C_i-basis at this temperature (Fig. 1) in the former cultivar. This has important implications in our understanding of why one cultivar is more or less sensitive to high temperatures. Simply by considering a finite g_m we change the perception from that the limitation of A_N has a biochemical nature to a diffusional one. Overall our results are consistent with the fact that RuBisCo and its temperature kinetics are expected not to change with a single species, even though these two cultivars had been bred in contrasting environments. This similarity could be consequence that both cultivars presented a similar RuBisCo enzyme. This is not always completely true, since although modest, significant intraspecific variability in RuBisCo kinetic parameters has been reported in some crops like barley, rice and wheat (Rinehart et al. 1983; Makino et al., 1987; Galmés et al., 2014). Bota et al., (2002) found no differences in the RuBisCo specificity for CO_2/O_2 between two cultivars of *Vitis vinifera*. Moreover, RuBisCO active sites are located in the large subunits, which are encoded by a unique gene rbcL in the chloroplast genome. Comparison of the rbcL sequences available for *Rkatsiteli, Meskhuri Mtsvane*, *Maxxa, Sultanina* and *Saperavi* grapevine cultivars in the GeneBank reveals identical amino acid composition for the large subunit (data no shown). Based on these evidences, we assume that the grapevine cultivars included in the present study have the same RuBisCo catalytic traits.

Although g_m has been described to vary between cultivars of grapevine (Pou et al., 2012; Tomàs et al., 2014), this is the first time that differences are observed in the response to temperature (Figure 1, 2). The differences in the response to temperature of g_m have been analyzed with a simplified model in nine species (von Caemmerer and Evans 2014). This model neglects the gas phase component of g_m and concentrates on the liquid and membrane. This makes the model to resolve the variation of g_m into two

parameters: the activation energy for membrane permeability to CO_2 and the effective liquid path length. In other words, the two main candidates behind the response to temperature are aquaporins and cell wall effective path length. Anatomical characteristics of leaves in both cultivars might be playing a role in the response observed. The effective path lengths for liquid diffusion are influenced by the magnitude of the surface of chloroplasts respect to mesophyll surface in the intercellular spaces, and also by the porosity of the cell wall. It is difficult to measure this last term and it is expected to change with the composition of the cell wall. Definitely, this is an interesting research line for the near future. On the other hand, the membrane permeability to CO_2 is affected by the composition of the membrane, e.g. the CO_2 permeability of lipid bilayers could be decreased by increasing the cholesterol content of the membrane (Itel, Al-Samir, Öberg et al., 2012). Aquaporins have been reported as the main candidate to explain g_m and its response to environmental variables (Flexas et al. 2012; Pou et al., 2013; Moshelion et al., 2014). von Caemmerer and Evans (2014) concluded with the application of their simplified model, that a high membrane permeability to CO_2 by inclusion of a large number of aquaporin would render the membrane g_m rather insensitive to temperature. Our results seem to be in agreement with this possibility, especially in the case of Grenache in which its temperature response appears to be pretty flat, as those of woody plants shown in von Caemmerer and Evans (2014). All these possibilities need to be tested and knowledge about them is needed to understand the mechanistic basis of the control of g_m to temperature.

Despite the difference in the response of g_m to temperature between variables, this parameter seems to be not critical in the determination of the reduction of A_N at other temperatures than optimum. Our analysis of contributions indicates that the biochemical component takes the lead (Fig. 3), especially at low temperatures. We are not aware of any study in which the analysis of contributions or limitations of photosynthesis with temperature has been comprehensively performed including temperature response functions of the whole set of variables which determines A_N, like for instance g_m. Most of the studies have been focused on the limitation exerted by g_m under water stress either in short-term control experiments (Flexas et al., 2009; Gallé et al., 2009) or in seasonal evolution under field conditions (Grassi and Maganani 2004). But most of the measurements were made at a reference temperature, usually 25 ºC. In most of those studies, only when water stress was severe it was found a biochemical limitation, being

the diffusional ones, both g_s and g_m, the most important (Flexas et al., 2009; Gallé et al., 2009;) under mild and moderate water stress. As our study was done under control conditions and with the same plants over a short period of time, no acclimation processes are assumed to have taken place. In the response to temperature our analysis suggests that the biochemical have a more important role than in the response to water stress. The photosynthetic apparatus is generally considered very resistant to mild and moderate water stress (Flexas et al., 2004; Flexas and Medrano, 2002). However, temperature affects strongly the V_c and J_m as it can be inferred from the exponential response curves obtained in this study (Fig. 1 and 2) or elsewhere (Kattge and Knorr, 2007). The integrity of the membranes and it structural properties play and important role explaining the response to temperature. Cell membranes have been reported to be especially sensitive to low temperatures, since they provoke a transition of membrane lipids from liquid crystalline to gel phase, modifying their properties (Porankiewicz et al., 1998). Our results line on this idea, since all the biochemical contribution to the reduced A_N at low temperatures was attributed to J (Fig. 6). Regeneration of RuBP is dependent on the electron transport rate, process which requires a high structured, organized and thermo stable membrane. The effect of low temperature on photosynthesis and growth has been specifically studied on grapevine (Flexas et al. 1999; Hendrickson et al., 2003, 2004). These authors concluded that the observed response at low temperatures was more likely a response to RuBP regeneration and/or increased electron transport to O_2, but not a problem of photoinhibition of PSII.

However, Semillon, in contrast with Grenache, showed some contributions due to RuBisCO, and represented by V_c, K_c and Γ^* (Fig. 5). Our explanation for this is the lower C_c operating point at which Semillon works, due to its lower g_s and g_m values in comparison to Grenache. This agrees with the reduction of g_m at 40 ºC, which together with the reduction in g_s makes the diffusional contributions to double in Semillon those of Grenache. It is puzzling to see how contributions of V_c and K_c counterbalance each other at either sides of the optimum temperature. This fact is out of the scope of this study, but it is likely related to the trade-off between the catalytic rate of Rubisco (K_{cat}) and its specificity factor. Galmés et al. (2014) and Whitney et al., (2011) have shown how plants have to choose between a fast RuBisCO or an efficient RuBisCO. The choice has much to do with the environment at which the species has evolved (Galmés et al., 2005). However, the impact of temperature in this tradeoff is not so much studied.

Our data on Semillon in Fig. 5b suggests that the response to temperature of V_c and K_c are tuned in such a way that the limitations of both variables are finely compensated in all the range of temperatures at which plant grows.

The optimum values for A_N we have found in this study (Figure 3) match well with the reputation of both cultivars. The average growing season for Semillon ranges from 14.9 ºC to 18.15 ºC, while for Grenache it ranges from 16.6 ºC to 20.1 ºC (Jones et al. 2006). At temperatures below optimum, both varieties had photosynthesis limited by biochemical processes, especially related to the regeneration of the RuBP, and therefore light reactions. Both cultivars share a similar pattern concerning the role of biochemical contributions to the reduction of A_N. The main differences between both cultivars are focused in the diffusional contributions. In Grenache they show up to play a major role than in Semillon, especially at temperatures below optimum. At temperatures above optimum the diffusional contributions are slightly higher in Semillon. This agrees well with the difference between cultivars in the response to temperature of g_m. However, the contributions analysis awarded the majority of the diffusional limitation to g_s. This cannot underplay the importance of the inclusion of temperature response of g_m in photosynthesis models, since only by doing so we can understand correctly the role of the biochemical and diffusional component in the limitation of A_N by temperature.

ACKNOWLEDGMENTS

REFERENCES

Bernacchi C.J., Pimentel C. & Long S.P. (2003) In vivo temperature response functions of parameters required to model RuBP-limited photosynthesis. *Plant, Cell & Environment*, **26**, 1419-1430.

Bernacchi C.J., Portis A.R., Nakano H., von Caemmerer S. & Long S. P. (2002) Temperature response of mesophyll conductance. Implications for the determination of Rubisco enzyme kinetics and for limitations to photosynthesis in vivo. *Plant Physiology*, **130**, 1992-1998.

Bernacchi C.J., Singsaas E.L., Pimentel C., Portis J,A.R. & Long S.P. (2001) Improved temperature response functions for models of Rubisco-limited photosynthesis. *Plant, Cell & Environment*, **24**, 253-259.

Bota J., Flexas J., Keys A.J., Loveland J., Parry M.A.J. & Medrano H. (2002) Specificity factor of ribulose-1, 5-bisphosphate carboxylase/oxygenase in grapevines (*Vitis vinifera L.*): first in vitro determination and comparison to in vivo estimations. *Vitis*, **41**, 163-168.

Buckley T.N. & Diaz-Espejo A. (2014) Partitioning changes in photosynthetic rate into contributions from different variables. *Plant, Cell & Environment.* Doi: 10.1111/pce.12459

Caemmerer S. & Evans J.R. (2014) Temperature responses of mesophyll conductance differ greatly between species. *Plant, Cell & Environment*. Doi: 10.1111/pce.12449

Cen Y.P. & Sage R.F. (2005) The regulation of ribulose-1,5-bisphosphate carboxylase activity in response to variation in temperature and atmospheric CO_2 partial pressure in sweet potato. *Plant Physiology* **139**, 1–12.

Diaz-Espejo A. (2013) New challenges in modelling photosynthesis: temperature dependencies of Rubisco kinetics. *Plant, Cell & Environment*, **36**, 2104-2107.

Diaz-Espejo A., Nicolas E. & Fernandez J.E. (2007) Seasonal evolution of diffusional limitations and photosynthetic capacity in olive under drought. *Plant, Cell & Environment*, **30**, 922-933.

Egea G., González-Real M.M., Baille A., Nortes P.A. & Diaz-Espejo A. (2011) Disentangling the contributions of ontogeny and water stress to photosynthetic limitations in almond trees. *Plant, Cell & Environment*, **34**, 962-979.

Ethier G.J. & Livingston N.J. (2004) On the need to incorporate sensitivity to CO_2 transfer conductance into the Farquhar–von Caemmerer–Berry leaf photosynthesis model. *Plant, Cell & Environment*, **27**, 137-153.

Evans J.R. & Von Caemmerer S. (2013) Temperature response of carbon isotope discrimination and mesophyll conductance in tobacco. *Plant, Cell & Environment*, **36**, 745-756.

Farquhar G.D., von Caemmerer S.V. & Berry J.A. (1980) A biochemical model of photosynthetic CO_2 assimilation in leaves of C3 species. *Planta*, **149**, 78-90.

Flexas J. & Diaz-Espejo A. (2014) Interspecific differences in temperature response of mesophyll conductance: food for thought on its origin and regulation. *Plant, Cell & Environment*, doi: 10.1111/pce.12476

Flexas J. & Medrano H. (2002) Drought-inhibition of photosynthesis in C3 plants: stomatal and non-stomatal limitations revisited. *Annals of Botany*, **89**, 183-189.

Flexas J., Badger M., Chow W.S., Medrano H. & Osmond C.B. (1999) Analysis of the relative increase in photosynthetic O_2 uptake when photosynthesis in grapevine leaves is inhibited following low night temperatures and/or water stress. *Plant Physiology*, **121**, 675-684.

Flexas J., Barbour M.M., Brendel O., *et al.,* (2012) Mesophyll diffusion conductance to CO_2: An unappreciated central player in photosynthesis. *Plant Science*, **193**, 70-84.

Flexas J., Barón M., Bota J. *et al.* (2009). Photosynthesis limitations during water stress acclimation and recovery in the drought-adapted Vitis hybrid Richter-110 (V. berlandieri × V. rupestris). *Journal of Experimental Botany*, **60**, 2361-2377.

Flexas J., Bota J., Galmes J., Medrano H. & Ribas-Carbó M. (2006) Keeping a positive carbon balance under adverse conditions: responses of photosynthesis and respiration to water stress. *Physiologia Plantarum*, **127**, 343-352.

Flexas J., Bota J., Loreto F., Cornic G. & Sharkey T.D. (2004) Diffusive and metabolic limitations to photosynthesis under drought and salinity in C3 plants. *Plant Biology*, **6**, 269-279

Flexas J., Díaz-Espejo A., Berry J.A., Cifre J., Galmes J., Kaldenhoff R., Medrano H. & Ribas-Carbó M. (2007) Analysis of leakage in IRGA's leaf chambers of open gas exchange systems: quantification and its effects in photosynthesis parameterization. *Journal of Experimental Botany*, **58**, 1533-1543.

Flexas J., Galmés J., Gallé A., Gulías J., Pou A., Ribas-Carbó M., Tomàs M. & Medrano H. (2010) Improving water use efficiency in grapevines: potential physiological targets for biotechnological improvement. *Australian Journal of Grape and Wine Research*, **16**, 106-121.

Flexas J., Ribas-Carbó M., Diaz-Espejo A., Galmes J. & Medrano H. (2008) Mesophyll conductance to CO_2: current knowledge and future prospects. *Plant, Cell & Environment*, **31**, 602-621.

Galle A., Florez-Sarasa I., Tomas M., Pou A., Medrano H., Ribas-Carbo M., & Flexas, J. (2009) The role of mesophyll conductance during water stress and recovery in tobacco (Nicotiana sylvestris): acclimation or limitation? *Journal of Experimental Botany*, **60**, 2379-2390.

Galmes J., Flexas J., Keys A.J., Cifre J., Mitchell R.A., Madgwick, P. J., ... & Parry, M. A. (2005). Rubisco specificity factor tends to be larger in plant species from drier habitats and in species with persistent leaves. *Plant, Cell & Environment*, **28**(5), 571-579.

Galmés J., Kapralov M.V., Andralojc P., Conesa M.À., Keys A.J., Parry M.A. & Flexas J. (2014) Expanding knowledge of the Rubisco kinetics variability in plant species: environmental and evolutionary trends. *Plant, Cell & Environment*. Doi: 10.1111/pce.12335

Genty B., Briantais J.M. & Baker N.R. (1989) The relationship between the quantum yield of photosynthetic electron transport and quenching of chlorophyll fluorescence. *Biochimica et Biophysica Acta (BBA)-General Subjects*, **990**, 87-92.

Grassi G. & Magnani F. (2005) Stomatal, mesophyll conductance and biochemical limitations to photosynthesis as affected by drought and leaf ontogeny in ash and oak trees. *Plant, Cell & Environment*, **28**, 834-849.

Greer D.H. & Weedon M.M. (2012) Modelling photosynthetic responses to temperature of grapevine (*Vitis vinifera cv. Semillon*) leaves on vines grown in a hot climate. *Plant, Cell & Environment*, **35**, 1050-1064.

Hannah L., Roehrdanz P.R., Ikegami M., Shepard A.V., Shaw M.R., Tabor G., ... & Hijmans R.J. (2013). Climate change, wine, and conservation. *Proceedings of the National Academy of Sciences*, **110**, 6907-6912.

Harley P.C., Loreto F., Di Marco G. & Sharkey T. D. (1992) Theoretical considerations when estimating the mesophyll conductance to CO_2 flux by analysis of the response of photosynthesis to CO_2. *Plant Physiology*, **98**, 1429-1436.

Hendrickson L., Ball M.C., Osmond C.B., Furbank R.T., Chow W.S. (2003) Assessment of photoprotection mechanisms of grapevines at low temperature. *Functional Plant Biology*, **30**, 631-642.

Hendrickson L., Ball M.C., Wood J.T., Chow W.S. & Furbank R.T. (2004) Low temperature effects on photosynthesis and growth of grapevine. *Plant, Cell & Environment*, **27,** 795–809.

IPCC, 2013. Stocker T. F., Dahe Q., Plattner G.K., (2013) Climate Change 2013: The Physical Science Basis. Working Group I Contribution to the Fifth Assessment

Report of the Intergovernmental Panel on Climate Change. Summary for Policymakers

Itel F., Al-Samir S., Öberg *et al.* (2012) CO_2 permeability of cell membranes is regulated by membrane cholesterol and protein gas channels. *The FASEB Journal*, **26**, 5182-5191.

Jones H.G. (2006) Climate and terroir: Impacts of climate variability and change on wine. Fine Wine and Terroir—The Geoscience Perspective. Geoscience Canada, eds Macqueen RW, Meinert LD (Geological Association of Canada, St John's, Newfoundland), 1–14.

Kattge J. & Knorr W. (2007) Temperature acclimation in a biochemical model of photosynthesis: a reanalysis of data from 36 species. *Plant, Cell & Environment,* **30**, 1176–1190.

Kawase M., Hanba Y.T. & Katsuhara M. (2013) The photosynthetic response of tobacco plants overexpressing ice plant aquaporin McMIPB to a soil water deficit and high vapor pressure deficit. *Journal of Plant Research*, **126**, 517-527.

Makino A., Mae T. & Ohira K. (1987) Variations in the contents and kinetic properties of ribulose-1, 5-bisphosphate carboxylases among rice species. *Plant and Cell Physiology*, **28**, 799-804.

Moshelion M., Halperin O., Wallach R., Oren R. & Way D.A. (2014) Role of aquaporins in determining transpiration and photosynthesis in water-stressed plants: crop water-use efficiency, growth and yield. *Plant, Cell & Environment*. Doi: 10.1111/pce.12410

Mullins M.G., Bouquet A. & Williams L.E. (1992) *Biology of the grapevine*. Cambridge University Press.

Perez-Martin, A., Michelazzo, C., Torres-Ruiz, J. M., Flexas, J., Fernández, J. E., Sebastiani, L., & Diaz-Espejo, A. (2014). Regulation of photosynthesis and stomatal and mesophyll conductance under water stress and recovery in olive trees: correlation with gene expression of carbonic anhydrase and aquaporins. *Journal of Experimental Botany*. Doi:10.1093/jxb/eru160.

Porankiewicz J., Selstam E., Campbell D. & Öquist G. (1998) Membrane lipid composition and restoration of photosynthesis during low temperature acclimation in Synechococcus sp. strain PCC 7942. *Physiologia Plantarum*, **104**, 405-412.

Pou A., Medrano H., Flexas J. & Tyerman S.D. (2013) A putative role for TIP and PIP aquaporins in dynamics of leaf hydraulic and stomatal conductances in grapevine under water stress and re-watering. *Plant, Cell & Environment*, **36**, 828-843.

Pou A., Medrano H., Tomàs M., Martorell S., Ribas-Carbó M. & Flexas J. (2012) Anisohydric behaviour in grapevines results in better performance under moderate water stress and recovery than isohydric behaviour. *Plant and Soil*, **359**, 335-349.

Prieto J., Louarn G., Perez Peña J., Ojeda H., Simonneau T. & Lebon E. (2012) A leaf gas exchange model that accounts for intra-canopy variability by considering leaf nitrogen content and local acclimation to radiation in grapevine *(Vitis vinifera L.) Plant, Cell & Environment*, **35**, 1313–1328.

Rinehart C.A., Tingey S.V. & Andersen W.R. (1983) Variability of reaction kinetics for ribulose-1, 5-bisphosphate carboxylase in a barley population. *Plant Physiology*, **72**, 76-79.

Sade N., Gallé A., Flexas J., Lerner S., Peleg G., Yaaran A. & Moshelion M. (2014) Differential tissue-specific expression of NtAQP1 in Arabidopsis thaliana

reveals a role for this protein in stomatal and mesophyll conductance of CO_2 under standard and salt-stress conditions. *Planta*, **239**, 357-366.

Salvucci M.E. & Crafts-Brandner S.J. (2004) Inhibition of photosynthesis by heat stress: the activation state of Rubisco as a limiting factor in photosynthesis. *Physiologia Plantarum,* **120**, 179–186.

Schrader S.M., Wise R.R., Wacholtz W.F., Ort D.R. & Sharkey T.D. (2004) Thylakoid membrane responses to moderately high leaf temperature in Pima cotton. *Plant, Cell & Environment,* **27**, 725–735.

Schultz H.R. & Stoll M. (2010) Some critical issues in environmental physiology of grapevines: future challenges and current limitations. *Australian Journal of Grape and Wine Research*, **16**, 4-24.

Schultz H.R. (2003) Extension of a Farquhar model for limitations of leaf photosynthesis induced by light environment, phenology and leaf age in grapevines (*Vitis vinifera L. cvv. White Riesling and Zinfandel*). *Functional Plant Biology*, **30**, 673-687.

Sharkey T.D. (2005) Effects of moderate heat stress on photosynthesis: importance of thylakoid reactions, Rubisco deactivation, reactive oxygen species, and thermotolerance provided by isoprene. *Plant, Cell & Environment*, **28**, 269–277.

Terashima I., & Ono K. (2002) Effects of $HgCl_2$ on CO_2 dependence of leaf photosynthesis: evidence indicating involvement of aquaporins in CO_2 diffusion across the plasma membrane. *Plant & Cell Physiology*, **43**, 70-78.

Teskey R., Wertin T., Bauweraerts I., Ameye M., McGuire M.A. & Steppe K. (2014). Responses of tree species to heat waves and extreme heat events. *Plant, Cell & Environment*. Doi: 10.1111/pce.12417

Tomás M., Medrano H., Brugnoli E., Escalona J.M., Martorell S., Pou A., Ribas-Carbó M. & Flexas J. (2014) Variability of mesophyll conductance in grapevine cultivars under water stress conditions in relation to leaf anatomy and water use efficiency. *Australian Journal of Grape and Wine Research*, **20**, 272-280.

Valentini R., Epron D., Angelis P.D., Matteucci G. & Dreyer E. (1995) In situ estimation of net CO_2 assimilation, photosynthetic electron flow and photorespiration in Turkey oak (*Q. cerris L.*) leaves: diurnal cycles under different levels of water supply. *Plant, Cell & Environment*, **18**, 631-640.

Walker B., Ariza L.S., Kaines S., Badger M.R. & Cousins A.B. (2013) Temperature response of in vivo Rubisco kinetics and mesophyll conductance in Arabidopsis thaliana: comparisons to Nicotiana tabacum. *Plant, Cell & Environment*, **36**, 2108-2119.

Warren C.R. & Dreyer E. (2006) Temperature response of photosynthesis and internal conductance to CO_2: results from two independent approaches. *Journal of Experimental Botany*, **57**, 3057-3067.

Warren C.R. (2008) Stand aside stomata, another actor deserves centre stage: the forgotten role of the internal conductance to CO_2 transfer. *Journal of Experimental Botany*, **59**, 1475-1487.

Whitney S.M., Sharwood R.E., Orr D., White S.J., Alonso H. & Galmés J. (2011) Isoleucine 309 acts as a C4 catalytic switch that increases ribulose-1, 5-bisphosphate carboxylase/oxygenase (rubisco) carboxylation rate in Flaveria. *Proceedings of the National Academy of Sciences*, **108**, 14688-14693.

Wise R.R., Olson A.J., Schrader S.M. & Sharkey T.D. (2004) Electron transport is the functional limitation of photosynthesis in field-grown Pima cotton plants at high temperature. *Plant, Cell & Environment*, **27**, 717–724.

Wullschleger S.D. (1993) Biochemical limitations to carbon assimilation in C3 plants – a retrospective analysis of the A/C$_i$ curves from 109 species. *Journal of Experimental Botany*, **44**, 907–920.

Yamori W., Noguchi K., Hanba Y.T. & Terashima I. (2006) Effects of internal conductance on the temperature dependence of the photosynthetic rate in spinach leaves from contrasting growth temperatures. *Plant & Cell Physiology*, **47**, 1069-1080.

4.2. On the quest of a mechanistic model of stomatal response to water stress

Martorell S., Buckley TN., Tomàs M., Flexas J., Escalona JM., Ribas-Carbó M., Medrano H., Diaz-Espejo A.

[1]Research Group on Plant Biology under Mediterranean Conditions, Departament de Biologia, Universitat de les Illes Balears, Carretera de Valldemossa Km 7.5, 07122 Palma de Mallorca, Illes Balears, Spain;

[2]Irrigation and Crop Ecophysiology Group, Instituto de Recursos Naturales y Agrobiología de Sevilla (IRNAS, CSIC). Avenida Reina Mercedes 10, 41012 Sevilla, Spain

ABSTRACT

Models of stomatal conductance (g_s) are a necessary tool to improve our understanding of water use and carbon fixation in plants, especially under water stress. Most of the attempts to model g_s have been made with empirical models, which limit the applicability of the results obtained. In this study three models are compared, two of them are semi-empirical models widely used in the literature, while the other one is a mechanistic model that has not been used at the leaf level in field ecophysiological studies yet. Leaf gas exchange data from grapevines in well water and water stress conditions were collected along a growing season in a field trial. Results showed that all models were able to predict g_s showing a similar fit in all the scenarios. In addition, the mechanistic model was able to predict two of the three physiological parameters, such as; hydraulic conductance (K_h) and osmotic potential (π). These variables predicted by the model were validated with measured values. Moreover, a change of sensitivity of abscisic acid respect to g_s was predicted. In the near future, the use of mechanistic models of g_s would be a powerful tool to infer on the mechanisms behind the stomata regulation and the prediction of g_s values.

INTRODUCTION

Stoma is the valve that regulates water loss and carbon gain, being the first resistance to CO_2 on the way to the chloroplasts. Despite of the stomata importance on leaf gas exchange process, there is not yet a clear knowledge of how stomata regulate their aperture and closure. Some coordinated mechanisms are responsible of the function of stomata (for rev. Buckley, 2005), however the high interaction between them make the regulation difficult to understand. Changes produced on turgor of guard cells are finally the responsible of the aperture and closure of stomatal pores.

There are some environmental parameters identified to produce changes on the aperture of stomatal pores such as: light, CO_2, soil water content (SWC) and vapor pressure deficit (VPD). Considering them, some attempts have been made to model g_s proposing models from empirical to mechanistic ones (Jarvis et al., 1976; Ball et al., 1987; Leuning 1995; Buckley et al., 2003; Peak and Mott, 2011). Empirical and semi-empirical models of g_s have been the most used as they are more mathematically tractable and easier to use (Buckley and Mott, 2013). Ball et al., (1987), proposed one of the most used semi-empirical models of g_s, known as "BWB model". It is based on

the correlation between g_s and photosynthesis rate, as well as the response to a series of ambient variables. On the other hand, another widely used semi-emperical model is a modification of the BWB model proposed by Leuning, (1995) called "BWB-L". It includes the response of g_s to VPD instead of the relative humidity. Although this modification improved the model performance (Van Wijk et al. 2000; Mo and Liu 2001; Arora 2003), other studies showed that it was almost the same or worse than BWB model (Cox et al. 1998; Gutschick and Simonneau 2002; Gutschick 2007). In general, both models (BWB and BWB-L) are able to predict g_s and are widely used in the literature (Egea et al., 2011), although their parameters are empirical without a physiological meaning. This fact difficult the use of these models since its empirical parameters needs to be adjusted to each specie and conditions (Damour et al., 2010; Egea et al., 2011; Buckley and Mott, 2013). Another drawback of these models is that water stress effects cannot be predicted without considering the variation of the empirical coefficients in response to water stress requiring the inclusion of a function response of the empirical parameters to water stress (Sala and Tenhunen, 1996; Wang and Leuning, 1998; van Wijk et al., 2000; Verhoef and Allen, 2000; Misson et al., 2004).

More recently, the knowledge integration generated by the physiological studies on stomata led to generate the first mechanistic models of g_s (Buckley et al., 2003; Peak and Mott 2011). In this case, Buckley et al., (2003) developed a mechanistic model (hereafter "BMF model") to predict g_s, being one of the best options to model g_s with a mechanistic basis. The "BMF" model is based on the relationship between the hydraulic mechanics of stomata function taking in account changes of volume in guard cells. This model assumes that turgor changes produced in guard cells are the responsible of the stomatal control. Successful results have been obtained modeling with some simplifications of this model (Buckley *et al.,* 2012; Diaz-Espejo *et al.,* 2012) taking advantage because all their parameters have a physiological meaning. Although mechanistic models exist, their use has not been incorporated in ecophysiological studies yet, being important to investigate on the use of these models in the near future to understand the stomatal regulation, and generate new hypothesis on stomatal control.

The main goals of this study are: i) to test the applicability of the BMF model with field data of grapevine under control and water stress conditions; ii) to compare the performance of the model with the other two widely used models, BWB and BWB-L;

iii) to confirm whether the parameters of the BMF model have full physiological meaning by comparing them with actual measurements; and iv) to use the model to infer the main mechanisms of regulation of g_s under water stress conditions.

MATERIALS AND METHODS

Site of the study and plant material

The experiment was conducted at the experimental field of the University of Balearic Islands during year 2012. Grapevines were three years old grafted on Richter-110 and planted in rows (distance between rows was 2.5 meters and plants 1 meter). They were conducted in a bilateral double cordon having between 10-12 canes per plant. Climatic conditions were typical of the Mediterranean area and consisted on an average temperature for the experimental period of 25.2 ºC, with temperature ranging from a maximum of 37.3ºC in August and a minimum of 13.4ºC in June. During this period mean relative humidity was 58% and average PPFD at noon 1700 μmol m^{-2} s^{-1}. The total amount of rainfall water was 0.4 mm during all the period of the experiment. Soil was a clay loam type 1.1 meters deep. Two irrigation treatments were applied; well watered (WW), which consisted on the application of the 0.7 ETo, dosage previously estimated to be enough to replenish the water used daily by the plants, and water stressed (WS), which consist in withholding irrigation during all the summer.

Gas exchange measurements

Leaf gas exchange was measured using a portable open flow gas exchange system (Li-6400; Li-Cor, Inc., Lincoln, NE, USA) equipped with a clear chamber (Li-6400-08). Environmental conditions in the chamber consisted on ambient light, air temperature matched to the ambient and CO_2 set to a concentration of 400 μmol mol^{-1}. Stomatal conductance (g_s), photosynthesis (A_N) and transpiration (E) were measured throughout the day between five or seven times per day on the days 12th of June; 10th of July and 27th of August. Five plants were measured at each hour at the diurnal cycles of gas exchange.

Parameterizing the BWB and BWB-L model

Ball, Wodroow and Berry (1987) model of stomatal conductance was parameterized for each date. The model presents the following equation:

$$g_s = g_{s0} + a_1 \frac{A\,h_s}{C_s} \quad (1)$$

where g_{s0} is residual stomatal conductance, a_1 refers to an empirical coefficient, A is net photosynthesis, and h_s and C_s are relative humidity and CO_2 concentration at the leaf surface respectively.

Leuning, (1995) modified the model to include the response of stomatal conductance to VPD. Leaving the model on this formulation:

$$g_s = g_{s0} + a_1 \frac{A}{(C_s - \Gamma)(1 + VPD/D_0)} \quad (2)$$

where VPD and C_s are the vapor pressure deficit and the CO_2 concentration at the leaf surface and D_0 and a_1 are empirical coefficients.

Both models have been parameterized and cross-validated with the gas exchange data measured in the experiment. To perform the cross validations we did the mean of the empirical parameters fitted to four individual plants leaving one plant out of this mean. The values from the plant leaved (not used before to obtain the mean of the parameters) were used to model the g_s with the mean values of the empirical parameters obtained before. The values obtained for g_s were plotted vs the measured ones and also versus their residues (Figure 2). These cross-validations were performed for all the plants and treatments.

Parameterizing BMF model of stomatal conductance

A modified version of the process based model of Buckley, Mott and Farquhar (2003) (hereafter, the BMF model) of stomatal conductance was used. This model is based on leaf, stomata water relations and the hypothesis that the regulation of the osmotic pressure of the guard cells is related to *ATP* production by the photosynthetic cells (using the model of Cowan and Faquhar (1980)). Also it has been assumed that turgor pressure of the epidermis represents the changes in water status of the leaf.

 The simplified version of the *BMF* model has the following equation:

$$g_s = \frac{naK(\Psi_s + \pi)}{K + na\mathrm{VPD}} \quad (3)$$

where K is leaf-specific hydraulic conductance, Ψ_s is soil water potential, π defines bulk leaf osmotic pressure and VPD refers leaf to vapor pressure deficit. n and a capture non-

hydraulic effects: a is mesophyll ATP concentration expressed relative to its maximum value and n is a lumped parameter representing other non-hydraulic factors:

$$n \equiv \mathcal{X}\beta\tau_m, \text{ and (4)}$$

$$a \equiv \tau/\tau_m, \text{ (5)}$$

where τ is ATP concentration in photosynthesizing cells, χ is a proportionality factor that scales the guard and epidermal cell turgor pressures to g_s, β is a proportionality factor that scales the product of τ and the epidermal turgor to changes in guard cell osmotic pressure and τ_m defines the maximum τ (the total pool of adenylates, ADP+ATP). Five approaches have been used to fit the stomatal conductance model: 1.- Fitting the 3 BMF parameters (K, n and π) simultaneously. 2.- Fitting K and n and using measured $\Psi\pi,_{FT}$ as a proxy of π. 3.- Fitting K and n and using measured $\Psi\pi,_{TLP}$ as a proxy of π. 4.- Fitting π and n and using measured values of K_h. 5.- Fitting n and using measured values of both K_h and π (the latter estimated using measured $\Psi\pi,_{TLP}$).

A cross validation has been performed with the best option to model stomatal conductance as explained before for the BWB and BWB-L models.

Midday, predawn leaf water potentials and Pressure Volume curves (P-V)

Leaf water potentials were measured at predawn and midday with a Scholander pressure bomb (Soil moisture Equipment Corp. Santa Barbara, CA, USA) measuring four replicates per treatment. Pressure volume curves were measured to obtain leaf turgor loss point and osmotic adjustment (Tyree and Hammel 1972). Leaves were collected the evening before measurements and rehydrated overnight before P-V determination. During the dehydration of leaves in the laboratory, leaf water potential was periodically measured with a pressure chamber (Soil moisture Equipment. Corp. Santa Barbara, CA, USA) and leaf weight was measured with an analytical balance (Kern ABT320-4M, 10^{-4} g resolution). The turgor loss point ($\Psi_{\pi,TLP}$) was identified as the inflection point of the $1/\Psi_{leaf}$ versus relative water content (RWC) curve. The fitting method proposed by Sack and Pasquet-Kok (2011) was used to fit the P-V curves. This method fits lines by the standard major axis (Model II regression) so that either variable can be predicted from the other and the parameter calculation is more robust.

ABA extraction, purification and quantification

ABA was determined by liquid chromatography–tandem mass spectrometry (UHPLC-MS-MS, Agilent 1290 Infinity, Waldbronn, Germany) following the method described by Gomez-Cadenas *et al.* (2002). Xylem leaf sap was extracted in the field with a Scholander pressure bomb at 10th July and 27th August at 9 o'clock (local hour). A maximum overpressure of 0.2 MPa was applied until 10-15 µL of sap were obtained, which occur typically after 2-3-min. The sap was collected in 0.5 mL vials and immediately frozen in liquid nitrogen in the field. Once in the lab, samples were stored until use in a -80 ºC freezer. Prior determination, sap was thawed at room temperature and 1 µL of deutered-ABA (δ-ABA), as an internal standard, was added to 10 µL of each sample. δ-ABA was prepared following (Gomez-Cadenas *et al.* 2002). Samples with the internal standard were then centrifuge at 15000 *g* for 15 min at 4ºC, prior to UHPLC-MS-MS analysis.

K_h measurements

Whole plant hydraulic conductance (K_{hplant}) was calculated considering K_{hplant} from the Ohm's law analogy for the soil–plant–atmosphere continuum (Lovisolo et al. 2002):

$$E = K_{hplant} \times (\Psi_{soil} - \Psi_{leaf}); (6)$$

where E, Ψ_{leaf} and Ψ_{soil} were transpiration rate, leaf water potential and soil water potential, respectively. Ψ_{md} was taken as Ψ_{leaf} and Ψ_{pd} was taken as a proxy for $\Psi_{soil.}$

RESULTS

BWB, BWB-L and BMF models were able to predict stomatal conductance for the whole period of measurements (Figure 1).
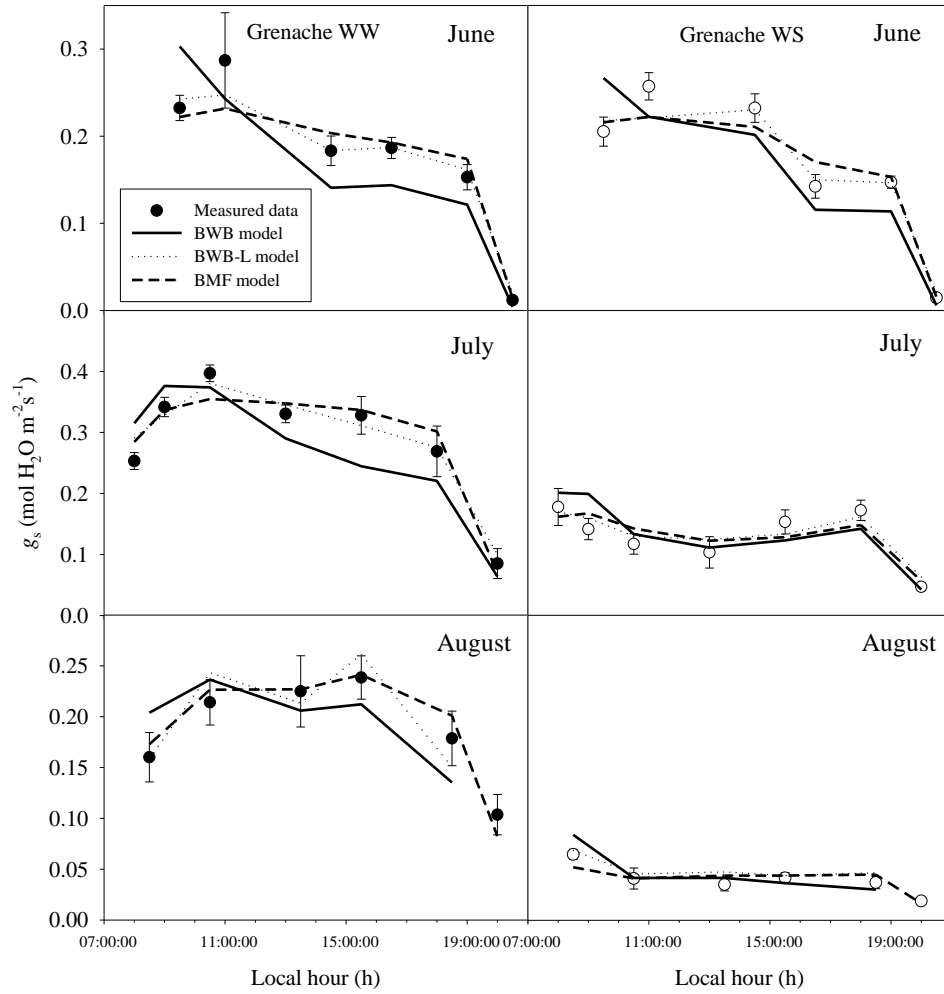
Figure 1: Diurnal cycles of stomatal conductance in three different dates of the experiment. Continuous line corresponded to BWB model prediction, dotted line to BWB-L model prediction and dashed line to BMF model prediction. Values are five replicates ± standard errors.

Date & Treatment	"m"+SE	"D$_0$" +SE	r^2	y = ax + b
BWB model				
June WW	8.8 ± 0.1[bc]	-	0.84	Y = 1.04x − 0.02
June WS	8.5 ± 0.2[b]	-	0.86	Y = 1.02x − 0.01
July WW	10.1 ± 0.5[c]	-	0.61	Y = 0.78x + 0.04
July WS	7.9 ± 0.5[b]	-	0.67	Y = 0.90x + 0.02
August WW	8.9 ± 0.3[bc]	-	0.57	Y = 0.78x + 0.03
August WS	5.9 ± 0.6[a]	-	0.69	Y = 1.21x − 0.01
BWB-L model				
June WW	5.4 ± 0.3[a]	17.4 ± 3.7[ab]	0.97	Y = 0.89x + 0.02
June WS	5.7 ± 0.5[a]	7.9 ± 2.0[a]	0.97	Y = 0.92x + 0.02
July WW	12.1 ± 2.8[ab]	28.9 ± 26.2[b]	0.89	Y = 0.83x + 0.05
July WS	14.1 ± 3.3[ab]	2.1 ± 0.8[a]	0.91	Y = 0.82x + 0.03
August WW	17.1 ± 4.0[b]	2.2 ± 0.8[a]	0.90	Y = 0.98x + 0.01
August WS	18.4 ± 3.2[b]	0.7 ± 0.2[a]	0.63	Y = 0.85x + 0.01

Table 1: Empirical parameters "m" and "D$_0$" obtained by the fit of BWB and BWB-L models of stomatal conductance. r^2 and equation values corresponded to the values obtained by the lineal regression between measured and modelled data of stomatal conductance (g_s). Values are mean of 5 replicates ± standard errors. Letters denote statistically differences between dates and treatments.

A good performance was found for BWB model in June, but not so good in July and August where g_s values were sub estimated (Table 1). The empirical parameter of the BWB model (*m*) maintained values around 8.5-10 under well water conditions (WW), however under water stress (WS) *m* reduced its value throughout the season having lower values as water stress increase (Table 1) arriving to 5.9. BWB-L model was able to predict g_s better than BWB. Empirical parameters of BWB-L model (D_0 and *m*) showed a distinct behavior; *m* increased its value throughout the season in both treatments and D_0 in general showed a slow decrease for WW treatment (13% for initial one), however for WS the values dropped to 66% of WW ones.

Date and treatment	π (MPa)	K (mmol m^{-2}s^{-1})	N	r^2	y = ax + b
BMF model					
June WW	- 1.2 ± 0.1^c	9.0 ± 1.2^{bc}	1.2 ± 0.1^a	0.85	Y = 0.81x + 0.03
June WS	- 1.2 ± 0.1^c	13.4 ± 3.4^c	1.1 ± 0.1^a	0.89	Y = 0.87x + 0.02
July WW	- 1.7 ± 0.1^{bc}	11.1 ± 2.8^c	1.5 ± 0.2^a	0.84	Y = 0.82x + 0.05
July WS	- 1.7 ± 0.2^{bc}	3.6 ± 0.3^{ab}	1.7 ± 0.1^a	0.79	Y = 0.75x + 0.03
August WW	- 2.2 ± 0.4^{ab}	3.6 ± 0.7^{ab}	6.9 ± 0.9^c	0.85	Y = 0.89x + 0.02
August WS	- 2.5 ± 0.3^a	1.2 ± 0.4^a	3.4 ± 0.6^b	0.77	Y = 0.77x + 0.01

Table 2: Physiological parameters, osmotic potential (π) hydraulic conductance (K_h) and ABA concentration (*n*), fitted using the mechanistic model of stomatal conductance (g_s) of Buckley et al., 2003. r^2 and equation values corresponded to the values obtained by the lineal regression between measured and modelled data of stomatal conductance (g_s). Values are mean of five replicates ± standard errors. Letters denote statistical differences between dates and treatments.

Table 2 shows the values of the three parameters of the BMF model, when the three parameters were fitted simultaneously without fixing any one of them with a measured value. In contrast with BWB and BWB-L, BMF model parameters, π, *K* and *n* have fully physiological meaning and can be used to infer the physiological processes taking place in the regulation of g_s. In general, it was observed an increase of π around 100% in both treatments throughout the season without any clear effect of treatment (Table 2). K_h showed usually higher values in WW plants than in plants of the WS treatment. However, in August, WW plants experienced a large drop in K_h, bringing them down to values similar to WS. In the WS treatment, that drop is already present for July values but continues dropping in August. The parameter *n*, related to ABA concentration, resulted quite constant during June and July in both treatments but showed an important increase in both treatments in August (Table 2).

The three models (BWB, BWB-L and BMF) were able to predict g_s as it can be observed by the cross-validations, explaining all the variability along the range of measurements (Figure 2).
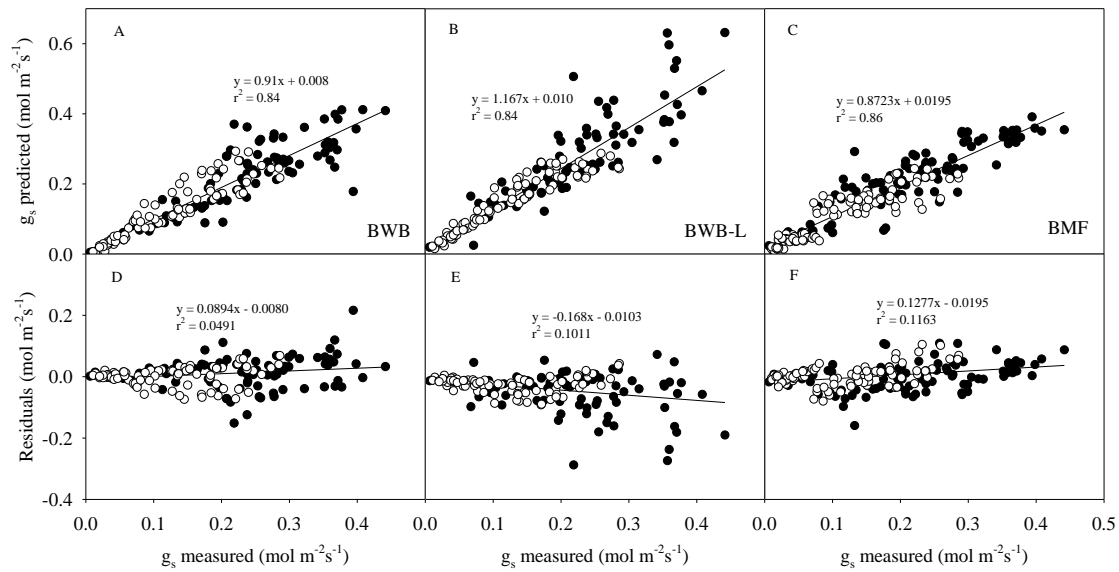
Figure 2: Cross validations obtained by using four parameters adjusted and data for one plant. Each graphic corresponds to a model fitted g_s and residuals itself.

BMF model

Although the adjustment of BMF model was good by fitting the three parameters at the same time, we investigated several options to fit the model using different approaches, since this model allows us the possibility of including measured parameters, like K_h or π. We were interested in testing if this would affect the robustness and applicability of the model. Also, we were interested in the comparison between simulated and measured parameters, as an ultimate proof of the mechanistic basis of the model. BMF was fitted using different options (see material and methods for a description and Table 3 for results) but the obtained results showed contrasting values with the adjusted parameters of the model (K_h, n and π). In all the approaches used to fit the model the relationship between ABA xylem sap and n parameter failed to correlate (Table 3). Fitting the tree parameters at the same time (Approach 1) gave us a nice relationship between hydraulic conductance measured and estimated from the model however the relationship between π estimated from the model and $\Psi_{\pi,TLP}$ measured with the pressure volume curves was not good. The second option, using the values of $\Psi_{\pi,FT}$ as π, fits well g_s but had a poorer adjustment of hydraulic conductance data. However, using the approach 3 where $\Psi_{\pi,TLP}$ corresponds to π, fits well g_s and the fitting of the hydraulic conductance was nice having values consistent with the measured ones (Figure 3). The fourth option using K_h measured from Ohm's law at midday fits also well g_s but the adjustment of π with

139

$\Psi_{\pi,TLP}$ was poor. For the fifth option using K_h measured and $\Psi_{\pi,TLP}$ as π, didn't show any relationship between n and xylem sap ABA concentration (Table 3).

Approach	Validation	g_s measured vs g_s modelled	Equation comparison (π)	Equation comparison (K_h)	Equation comparison (n)
1	Fitting 3	y=0.92x + 0.014	y= 1.68x - 0.83 r^2= 0.282	y=0.82x + 0.15 r^2= 0.524	y=-0.011x+5.98 r^2= 0.387
2	$\Psi_{\pi,FT} = \pi$	y=0.92x + 0.012	-	y=1.31x + 0.56 r^2= 0.588	y=-0.015x+10.43 r^2= 0.130
3	$\Psi_{\pi,TLP} = \pi$	y=0.92x + 0.014	-	y= 0.93x - 0.45 r^2= 0.761	y=-0.009x+6.07 r^2= 0.202
4	$K_{hplant} = K_h$	y=0.92x + 0.014	y= 0.57x + 0.48 r^2= 0.169	-	y=-0.03x+13.44 r^2= 0.404
5	$K_{hplant} = K_h$ $\Psi_{\pi,TLP} = \pi$	y=0.95x + 0.007	-	-	y=0.004x+2.27 r^2= 0.029

Table 3: Linear regression equations obtained using five different approaches to fit the BMF model. Each BMF physiological parameter has a linear regression with the physiological parameter measured with the r^2 obtained.

All approaches were able to fit g_s values but not all the options have a good relationship between estimated and measured parameters. For this reason the third option (using $\Psi_{\pi,TLP}$ as π) was one of the best options used to fit the model. In that case plotting K_h measured with the K_h predicted by the model gave a nice relationship between both parameters (Figure 3). This K_h was well predicted with the BMF model and was the best option to have a nice accuracy in the estimation of g_s.
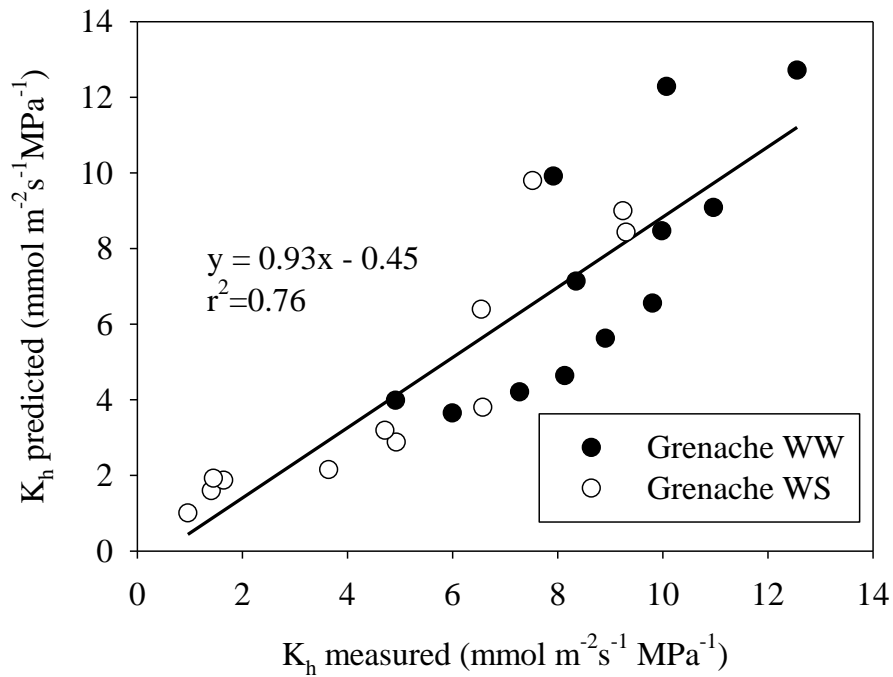
Figure 3: Linear regression between estimated hydraulic conductance (K_h) using BMF model and measured K_h. White circles denote water stress treatment (WS) and black circles well water treatment (WW).

Also, no relationship was observed when ABA xylem sap was plotted vs n. In that case, the ABA concentration was constant or not significantly variable in xylem sap between both dates and treatments at which it was measured but g_s changed (Figure 4). However, it was observed how the relationship between g_s and ABA was different between both dates and this could indicate a possible change of sensitivity of g_s to ABA (Figure 4C). Observing the tendency of the slope of the relationship between g_s and ABA and also the change of the parameter n, in general it can be observed an inverse behavior between both parameters that could indicate that n is more associated to the g_s sensitivity of ABA.
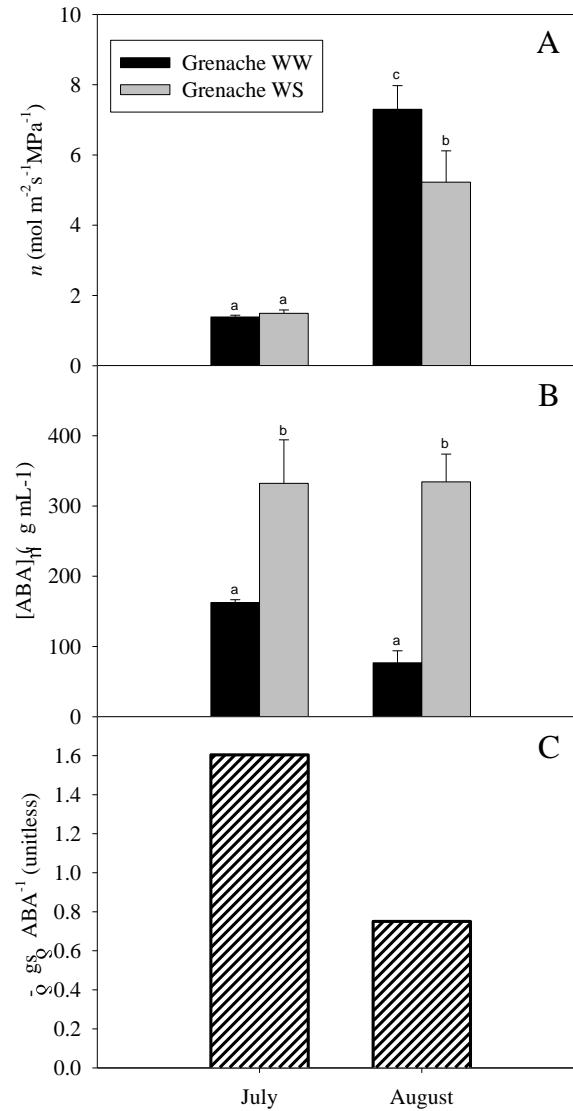
Figure 4: A) ABA concentration values obtained by the prediction of BMF in well watered (WW) and water stress (WS) treatments at July and August dates. B) Measured values of ABA concentration in xylem sap in well watered (WW) and water stress (WS) treatments at July and August dates. C) Slope of the relationship between ABA xylem sap and g_s in both treatments at July and August dates.

Comparing the different parameters adjusted by the models it can be observed as some parameters have the same tendency (Figure 5), although BWB and BWB-L parameters are basically empirical parameters and BMF model present physiological based parameters. In general the same pattern is observed between D_0 from BWB-L and K_h from BMF models, and not as clear as before but it is also observed an increase on the n throughout the season which can be related in part with the increase in the m parameter of the BWB-L.
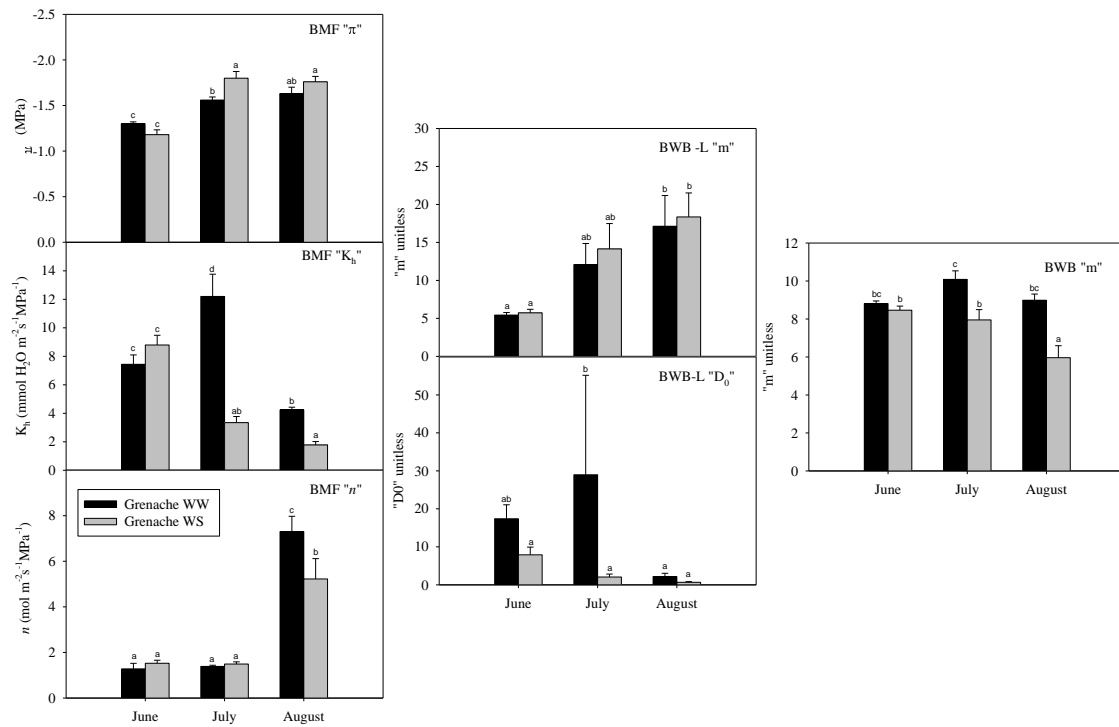
Figure 5: Evolution of the model parameters obtained by the fit of the three models (BWB, BWB-L and BMF models) in June, July and August dates in well water (WW, black) and water stress (WS, grey), treatments. Letters denote significant differences between dates and treatments within the same parameter $p < 0.05$. Each mean represent five replicates $\pm$ standard error.

Also, using the BMF model we are also able to model photosynthesis (Figure 6). Farquhar et al., 1980 model of photosynthesis is intrinsic in the BMF model. That leads also to simulate A_N and obtain a good agreement between measured and modelled A_N in water stress and well water conditions (Figure 7).
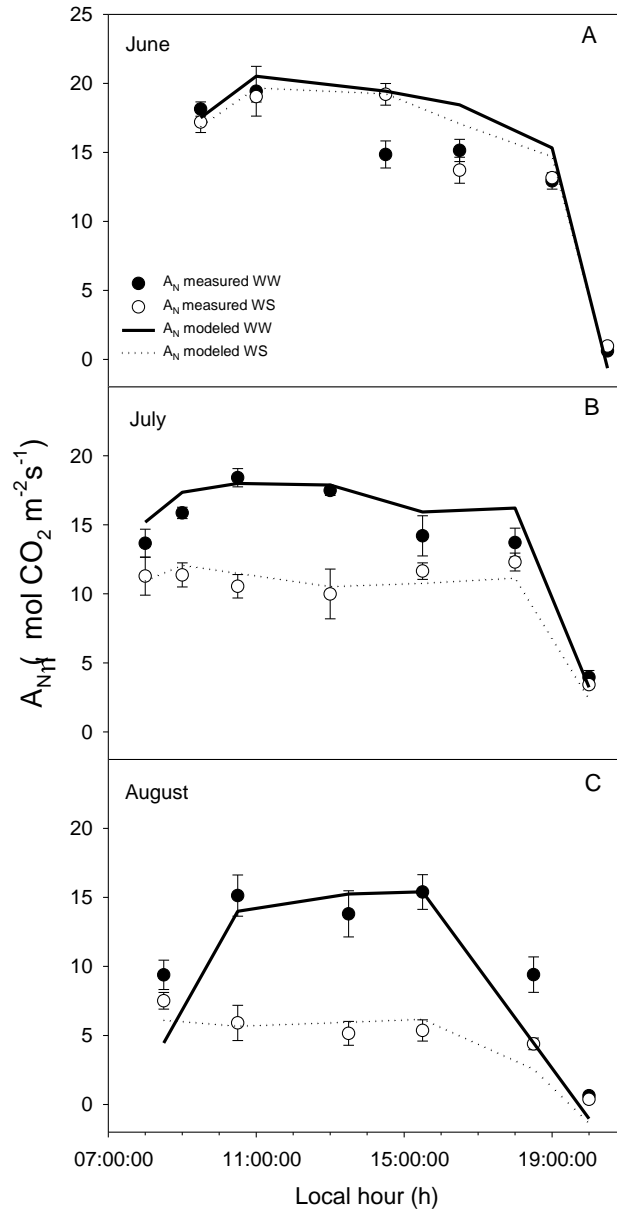
Figure 6: Diurnal variations of net Photosynthesis (A_N) under Well water conditions (black dots) and water stress (white dots). Lines represent modeled values obtained by the coupling of the BMF model with the Photosynthesis model of Farquhar et al., 1980. Each point represent five replicates ± standard error.
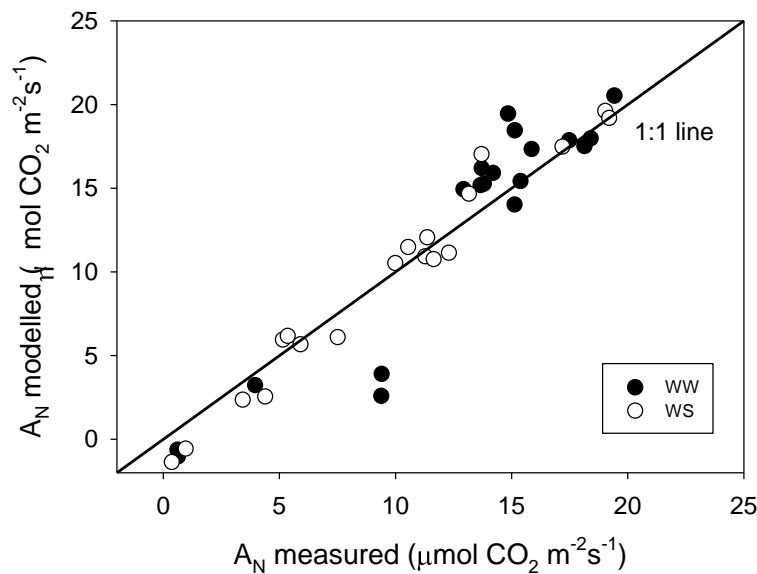
Figure 7: Linear regression between modelled and measured net Photosynthesis (A_N) in well water conditions (black dots) and water stress (white dots). Line plotted in the graph is 1:1. Data presented an $r^2 = 0.92$ and a significance $p < 0.0001$

DISCUSSION

Modelling leaf gas exchange under water stress conditions has become one of the biggest challenges for ecophysiologists in the last two decades (Sala and Tenhunen, 1996; Wang and Leuning, 1998; Diaz-Espejo et al., 2006; 2012; Keenan et al., 2010; Damour et al., 2010; Medlyn et al., 2011; De Egea et al., 2011; Gang et al., 2012). It is recognized that drought is one of the main limiting factor for plant productivity around the world and it is somehow imperative its inclusion in leaf, canopy or global circulation models (GCM) of transpiration and photosynthesis. In order to do so, we need to include the response of stomata to water stress, since it is now widely accepted that this is the first and main factor that contributes to the reduction of photosynthesis under natural conditions (Lawlor and Cornic, 2002; Flexas and Medrano, 2002; Medrano et al., 2002). Unfortunately, all the models used so far to face that issue have a strong empirical basis, which limits strongly their applicability. In this work, we have been able to use for the first time a process-based model of stomatal conductance successfully. This model (BMF), though a simplified version of the original (Buckley, Mott and Farquhar, 2003), has been proven to be robust and simulate the seasonal evolution of g_s in grapevines under field conditions satisfactorily. Even more, the BMF model can be used to infer the mechanisms behind the response of stomata to water

145

stress, and which is their seasonal evolution, opening the gate to new ecophysiological studies.

Models comparison

This is the first time that the BMF is compared with the most widely used semi-empirical models of g_s (BWB and BWB-L). Our data showed that all the models simulate well the diurnal course of g_s in three different dates along the season and in two watering treatments (Figure 1). The BWB model showed less resolution to predict stomatal conductance throughout the season. This could be consequence that BWB was not able to simulate g_s correctly when C_s is equal to the CO_2 compensatory point (Γ) (Leuning, 1990) or that stomata respond more precisely to VPD rather than to relative humidity (Mott and Parkhurst 1991; Aphalo and Jarvis, 1991). Both options were taken into account by Leuning (1995) and incorporated it at the BWB-L model. It was able to predict more precisely g_s, but had the disadvantage respect to BWB that it needs to adjust two empirical parameters instead of just one. Also as we performed the adjustment we used A_N as an input parameter for both models (BWB and BWB-L) which also helps to predict g_s as a high relationship exist between both parameters. Still the main limitation of both models is that they were not able to simulate correctly the water stress response of g_s unless the empirical parameters values were changed accordingly to water stress level (Sala & Tenhunen, 1996; Wang & Leuning 1998; Van Wijk et al., 2000; Misson et al., 2004; Damour et al., 2010; Egea et al., 2011).

Another option is the use of g_s process-based models, based on the physiological processes taking place in plants. The use of mechanistic models of stomatal conductance take advantage on BWB and BWB-L as it is able to predict water stress situations as their parameters variation to water stress are well established. Their parameters have been studied largely being a large number of studies working on K_h and water stress (Sperry and Tyree, 1988; Tyree and Sperry, 1988; Sperry and Tyree, 1990; Lovisolo and Schubert 1998), osmotic potential and water stress (Hsiao et al., 1976; Morgan, 1984) and ABA and water stress (Dodd, 2005). This give us the chance to investigate how K_h, π and n are influenced by water stress and also how these parameters are related to the final adjustment of g_s. Regulation of those parameters is going to be crucial to understand better the g_s behavior under actual field conditions.

BMF model

As BMF is not a commonly used model in the literature we investigated different options to fit it. All the approaches used were able to fit well g_s, but not all of them adjusted well with the measured parameters (Table 3). In this case, we choose a series of physiological parameters that can be measured and compared with the parameters obtained by the model, i.e. $\Psi_{\pi,TLP}$, $\Psi_{\pi,FT}$, $K_{h,plant}$ and [ABA] at xylem sap. As it is supposed that the BMF is a mechanistic model and its parameters have full physiological meaning, it should be possible to measure the parameters and to use them directly in the model. This is the case especially with K_h and π. The other parameter, n, although related to [ABA] is not straight forward since it represents a sensitivity of guard cells to ABA. Related to this I has been observed that the best option to fit *BMF* model was the approach 3 using $\Psi_{\pi,TLP}$ as π and adjusting only two parameters (K_h and n). A nice relationship was found between hydraulic conductance for the modeled and the measured values (Figure 3) being able to predict the decrease of K_h in water stress conditions (Lovisolo et al., 1998; Lovisolo et al., 2002; Choat et al., 2010; Pou et al., 2012). The relationship for g_s measured vs. modeled was close to one (0.93) indicating a nice adjustment of the BMF model with the $\Psi_{\pi TLP}$ as an input parameter. On the other hand, the relationship between n and ABA concentration in the xylem sap was not good. This, in fact, could be consequence that ABA xylem sap was not the one at which stomata is responding. Some reports found that ABA was synthesized in leaves rather than in roots (Holbrook et al., 2002; Christmann et al., 2005). Although of that, it was observed that with this ABA and also the slope of the relationship between g_s and ABA (Figure 4C) the parameter n simulated better the change of sensitivity of ABA in response to g_s than the ABA concentration values itself. This would led to think that some relationship exist between sensibility of ABA and stomatal conductance, also corroborated by the model. To validate the n parameter more measurements are needed to be performed on leaf ABA and know how this parameter can be related with it. Another point to consider is that [ABA] in the plant change along the day as Tallman (2004) showed. This means that the time of the sampling of ABA might be critical and especial care must be taken when designing experiments.

Evolution of the parameters

BWB and BWB-L parameters have not got any physiological meaning and the variability between the parameters is totally empirical and unpredictable. In some works

it have been tried to give a mechanistic basis of this parameters pointing out that m could represent ABA as well as D_0 would defines K_h (Dewar, 2002). This coordination is observed in our Figure 5 which showed the same pattern between D_0 and K_h linking out both models. But although of having the same pattern the principal advantage in this case is that BMF model is able to predict a real physiological value. In this case, hydraulic conductance is predicted to decrease during water stress as it has been observed in response to sustained soil water deficit in grapevines (Lovisolo and Shubert, 1998; Lovisolo et al., 2008; Choat et al., 2010; Brodersen et al., 2013). Moreover, π which is highly related to osmotic adjustment, showed a higher value through the season as it has been reported in grapevines too (During 1984; Rodrigues et al., 1993; Patakas and Noitsakis, 1999, 2001; Patakas et al., 2002; Martorell et al., 2014). This could be consequence that osmolites are being accumulated in leaves by leaf age effects (Patakas and Noitsakis, 2001). In the case of n in general seems that higher ABA concentrations are observed in the leaf at the end of the season. This is in both cases in the well water and water stress treatments as predicted by the model. More studies are necessary to see the role of ABA at the leaf scale compared with the BMF model, but we can infer that n has to be more related to leaf ABA than xylem ABA.

Moreover, BMF model is able to predict photosynthesis well (Figures 6 and 7). This is somehow expected because it already includes the FvCB (Farquhar *et al.*, 1980) model of photosynthesis. But it does mainly because, as we mentioned before, most of the limitation of A_N is due to stomatal closure.

As a main conclusion, the BMF model has been proven to be a good tool to improve our knowledge on stomatal regulation and also on the prediction of g_s. The inclusion of BMF model in global circulation models and also in the ecosystems models can improve the prediction of water use and also carbon gain around the world, referencing the findings with the physiological parameters governing each region. Before that, the model must be tested in more species, and must demonstrate its performance in different types of vegetation. In this sense, it is very promising to focus on the use of the vast amount of ecophysiological information available on plant response to water stress. Especially in the effect of water stress on hydraulic conductance and osmotic adjustment, two of the key parameters in the BMF model.

ACKNOWLEDGMENTS

REFERENCES

Aphalo P.J. & Jarvis P.G. (1991) Do stomata respond to relative humidity? *Plant, Cell & Environment*, **14**, 127-132.

Arora V.K. (2003) Simulating energy and carbon fluxes over winter wheat using coupled land surface and terrestrial ecosystem models. *Agricultural and Forest Meteorology*, **118**, 21-47.

Ball J.T., Woodrow I.E. & Berry J.A. (1987) A model predicting stomatal conductance and its contribution to the control of photosynthesis under different environmental conditions. In *Progress in photosynthesis research* (pp. 221-224). Springer Netherlands.

Brodersen C.R., McElrone A.J., Choat B., Lee E.F., Shackel K.A. & Matthews M.A. (2013) In vivo visualizations of drought-induced embolism spread in *Vitis vinifera*. *Plant physiology*, **161**, 1820-1829.

Buckley T. N. & Mott K. A. (2013) Modelling stomatal conductance in response to environmental factors. *Plant, Cell & Environment*, **36**, 1691-1699.

Buckley T.N. (2005) The control of stomata by water balance. *New Phytologist*, **168**, 275-292.

Buckley T.N., Mott K.A. & Farquhar G.D. (2003) A hydromechanical and biochemical model of stomatal conductance. *Plant, Cell & Environment*, **26**, 1767-1785.

Buckley T.N., Turnbull T.L. & Adams M.A. (2012) Simple models for stomatal conductance derived from a process model: cross-validation against sap flux data. *Plant, Cell & Environment*, **35**, 1647-1662.

Choat B., Drayton W.M., Brodersen C., Matthews M.A., Shackel K.A., Wada H. & Mcelrone A. J. (2010) Measurement of vulnerability to water stress-induced cavitation in grapevine: a comparison of four techniques applied to a long-vesseled species. *Plant, Cell & Environment*, **33**, 1502-1512.

Christmann A., Hoffmann T., Teplova I., Grill E. & Müller A. (2005) Generation of active pools of abscisic acid revealed by in vivo imaging of water-stressed Arabidopsis. *Plant Physiology*, **137**, 209-219.

Cox P.M., Huntingford C. & Harding R.J. (1998) A canopy conductance and photosynthesis model for use in a GCM land surface scheme. *Journal of Hydrology*, **212**, 79-94.

Damour G., Simonneau T., Cochard H. & Urban L. (2010) An overview of models of stomatal conductance at the leaf level. *Plant, Cell & Environment*, **33**, 1419-1438.

Dewar R.C. (1995) Interpretation of an empirical model for stomatal conductance in terms of guard cell function. *Plant, Cell & Environment*, **18**, 365-372.

Dewar R.C. (2002) The Ball–Berry–Leuning and Tardieu–Davies stomatal models: synthesis and extension within a spatially aggregated picture of guard cell function. *Plant, Cell & Environment*, **25**, 1383-1398.

Diaz-Espejo A., Buckley T.N., Sperry J.S. *et al.* (2012) Steps toward an improvement in process-based models of water use by fruit trees: a case study in olive. *Agricultural Water Management*, **114**, 37-49.

Diaz-Espejo A., Walcroft A.S., Fernández J.E., Hafidi B., Palomo M.J. & Girón I.F. (2006). Modeling photosynthesis in olive leaves under drought conditions. Tree Physiology, 26, 1445-1456.

Dodd I.C. (2005) Root-to-shoot signalling: assessing the roles of 'up'in the up and down world of long-distance signalling in planta. In *Root Physiology: from Gene to Function* (pp. 251-270). Springer Netherlands.

During H. (1984). Evidence ior osmotic adjustment to drought in grapevines.*Vitis*, *23*, 1-10.

Egea G., Verhoef A. & Vidale P.L. (2011) Towards an improved and more flexible representation of water stress in coupled photosynthesis–stomatal conductance models. *Agricultural and Forest Meteorology*, **151**, 1370-1384.

Farquhar G.D., von Caemmerer S.V. & Berry J.A. (1980) A biochemical model of photosynthetic CO_2 assimilation in leaves of C3 species. *Planta*, *149*, 78-90.

Flexas J. & Medrano H. (2002) Drought-inhibition of photosynthesis in C3 plants: stomatal and non-stomatal limitations revisited. *Annals of Botany*, **89**, 183-189.

Gómez-Cadenas A., Pozo O.J., García-Augustín P. & Sancho J.V. (2002) Direct analysis of abscisic acid in crude plant extracts by liquid chromatography-electrospray/tandem mass spectrometry. *Phytochemical Analysis*, **13,** 228-234.

Gutschick V.P. & Simonneau T. (2002) Modelling stomatal conductance of field-grown sunflower under varying soil water content and leaf environment: comparison of three models of stomatal response to leaf environment and coupling with an abscisic acid-based model of stomatal response to soil drying. *Plant, Cell & Environment*, **25**, 1423-1434.

Gutschick V.P. (2007) Plant acclimation to elevated CO_2-From simple regularities to biogeographic chaos. *Ecological Modelling*, **200**, 433-451.

Holbrook N.M., Shashidhar V.R., James R.A. & Munns R. (2002) Stomatal control in tomato with ABA-deficient roots: response of grafted plants to soil drying. *Journal of Experimental Botany*, *53*, 1503-1514.

Hsiao T.C., Acevedo E., Fereres E. & Henderson D.W. (1976) Water stress, growth, and osmotic adjustment. *Philosophical Transactions of the Royal Society of London. B, Biological Sciences*, **273**, 479-500.

Jarvis P.G. (1976) The interpretation of the variations in leaf water potential and stomatal conductance found in canopies in the field. *Philosophical Transactions of the Royal Society of London. B, Biological Sciences*, **273**, 593-610.

Keenan T., Sabate S. & Gracia C. (2010) Soil water stress and coupled photosynthesis–conductance models: Bridging the gap between conflicting reports on the relative roles of stomatal, mesophyll conductance and biochemical limitations to photosynthesis. *Agricultural and Forest Meteorology*, **150**, 443-453.

Lawlor D.W. & Cornic G. (2002) Photosynthetic carbon assimilation and associated metabolism in relation to water deficits in higher plants. *Plant, Cell & Environment*, **25**, 275-294.

Leuning R. (1990) Modelling stomatal behaviour and and photosynthesis of Eucalyptus grandis. *Functional Plant Biology*, **17**, 159-175.

Leuning R. (1995) A critical appraisal of a combined stomatal-photosynthesis model for C3 plants. *Plant, Cell & Environment*, **18**, 339-355.

Lovisolo C. & Schubert A. (1998) Effects of water stress on vessel size and xylem hydraulic conductivity in Vitis vinifera L. *Journal of Experimental Botany*, **49**, 693-700.

Lovisolo C., Hartung W. & Schubert A. (2002) Whole-plant hydraulic conductance and root-to-shoot flow of abscisic acid are independently affected by water stress in grapevines. *Functional Plant Biology*, **29**, 1349-1356.

Lovisolo C., Perrone I., Hartung W. & Schubert A. (2008) An abscisic acid-related reduced transpiration promotes gradual embolism repair when grapevines are rehydrated after drought. *New Phytologist*, **180,** 642-651.

Martorell S., Medrano H., Tomàs M., Escalona JM., Flexas J., Díaz-Espejo A., Plasticity of vulnerability to leaf hydraulic dysfunction during acclimation to drought in grapevines: an osmotic-mediated process. *Physiologia Plantarum* Doi: 10.1111/ppl.12253

Medrano H., Escalona J.M., Bota J., Gulias J. & Flexas J. (2002) Regulation of photosynthesis of C3 plants in response to progressive drought: stomatal conductance as a reference parameter. *Annals of Botany*, **89**, 895-905.

Misson L., Panek J.A. & Goldstein A.H. (2004) A comparison of three approaches to modeling leaf gas exchange in annually drought-stressed ponderosa pine forests. *Tree Physiology*, **24**, 529-541.

Mo X. & Liu S. (2001) Simulating evapotranspiration and photosynthesis of winter wheat over the growing season. *Agricultural & Forest Meteorology*, **109**, 203-222.

Morgan J.M. (1984) Osmoregulation and water stress in higher plants. *Annual Review of Plant Physiology*, **35**, 299-319.

Mott K.A. & Parkhurst D.F. (1991) Stomatal responses to humidity in air and helox. *Plant, Cell & Environment*, **14**, 509-515.

Patakas A. & Noitsakis B. (2001) Leaf age effects on solute accumulation in water-stressed grapevines. *Journal of plant physiology*, **158**, 63-69.

Patakas A. & Nortsakis B. (1999) Mechanisms involved in diurnal changes of osmotic potential in grapevines under drought conditions. *Journal of plant physiology*, **154**, 767-774.

Patakas A., Nikolaou N., Zioziou E., Radoglou K. & Noitsakis B. (2002) The role of organic solute and ion accumulation in osmotic adjustment in drought-stressed grapevines. *Plant Science*, **163**, 361-367.

Peak D. & Mott K.A. (2011) A new, vapour-phase mechanism for stomatal responses to humidity and temperature. *Plant, Cell & Environment*, **34**, 162-178.

Pou A., Medrano H., Tomàs M., Martorell S., Ribas-Carbó M. & Flexas J. (2012) Anisohydric behaviour in grapevines results in better performance under moderate water stress and recovery than isohydric behaviour. *Plant and Soil*, **359**, 335-349.

Rodrigues M.L., Chaves M.M., Wendler R., David M.M., Quick W.P., Leegood R.C., Stitt M. & Pereira, J. S. (1993) Osmotic adjustment in water stressed grapevine leaves in relation to carbon assimilation. *Functional Plant Biology*, **20**, 309-321.

Sack L. & Pasquet-Kok J & Prometheuswiki contributors. (2011) Leaf pressure–volume curve parameters. *PrometheusWiki website: http://prometheuswiki. publish. csiro. au/tikiindex. php*.

Sala A. & Tenhunen J.D. (1996) Simulations of canopy net photosynthesis and transpiration in *Quercus ilex* L. under the influence of seasonal drought. *Agricultural & Forest Meteorology*, **78**, 203-222.

Sperry J.S. & Tyree M.T. (1988) Mechanism of water stress-induced xylem embolism. *Plant Physiology*, **88**, 581-587.

Sperry J.S. & Tyree M.T. (1990) Water-stress-induced xylem embolism in three species of conifers. *Plant, Cell & Environment*, **13**, 427-436.

Tallman G. (2004) Are diurnal patterns of stomatal movement the result of alternating metabolism of endogenous guard cell ABA and accumulation of ABA delivered to the apoplast around guard cells by transpiration? *Journal of Experimental Botany, 55*, 1963–1976.

Tyree M.T. & Hammel H.T. (1972) The measurement of the turgor pressure and the water relations of plants by the pressure-bomb technique. *Journal of Experimental Botany*, **23**, 267-282.

Tyree M.T. & Sperry J.S. (1988) Do woody plants operate near the point of catastrophic xylem dysfunction caused by dynamic water stress? Answers from a model. *Plant Physiology*, **88**, 574-580.

Van Wijk M.T., Dekker S.C., Bouten W., Bosveld F.C., Kohsiek W., Kramer K., & Mohren G.M.J. (2000) Modeling daily gas exchange of a Douglas-fir forest: comparison of three stomatal conductance models with and without a soil water stress function. *Tree Physiology*, **20**, 115-122.

Verhoef A. & Allen S.J. (2000) A SVAT scheme describing energy and CO_2 fluxes for multi-component vegetation: calibration and test for a Sahelian savannah. *Ecological Modelling*, **127**, 245-267.

Wang Y.P. & Leuning R. (1998) A two-leaf model for canopy conductance, photosynthesis and partitioning of available energy I:: Model description and comparison with a multi-layered model. *Agricultural and Forest Meteorology*, **91**, 89-111.

5. UPSCALING FROM LEAF TO WHOLE CANOPY PROCESSES: CHARACTERZING THE LEAF POSITION AND MICROCLIMATE EFFECTS OF GRAPEVINE CANOPIES

5.1. Hydraulic constraints can explain the sub-optimal distribution of photosynthetic capacity in plant canopies due to diffusional limitations

Martorell S[1], Buckley TN[2], Tomàs M[1], Escalona JM[1], Ribas-Carbó M[1], Medrano H[1], Diaz-Espejo A[3]

[1] Research Group on Plant Biology under Mediterranean Conditions, Departament de Biologia, Universitat de les Illes Balears, Carretera de Valldemossa Km 7.5, 07122 Palma de Mallorca, Illes Balears, Spain.

[2] IA Watson Grains Research Centre, Faculty of Agriculture and Environment, The University of Sydney, Narrabri, NSW Australia.

[3] Irrigation and Crop Ecophysiology Group, Instituto de Recursos Naturales y Agrobiología de Sevilla (IRNAS, CSIC). Avenida Reina Mercedes 10, 41012 Sevilla, Spain.

ABSTRACT

Plant canopies are a complex system to study the physiological parameters regulating gas exchange. Some ways have been used to simplify the upscaling of photosynthesis to the total canopy, but results found with these ways highlight the need to introduce more realism to predict canopy photosynthesis. In this study we worked with the canopy of a crop, grapevine on conventional trellis system, with the Grenache grapevine cultivar measuring gas exchange and photosynthetic capacity in 14 crown positions. Results indicate that carboxylation rate (V_c) was distributed through the canopy being well correlated with the cumulative radiation observed in each position. However maximum photosynthesis rate wasn't well correlated with the previous correlation being differently regulated in the west and east canopy positions. That highlight that other constrains than average intercepted light were modifying photosynthesis rates. We found that stomatal conductance (g_s) was an important limitation to the photosynthesis rate. After some analysis we found that hydraulic conductance seems a putative candidate to regulate g_s at the conditions encountered in this study at the different positions of the grapevine canopy leading to have a suboptimal A_N distribution.

Key words: Grapevine canopy, hydraulic conductance, stomatal conductance, Photosynthesis contributions.

INTRODUCTION

Light is considered the key environmental driver in plant canopies (Niinemets and Anten 2009). All leaves receive a limited amount of irradiance and it can vary according to the position occupied in the crown. Ranges of 20-50 fold between canopy top and bottom in closed plant stands are usual (Lieffers et al., 1999) and a range of 100-fold of difference between top and down in tropical rainforest is the maximum observed (Valladares, 2003; Kitajima et al., 2005). Light has been observed to be well correlated with nitrogen content in leaves (DeJong and Doyle, 1985); however nitrogen is a limiting element in soil and its uptake and assimilation by plants is limited due to the high cost of energy in the assimilation process (Gutschick, 1981; Field and Mooney, 1986; Chapin et al., 1987). Taking into consideration the last statements, both (light and nitrogen) have been postulated as the most limiting resources within the canopy, limiting the photosynthesis rate (Field and Mooney, 1986; Evans, 1989). The relationship between nitrogen and light led to think that light is well related to the

photosynthetic capacity since most of the nitrogen in leaves is used for the construction of the photosynthetic apparatus (Evans, 1989). Even thought, when photosynthetic capacity is represented versus integrated light a curvilinear scattered response is commonly observed indicating that maximum photosynthetic rate saturates at intermediate light intensities and therefore, the photosynthetic capacity per unit of incident irradiance declines up through the crown (Buckley et al., 2013). This fact complicates the attempts to explain and model the variability and patterns of distribution of leaf nitrogen and photosynthetic capacity within canopies.

One of the most extended hypotheses for resources distribution within canopies is the optimization theory (Cowan and Farquhar, 1977). However, this theory suggests that for an optimal allocation of resources, nitrogen and photosynthetic capacity have to present a linear relationship between them and light interception. As a linear relationship is seldom found in real canopies this has driven to several authors (Dewar et al., 2012; Peltoniemi et al., 2012; Niinemets, 2012; Buckley et al., 2013) to conclude that other constrains along the canopy are playing a role in the determination of photosynthesis.

One of the physiological targets that have special influence on photosynthesis is stomatal conductance (g_s). Cowan and Farquhar (1977) suggested that g_s optimize water loss and maximize carbon gain (optimization theory). Under this hypothesis g_s and photosynthesis are well related and both are taken in account to estimate the whole canopy photosynthesis. But this theory fails to predict photosynthesis of the global canopy observing in general over estimations of canopy photosynthesis rates (Anten et al., 2000). Limitations for the theory could be due to environmental variables such as temperature, humidity and windiness. These environmental variables have been reported to affect leaf photosynthesis and could explain the deviation between optimal profiles and the real values (Niinemets and Valladares, 2004). Recently, some studies have reported other possibilities to explain the disjunction between the theory and the real data (Dewar et al., 2012; Peltoniemi et al., 2012; Niinemets, 2012; Buckley et al., 2013), concluding that H_2O and CO_2 pathways are possible limitations to the optimization theory.

On one hand, it has been observed how mesophyll conductance (g_m) vary according to the leaf position into the canopy (Niinemets et al., 2006; Woodruff et al 2009; Mullin et al., 2009; Whitehead et al., 2011; Han, 2011; Cano et al., 2013). Buckley and Warren (2014) modelled g_m variation across a canopy profile and conclude that CO_2 pathways need to be optimized to have an optimum photosynthesis. On the other hand, hydraulic

conductance has also been observed to vary between sun and shaded leaves (Sack et al., 2003; Brodribb and Jordan 2011; Nardini et al., 2012). Peltoniemi et al., (2012) introduced kh in a model of gs and conclude the need to have a optimized K_h to obtain an optimized A_N.

The main goal of this work is to investigate the possible constrains affecting A_N distribution along a grapevine canopy and find which physiological parameters are driving the suboptimal distributions encountered within the canopy in different studies.

MATERIAL & METHODS

Plant material

The experiment was conducted from 17 to 24 August 2012 at the experimental field of the University of Balearic Islands on grapevine plants of Grenache cultivar during summer 2012. Plants were three years old grafted on Richter-110 and planted in rows (distance between rows was 2.5 m and plants 1 m). They were conducted in a bilateral double cordon having between 10-12 canes per plant and were irrigated with 9 liters per day and plant (around 70% of ETo), an amount that had been established as adequate under our experimental conditions to sustain high plant water status. Four plants and 14 crown positions of each plant were selected for gas exchange measurements. Four of these positions were on the east face of the crown (positions 1-4), two were on the top of the crown (5 & 6), four were on the west face (7-10), and four were located in the inner part of the crown (11-14). These crown positions are illustrated in Figure 1. Meteorological variables were recorded by a meteorological station located in the same field site (Meteodata 3000, Geonica, Spain.).

Gas exchange measurements

Diurnal gas exchange measurements were taken at the fourteen crown positions on 23th of August using an open flow gas exchange system (Li-6400, Li-Cor) equipped with a clear chamber (Li-6400-08). Net photosynthesis (A_N) and stomatal conductance (g_s) were measured through the day at different time hours (09:15, 11:00, 13:45, 16:00 and 18:30, CEDT). Air temperature and humidity in the chamber was set to match ambient and c_a was set at 400 µmol mol^{-1}. Of the 280 expected measurements (5 times x 14 positions x 4 individuals), 10 were lost due to errors in the data collection, leaving 270 measurements.
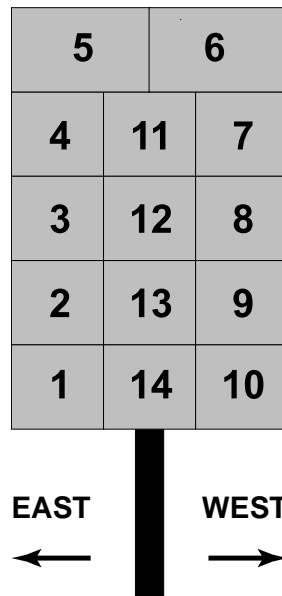
Figure 1: Diagram showing the 14 position measured throught the canopy

Estimating photosynthetic parameters

At each of the four plant crowns photosynthetic parameters were estimated as follows. The response of net photosynthesis (A_N) to intercellular CO_2 (c_i) were performed using an open flow gas exchange system (Li-6400; Li-Cor, Inc., Lincoln, Nebraska) equipped with a leaf chamber fluorimeter (Li-6400-40;Li-Cor). Curves were performed under saturated light (1500 μmol m^{-2}s^{-1}), with block temperature controlled at 30°C. Ambient CO_2 (c_a) was allowed to change between 50 and 1600 μmol mol^{-1}. After steady state was reached at 400 μmol mol^{-1}, C_a was lowered stepwise from 400 to 50 μmol mol^{-1}, then returned to 400 μmol mol^{-1} and increased stepwise to 1600 μmol mol^{-1}. A total of 16 points were recorded for each curve. V_m, J_m and g_m were estimated by the curve fitting method proposed by Ethier & Livingston (2004). The values were corrected to 25°C using the temperature responses measured on leaves of the same variety (chapter 4.1 of this thesis and Buckley et al., 2014).

BMF model of stomatal conductance

A modified version of the process based model of Buckley, Mott and Farquhar (2003) (hereafter, the BMF model) of stomatal conductance was used. This model is based on leaf, stomata water relations and the hypothesis that the regulation of the osmotic pressure of the guard cells is related to ATP production by the photosynthetic cells (using the model of Cowan and Faquhar (1980)). The model also assumes that turgor pressure of the epidermis represents the changes in water status of the leaf.

The simplified version of the BMF model has the following equation:

159

$$g_s = \frac{naK(\Psi_s + \pi)}{K + na\text{VPD}} \quad (1)$$

where K is leaf-specific hydraulic conductance, Ψ_s is soil water potential, π is bulk leaf osmotic pressure and VPD is leaf to air water vapor mole fraction gradient. n and a capture non-hydraulic effects: a is mesophyll ATP concentration expressed relative to its maximum value and n is a lumped parameter representing other non-hydraulic factors:

$n \equiv \mathcal{X}\beta\tau_m$, (2) and

$a \equiv \tau/\tau_m$, (3)

Were τ is ATP concentration in photosynthesizing cells, χ is a proportionality factor that scales the guard and epidermal cell turgor pressures to g_s, β is a proportionality factor that scales the product of τ and the epidermal turgor to changes in guard cell osmotic pressure and τ_m is the maximum τ (the total pool of adenylates, ADP+ATP).

Osmotic potential determination

Leaves from each position and plant crown were collected, frozen in liquid nitrogen and stored at -80ºC until its analysis. One 7-mm diameter disc per leaf was sampled with a cork borer. It was punctured 15-20 times with forceps to speed equilibration and immediately loaded in a C-52 thermocouple psychrometer chamber (Wescor Inc., Logan, UT) connected to a data logger (PSYPRO, Wescor). Equilibrium was reached in ~30 min. After that osmotic potential was obtained.

Limitation analysis of g_s

We performed the analysis of limitations proposed by Rodriguez-Dominguez et al (personal communication). The stomatal limitations can be hydraulic and non-hydraulic limitation (y_h and y_{nh} respectively). Hydraulic limitation was defined to be due to investments in hydraulic conductance, K ($y_h = \delta \ln g_s / \delta \ln K$) and the non-hydraulic limitation were due to limitations in the product na ($y_{nh} = \delta \ln g_s / \ln(na)$). The derivatives are as follow:

$$y_h \equiv \frac{\partial \ln g_s}{\partial \ln K} = \frac{na}{\dfrac{K}{\Delta w} + na}, (4) \; and$$

$$y_{nh} \equiv \frac{\partial lng_s}{\partial \ln na} = \frac{\frac{k}{\Delta W}}{\frac{K}{\Delta W} + na} = 1 - y_h \quad (5)$$

Contributions analysis

The contributions analysis proposed by Buckley and Diaz-Espejo (2014) were used to partition changes in photosynthesis into contributions from the underlying variables. This new approach uses numerical integration having the advantage to avoid the bias caused by the discrete approximations and avoiding the need to compute partial derivatives for each variable and relying instead on substitution in the photosynthesis model. This approach is easily extended to encompass effects of changes in any photosynthetic variable, under any conditions.

This approach integrates changes produced in A across the interval between reference value and comparison points and the resulting contributions are expressed as percentages of the value of A at a reference point (A_{ref}). The contribution from a variable x_j to a change in A is defined as:

$$\rho_{xj} \equiv \frac{100}{A_{ref}} \cdot \sum_{k=0}^{n-1} \left[\delta A \big| \delta x_j \right]_k^{k+1}$$

Similarly, it can be calculated the total contribution from diffusional conductances (g_{sc}, g_m and g_{bc});

$$\rho_{diff} \equiv \frac{100}{A_{ref}} \cdot \sum_{k=0}^{n-1} \left[\delta A \big| \delta g_{sc}, \delta g_{bc}, \delta g_m \right]_k^{k+1}$$

and the total contribution from variables that involve the biochemistry of photosynthesis;

161

$$\rho_{bio} \equiv \frac{100}{A_{ref}} \cdot \sum_{k=0}^{n-1} \left[\begin{array}{c} \delta A \big| \delta V_{cmax}, \delta J_{max}, \delta V_{tpu}, \delta R_d, \\ \delta K_c, \delta K_o, \delta \Gamma_*, \delta \phi, \delta \theta_j, \delta i \end{array} \right]_k^{k+1}$$

RESULTS

Our data confirmed the results found in most studies, in which photosynthetic capacity of leaves (V_c) within a canopy followed a curvilinear response to daily cumulative PPFD (Fig. 2a). Also the correlation between V_c and leaf nitrogen by area (N_a) was linear for the whole canopy positions measured (Fig. 2b) showing a direct role of nitrogen in the construction of the photosynthetic machinery of leaves.
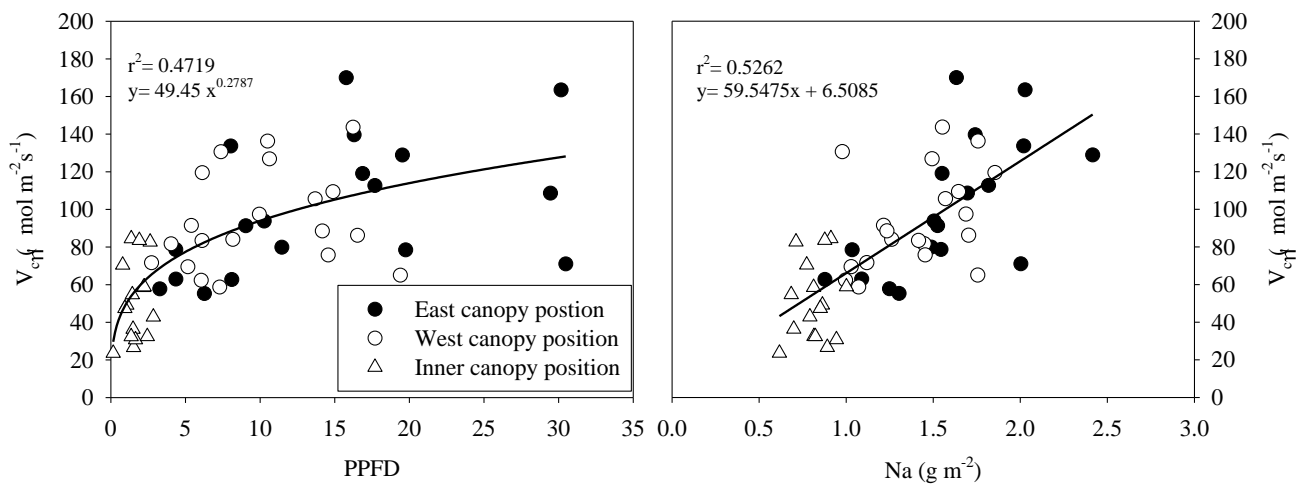

Figure 2: Carboxylation rate versus a) integral PAR received during one day b) total nitrogen content per area (Na). Each point is an individual measurement.

However, leaves located in the west side of the canopy tended to show lower maximum photosynthesis rate ($A_{N,max}$) than those in the east for a given cumulative radiation (Figure 3a). This pattern was also observed in the maximum stomatal conductance ($g_{s,max}$) (Figure 3B) highlighting a different regulation effect on both sides of the canopy for $A_{N,max}$.
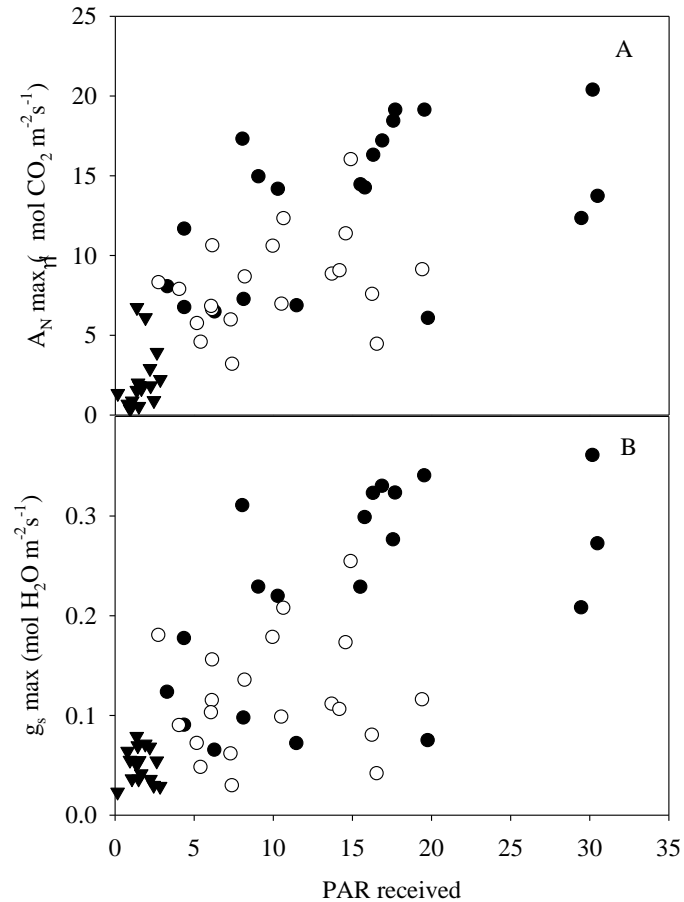
Figure 3: Integral PAR received during one day versus a) maximum Photosynthetic rate observed in each position (A_{Nmax}) and b) maximum stomatal conductance observed in each position (g_{smax}). Values are individual measurements.

To study the possible change of contributions to plant photosynthesis in the different locations of the crown we investigated the biochemical and diffusional contributions affecting each location. For this purpose we applied the contribution analysis proposed by Buckley & Diaz-Espejo, (2014) in each canopy position. In general, it was observed that diffusional contributions were higher than biochemical in sunny exposed leaves of the canopy (Figure 4). The pattern of diffusional contributions were irregular along the different locations studied in the canopy, having less contributions in the east part of the canopy and higher contributions in the west. Also, the highest total contributions were observed in the inner parts of the canopy showing a higher proportion of biochemical contributions than diffusional ones.
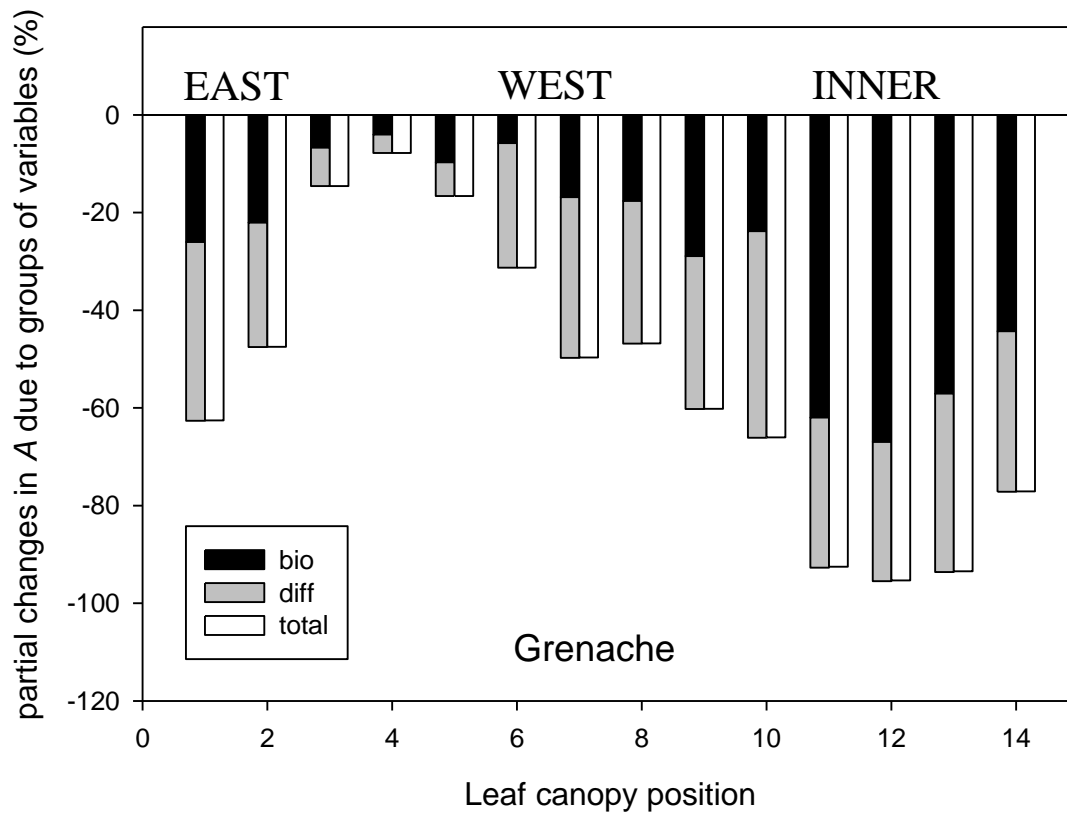
Figure 4: Analysis of contributions with total contributions (blank bars) and biochemical (black bars) and diffusional (grey bars). Values are means of four replicates per position

When diffusional contributions were partitioned into stomatal and mesophyll conductance it was observed that diffusional contributions were highly attributed to stomatal conductance, having in most of the cases the highest value of the contribution (Figure 5). Positions 4 and 5 presented relatively much less stomatal conductance contributions to changes in A_N than positions 6 and 7, despite of having similar accumulative irradiance along the day.
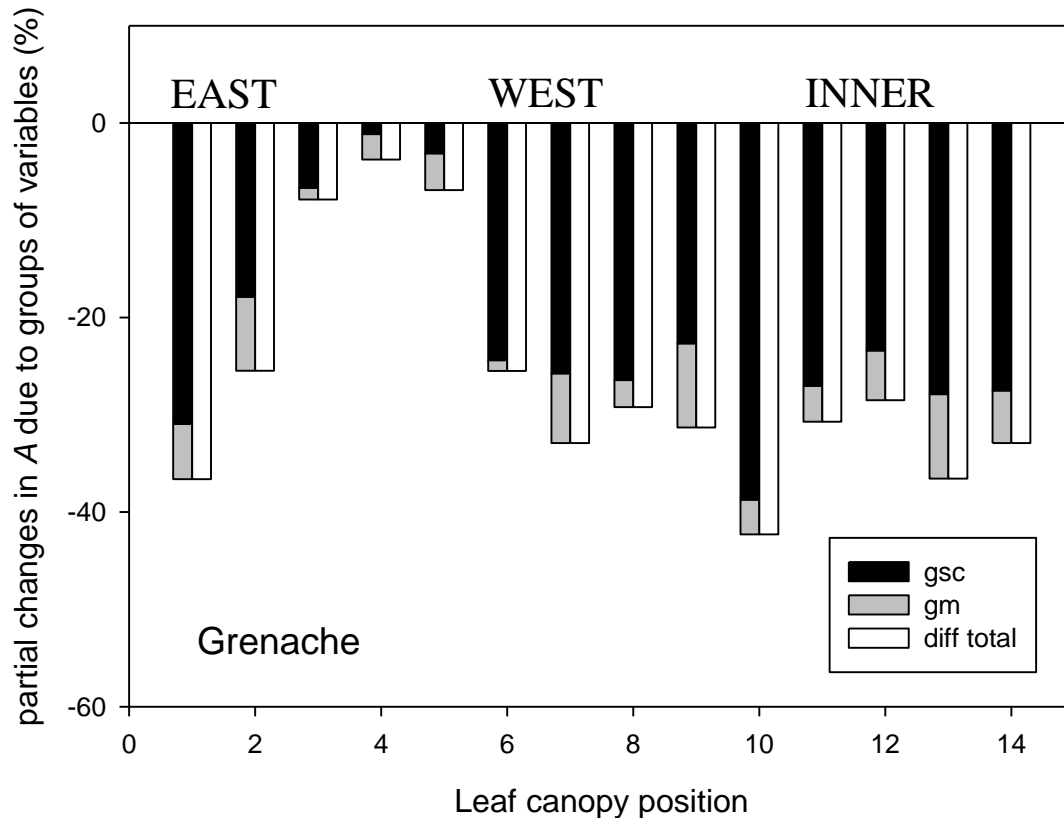
Figure 5: Partitioning of diffusional contributions into stomatal conductance contributions (black bars) and mesophyll conductance contributions (grey bars). Values are means of four replicates per position.

Once identified g_s as a major limitation in A_N, we used the Buckley et al., (2003) model of stomatal conductance to obtain the key physiological parameters regulating stomatal conductance. No significant differences were found in the osmotic potential of leaves at the different locations (data not shown; averaged $\pi = 1.71$; P<0.05). However, we found more variability in the other two parameters of the model: hydraulic conductance (K) and n, a parameter which has been associated to the non-hydraulic response (chemical signaling) and therefore, putatively related to ABA. K obtained by the fit of the model showed a curvilinear response to accumulative PPFD similar to V_c, (Fig. 6a), although at this time differentiating between east and west side locations. It was observed how leaves located in the east side had, in general, higher values of K than leaves located at the west site for a given accumulative PPFD. When K was plotted against V_c, two trends emerged also (Fig. 6b), although scattered. That trends showed that the correlation between hydraulic and photosynthetic capacity of leaves were different depending on the site of the canopy studied.
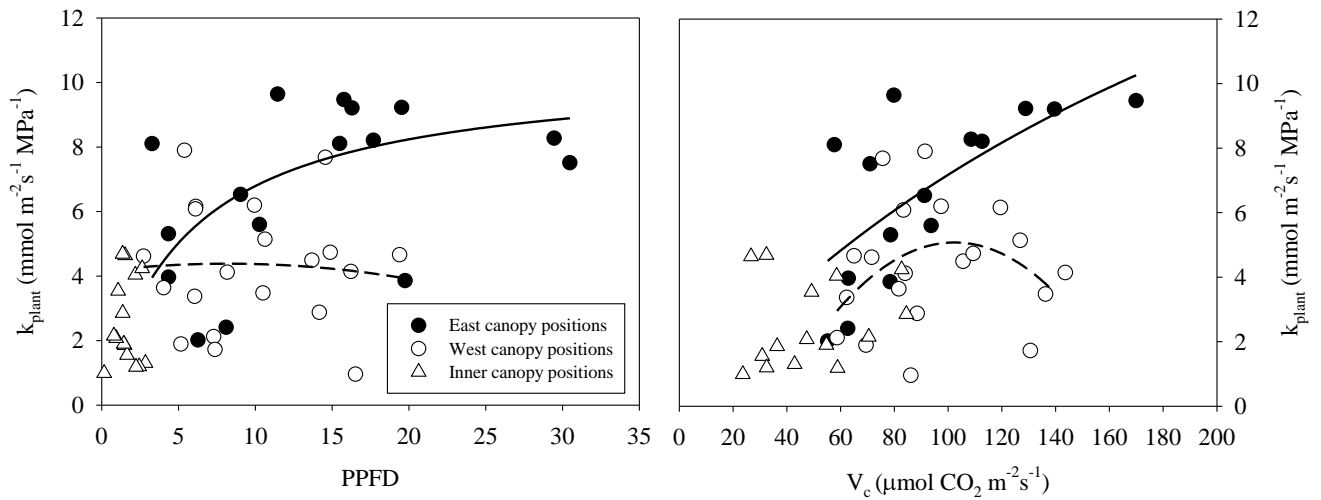
Figure 6: K value predicted from the Buckley et al., (2003) model of stomatal conductance versus a) integral PAR received during one day b) carboxylation rate (V_c). Each point is an individual measurement.

Therefore, location, especially related to orientation, had a major role in the distribution of the physiological parameters regulating stomatal conductance. A trend emerged clearer when averages per location were calculated for the physiological parameters obtained by the BMF model. *K* was consistently higher in the locations of the east side of the canopy than in the west side (Fig, 7a). Similarly, *n* followed a pattern within the canopy, although in this case opposite to *K* (Fig. 7b). Locations in the east presented on average higher values than those in the west. Both parameters were correlated (P<0.01) and showed a negative linear relationship (r^2= 0.56).
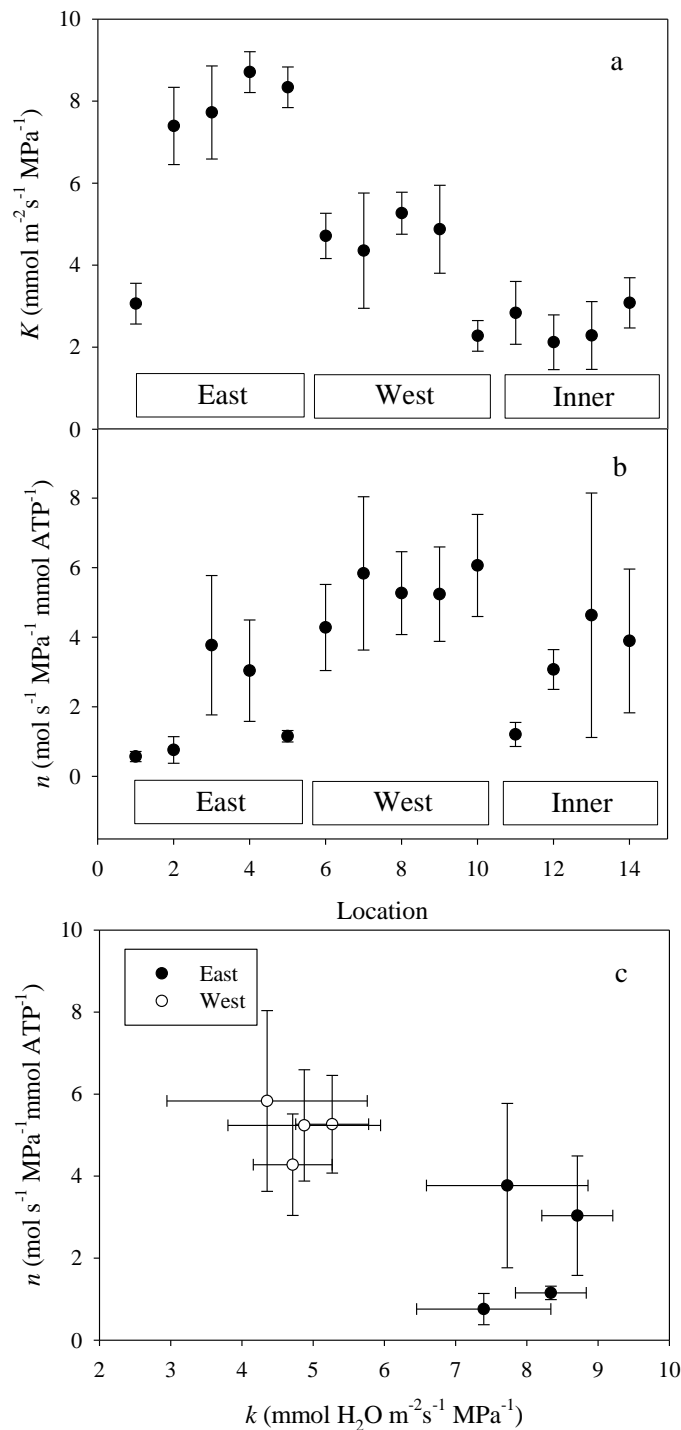
Figure 7: Model parameters (*K* and *n*) related to each position in the canopy (a b graphs). C) Relationship between n and k between east and west site of the canopy. Points represent average values of four measurements ± standard error.

Finally, to quantify the role of hydraulic and non-hydraulic signals limiting g_s we applied an analysis of limitations on the BMF model. We selected 5 representative leaves for east and west canopy locations, where PPFD peak was received before or after noon (Fig. 8a for east, Fig. 8b for west). For each canopy position we also

represent the atmospheric demand (VPD), which was very similar between both orientations (Figures 9c and 9d). However the most important aspect to highlight was that in east locations high PPFDs values were achieved when VPD was still relatively low, meanwhile the peak of PPFD in west locations occurred when VPD was the highest. In terms of hydraulic limitations (γ_h) the diurnal evolution in east and west were different (Fig 9e and 9f). Locations at east presented their peaks in γ_h around noon with average maximum values of 0.90 (Fig 9 e) but throughout the afternoon γ_h was reduced (e.g. after 16:00 GMT γ_h was lower than 0.5). In the west locations γ_h was maintained at values over 0.5 early in the morning and close to 1 for most of the day (Fig. 9 f). As a consequence, the limitations due to non-hydraulic signals (γ_{nh}) showed very low values for most of the day except on the last hours of the day.
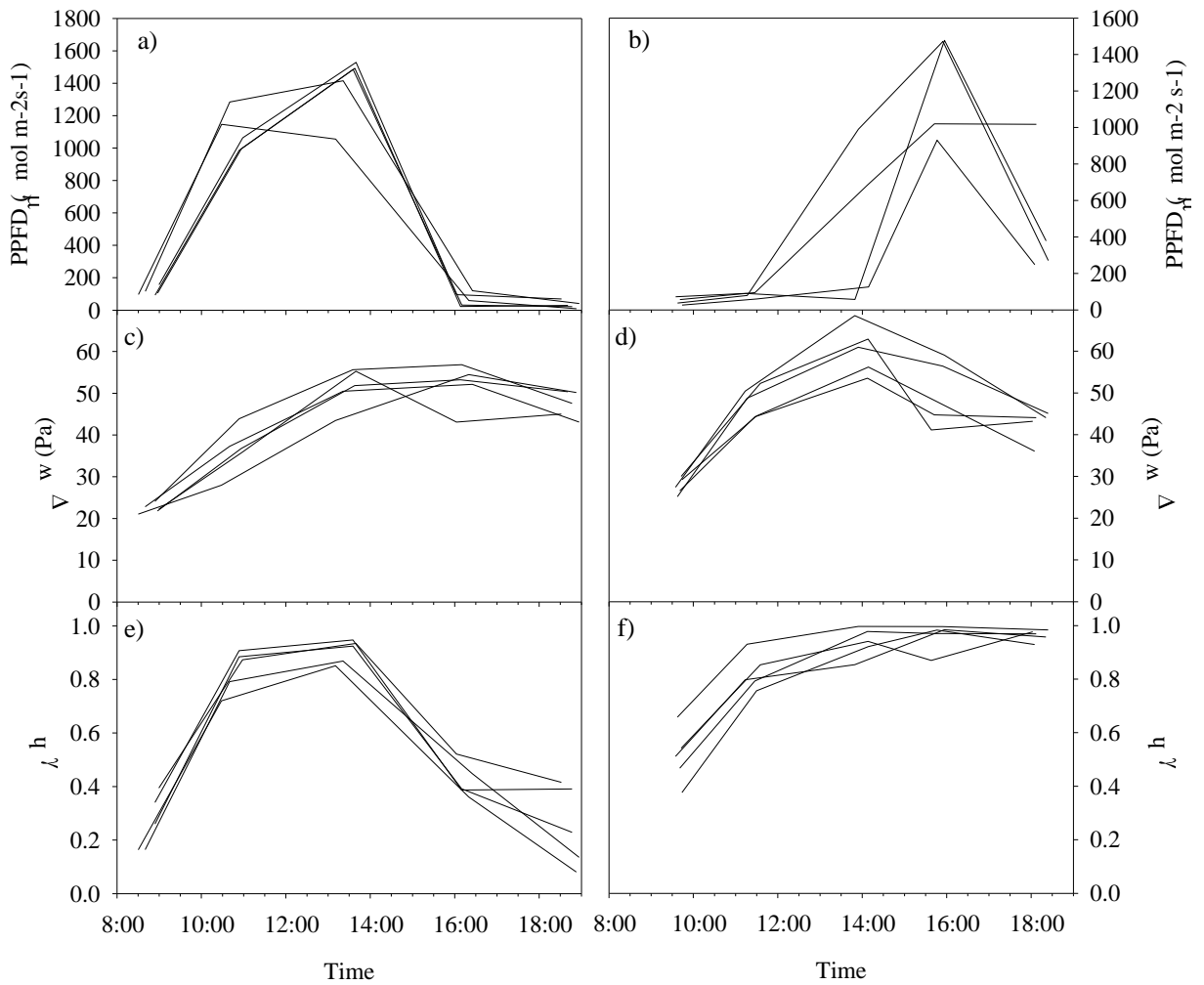

Figure 8: Diurnal cycles of photosynthetic active radiation (PAR) and air leaf water gradient (ΔW) from five leaves located in the east (a, c) and west (b, d). Hydraulic limitation of stomatal conductance in the east (e) and west (f) face of the canopy.

DISCUSSION

Our results suggest that diffusional limitations due to g_s can be the principal cause to observe suboptimal distribution of photosynthesis around the canopy. Some authors have highlighted this possibility in the past in real canopies (Grassi and Magnani 2005; Niinemets et al., 2005; 2006; Warren and Adams 2006; Diaz-Espejo et al., 2007) arguing that this situation could be consequence of water stress, drought, high temperatures or photo inhibition. But also, behind of this limitations there could be other processes as it is the case of hydraulic conductance (K_h). Recently, Peltoniemi et al., 2012 modeled that photosynthesis was not able to be optimized if K_h was not optimized too.

The gradients in photosynthetic capacity distribution across a crown profile have been widely associated to reflect the acclimation of leaves to light conditions encountered in the canopy as a major driver of changing conditions. Despite of that, the regulation mechanism of these variations in photosynthetic capacity are not fully understood (kull and Kruijit, 1999; Pons et al., 2001; Yano and Terashima, 2004; Terashima, et al., 2006; Niinemets and Anten, 2009) having contrasting results between measured nitrogen distribution and optimal distribution (Prieto et al, 2010?? Hay dos citasAnten et al., 2000). In the same way, for the use of the water resource, it was also demonstrated a high canopy variation of the leaf water use efficiency which was significantly related with the average intercepted PPFD in the different leaf positions in a grapevine canopy. There is a close relationship between N_a and photosynthetic capacity (Figure 1) because the major part of nitrogen is used to construct the photosynthetic apparatus (Evans, 1989). This close relationship led to think that light received at each locations of the leaves are the principal constraint affecting photosynthetic machinery. Also with the hypothesis that plants maximize carbon gain, stomatal conductance (g_s) is already included in the hypothesis and led to assume that stoma has an optimized behavior. However, results showed that optimization models underestimate canopy photosynthesis results (Anten et al., 2000).

Some experiments showed that growth can be differently regulated depending on the micro-environmental conditions at the moment that the peak of radiation occurs (Barden, 1996, Cavender-Bares et al., 1998). By these experiments it was concluded that although receiving the same amount of light in east and west sides, the east was

able to use light more efficiently due to the asymmetry of microclimate conditions. That would question the hypothesis that light is the most important environmental variable and would reinforce the need to search for more constraints along the canopy that could reinforce the idea of a suboptimal distribution of A_N. In this study we obtained the same carboxylation capacity for each side of the canopy for Grenache grapevine cultivar (Fig 2) that could indicate that both sides were able to have the same assimilation rates. However a differential $A_{N,max}$ was observed between both sides of the canopy (Figure 3) leading to think that some constraints were affecting photosynthesis other than light as the main driver of photosynthesis.

The application of the contribution analysis proposed by Buckley & Diaz-Espejo (2014) helped us to understand which were the real contributions affecting A_N. It was observed that diffusional contributions were the highest component limiting photosynthesis in the west side of the canopy respect to the east (Fig 4). Those results were in accordance with the results of Warren and Buckley (2013) which predicted that CO_2 pathways need to be optimized to have an optimized photosynthesis. This situation generates an asymmetry between both sides playing diffusional contributions a differential role in both parts of the canopy and being the principal driver of changes observed in $A_{N,max}$. Partitioning diffusional contributions in g_s and g_m contributions was useful to identify the principal regulator of A_{Nmax} change between both sides. g_m contributions were lower and seem not to be as the major contribution of the changes observed in $A_{N,max}$, but they were also present and were part of the observed change between both sides. On the other hand, g_s contributions were higher being the responsible of the differential A_N rate between both sides of the canopy. VPD could be invoked to explain the differential contributions between both sides (Diaz-Espejo et al., 2007), but also other constraints need to be invoked to reach the change observed in stomatal conductance.

It is well known that stomata operate due to changes of turgor on guard cells (Buckley, 2005). Those changes of turgor are dependent in various processes as could be active or passive. One way to study those changes is the application of the BMF mechanistic model of g_s. BMF model permits to extract the physiological parameters related to the control of stomata leading to have an idea about the main constraints limiting g_s and consequently A_N. It has been observed that BMF model was able to reproduce K and also ABA behavior with the data measured (Diaz-Espejo et al., 2012; Rodriguez-Dominguez in press, Martorell et al., in press). Two relationships were obtained by K

predicted using BMF model and the cumulative radiation received (Figure 6) with a clear differentiation between west and east site have been observed although is scattered. These results could be explained in relation to the recent results of Peltoniemi et al., 2012, who concluded that carbon gain has to be optimized with hydraulic conductance. Also two relationships were found between V_c, and K reinforcing the idea that K is not necessarily related to A_N rate. Those results were important because of the importance that water pathways can be one of the major challenges to improve the optimization theory since water pathways seems to play a really important role on the stomatal control. There are evidences that K vary between light regimes and can be different in light conditions (Sack et al., 2003; Brodribb and Jordan 2011; Nardini et al., 2012). This K also can vary along the canopy and may depend on the micro-environmental conditions encountered around the canopy, making this K variable and responsible of the stomata control. This need to be tested measuring K in different moments of the day and different positions around the canopy, but also a variation of K_{leaf} during the day has been observed in the field (Johnson et al., 2009, Zufferey et al 2011).

Leaf position around the canopy can be also another way to show the variation of the parameters of the g_s model and show differences clearer. Figure 7a shows how K was distributed asymmetrically around the canopy being east positions able to have higher values of K than west positions explaining some limitation due to this fact. In contrast n values were lower on east and higher on west, supposed to be related to micro environmental conditions encountered each part of the canopy as has been hypothesized in different studies (Barden, 1996; Cavender-Bares et al., 1998). A negative relationship was found between both parameters when both were plotted in a graph observing that they have some relationship between them. One of the most drivers of these differences would be the micro-environmental conditions encountered around the canopy. East site receive high PPFD intensities t when VPD is not as high as in the midday when VPD is the highest and it is when west side starts to receive the sun. Otherwise, in the east positions, High light is received when water supply to the leaf is still high and stomata can be open. By contrary the south face leaves receive the highest PPFD intensities when water supply is more difficult and in consequence stomata tend to be more clesed.

To see the limitations that are working on stomatal conductance we performed an analysis to quantify how stomatal conductance is limited by the hydraulic component

and the chemical signals (Rodríguez-Domínguez et al., submitted). That analysis show a differential regulation of both components observing that hydraulic constraints are the major challenges limiting g_s in both parts of the canopy and they became higher when maximum light intensity is applied to leaves (Rodriguez-Dominguez unpublished). That reinforce the paper played by the hydraulic conductance on the control of stomata and reinforce the recent hypothesis launched by Peltoniemi et al., 2013 that hydraulic conductance could play a really important role on the optimization of carbon gain. This led to think how hydraulic conductance has to be modeled to be included in the models to improve the predictions of the optimization theory.

In conclusion our data show that other factors than light limit carbon gain in grapevines canopies. This is reflected in the non-linear relationship between photosynthetic capacity and PPFD accumulated. Although optimization theory predicts that photosynthetic capacity should scale linearly with radiation, deviation of the theory in actual canopies have been explained in terms of the existence of other constraints, like hydraulic limitations or diffusional limitations. This might be the case in our grapevine canopies. Locations in the canopy receiving the peak of radiation at a moment of high evaporative demand must overcome the limitations imposed by hydraulic limitations, which induce at the same time stomatal closure and diffusional limitation of photosynthesis. This would make during the ontogeny and acclimation process later on to an adjustment of the hydraulic conductivity and photosynthetic capacity that we observed. Leaves of all locations force their hydraulic systems to their limits as our limitation analysis suggests, although in a different fashion depending on the location, which is determined by the combination of air evaporative demand and radiation availability in time. In our environment characterized by an extremely high evaporative demand it is believable that hydraulic limitations imposed the major restrictions to g_s, but at the same time it raises the question on the role played by non-hydraulic signals. They look to play an important role in the regulation of g_s especially in those moments of low radiation and Δw. However, it looks like that ABA is not directly related to this regulatory role, and in any case associated to water stress since our plants were fully irrigated. Further experiments should focus on two aspects: what determines the distribution of K in the canopy, and why non-hydraulic factors correlate with it.

REFERENCES

Anten N.P. Hikosaka K. & Hirose T. (2000) Nitrogen utilisation and the photosynthetic system. *Leaf development and canopy growth*, **21** 171-203.

Anten N.P.R., Hikosaka K. & Hirose T. (2000) Nitrogen utilization and the photosynthetic system. In: MarshalB, Roberts J, eds.Leaf development and canopy growth. *Sheffield Academic, Sheffield, UK,* 171–203.

Barden L.S. (1996). A comparison of growth efficiency of plants on the east and west sides of a forest canopy gap. *Bulletin of the Torrey Botanical Club*, 240-242.

Brodribb T.J. & Jordan G. J. (2011) Water supply and demand remain balanced during leaf acclimation of Nothofagus cunninghamii trees. *New Phytologist*, *192*, 437-448.

Buckley T.N. & Warren C.R. (2014) The role of mesophyll conductance in the economics of nitrogen and water use in photosynthesis. *Photosynthesis research*, **119**, 77-88.

Buckley T.N., Cescatti A. & Farquhar G.D. (2013) What does optimization theory actually predict about crown profiles of photosynthetic capacity when models incorporate greater realism? *Plant, Cell & Environment*, **36**, 1547-1563.

Buckley T.N., Martorell S., Diaz-Espejo A., Tomàs M. & Medrano H. (2014) Is stomatal conductance optimized over both time and space in plant crowns? A field test in grapevine (Vitis vinifera). *Plant, Cell & Environment*

Buckley T.N., Miller J.M. & Farquhar G.D. (2002). The mathematics of linked optimisation for water and nitrogen use in a canopy. *Silva Fennica*, **36**, 639-669.

Buckley T.N., Mott K.A. & Farquhar G.D. (2003) A hydromechanical and biochemical model of stomatal conductance. *Plant, Cell & Environment*, **26**, 1767-1785.

Cano F.J., Sánchez-gomez D., Rodríguez-Calcerrada J., Warren C.R., Gil L. & Aranda I. (2013) Effects of drought on mesophyll conductance and photosynthetic limitations at different tree canopy layers. *Plant, Cell & Environment*, **36**, 1961-1980.

Chapin F.S., Bloom A.J., Field C.B. & Waring R.H. (1987) Plant responses to multiple environmental factors. *Bioscience*, **37**, 49-57.

Cowan I.R. & Farquhar G.D. (1977) Stomatal function in relation to leaf metabolism and environment. *Symposium of the Society for Experimental Biology* **31,** 471–505.

Diaz-Espejo A., Nicolas E., & Fernandez J.E. (2007) Seasonal evolution of diffusional limitations and photosynthetic capacity in olive under drought. *Plant, Cell & Environment*, **30**, 922-933.

Evans J.R. (1989) Photosynthesis and nitrogen relationships in leaves of C3 plants. *Oecologia*, *78*, 9-19.

Evans J.R. (1989) Photosynthesis and nitrogen relationships in leaves of C3 plants. *Oecologia*, *78*, 9-19.

Field C. & Mooney H.A. (1986) The photosynthesis-nitrogen relation-ship in wild plants. In: Givinsh TJ (ed) On the economy of form and function. Cambridge University Press, Cambridge, pp 25-55

Gutschick V.P. (1981) Evolved strategies in nitrogen acquisition by plants.*American Naturalist*, 607-637.

Han Q. (2011). Height-related decreases in mesophyll conductance, leaf photosynthesis and compensating adjustments associated with leaf nitrogen concentrations in Pinus densiflora. *Tree physiology*, **31**, 976-984.

Kitajima K., Mulkey S.S. & Wright S.J. (2005) Variation in crown light utilization characteristics among tropical canopy trees. *Annals of Botany*, **95**, 535-547.

Kull O. & Kruijt B. (1999) Acclimation of photosynthesis to light: a mechanistic approach. *Functional Ecology*, **13**, 24-36.

Lieffers V.J., Messier C., Stadt K.J., Gendron F. & Comeau P.G. (1999) Predicting and managing light in the understory of boreal forests. *Canadian Journal of Forest Research*, **29**, 796-811.

Mullin L.P., Sillett S.C., Koch G.W., Tu K.P. & Antoine M.E. (2009) Physiological consequences of height-related morphological variation in Sequoia sempervirens foliage. *Tree Physiology*, **29**, 999-1010.

Nardini A., Pedá G. & Salleo S. (2012) Alternative methods for scaling leaf hydraulic conductance offer new insights into the structure–function relationships of sun and shade leaves. *Functional Plant Biology*, **39**, 394-401.

Niinemets U. & Valladares F. (2004) Photosynthetic acclimation to simultaneous and interacting environmental stresses along natural light gradients: optimality and constraints. *Plant Biology,* **6**, 254–68.

Niinemets Ü. (2012) Optimization of foliage photosynthetic capacity in tree canopies: towards identifying missing constraints. *Tree physiology*, **32**, 505-509.

Niinemets Ü. & Anten N.P. (2009) Packing the photosynthetic machinery: from leaf to canopy. In *Photosynthesis in silico* (pp. 363-399). Springer Netherlands.

Niinemets Ü., Cescatti A., Rodeghiero M. & Tosens T. (2006) Complex adjustments of photosynthetic potentials and internal diffusion conductance to current and previous light availabilities and leaf age in Mediterranean evergreen species Quercus ilex. *Plant, Cell & Environment*, **29**, 1159-1178.

Peltoniemi M.S., Duursma R.A. & Medlyn B.E. (2012) Co-optimal distribution of leaf nitrogen and hydraulic conductance in plant canopies. *Tree physiology*, **32**, 510-519.

Pons T.L., Jordi W. & Kuiper D. (2001) Acclimation of plants to light gradients in leaf canopies: evidence for a possible role for cytokinins transported in the transpiration stream. *Journal of Experimental Botany*, **52**, 1563-1574.

Sack L., Cowan P.D., Jaikumar N. & Holbrook N.M. (2003) The 'hydrology' of leaves: co-ordination of structure and function in temperate woody species. *Plant, Cell & Environment*, **26**, 1343-1356.

Soar C.J., Speirs J., Maffei S.M. & Loveys B.R. (2004) Gradients in stomatal conductance, xylem sap ABA and bulk leaf ABA along canes of Vitis vinifera cv. Shiraz: molecular and physiological studies investigating their source. *Functional Plant Biology*, **31**, 659-669.

Terashima I., Hanba Y.T., Tazoe Y., Vyas P. & Yano S. (2006). Irradiance and phenotype: comparative eco-development of sun and shade leaves in relation to photosynthetic CO_2 diffusion. *Journal of Experimental Botany*, **57**, 343-354.

Valladares F. (2003) Light heterogeneity and plants: from ecophysiology to species coexistence and biodiversity. In *Progress in Botany* (pp. 439-471). Springer Berlin Heidelberg.

Whitehead D., Barbour M.M., Griffin K.L., Turnbull M.H. & Tissue D.T. (2011) Effects of leaf age and tree size on stomatal and mesophyll limitations to photosynthesis in mountain beech (Nothofagus solandrii var. cliffortiodes). *Tree Physiology*, **31**, 985-996.

Woodruff D.R., Meinzer F.C., Lachenbruch B. & Johnson D.M. (2009) Coordination of leaf structure and gas exchange along a height gradient in a tall conifer. *Tree Physiology*, **29**, 261-272.

Yano S. & Terashima I. (2004) Developmental process of sun and shade leaves in Chenopodium album L. *Plant, Cell & Environment*, **27**, 781-793.

5.2. Is stomatal conductance optimised over both time and space in plant crowns? A field test in grapevine (*Vitis vinifera*).

Thomas N Buckley [†,1,] **Sebastia Martorell** [†,2] **Antonio Diaz-Espejo** [3] **Magdalena Tomàs** [2] **Hipólito Medrano** [2]

[1] IA Watson Grains Research Centre, Faculty of Agriculture and Environment, The University of Sydney, Narrabri, NSW Australia.

[2] Research Group on Plant Biology under Mediterranean Conditions, Departament de Biologia, Universitat de les Illes Balears, Carretera de Valldemossa Km 7.5, 07122 Palma de Mallorca, Illes Balears, Spain.

[3] Irrigation and Crop Ecophysiology Group, Instituto de Recursos Naturales y Agrobiología de Sevilla (IRNAS, CSIC). Avenida Reina Mercedes 10, 41012 Sevilla, Spain.

[†] **These authors contributed equally to the authorship of this work**

ABSTRACT

Crown carbon gain is maximised for a given total water loss if stomatal conductance (g_s) varies such that the marginal carbon product of water ($\partial A/\partial E$) remains invariant both over time and among leaves in a plant crown, provided the curvature of assimilation rate (A) vs transpiration rate (E) is negative. We tested this prediction across distinct crown positions *in situ* for the first time, by parameterising a biophysical model across 14 positions in four grapevine crowns (*Vitis vinifera*), computing optimal patterns of g_s and E over a day and comparing these to observed patterns. Observed water use was higher than optimal for leaves in the crown interior, but higher than optimal in most other positions. Crown carbon gain was 18% lower under measured g_s than under optimal g_s. Positive curvature occured in 39.6% of cases due to low boundary layer conductance (g_{bw}), and optimal g_s was zero in 11% of cases because $\partial A/\partial E$ was below the target value at all g_s. Some conclusions changed if we assumed infinite g_{bw}, but optimal and measured E still diverged systematically in time and space. We conclude that the theory's spatial dimension and assumption of positive curvature require further experimental testing.

Keywords: optimisation, stomata, boundary layer, water use efficiency, carbon water balance.

INTRODUCTION

Water is a major factor limiting plant growth and carbon sequestration in both natural and agricultural systems. To predict and manage these systems and to direct basic research into the underlying biological controls, we need formal mathematical models that can both predict and explain how carbon and water exchange are coordinated and regulated by stomatal conductance (g_s). However, no process-based model of g_s that can achieve this has yet gained consensus, and phenomenological models merely reproduce observed patterns of g_s, so they have limited ability to explain stomatal behaviour (Damour *et al.*, 2010, Buckley & Mott, 2013). Another approach, optimisation theory, attempts to deduce g_s from the hypothesis that stomatal behaviour tends to maximise carbon gain (net CO_2 assimilation rate, A) for a given water loss (transpiration rate, E) (Cowan & Farquhar, 1977). The rationale for this hypothesis is that natural selection has presumably favoured genotypes with more nearly optimal use

of limiting resources, including water (Cowan & Farquhar, 1977, Cowan, 2002, Mäkelä *et al.*, 2002).

Formally, the optimisation hypothesis states that, among all possible spatio-temporal distributions of g_s that yield the same total transpiration rate, total carbon gain will be greatest for the distribution in which the ratio of the marginal sensitivities of *A* and *E* to g_s (($\partial A/\partial g_s$)/($\partial E/\partial g_s$)), often abbreviated as $\partial A/\partial E$ and referred to in this study as the *marginal carbon product of water*) is invariant within the domain in which total transpiration rate can be considered constant (Cowan & Farquhar, 1977). That domain is typically taken to be one day (at longer time scales, the total water supply available to the canopy, and with it the target value μ for $\partial A/\partial E$, may change). This result assumes that the *A* vs *E* curve generated by varying g_s has negative curvature; i.e., $\partial A/\partial E$ always declines when *E* increases by stomatal opening ($\partial^2 A/\partial E^2 < 0$). Pioneering work by Farquhar (1973) and Cowan and Farquhar (1977) showed that the patterns of stomatal behaviour predicted by this hypothesis share important qualitative features with observed behaviour, including reduced g_s under high evaporative demand or low light (photosynthetic photon flux density, PPFD).

The subsequent four decades have seen this theory tested many times – most commonly in relation to controlled variations in individual environmental variables such as evaporative demand, but also in relation to natural variation in environmental conditions *in situ* (e.g., Farquhar *et al.*, 1980a, Meinzer, 1982, Williams, 1983, Ball & Farquhar, 1984, Küppers, 1984, Sandford & Jarvis, 1986, Guehl & Aussenac, 1987, Fites & Teskey, 1988, Berninger *et al.*, 1996, Hari *et al.*, 1999, Thomas *et al.*, 1999, Schymanski *et al.*, 2008, Way *et al.*, 2011). However, two critical elements of the original theory remain largely untested: neither its spatial dimension – that is, the prediction that $\partial A/\partial E$ should not vary among leaves at distinct crown positions within the same individual – nor the assumption that $\partial^2 A/\partial E^2 < 0$ have ever been tested in the field. The prediction that the target value of $\partial A/\partial E$ should be the same for all leaves in the canopy follows from the premise that the plant has a single total water supply, and the ability, in principle, to distribute water arbitrarily among leaves. The original Cowan-Farquhar theory does not distinguish temporal and spatial variations in $\partial A/\partial E$, either of which will reduce whole-canopy carbon gain (provided $\partial^2 A/\partial E^2 < 0$).

Furthermore, few tests have accounted for variations in mesophyll and boundary layer conductances (g_m and g_{bc}, respectively), both of which restrict CO_2 diffusion and can strongly influence the predictions and assumptions of optimisation theory (Buckley *et al.*, 1999, Buckley *et al.*, 2013, Buckley & Warren, 2013).

The objective of this study was to test the spatial dimension of the optimisation hypothesis and its assumption of negative curvature in *A* vs *E*, while accounting for mesophyll and boundary layer conductances. We parameterised a biochemical gas exchange model (which included mesophyll conductance and its temperature response) for one leaf at each of 14 standardised positions in each of four individual crowns of grapevine (*Vitis vinifera* L. var Grenache), and then monitored *in situ* environmental conditions and stomatal conductance for each of those leaves over time across a single day. We used these data to test the theory's assumption that $\partial^2 A/\partial E^2 < 0$, to infer the optimal spatio-temporal distributions of g_s (and *E*), and to compare the inferred optimal patterns with observed patterns.

MATERIALS AND METHODS

Study system

This study was conducted from 17 to 24 August 2012 in the experimental field of the University of Balearic Islands during summer 2012 on grapevines of Grenache varietal. Soil was a clay loam type 1.5 m deep. Plants were 3-years-old grafted on rootstock Richter-110 and planted in rows (distance between rows was 2.5 m and between plants, 1 m). Plants were situated in a bilateral double cordon having between 10-12 canes per plant. Plants had been irrigated throughout the summer with 9.0 liters per plant per day, an amount that had been established as adequate to sustain high plant water status in a previous experiment. Predawn water potential of plants on the day of *in situ* gas exchange measurements (22 August 12) was -0.24 ± 0.06 MPa.

Four plants and 14 crown positions of each plant were selected for gas exchange measurements. Four of these positions were on the east face of the crown (positions 1-4), two were on the top of the crown (5 & 6), four were on the west face (7-10), and four were located in the inner part of the crown (11-14). These crown positions are illustrated in Figure 1
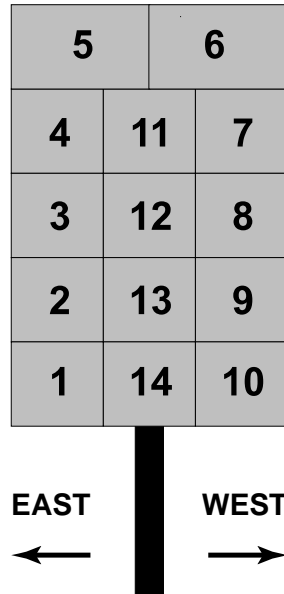
Figure 1: Diagram illustrating the 14 crown positions at which leaf gas exchange was measured in this study. The diagram represents a cross-section of the grapevine crown, looking southwards along the long axis of a planting row, with east (sunrise) to the left and west (sunset) to the right. Positions 1-10 are on the crown exterior, and positions 11-14 are in the crown interior.

Meteorological measurements

A meteorological station (Meteodata-3000) located in the experimental field with sensors of wind speed (Young 81000, R.M. Young company, Traverse City, Michigan) and air temperature and relative humidity (Young 41382, Young company) were used. The height of the wind speed sensor was 2.7 meters above the soil (approximately 0.5 meters above the upper part of the canopy).

Variable	Symbol	Units	Value
net CO_2 assimilation rate	A	μmol m^{-2} s^{-1}	varies
leaf absorptance to photosynthetic photon flux	α	-	0.92
demand or supply limited value of A	A_d, A_s	μmol m^{-2} s^{-1}	varies
RuBP-carboxylation or regeneration limited value of A_d	A_v, A_j	μmol m^{-2} s^{-1}	varies
ambient CO_2 mole fraction	c_a	μmol mol^{-1}	400
intercellular or chloroplastic CO_2 mole fraction	c_i, c_c	μmol mol^{-1}	varies
molar heat capacity of air	c_p	J mol^{-1} K^{-1}	29.2
curvature of A vs E relationship	$\partial^2 A/\partial E^2$	μmol m^2 s mmol^{-2}	varies
saturation vapour pressure deficit of air	D_a	Pa	varies
marginal carbon product of water	$\partial A/\partial E$	μmol mmol^{-1}	varies
leaf characteristic dimension	d_{leaf}	m	0.1
effective leaf-air water vapour mole fraction gradient	Δw	mmol mol^{-1}	varies
leaf transpiration rate	E	mmol m^{-2} s^{-1}	varies
leaf emissivity to IR	ε_{leaf}	-	0.95
fraction of absorbed photons that do not contribute to photochemistry	f	-	0.23
absorbed shortwave radiation	Φ	J m^{-2} s^{-1}	varies
fraction of infrared radiation that comes from the sky	f_{ir}	-	varies
psychrometric constant	γ	Pa K^{-1}	66.0
photorespiratory CO_2 compensation point (at 25°C)	Γ_* (Γ_{*25})	μmol mol^{-1}	varies (36.2)
leaf boundary layer conductance to heat, water or CO_2	g_{bh}, g_{bw}, g_{bc}	mol m^{-2} s^{-1}	varies
mesophyll conductance to CO_2	g_m	mol m^{-2} s^{-1}	varies
radiation conductance	g_{Rn}	mol m^{-2} s^{-1}	varies
stomatal conductance to water or CO_2	g_s, g_{sc}	mol m^{-2} s^{-1}	varies
maximum stomatal conductance	g_{smax}	mol m^{-2} s^{-1}	varies
optimal stomatal conductance	g_{so}	mol m^{-2} s^{-1}	varies
total leaf conductance to water or CO_2	g_{tw}, g_{tc}	mol m^{-2} s^{-1}	varies
potential electron transport rate	J	μmol m^{-2} s^{-1}	varies
light-limited (capacity-saturated) value of J	J_i	μmol m^{-2} s^{-1}	varies
capacity-limited (light-saturated) value of J (at 25°C)	J_m (J_{m25})	μmol m^{-2} s^{-1}	varies
Michaelis constant for RuBP carboxylation or oxygenation	K_c, K_o	μmol mol^{-1}	varies
canopy extinction coefficient for diffuse irradiance	k_d	-	0.8
cumulative leaf area index	L	m^2 m^{-2}	varies
target value for $\partial A/\partial E$	μ	μmol mmol^{-1}	1.28-1.59
mole fraction of oxygen	O	μmol mol^{-1}	2.1·10^5
atmospheric pressure	P_{atm}	Pa	1.0·10^5
photosynthetic photon flux density	PPFD	μmol m^{-2} s^{-1}	varies
curvature parameter for relationship of A_d to A_v and A_j	θ_A	-	0.99
curvature parameter for relationship of J to J_m and J_i	θ_J	-	0.90
non-photorespiratory CO_2 release (at 25°C)	R_d (R_{d25})	μmol m^{-2} s^{-1}	varies
net isothermal radiation	R_n^*	J m^{-2} s^{-1}	varies
Stefan-Boltzmann constant	σ	J m^{-2} s^{-1} K^{-4}	5.67·10^{-8}
air temperature (in Kelvins)	T_{air} ($T_{air,K}$)	^{o}C (K)	varies
leaf temperature	T_{leaf} ($T_{leaf,K}$)	^{o}C (K)	varies
carboxylation capacity (at 25°C)	V_m (V_{m25})	μmol m^{-2} s^{-1}	varies
wind speed	v_{wind}	m s^{-1}	varies
water vapour mole fraction of intercellular spaces or air	w_i, w_a	mmol mol^{-1}	varies

Table1: List of variables and parameters referred to in this study, including symbols, units and values where appropriate.

Biophysical gas exchange model

We used the photosynthesis model of Farquhar et al (1980b) and the gas-exchange equations of von Caemmerer and Farquhar (1981) to simulate CO_2 and H$_2$O exchange

in grapevine. Briefly, the net CO_2 assimilation rate due to biochemical demand (A_d) is computed from RuBP-carboxylation-limited and –regeneration-limited rates (A_v and A_j) (a list of symbols is given in Table1:

$$(1) \quad A_v = V_m \frac{c_c - \Gamma_*}{c_c + K_c\left(1 + O/K_o\right)} - R_d, \text{ and}$$

$$(2) \quad A_j = \tfrac{1}{4} J \frac{c_c - \Gamma_*}{c_c + 2\Gamma_*} - R_d,$$

where V_m is carboxylation capacity, J is potential electron transport rate, c_c is chloroplastic CO_2 concentration, Γ_* is photorespiratory CO_2 compensation point, K_c and K_o are the Michaelis constants for RuBP carboxylation and oxygenation, respectively, O is oxygen concentration and R_d is the rate of non-photorespiratory CO_2 release. Actual assimilation rate is calculated as the hyperbolic minimum of A_v and A_j (the lesser root A_d of $\theta_A A_d^2 - A_d(A_v + A_j) + A_v A_j = 0$, where θ_A is a dimensionless curvature parameter less than unity); this accounts for co-limitation by both carboxylation and regeneration near the transition between the two limitations, and it smoothes the transition, ensuring differentiability as required for continuous optimisation. We calculated J as the hyperbolic minimum of light-limited and light-saturated rates, J_m and J_i (the lesser root J of $\theta_J J^2 - J(J_m + J_i) + J_m J_i = 0$; $J_i = 0.5\alpha \cdot (1 - f) \cdot \text{PPFD}$, α is the leaf absorptance to photosynthetic irradiance and f is the fraction of absorbed photons that do not contribute to photochemistry).

The supply of CO_2 by diffusion to the sites of carboxylation (A_s) was modeled as

$$(3) \quad A_s = g_{tc}\left(c_a - c_c\right),$$

where g_{tc} is total conductance to CO_2, given by

$$(4) \quad g_{tc} = \left(g_{sc}^{-1} + g_{bc}^{-1} + g_m^{-1}\right)^{-1},$$

where g_{sc} is stomatal conductance to CO_2 ($g_s/1.6$ where g_s is stomatal conductance to H_2O), g_{bc} is boundary layer conductance to CO_2 and g_m is mesophyll conductance to

CO_2. At steady state, the supply and demand rates are equal ($A_d = A_s$), so the actual net CO_2 assimilation rate, A, is given by the intersection of A_d and A_s:

(5) $A = A_d \cap A_s$.

This intersection leads to a quartic (4th-order polynomial) expression for c_c, whose coefficients are functions of the parameters in Eqns 1-3, and which is readily solved for c_c (e.g., Abramowitz & Stegun, 1972). Transpiration rate (E) is given by

(6) $E = g_{tw} \Delta w$,

where

(7) $g_{tw} = \left(g_s^{-1} + g_{bw}^{-1} \right)^{-1}$, and

(8) $\Delta w = \dfrac{w_i - w_a}{1 - \frac{1}{2} \cdot 0.001 \cdot \left(w_i + w_a \right)}$,

in which g_{bw} is boundary layer conductance to H_2O and w_i and w_a are the water vapour mole fractions in the intercellular spaces and the ambient air, respectively. We assumed that the air spaces were saturated with water vapour, so that w_i was given by

(9) $w_i = 6.112 \cdot \exp\left(17.62 \cdot T_{leaf} \middle/ \left(243.13 + T_{leaf} \right) \right) \middle/ P_{atm}$,

where T_{leaf} is leaf temperature in $^\circ$C (World Meteorological Organization, 2008). The expression in the numerator of Eqn 9 gives the saturation partial pressure of water, and P_{atm} is total atmospheric pressure. We estimated *in situ* leaf temperature using the isothermal net radiation approximation as described by Leuning et al. (1995) and modified to molar units:

(10) $T_{leaf} = T_{air} + \dfrac{\gamma R_n^* / c_p - D_a g_{tw}}{s g_{tw} + \gamma \left(g_{bh} + g_{Rn} \right)}$

where T_{air} is air temperature, γ is the psychrometric constant, c_p is the molar heat capacity of air, D_a is the saturation vapour pressure deficit of air, and s is the derivative of saturation vapour pressure with respect to temperature. g_{Rn} is the radiation conductance, given by

$$(11) \quad g_{Rn} = 4\varepsilon_{leaf}k_d f_{ir}\sigma T_{air}^3 / c_p \, ,$$

where ε_{leaf} is leaf emissivity to longwave radiation, σ is the Stefan-Boltzmann constant, k_d is the canopy extinction coefficient for diffuse irradiance (0.8; Leuning *et al.*, 1995), and f_{ir} is the fraction of the leaf's incoming infrared radiation that comes directly from the sky. In simulations on horizontally continuous canopies, f_{ir} is generally taken as exp(-$k_d L$) where L is cumulative leaf area index (e.g., Leuning *et al.*, 1995). We computed f_{ir} in this fashion for interior crown leaves (positions 11-14); for positions on the lateral crown exterior (positions 1-4 and 7-10), we computed f_{ir} as the fraction of each leaf's upwards sky view occupied by actual sky rather than by the adjacent canopy (β/180, where β (degrees) is the angle at which sky appears above the adjacent canopy, as viewed from the crown position in question). We used $f_{ir} = 1.0$ for the two positions at the top of the crown (positions 5 and 6). R_n^* is the isothermal net radiation, given by

$$(12) \quad R_n^* = \Phi - (1 - \varepsilon_{atm})k_d f_{ir}\sigma T_{air,K}^4$$

where Φ is absorbed shortwave radiation, ε_{atm} is atmospheric emissivity to longwave radiation, given by $0.642 \cdot (0.001 \cdot P_{atm} \cdot w_a / T_{air,K})^{1/7}$ for P_{atm} in Pa and w_a in mmol mol^{-1} (Leuning *et al.*, 1995), and $T_{air,K}$ is T_{air} in Kelvins. Note that this assumes a canopy IR emissivity of unity. We calculated Φ by assuming incident shortwave radiation was equal to 0.5666·PPFD (0.5666 is the ratio of total shortwave energy to photosynthetic photon flux in extraterrestrial solar radiation; de Pury & Farquhar, 1997), and that this radiation was half visible and half near-infrared (Leuning *et al.*, 1995), with leaf absorptances of 0.92 and 0.2, respectively (0.92 was the mean observed PAR absorptance of leaves in this study, and 0.2 is the complement of NIR reflection and transmission coefficients, both of which are approximately 0.4; Gates *et al.*, 1965). This gives $\Phi = (0.5 \cdot 0.92 + 0.5 \cdot 0.2) \cdot 0.5666 \cdot$PPFD $= 0.3173 \cdot$PPFD.

Equation 10 requires a value for boundary layer conductances to heat (g_{bh}) and water (g_{bw}, which is embedded in g_{tw} (Eqn 7)), and Eqn 4 requires boundary layer conductance to CO_2 (g_{bc}). We assumed $g_{bc} = g_{bw}/1.37$ and $g_{bw} = 1.08 \cdot g_{bh}$ and simulated g_{bh} using an expression based on forced (wind-driven) convection (Leuning *et al.*, 1995):

$$(13) \quad g_{bh} = 0.123\left(v_{wind}/d_{leaf}\right)^{0.5}$$

where v_{wind} is wind speed and d_{leaf} is the leaf's characteristic dimension (approximately equivalent to its average downwind width; 0.1 m in this study). This ignores the possibility of free convection driven by buoyancy of air warmed by the leaf. However, most available data and theoretical studies suggest that free convection contributes only negligibly to heat exchange under natural conditions, even at very low wind speeds, and that modeling g_{bh} based on forced convection alone provides accurate predictions (Leuning, 1988, Brenner & Jarvis, 1995, Grantz & Vaughn, 1999, Roth-Nebelsick, 2001). We simulated the attenuation of wind speed through the canopy profile by

$$(14) \quad v_{wind} = v_{wind(top)} \cdot \exp(-0.5L)$$

where L is cumulative leaf area index ($m^2 \ m^{-2}$) and $v_{wind(top)}$ is the wind speed measured above the canopy. To calculate L for each canopy position, we summed the leaf area index of all canopy regions (as defined by Figure 1) above that position. To measure those leaf area indices, we measured the total leaf area in each canopy region for each of six individuals, then divided these areas by the projected areas of each region to give the leaf area index contributed by that region. The resulting values of L are given in Table 2.

position	L
1	3.1
2	2.6
3	2.1
4	1.8
5	0
6	0
7	1.5
8	1.8
9	2.4
10	2.7
11	1.6
12	2.1
13	2.6
14	3.3

Table 2: Cumulative leaf area index (L, m^2 m^{-2}) at each of the 14 canopy positions illustrated in Figure 1, used to estimate wind speed at each position (Eqn 14).

Parameterising the gas exchange model

We estimated photosynthetic parameters for each of 56 leaves (four individuals x 14 canopy positions) as follows. We measured the response of leaf net CO_2 assimilation rate (A) to intercellular CO_2 mole fraction (c_i) using an open flow gas exchange system (Li-6400; Li-Cor, Inc., Lincoln, Nebraska) equipped with an integrated leaf chamber fluorometer (Li-6400-40; Li-Cor). Curves were performed under saturating light (1500 μmol $m^{-2}s^{-1}$), with block temperature controlled at 30ºC. Ambient CO_2 (c_a) was set between 50 and 1600 μmol mol^{-1} and chamber humidity was set to track ambient conditions. After steady state photosynthesis was reached, c_a was lowered stepwise from 400 to 50 μmol mol^{-1}, returned to 400 μmol mol^{-1} and increased stepwise to 1600 μmol mol^{-1}. A total of 16 points were recorded for each curve. We then estimated g_m, V_m and J_m by the curve fitting method proposed by Ethier & Livingston (2004). To simulate changes in these parameters with temperature, we corrected these values to 25ºC (as g_{m25}, V_{m25} and J_{m25}, respectively) using temperature responses measured on leaves of the same variety, grown in pots at the same site and transported to the laboratory to allow plants to acclimate to constant temperature and other atmospheric conditions. Temperature responses were measured by repeating CO_2 response curves at 15, 20, 25, 30, 35 and 40 ºC, using the same protocol described above but with the expanded temperature control kit (Li-6400-88, Li-Cor) added to the gas exchange system. The temperature response data are shown in Figure 2. Temperature response functions were as follows:

$$(15) \quad V_m\left(T_{leaf,K}\right) = V_{m25} \cdot \exp\left(a_v\left(T_{ref}^{-1} - T_{leaf,K}^{-1}\right)\right),$$

$$(16) \quad J_m\left(T_{leaf,K}\right) = J_{m25} \cdot \exp\left(a_j\left(T_{ref}^{-1} - T_{leaf,K}^{-1}\right)\right) \cdot \left(\frac{1 + \exp\left(b_j\right)}{1 + \exp\left(b_j + c_j\left(T_{ref}^{-1} - T_{leaf,K}^{-1}\right)\right)}\right), \text{ and}$$

$$(17) \quad g_m\left(T_{leaf}\right) = g_{m25} \cdot \exp\left(-d\left(\ln\left(T_{leaf}/T_{opt}\right)\right)^2\right),$$

where $T_{ref} = 298.15$ K, $T_{leaf,K}$ is leaf temperature in Kelvins, and a_v, a_j, b_j, c_j, d and T_{opt} are empirical parameters: $a_v = 7350.45$ K, $a_j = 6710.22$ K, $b_j = -2.15188$ (unitless), $c_j = 13807.8$ K, $d = 0.71027$ (unitless) and $T_{opt} = 36.75$ °C. Other parameters were taken from literature: 25°C values and temperature responses for Rubisco kinetic parameters (K_c and K_o) and the photorespiratory CO_2 compensation point (Γ_*) were taken from Bernacchi *et al.* (2003). Non-photorespiratory CO_2 release in the light at 25°C (R_{d25}) was estimated from photosynthetic response curves as $0.0089 \cdot V_{m25}$ according de Pury and Farquhar (1997), and the temperature response of R_d was taken from Bernacchi *et al.* (2003).
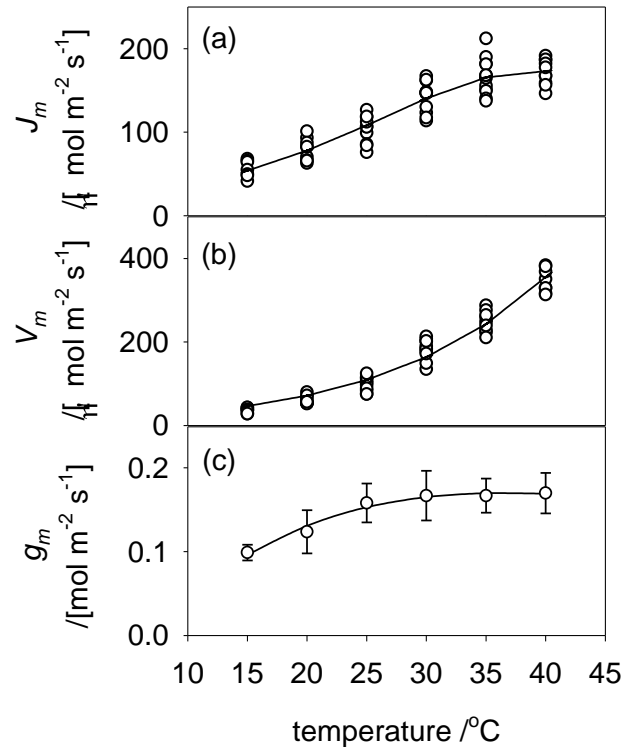

Figure 2: Temperature responses for photosynthetic parameters measured in grapevine for this study (symbols) and response curves fitted to these measurements (lines; Eqns 15-17 in the main text). (b) Electron transport capacity, J_m, (a) carboxylation capacity, V_m, (c) mesophyll conductance to CO_2, g_m.

Measuring leaf gas exchange in situ

At each of five times on a given day (approximately 0915, 1100, 1345, 1600 and 1830, CEDT), we used an open flow gas exchange system (Li-6400, Li-Cor) equipped with a clear chamber (Li-6400-08) to obtain a 30-second average measurement of stomatal conductance and incident PPFD on each of the leaves for which we had previously estimated photosynthetic parameters as described above. Prior to each measurement, we observed the leaf's orientation, and oriented the chamber such that the PPFD sensor surface was parallel to the original plane of the leaf; this ensured that the PPFD thus measured was very similar to the PPFD actually experienced by the leaf prior to measuring g_s. c_a was set at 400 μmol mol^{-1} and chamber air temperature and humidity were set to match ambient. Of the 280 expected measurements (5 times x 14 positions x 4 individuals), 10 were lost due to clerical errors, leaving 270 measurements.

Computing $\partial A/\partial E$

We calculated $\partial A/\partial E$ numerically, as follows. We computed A and E from the gas exchange model outlined above, added a very small increment ($1.0 \cdot 10^{-6}$ mol m^{-2} s^{-1}) to stomatal conductance and estimated $\partial A/\partial E$ as the ratio of the resulting increases in A and E. This ensured that changes in leaf temperature (T_{leaf}) resulting from the simulated increment in g_s, and the effects of those temperature changes on both A and E, would be calculated accurately (analytical description of the effects of changing T_{leaf} would be overly complex and prone to error, due to the many photosynthetic parameters affected by T_{leaf}). We verified that this numerical approach did not suffer from discretisation error by computing $\partial A/\partial E$ both numerically and analytically (using expressions given by Buckley *et al.*, 2002) while holding leaf temperature constant; the two resulting values of $\partial A/\partial E$ were indistinguishable (not shown).

Computing optimal stomatal conductance

For each point in time at each crown position, we computed optimal stomatal conductance as follows. First, we generated the theoretical A vs E relationship for that point by varying g_s from $2.0 \cdot 10^{-4}$ to 2.0 mol m^{-2} s^{-1} in 10,000 steps. We then classified each point into one of three categories based on the nature of the resulting A vs E relationship. In Category I, $\partial A/\partial E$ declines monotonically as g_s increases (i.e., $\partial^2 A/\partial E^2$

< 0). In Category II, $\partial A/\partial E$ increases at low g_s, reaches a maximum and then decreases at higher g_s (i.e., $\partial^2 A/\partial E^2 > 0$ at low g_s and $\partial^2 A/\partial E^2 < 0$ at high g_s). In Category III, $\partial A/\partial E$ is below its crown-wide target value (μ, discussed below) for all positive g_s (typically because PPFD is quite low or Δw is quite high). Examples of relationships between g_s and $\partial A/\partial E$ for five randomly chosen instances of each Category are shown in Figure 3A.
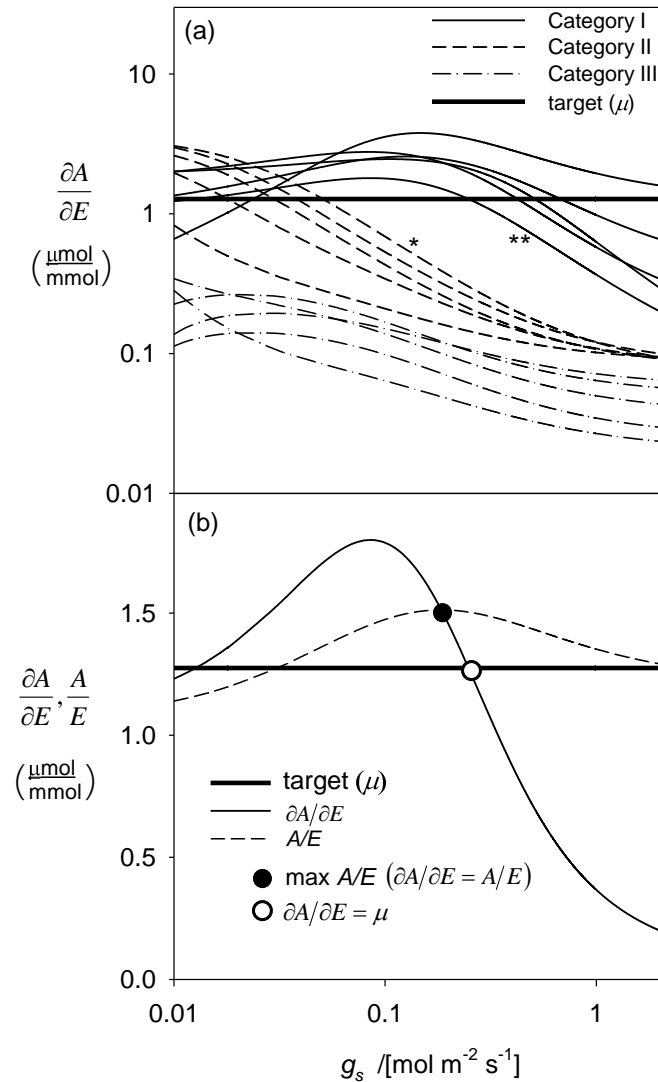

Figure 3: (A) Relationships between the marginal carbon product of water and g_s for four randomly chosen leaves in each of Category I (for which $\partial^2 A/\partial E^2 < 0$; dashed lines) and Category II (for which $\partial^2 A/\partial E^2 > 0$ at low g_s; solid lines); the thick black horizontal line represents the target value for $\partial A/\partial E$ (μ). (B) The relationships between g_s and $\partial A/\partial E$ (solid line) and instantaneous water use efficiency, A/E (dashed line) for one leaf in Category II, showing that A/E is maximised at a lower g_s (left-hand vertical grey line) than the g_s at which $\partial A/\partial E$ equals the crown-wide target value, μ (right-hand vertical grey line). μ is shown by the horizontal black line. (The curves marked with asterices in A also appear in Figure 4.)

188

Identification of optimal g_s (g_{so}) differs for each of these categories. For Category III, g_{so} is zero. The category most clearly relevant to the original Cowan-Farquhar theory is Category I; in this case, g_{so} is the value of g_s for which $\partial A/\partial E$ equals a target value, μ, that is invariant among leaves in the crown and over time (the choice of μ is discussed below). For Category II, there exists a realistic positive g_s that maximises instantaneous water use efficiency, WUE $= A/E$; this occurs when $A/E = \partial A/\partial E$ (Buckley et al., 1999) (Figure 3B). WUE is always greater at that value of g_s than for any other value, including any value (or values) for which $\partial A/\partial E = \mu$. However, although this value of g_s would maximise WUE for a Category II leaf considered by itself, it is not optimal for the crown as a whole. For example, imagine a Category I leaf and a Category II leaf both initially at $\partial A/\partial E = \mu$ (Figure 4A). Consider the effect of reducing E and g_s in the Category II leaf in order to bring it to the point of maximum WUE, where $\partial A/\partial E = A/E$, and redistributing the water thus saved to the Category I leaf (Figure 4B). The total change in assimilation rate resulting from this redistribution is

$$(18) \qquad \delta A_{total} = \int \left(\frac{\partial A}{\partial E}_{I} - \frac{\partial A}{\partial E}_{II} \right) dE ,$$

where the subscripts I and II refer to variables in the Category I and II leaves, respectively. Because $\partial A/\partial E$ is greater in the Category II leaf than in the Category I leaf across the range of g_s spanning this redistribution (4B), the integrand in Eqn 18 is negative, so the net change in assimilation rate for both leaves combined is also negative (Figure 4C). Thus, the optimal solution when some leaves are in Category II is to increase transpiration in those leaves at the expense of other leaves until $\partial A/\partial E$ is invariant among all transpiring leaves.

We identified the optimal g_s in both Category I and II leaves by searching the array of 10,000 g_s and $\partial A/\partial E$ values in reverse (i.e., beginning at high g_s and proceeding towards low g_s), finding the first point where $\partial A/\partial E > \mu$, and identifying optimal g_s as the average of the two values spanning the change in sign of $\partial A/\partial E$. In 21 instances of Category II points, (7.8% of all points), maximum WUE occurred at $g_s > 2.0$ mol m^{-2} s^{-1}; in these cases, we set g_{so} to 2.0 mol m^{-2} s^{-1} on the grounds that values greater than that are not physiologically realistic. We compared the resulting distributions of water loss

with alternative simulations in which g_{so} was either capped at 1.0 mol m^{-2} s^{-1} or allowed to take on arbitrarily high values, and the results were nearly identical (not shown); this is because boundary layer conductance (g_{bw}) was typically quite low in those instances, so that E was relatively insensitive to changes in g_s.
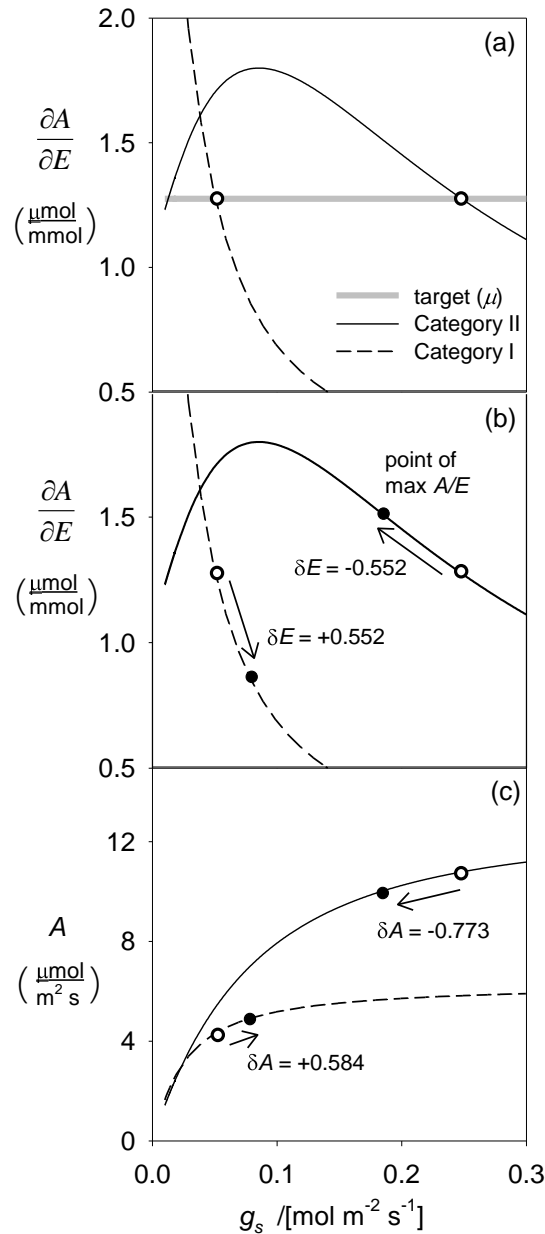

Figure 4: Illustration of the effect of redistributing water loss from a Category II leaf (solid lines) to a Category I leaf (dashed lines) in order to maximise water use efficiency (A/E) in the former. (A, open symbols): initial condition, in which $\partial A/\partial E$ equals the crown-wide target value, μ, for both leaves. (B, closed symbols): condition after redistribution of water loss ($\delta E = 0.552$ mmol m^{-2} s^{-1}) from the Category II leaf to the Category I leaf. (C): Relationships between net CO_2 assimilation rate, A, and stomatal conductance, g_s, for both leaves, with symbols representing the initial and final conditions as in A and B. The net change in A resulting from redistribution is negative. (Note that the Category I and II leaves correpond to the curves marked with one and two asterices, respectively, in Figure 4A.)

190

We identified the target value for $\partial A/\partial E$ (μ) separately for each individual by adjusting an initial estimate of μ repeatedly (re-optimising g_s for all measurement points at each value of μ) until the whole-crown diurnal total water loss computed for the optimal pattern of g_s was as close as possible to the total water loss computed for the measured pattern of g_s. Because changes in μ sometimes caused one or more measurement points to change categories, the relationship between μ and total crown water loss was not smooth, so it was not possible to achieve arbitrarily precise agreement in crown total water use between optimal and measured g_s distributions. However, the two values agreed to within 1.53% in all cases, and to within 0.21% when summed over all four crowns. To account for the effect of small remaining differences between measured and optimised crown water loss on comparisons of total carbon gain, we applied an approximate correction to total carbon gain: (Corrected optimal crown A) = (Computed optimal crown A) × (Measured crown E)/(Computed optimal crown E).

Numerical methods

All of the calculations described above were implemented in Microsoft Excel, in some cases using algorithms coded in VBA and in other cases using worksheet formulas. The Excel file containing the code is available from the authors upon request.

Statistical tests of the optimisation hypothesis

We chose to compare transpiration rate, rather than stomatal conductance itself, between optimal and measured patterns, for two reasons. First, mean optimal g_s was many times greater than mean measured g_s in some leaves, due to low boundary layer conductance (when g_{bw} is low, E is nearly insensitive to g_s at high g_s), and this made direct comparisons between measured and optimal patterns of g_s somewhat uninformative. Second, because optimisation theory is concerned with optimal allocation of finite resources, we felt it was more informative to compare distributions of the resource itself (water loss, E) rather than the biological parameter (g_s) that controls how that resource is distributed.

Residuals of E (optimal minus measured E) were distributed highly non-normally (as were the residuals of g_s), and normality could not be adequately improved by any transformation, so we used non-parametric tests (Kruskal-Wallis rank sum test) to

assess the probability that observed systematic differences in residual E among crown positions, among times of day, and among times of day at each crown position, were due to chance alone. We also assessed variation in mesophyll conductance (g_{m25}) with crown position using the Kruskal-Wallis test. Variations in photosynthetic capacity (V_{m25} and J_{m25}) were distributed normally, and were assessed by traditional analysis of variance in linear models. All analyses were performed in base R (R Core Team, 2013).

RESULTS

Photosynthetic capacity and irradiance

Photosynthetic capacity estimated from CO_2 response curves (V_{m25} and J_{m25}) differed significantly among crown positions (p < 0.0001 for both variables) (Fig 5 A,B). Mesophyll conductance (g_{m25}, Fig 5 C) also differed among positions (p = 0.013). Each of these variables was generally greater in the upper crown (positions 4-7; Figure 1
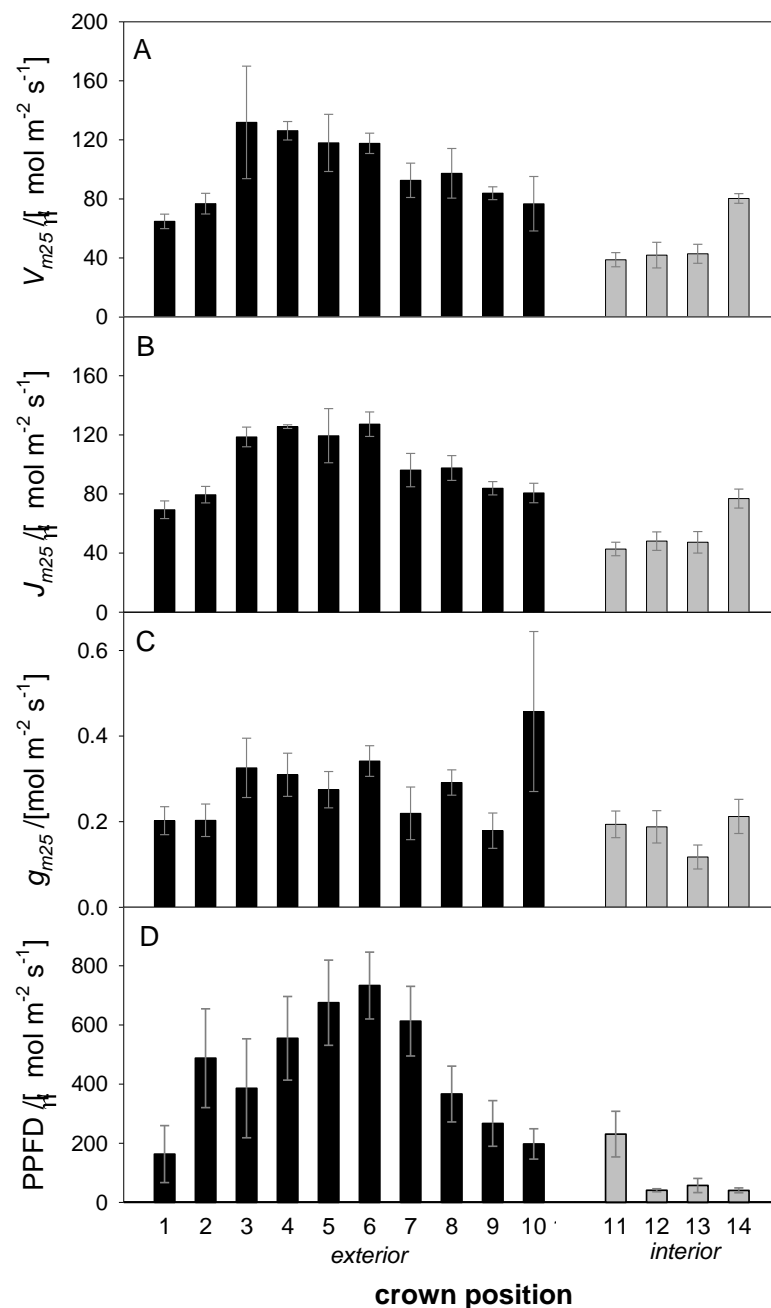
Figure 5: Gas exchange parameters (A, carboxylation capacity at 25°C, V_{m25}; B, electron transport capacity at 25°C, J_{m25}; C, mesophyll conductance at 25°C, g_{m25}) and incident photosynthetic photon flux density on the day of *in situ* measurements (D, PPFD) at each of 14 crown positions (see diagram in Figure 1). Black bars, exterior crown; grey bars, interior crown. Sample means ± SE.

For comparison, mean PPFD measured *in situ* on the day of diurnal measurements (22 Aug 2012) was greatest at the top of the crown and decreased down the sides of the crown, and PPFD was very low at the three lower interior crown positions (12-14) (Fig 5D).

Atmospheric conditions and associated leaf variables

Atmospheric conditions on 22 Aug 2012 were warm, calm and dry: air temperature ranged from 28.7 to 35.1°C, ambient humidity ranged from 12.0 to 15.5 mmol mol^{-1} (16.5 to 25.4% relative humidity) and 1-hour mean wind speed ranged from 0.5 to 1.1 m s^{-1} (Fig6.).
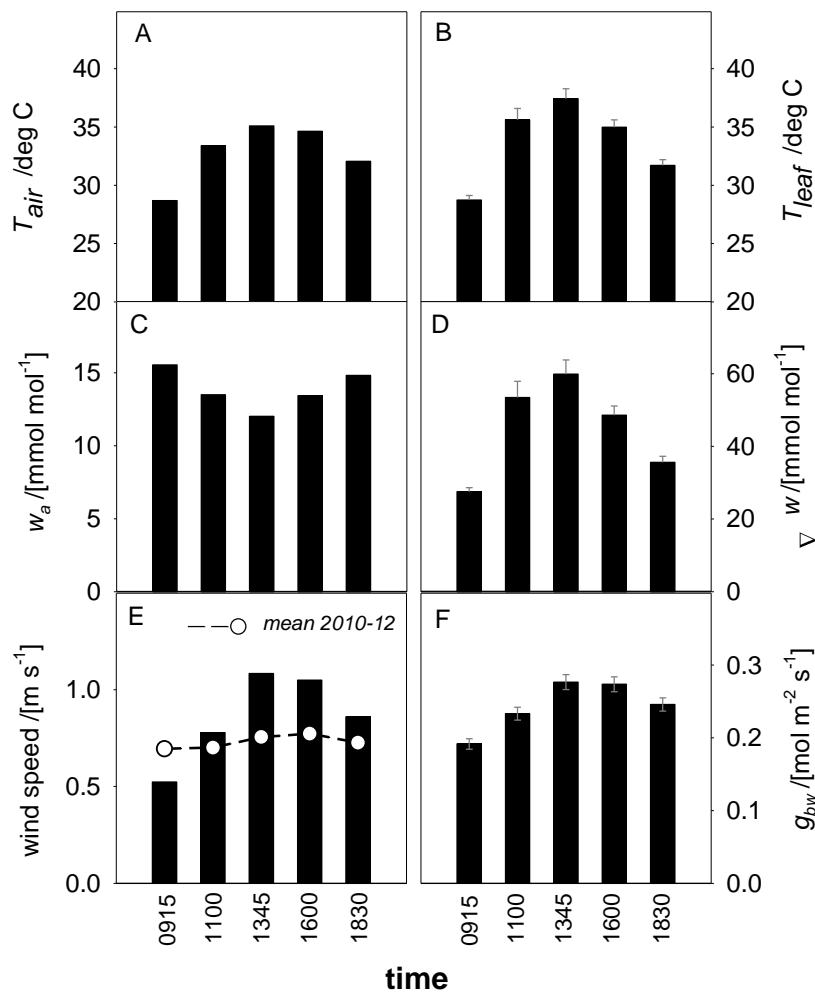

Figure 6: Environmental conditions measured at a meteorological station adjacent to the study site (A,C,E), and crown averages of associated leaf-level variables calculated from energy balance, based on those environmental conditions (B,D,F). A, air temperature (T_{air}); B, leaf

temperature (T_{leaf}); C, ambient water vapour mole fraction (w_a); D, effective leaf-to-air water vapour mole fraction gradient (Δw); E, wind speed (v_{wind}) measured on the day of the study (bars) and averaged over June-August in 2010-2012 (line and symbols); F, boundary layer conductance to water (g_{bw}). For B, D and E, error bars are SEs among four individual crowns.

Based on energy balance calculations, crown average leaf temperature (Fig 6 B) ranged from 28.7 to 37.4^{o}C, evaporative demand (Δw, Fig 6 D) ranged from 27.5 to 59.9 mmol mol^{-1} and boundary layer conductance (g_{bw}, 6 F) ranged from 0.19 to 0.28 mol m^{-2} s^{-1}, and each of these variables peaked in early afternoon (1345). Stomatal conductance and water use were moderate despite these conditions, with crown average g_s ranging from a minimum of 0.06 mol m^{-2} s^{-1} (at 1830) to a maximum of 0.13 (at 1100), and transpiration rate reaching a maximum of 4.4 mmol m^{-2} s^{-1} (at 13:45) (Fig 7).
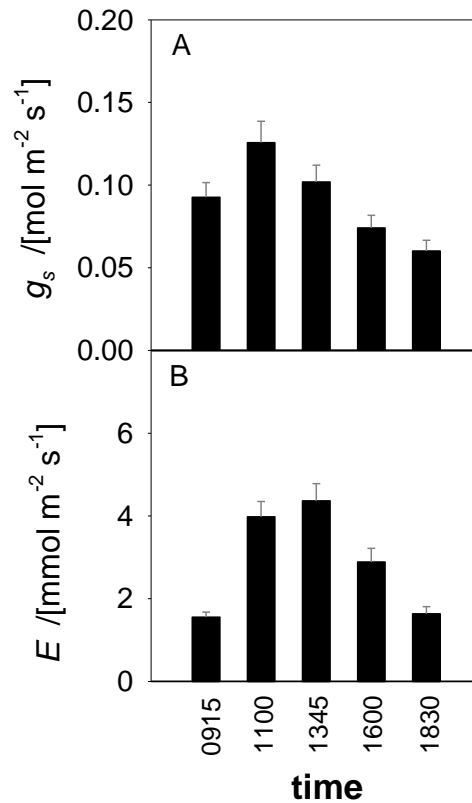

Figure 7: In situ measurements of stomatal conductance, g_s (A), and values of transpiration rate, E (B) calculated from measured g_s, averaged over 14 crown positions. Error bars are SEs among four individual crowns.

Categorisation of A vs E curves for each point

For each of 270 *in situ* measurement points, we calculated theoretical instantaneous relationships between A and E as described in *Materials and Methods*. Of these 270

points, 49.3% (133/270) were in Category I, for which $\partial A/\partial E$ declines monotonically with increasing g_s. Due to the combination of high irradiance and evaporative demand and low boundary layer conductance, we observed positive curvature in the A vs E relationship ($\partial^2 A/\partial E^2 > 0$) in 39.6% (107/270) of A vs E curves. These points fall into Category II, in which $\partial A/\partial E$ increases at low g_s and decreases at high g_s. Another 11.1% (30/270) were in Category III (optimal g_s was zero because $\partial A/\partial E$ was below the target value, μ, for all positive g_s).
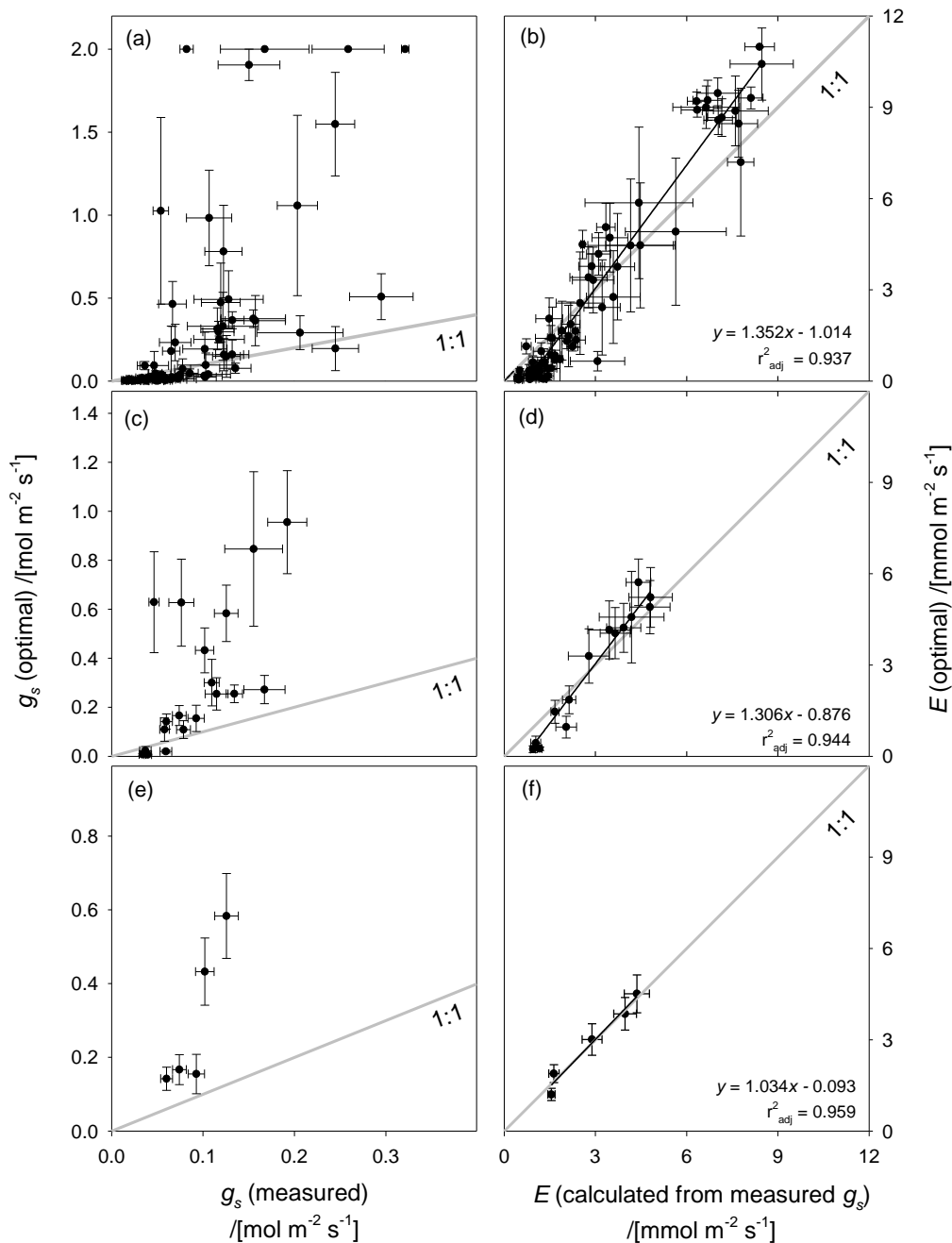
Optimal vs observed gas exchange patterns

Figure 8: Measured vs optimal stomatal conductance to H_2O g_s (A, C, E) and transpiration rate, E (B, D, F). A, B: averages within each of 70 combinations of crown position and measurement time. C, D: averages over all measurement times within each of 14 crown positions. E, F: averages over all crown positions at each of five measurement times. Error bars are SEs among four individual crowns. Grey lines in B,D,F: one-to-one line. Note the y-axis scales differ in A, C and E.

The optimal values of g_s were generally quite high, yet this had a smaller effect on total conductance (g_{tw}) and hence transpiration rate (E) than one might expect, due to the low boundary layer conductances. As a consequence, mean g_s predicted by optimisation greatly overestimated measured g_s in many cases, even though total crown water use was identical between the optimal and observed patterns of g_s. This is shown in panels A, C and E of Figure 8, which present measured and predicted g_s in three ways: without any grouping (Fig 8 A), grouped by position and averaged over time (Fig 8 C), or grouped by time and averaged among positions (Fig 8 E).

Because the low boundary layer conductances led to such skewed differences between observed and optimal g_s, comparisons between observed and optimal transpiration rate (E) are more informative, and are presented in panels B, D and F of Figure 8.
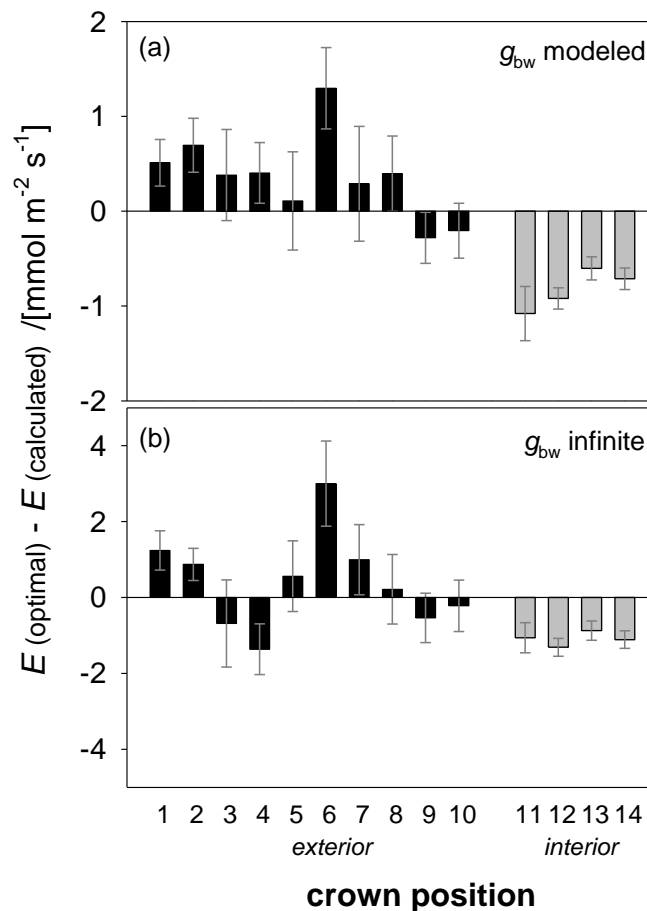
Figure 9: Residuals of transpiration rate (optimal minus measured *E*): diurnal means in relation to crown position. A, optimal *E* computed using boundary layer conductance, g_{bw}, modeled based on measured wind speed. B, optimal *E* computed assuming negligible boundary layer resistance (infinite g_{bw}). Error bars are SEs among four individual crowns. Note the y-axis scales differ in A and B.

Optimal *E* was generally greater than measured *E* in cases where measured *E* itself was higher than the crown average (Figs 8 B,D). This pattern largely reflected a reallocation of water loss from the interior crown (positions 11-14) to the upper and east-facing exterior crown (positions 1-6), as illustrated in Fig 9 A. Residuals of *E* (optimal minus measured *E*) differed significantly among positions ($p < 0.0001$). Optimal *E* was also lower than measured *E* in the middle of the day, and higher in the late afternoon (Fig 10 A) ($p < 0.05$).

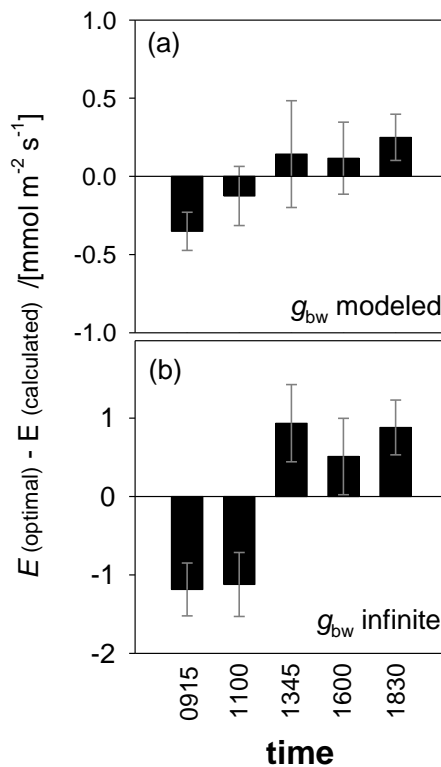**Figure 10:** Residuals of transpiration rate (optimal minus measured *E*): averages over 14 crown positions, shown in relation to time. A, optimal *E* computed using boundary layer conductance, g_{bw}, modeled based on measured wind speed. B, optimal *E* computed assuming negligible boundary layer resistance (infinite g_{bw}). Error bars are SEs among four individual crowns. Note the y-axis scales differ in A and B.

Additionally, the variation over time in residuals of E differed among crown positions (Fig 11) (these changes were significant for positions 1, 2, 4, 6, 8 and 10; $p < 0.05$). The clearest pattern in this regard was for optimal E to be greater than measured E in the first half of the day on the eastern crown and in the second half of the day on the western crown (Figs 11 A,C). Thus, the spatial pattern of differences between optimal and measured E among exterior crown positions shown in Fig 9 partly reflects a time-by-position interaction.
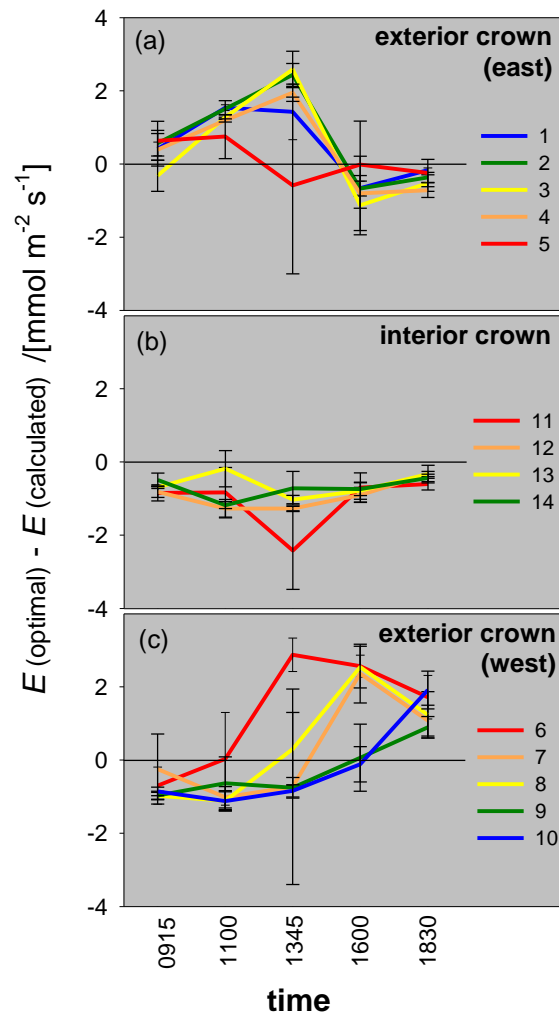

Figure 11: Residuals of transpiration rate (optimal minus measured E) over time for each of 14 crown positions: A, positions 1-5 (the eastern side of the crown); B, positions 11-14 (the interior crown); C, positions 6-10 (the western side of the crown). Error bars are SEs among four individual crowns.

Effects of gas exchange distributions on total carbon gain

To assess how whole plant carbon/water balance would be impacted by these differences between measured and optimal patterns of water use, we computed total diurnal carbon gain for each crown in three ways: using either the measured or optimal spatio-temporal distributions of g_s or using a constant value of g_s, while controlling for total crown water loss in each case. We found that a constant g_s yielded $71.7 \pm 0.6\%$ of the total carbon gain achieved by the optimal g_s distribution, whereas the observed g_s distribution achieved $81.8 \pm 0.3\%$ of the optimum (Fig 12).
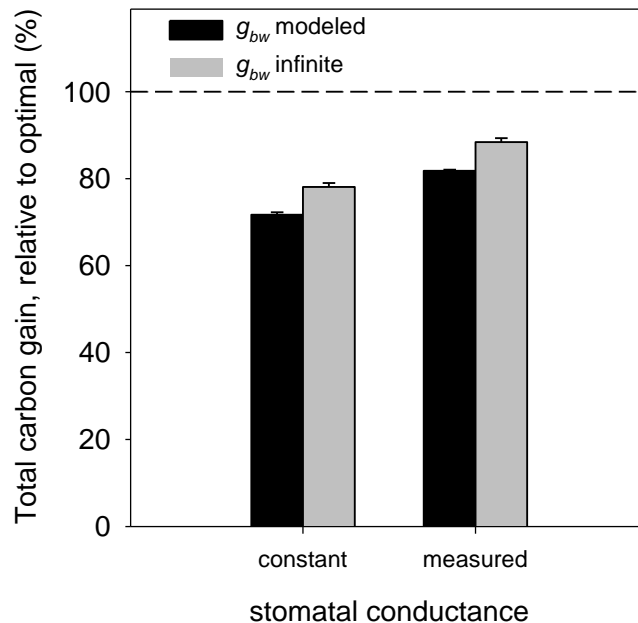

Figure 12: Total diurnal carbon gain calculated using either constant g_s, measured g_s or optimised g_s, expressed as a percentage of optimised values. Error bars are SEs among four individual crowns.

Effects of aerodynamic coupling (boundary layer conductance)

Because boundary layer conductance impacts the validity of the assumption that $\partial^2 A/\partial E^2 < 0$, which underlies optimisation theory, we repeated all calculations under an alternative scenario in which g_{bw} was imagined to be extremely large (which we simulated by setting wind speed to $3 \cdot 10^8$ m s^{-1}). The purpose of comparing the original results to this alternative scenario was to assess the sensitivity of inferred optima to assumptions about aerodynamic coupling between leaves and the air. Some conclusions were qualitatively similar between the "decoupled" and "coupled" scenarios: for

example, in both scenarios, the optimal pattern shifted water use from the interior crown to the upper exterior crown (cf. Figs 9 A,B), and from early in the day to later in the day. However, some conclusions differed as well. For example, the optimal pattern shifted water use away from positions 3 & 4 on the east face (cf. Figs 9 A,B). The magnitude of redistribution of water loss required to achieve the optimum was also greater at many positions in the coupled scenario than in the decoupled scenario (e.g., position 6; cf. Figs 9 A,B), although the difference in total carbon gain between the observed g_s distribution and the theoretical optimum was smaller in the coupled scenario (11.6% vs. 18.2%) (Fig 12)
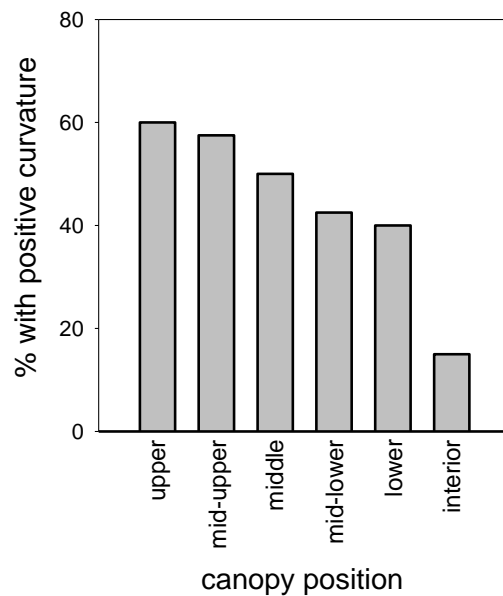
Figure 13: Proportion (as percent) of measurement points for which positive curvature in the relationship between assimilation rate and transpiration rate was observed. Position categories are as follows: upper (positions 5 and 6), mid-upper (positions 4 and 7), middle (positions 3 and 8), mid-lower (positions 2 and 9), lower (positions 1 and 10), interior (positions 11-14). Position numbers are shown in Figure 1.

DISCUSSION

Our objective was to test two aspects of stomatal optimisation theory that have largely been ignored by previous studies. Most work has focused on the prediction that stomata should keep the marginal carbon product of water, $\partial A/\partial E$, invariant over time. However, the theory also predicts that stomata must hold $\partial A/\partial E$ invariant in space (i.e., among leaves in distinct environments within the same individual crown) and it assumes that water loss earns diminishing returns in terms of carbon gain (i.e., the

curvature of A vs E is negative: $\partial^2 A/\partial E^2 < 0$) (Cowan & Farquhar, 1977), yet these aspects of the theory remain largely untested. Our results suggest that neither the spatial aspect of the theory nor its assumption of positive curvature hold in grapevine canopies under the hot, dry, sunny and calm conditions typical of Mediterranean summer at our study site. We found that the measured spatial pattern of water use differed systematically from the optimal pattern, with some regions of the crown using more water than the optimum and other regions using less. We also found positive curvature in A vs E for 40% of leaf measurements, largely due to low boundary layer conductance. In addition, we found that if we had simply assumed negligible boundary layer resistance, as many applications of the theory have assumed, then the resulting predictions would have diverged substantially from the true optima, thereby altering some conclusions about the relationship between observed and optimal patterns.

Positive curvature in A vs E and its implications

Water loss typically brings diminishing returns of carbon gain, because stomatal opening tends to reduce the gradient for leaf CO_2 uptake more than that for H_2O loss. As g_s increases, intercellular CO_2 increases, which decreases the CO_2 gradient. Although a related effect occurs with transpiration – that is, increased E can decrease the evaporative gradient (Δw) by increasing ambient humidity – this effect is generally smaller than the CO_2 effect because the volume of air even in a dense canopy is vastly larger than the volume of the intercellular air spaces (Cowan, 1977, Buckley *et al.*, 1999). In this case, there is no instantaneous optimum for the tradeoff between carbon gain and water loss: carbon gain per unit of water loss (instantaneous water use efficiency, WUE = A/E) is greatest in the limit of zero g_s, which is a trivial solution. (This is what led Cowan and Farquhar (1977) to ask what pattern of g_s maximises total carbon gain for a given total water loss, which leads to the invariant-$\partial A/\partial E$ solution.) However, increased g_s can strongly reduce Δw when boundary layer conductance (g_{bw}) is low. This is because low g_{bw} weakens convective heat transfer, increasing the scope of evaporative cooling to reduce leaf temperature and therefore Δw (Jones, 1992). The resulting changes in Δw can lead to positive curvature in A vs E (Cowan, 1977, Buckley *et al.*, 1999). In such conditions, there is an instantaneous optimum for leaf-scale WUE, which occurs when $\partial A/\partial E = A/E$ (the point at which the tangent line to the A vs E curve

goes through the origin) (Buckley *et al.*, 1999). As a result, it is initially unclear whether the invariant-∂A/∂E solution still applies in such conditions.

Buckley *et al.* (1999) suggested that if curvature is positive but a leaf cannot maintain *E* high enough to reach the maximum *A/E*, then the leaf should close some stomata entirely and open others more widely to achieve the optimum in the latter areas; i.e., spatially heterogeneous g_s is beneficial in this case. A related argument can be made at the crown level. If some leaves have negative curvature and others have positive curvature, then water loss should be reallocated from the former to the latter to allow the latter to maximise WUE. This will reduce *E* in the negative-curvature leaves, thereby increasing ∂A/∂E and WUE in those leaves as well and ensuring that the reallocation improves WUE throughout the crown. Furthermore, whole-crown WUE is maximised by increasing g_s even further in leaves with positive curvature – i.e., beyond the point at which WUE is maximised for those individual leaves – as explained in the text surrounding Equation 18 and illustrated in Figure 4.

The Cowan and Farquhar (1977) solution therefore applies even if positive curvature occurs, provided curvature eventually becomes negative at higher g_s. There are two exceptions to this solution. First, stomata should simply open as far as possible in leaves in which ∂A/∂E is always greater than the crown-wide target value (μ). This scenario applied in 7.8% of measured leaves in the present study. In these cases, boundary layer conductance was very low, so that changes in g_s had very little effect on ∂A/∂E at high g_s. Second, stomata should simply close in leaves for which the crown-wide target value of ∂A/∂E (μ) cannot be reached for any g_s ("Category III" leaves in our terminology; Fig 3A); this scenario applied in 11.1% of leaves in this study.

The implications of positive curvature will depend on how often, in nature, boundary layer conductance is low enough to allow positive curvature to occur. Wind speed above the canopy ranged from 0.5 – 1.1 m s^{-1} in our study, and positive curvature occurred across this range. This range is low but not particularly unusual for our site: mean daytime summer wind speed was 0.69 – 0.77 m s^{-1} over 2010-12 (Fig 6 e). Another study on grapevine (Daudet *et al.*, 1998) found wind speed was below 1.0 m s^{-1} for 13% of a typical day, and Jones et al. (2002) found wind speed rarely exceeded 1.3

m s^{-1} during two of four days in a field study on grapevine. Similar ranges have been reported in other species (e.g., 1-2 m/s, cotton, Grantz & Vaughn, 1999). Wind speed is much lower inside the crown because of wind attenuation by the canopy itself (e.g., Oliver, 1971, Daudet *et al.*, 1999, Grantz & Vaughn, 1999). However, this was not a dominant factor in causing positive curvature in the present study, as the occurrence of positive curvature actually decreased with depth in the canopy (Figure 13). We conclude that the occurrence of positive curvature in *A* vs *E* may not be as rare as previously thought, and that the matter requires further experimental study.

Why is the spatial distribution of water loss sub-optimal?

We found that the observed distribution of water loss among leaves did not match the optimal pattern, that the residuals were systematically related to crown position, and that these deviations reduced crown carbon gain by 18% compared to the optimum. It is helpful here to reiterate the rationale for this definition of "optimal": total carbon gain will be greatest for a given total water loss if $\partial A/\partial E$ is invariant (provided $\partial^2 A/\partial E^2 > 0$). That statement is independent of spatial or temporal scale, and is a generic mathematical result from the calculus of variations (Cowan & Farquhar, 1977). It says that among all possible spatiotemporal distributions of g_s that give the same total crown water loss, carbon gain is greatest for the distribution in which $\partial A/\partial E$ is invariant. A separate question is, at what scale is it biologically meaningful to view total water loss as invariant (Cowan, 1982, Cowan, 1986, Mäkelä *et al.*, 1996, Buckley & Schymanski, 2013)? In the next section ("*Is the optimisation problem correctly posed?*"), we discuss the possibility that it is not biologically appropriate to view total crown water loss as invariant, regardless of time scale. In this section we discuss other possible explanations for the observed spatial deviations from optimality. One involves delays in stomatal opening. We found that optimal water loss typically exceeded observed water loss whenever the sun was oriented most directly towards a particular crown position (e.g., Fig 11). It is possible that stomata in these positions could not respond quickly enough to the peak in PPFD to achieve optimal water loss. This effect would be exacerbated by low g_{bw}, which requires large changes in g_s to achieve a given change in water loss. Vico *et al.* (2011) suggested that delays in stomatal opening and closing in response to changes in PPFD create a quasi-optimal pattern of g_s, arguing that the costs of stomatal regulation itself must be subtracted from leaf net carbon gain in computing the optimum, so that the true optimum includes a finite time constant for stomatal

adjustments to PPFD. This is unlikely to explain our results, given that the carbon cost of stomatal movements was on the order of 0.25% of net assimilation rate in the simulations presented by Vico *et al* (2011) – far less than the potential improvement in carbon gain that could have been achieved by optimal stomatal control in our study.

Medlyn et al (2011; 2013) suggested that stomata lack the physiological machinery to detect the shift between carboxylation- and regeneration-limited photosynthesis. Those authors noted that stomatal responses to short-term changes in atmospheric CO_2 were approximately optimal under regeneration- but not carboxylation-limited conditions, so they suggested that stomata were only capable of optimal behaviour under regeneration-limited conditions (i.e., under sub-saturating PPFD). Our results offer qualified support for that idea, as deviations from optimality at a given position tended to be greater when the sun was oriented more directly towards that position, at which time PPFD would likely be saturating.

The spatial distribution of photosynthetic nitrogen may also have contributed to these deviations. The ratio of carboxylation capacity to PPFD was eight times greater in the interior crown (positions 11-14) than on the upper exterior crown (positions 4-7) (Fig 5) – consistent with other reports that capacity is not proportional to local irradiance, contrary to the predictions of optimisation theory for distribution of photosynthetic nitrogen (Evans, 1993, Hirose & Werger, 1994, Hollinger, 1996, de Pury & Farquhar, 1997, Makino *et al.*, 1997, Bond *et al.*, 1999, Friend, 2001, Frak *et al.*, 2002, Kull, 2002, Lloyd *et al.*, 2010, Buckley *et al.* 2013). It is well established that g_s is highly correlated with photosynthetic capacity (Wong *et al.*, 1979). If this correlation represents a mechanistic constraint on stomatal regulation – i.e., if the mechanisms that stomata have presumably evolved to optimise carbon/water balance include a physiological "response" to photosynthetic capacity or some proxy thereof – then such a response may present a physiological barrier to achieving optimal distributions of water loss in situations where photosynthetic capacity is suboptimally distributed. This highlights the important linkage between the economics of water loss and photosynthetic nitrogen use in plant crowns (Field, 1983, Buckley *et al.*, 2002, Farquhar *et al.*, 2002, Peltoniemi *et al.*, 2012, Buckley *et al.*, 2013, Buckley & Warren, 2013, Palmroth *et al.*, 2013).

Is the optimisation problem correctly posed?

The requirement that $\partial A/\partial E$ be spatially invariant within the crown assumes that water loss can be arbitrarily allocated among leaves and over time within the crown. However, hydraulic constraints may make it impossible for leaves in some crown positions to achieve optimal water loss rates while also maintaining water potential above thresholds for catastrophic loss of hydraulic conductivity. Although this could be remedied by increasing hydraulic conductance to such leaves by re-allocating carbon, such re-allocation may itself be sub-optimal, for two reasons. One is that stem carbon serves other functions, including mechanical support. Another is that hydraulic limitations to water loss may only manifest during brief periods in the growing season, in which case the large carbon investment needed to achieve optimal distribution of water loss may outweigh any resulting gains in crown water use efficiency. Thus, each leaf may in fact require a different target value for $\partial A/\partial E$ to reflect the realities of its water supply constraints. A full exploration of this idea requires more intensive theoretical analysis.

CONCLUSIONS

We found systematic divergence between observed and optimal spatial patterns of water use, and evidence of widespread positive curvature ($\partial^2 A/\partial E^2 > 0$) in grapevine crowns under hot, dry and calm conditions. Positive curvature resulted from aerodynamic decoupling between the crown and atmosphere. Our results suggest caution is warranted when using optimisation theory to predict g_s at the crown scale, and that further study is required to assess the occurrence of conditions leading to positive curvature. We also suggest it may be necessary to revise optimisation theory to account for variations in hydraulic capacity within a crown.

ACKNOWLEDGEMENTS

Schymanski and Graham Farquhar for helpful conversations, and two anonymous reviewers and the Associate Editor, Dr Danielle Way, for helpful comments on an earlier draft. We are particularly indebted to a reviewer who noted a critical error in our identification of optimal g_s in Category II leaves.

REFERENCES

Abramowitz M. & Stegun I.A. (1972) Solutions of quartic equations. In: *Handbook of Mathematical Functions with Formulas, Graphs and Mathematical Tables*, pp. 17-18. Dover, New York.

Ball M.C. & Farquhar G.D. (1984) Photosynthetic and Stomatal Responses of Two Mangrove Species, Aegiceras corniculatum and Avicennia marina, to Long Term Salinity and Humidity Conditions. *Plant Physiology*, **74**, 1-6.

Bernacchi C., Pimentel C. & Long S. (2003) In vivo temperature response functions of parameters required to model RuBP-limited photosynthesis. *Plant, Cell & Environment*, **26**, 1419-1430.

Berninger F., Mäkelä A. & Hari P. (1996) Optimal control of gas exchange during drought: empirical evidence. *Annals of Botany*, **77**, 469-476.

Bond B.J., Farnsworth B.T., Coulombe R.A. & Winner W.E. (1999) Foliage physiology and biochemistry in response to light gradients in conifers with varying shade tolerance. *Oecologia*, **120**, 183-192.

Brenner A.J. & Jarvis P.G. (1995) A heated leaf replica technique for determination of leaf boundary layer conductance in the field. *Agricultural and Forest Meteorology*, **72**, 261-275.

Buckley T.N., Cescatti A. & Farquhar G.D. (2013) What does optimisation theory actually predict about crown profiles of photosynthetic capacity, when models incorporate greater realism? *Plant, Cell & Environment*, **36**, 1547-1563.

Buckley T.N., Farquhar G.D. & Mott K.A. (1999) Carbon-water balance and patchy stomatal conductance. *Oecologia*, **118**, 132-143.

Buckley T.N., Miller J.M. & Farquhar G.D. (2002) The mathematics of linked optimisation for nitrogen and water use in a canopy. *Silva Fennica*, **36**, 639-669.

Buckley T.N. & Mott K.A. (2013) Modeling Stomatal Conductance in Response to Environmental Factors. *Plant, cell & environment*.

Buckley T.N. & Schymanski S.J. (2013) Stomatal optimisation in relation to atmospheric CO2. *New Phytologist*.

Buckley T.N. & Warren C.R. (2013) The role of mesophyll conductance in the economics of nitrogen and water use in photosynthesis. *Photosynthesis Research*, (**doi 10.1007/s11120-013-9825-2**).

Caemmerer S. & Farquhar G.D. (1981) Some relationships between the biochemistry of photosynthesis and the gas exchange of leaves. *Planta*, **153**, 376-387.

Cowan I. (2002) Fit, fitter, fittest; where does optimisation fit in? *Silva Fennica*, **36**, 745-754.

Cowan I.R. (1977) Stomatal behaviour and environment. *Advances in Botanical Research*, **4**, 117-228.

Cowan I.R. (1982) Water use and optimization of carbon assimilation. In: *Encyclopedia of plant physiology. 12B. Physiological plant ecology* (eds O.L. Lange, C.B. Nobel, C.B. Osmond, & H. Ziegler), pp. 589-630. Springer-Verlag, Berlin.

Cowan I.R. (1986) Economics of carbon fixation in higher plants. In: *On the economy of plant form and function* (ed T.J. Givnish), pp. 133-170. Cambridge University Press, Cambridge.

Cowan I.R. & Farquhar G.D. (1977) Stomatal function in relation to leaf metabolism and environment. *Symposium of the Society for Experimental Biology*, **31**, 471-505.

Damour G., Simonneau T., Cochard H. & Urban L. (2010) An overview of models of stomatal conductance at the leaf level. *Plant, Cell & Environment*, **33**, 1419-1438.

Daudet F., Le Roux X., Sinoquet H. & Adam B. (1999) Wind speed and leaf boundary layer conductance variation within tree crown: consequences on leaf-to-atmosphere coupling and tree functions. *Agricultural and Forest Meteorology*, **97**, 171-185.

Daudet F., Silvestre J., Ferreira M., Valancogne C. & Pradelle F. (1998) Leaf boundary layer conductance in a vineyard in Portugal. *Agricultural and forest meteorology*, **89**, 255-267.

de Pury D.G.G. & Farquhar G.D. (1997) Simple scaling of photosynthesis from leaves to canopies without the errors of big-leaf models. *Plant, Cell and Environment*, **20**, 537-557.

Ethier G. & Livingston N. (2004) On the need to incorporate sensitivity to CO_2 transfer conductance into the Farquhar–von Caemmerer–Berry leaf photosynthesis model. *Plant, Cell & Environment*, **27**, 137-153.

Evans J.R. (1993) Photosynthetic acclimation and nitrogen partitioning within a lucerne canopy. II. Stability through time and comparison with a theoretical optimum. *Australian Journal of Plant Physiology*, **20**, 69-82.

Farquhar G.D. (1973) *A study of the responses of stomata to perturbations of environment*, The Australian National University.

Farquhar G.D., Buckley T.N. & Miller J.M. (2002) Stomatal control in relation to leaf area and nitrogen content. *Silva Fennica*, **36**, 625-637.

Farquhar G.D., Schulze E.D. & Kuppers M. (1980a) Responses to humidity by stomata of Nicotiniana glauca L. and Corylus avellana L. are consistent with the optimization of carbon dioxide uptake with respect to water loss. *Australian Journal of Plant Physiology*, **7**, 315-327.

Farquhar G.D., von Caemmerer S. & Berry J.A. (1980b) A biochemical model of photosynthetic CO_2 assimilation in leaves of C_3 species. *Planta*, **149**, 78-90.

Field C.B. (1983) Allocating nitrogen for the maximization of carbon gain: leaf age as a control on the allocation program. *Oecologia*, **56**, 341-347.

Fites J. & Teskey R. (1988) CO2 and water vapor exchange of Pinus taeda in relation to stomatal behavior: test of an optimization hypothesis. *Canadian Journal of Forest Research*, **18**, 150-157.

Frak E., Le Roux X., Millard P., Adam B., Dreyer E., Escuit C., Sinoquet H., Vandame M. & Varlet-Grancher C. (2002) Spatial distribution of leaf nitrogen and photosynthetic capacity within the foliage of individual trees: disentangling the effects of local light quality, leaf irradiance, and transpiration. *Journal of Experimental Botany*, **53**, 2207-2216.

Friend A.D. (2001) Modelling canopy CO2 fluxes: are 'big-leaf' simplifications justified? *Global Ecology and Biogeography*, **10**, 603-619.

Gates D.M., Keegan H.J., Schleter J.C. & Weidner V.R. (1965) Spectral properties of plants. *Applied optics*, **4**, 11-20.

Grantz D.A. & Vaughn D.L. (1999) Vertical profiles of boundary layer conductance and wind speed in a cotton canopy measured with heated brass surrogate leaves. *Agricultural and Forest Meteorology*, **97**, 187-197.

Guehl J.-M. & Aussenac G. (1987) Photosynthesis Decrease and Stomatal Control of Gas Exchange in Abies alba Mill. in Response to Vapor Pressure Difference. *Plant Physiology*, **83**, 316-322.

Hari P., Mäkelä A., Berninger F. & Pohja T. (1999) Field evidence for the optimality hypothesis of gas exchange in plants. *Australian Journal of Plant Physiology*, **26**, 239-244.

Hirose T. & Werger M.J.A. (1994) Photosynthetic capacity and nitrogen partitioning among species in the canopy of a herbaceous plant community. *Oecologia*, **100**, 203-212.

Hollinger D.Y. (1996) Optimality and nitrogen allocation in a tree canopy. *Tree Physiology*, **16**, 627-634.

Jones H.G. (1992) *Plants and microclimate*. (2nd ed.). Cambridge University Press, Cambridge.

Jones H.G., Stoll M., Santos T., de Sousa C., Chaves M.M. & Grant O.M. (2002) Use of infrared thermography for monitoring stomatal closure in the field: application to grapevine. *Journal of Experimental Botany*, **53**, 2249-2260.

Kull O. (2002) Acclimation of photosynthesis in canopies: models and limitations. *Oecologia*, **133**, 267-279.

Küppers M. (1984) Carbon Relations and Competition between Woody Species in a Central European Hedgerow. II. Stomatal Responses, Water Use, and Hydraulic Conductivity in the Root/Leaf Pathway. *Oecologia*, **64**, 344-354.

Leuning R. (1988) Leaf temperatures during radiation frost Part II. A steady state theory. *Agricultural and Forest Meteorology*, **42**, 135-155.

Leuning R., Kelliher F.M., de Pury D.G.G. & Schulze E.D. (1995) Leaf nitrogen, photosynthesis, conductance and transpiration: scaling from leaves to canopies. *Plant, Cell and Environment*, **18**, 1183-1200.

Lloyd J., Patino S., Paiva R.Q., Nadrdoto G.B., Quesada C.A., Santos A.J.B., Baker T.R., Brand W.A., Hilke I., Gielmann H., Raessler M., Luizao F.J., Martinelli L.A. & Mercado L.M. (2010) Optimisation of photosynthetic carbon gain and within-canopy gradients of associated foliar traits for Amazon forest trees. *Biogeosciences*, **7**, 1833-1859.

Mäkelä A., Berninger F. & Hari P. (1996) Optimal control of gas exchange during drought: theoretical analysis. *Annals of Botany*, **77**, 461-467.

Mäkelä A., Givnish T.J., Berninger F., Buckley T.N., Farquhar G.D. & Hari P. (2002) Challenges and opportunities of the optimality approach in plant ecology. *Silva Fennica*, **36**, (in press).

Makino A., Sato T., Nakano H. & Mae T. (1997) Leaf photosynthesis, plant growth and nitrogen allocation in rice under difference irradiances. *Planta*, **203**, 390-398.

Meinzer F. (1982) The effect of vapor pressure on stomatal control of gas exchange in Douglas fir (Pseudotsuga menziesii) saplings. *Oecologia*, **54**, 236-242.

Oliver H. (1971) Wind profiles in and above a forest canopy. *Quarterly Journal of the Royal Meteorological Society*, **97**, 548-553.

Palmroth S., Katul G.G., Maier C.A., Ward E., Manzoni S. & Vico G. (2013) On the complementary relationship between marginal nitrogen and water-use efficiencies among Pinus taeda leaves grown under ambient and CO2-enriched environments. *Annals of botany*, **111**, 467-477.

Peltoniemi M.S., Duursma R.A. & Medlyn B.E. (2012) Co-optimal distribution of leaf nitrogen and hydraulic conductance in plant canopies. *Tree Physiology*, **32**, 510-519.

Press W.H., Teukolsky S.A., Vetterling W.T. & Flannery B.P. (1992) *Numerical recipes in C++: the art of scientific computing*. (2 ed.). Cambridge University Press, Cambridge, UK.

Roth-Nebelsick A. (2001) Computer-based analysis of steady-state and transient heat transfer of small-sized leaves by free and mixed convection. *Plant, Cell & Environment*, **24**, 631-640.

Sandford A.P. & Jarvis P.G. (1986) Stomatal responses to humidity in selected conifers. *Tree Physiology*, **2**, 89-103.

Schymanski S.J., Roderick M.L., Sivapalan M., Hutley L.B. & Beringer J. (2008) A canopy-scale test of the optimal water-use hypothesis. *Plant, Cell & Environment*, **31**, 97-111.

Team R.C. (2013) R: A language and environment for statistical computing. R Foundation for Statistical Computing, Vienna, Austria.

Thomas D.S., Eamus D. & Bell D. (1999) Optimization theory of stomatal behaviour: II. Stomatal responses of several tree species of north Australia to changes in light, soil and atmospheric water content and temperature. *Journal of Experimental Botany*, **50**, 393-400.

Vico G., Manzoni S., Palmroth S. & Katul G. (2011) Effects of stomatal delays on the economics of leaf gas exchange under intermittent light regimes. *New Phytologist*, **192**, 640-652.

Way D.A., Oren R., Kim H.-S. & Katul G.G. (2011) How well do stomatal conductance models perform on closing plant carbon budgets? A test using seedlings grown under current

and elevated air temperatures. *Journal of Geophysical Research: Biogeosciences*, **116**, G04031.

Williams W.E. (1983) Optimal water-use efficiency in a California shrub. *Plant, Cell & Environment*, **6**, 145-151.

Wong S.C., Cowan I.R. & Farquhar G.D. (1979) Stomatal conductance correlates with photosynthetic capacity. *Nature*, **282**, 424-426.

World Meteorological Organization (2008) *Guide to Meteorological Instruments and Methods of Observation*. WMO, Geneva, Switzerland.

6. GENERAL DISCUSSION

Water is the main resource for plants life resulting in determinant factor for plant distribution and growth in wide world areas, thus adaptation to water scarcity has excerted an important pressure in the evolution of plant species (Engelbrecht *et al*. 2007; Morison *et al.* 2008; Kursar *et al.* 2009). Water loss becomes unavoidable for plants because photosynthesis needs wide surfaces for light interception (leaves) and also needs to facilitate the CO_2 flux to the mesophyll. CO_2 and water flows occur at the stomata but water gradient is thousands of times larger than CO_2 thus moles of water loss are between 100 and 1000-fold those of CO_2 captured by photosynthesis. Therefore, transpiration becomes unavoidable for plant and regulation of leaf area and stomatal aperture are clearly an important part of plant adaptation and acclimation to drought prone environments.

Therefore, regulation of stomatal conductance (g_s) is a key point to understand plant's water economy and the implications of this economy on plant adaptation to drought, evolution and ecology trying to understand the best strategies to save water in agro-ecosystems (Farquhar and Sharkey, 1982; Schulze et al., 1994; Medrano *et al.*,2002, 2003; Hetherington and Woodward, 2003; Chaves et al, 2007; Brodribb and McAdam, 2011). Control of stomatal aperture is a hot issue in plant physiology research, being subject to an impressive amount of work, both on the basis of plant physiology and ecophysiology as well as for the water saving objectives in agronomy (Buckley, 2005; Damour et al., 2010; Medlyn et al., 2011; Diaz-Espejo et al., 2012; Buckley and Mott, 2013). From this grounds, it is evident that there is a multi-control of stomatal aperture and that it would be interesting to contrast simultaneously the weight of single characters such as leaf water relations, osmotic adjustment, hydraulic conductivity and abscisic acid variations, to better explain their weight on g_s regulation under field conditions and to contrast the capacity of different models to predict the g_s variations.

The main goal of the present thesis is to integrate key points of stomatal control in order to identify their relative importance to particular adjustments. Previous experience showed the need to undertake deeper research on leaf and stem water relations and leaf hydraulic conductance as well as to introduce an innovative modeling approach to gain new perspectives to integrate previous knowledge. This should allow new tests of the capacity of mechanistic models to improve our knowledge of this complex control and

to better understand the responses by plants to drought, as well as the observed differences of such responses.

The results of this Thesis have been structured in three chapters (2, 3, 4) corresponding to seven scientific publications derived from the experimental work. The specific relevance of the findings is discussed in each chapters, dealing with some of the general objectives previously described. Therefore, this General Discussion intends to provide an integrated view of all physiological processes that affect stomatal regulation and highlight the advances obtained from the present results in the understanding of the stomatal regulation. This discussion is structured on the basis of the general objectives of the thesis.

1. - Physiological mechanism regulating g_s under water stress.

The first objective of this thesis was **to improve the present knowledge on the role of water relations, leaf gas exchange, ABA and hydraulic conductance of stem and leaves on the regulation of stomatal conductance and photosynthesis.**

Stoma is composed of two guard cells hydraulically connected to mesophyll cells and their surrounding (Buckley, 2005). Therefore, stomata closure and aperture is consequence of turgor changes of guard cells which are connected with adjacent cells of the mesophyll and epidermic ones. Cell turgor responds to changes of different physiological parameters such as leaf water potential, water supply to the leaf, hydraulic conductivity, chemical signals like ABA and others (Farquhar and Sharkey, 1982; Ball et al., 1987; Leuning, 1990, 1995; Dodd, 2005; Buckley, 2005).

Regarding to the coordination mechanisms regulating stomatal conductance, Chapter 3.1 shows the existence of a consistent coordination between stomatal closure and turgor loss point related to the water potential at which stomata close. Turgor loss point water potential coincides with the point at which 50% of stem cavitation occurs (P_{50}) which integrates a general plant response to water stress (Martorell et al., 2014a). These results are in agreement with Choat *et al.,* (2012) showing that different species from drought prone areas are living usually near P_{50} values of stem hydraulic conductance. Chapter 3.1 shows that leaf turgor loss and stomatal closure thresholds occur at leaf water potentials just above P_{50} stem water potential, suggesting that stomatal closure plays a protective role by delaying the occurrence of extensive embolism in the stem (Jones & Sutherland 1991; Sparks & Black 1999). It also shows the existence of a high degree of coordination between leaf and stem traits which has

been described as typical for isohydric behaviour (Tardieu and Simonneau, 1998; Domec & Johnson 2012).

Another proposed regulator of stomatal conductance is the hydraulic conductivity of leaves. Our data shows, for the first time, that leaf hydraulic vulnerability to dysfunction (measured by P_{80}, the water potential causing 80% loss of conductivity) decreased over summer in grapevine, and that P_{80} was strongly correlated with turgor loss point (Martorell et al., 2014b). This indicates that hydraulic conductivity is not constant, being able to change with leaf age and the vulnerability of leaf conductance is able to acclimate to water stress. Moreover, the maintenance of K_{leaf} at more negative Ψ_{leaf} values is strongly correlated to osmotic adjustment, (Martorell et al. 2014b) suggesting that maintenance of turgor pressure may be involved in the plastic acclimation of leaf hydraulic vulnerability to dysfunction, measured as P_{80}. Previous studies have shown P_{50} and P_{80} to be lower in species from arid and semiarid environments (Blackman *et al.* 2010, Scoffoni *et al.* 2012, Nardini *et al.* 2012), understanding such differences as an adaptation to arid regions (Nardini *et al.* 2012). This Thesis also provides evidence that the observed acclimation of leaf hydraulic vulnerability to drought is caused, at least in part, by osmotic adjustment. These adjustments may help to maintain the conductivity of the extra-xylary pathway for water flow in two ways. First, maintaining turgor to prevent excessive cell shrinkage during water stress (Sancho-Knapik *et al.* 2011, Scoffoni *et al.* 2012, Scoffoni *et al.* 2014), thereby maintaining cell to cell pathways (symplastyc and transcellular paths) and preventing a reduction in evaporative surface in the intercellular spaces (Scoffoni *et al.* 2014). Second, maintenance of turgor may be required to sustain high conductivity of the symplastic pathway as turgor may directly modulate aquaporin function (Kim and Steudle 2007, Cochard *et al.* 2007).

This result highlights the relevance of the extra-xylary component of K_{leaf} and shows again the importance of cell turgor and osmotic adjustment over the regulation of K_{leaf} and in consequence over stomatal conductance. Enhancement of K_{leaf} at lower water potentials, which might help to explain the established contrasting reputation of the two cultivars measured, points out the extra-xylary component of K_{leaf} as one of the most plastic components of the hydraulic acclimation of plants to water stress.

As a follow up of those experiments demonstrating the relevance of osmotic adjustment and turgor maintenance on the g_s response to water stress as well as their

importance to understand K_h variations with leaf age, the behavior of two grapevine cultivars, Grenache and Tempranillo, with contrasting reputation as more and less adapted to drought environments (Jones, 2006; Van Leeuwen *et al.* 2013) were compared. Consistent with previous reports in potted plants, Grenache showed slightly higher water use efficiency (WUE) than Tempranillo (Flexas *et al.* 2010; Tomàs *et al.* 2012). WUE was higher in Grenache in al treatments, although it was for more evident under sever water stress.

Osmotic adjustment seemed to be responsible for the sustained higher values of $\Delta\Psi$ in Tempranillo as compared to Grenache under water stress in both years. Osmotic adjustment could also contribute to delay the effects of water stress in Tempranillo enabling it to maintain turgor at lower water potential (Kubiske and Abrams 1990; Sack et al. 2003; Bartlett et al. 2012; Martorell et al. 2014 k leaf). Consequently, osmotic adjustment is an important contribution to maintain stomata opened at lower water potentials (Martorell et al., 2014 varietats).

Data in this Thesis is not determinant to mark a differential behavior of both cultivars for the g_s dependency of Ψ_{pd}. Although, when maximum stomatal conductance was plotted against Ψ_{md}, a particular relationship was found for each cultivar, and in general, for the same Ψ_{md} the corresponding g_s was slightly higher for Tempranillo than Grenache. These results were not consistent to qualify these cultivars as iso or anysohydric.

There was a good correlation between ABA and Ψ_{pd} which was coincident for both cultivars. However, this relationship was clearly dependent on the sampling time with a dramatic change between July and August leading to two clearly differentiated regression lines. Interestingly, Grenache showed constitutively higher values of ABA than Tempranillo for the same water stress levels adding a differential characteristic between both cultivars in the dependence of ABA from Ψ_{pd}.

The dependency of g_s from K_{hplant} presented a cultivar dependent relationship so that Tempranillo showed for similar K_{hplant} higher g_s values thus showing that Tempranillo and Grenache had different sensibility against hydraulic restrictions being both with similar sensitivity (slope). Again, the higher osmotic adjustment component of Tempranillo could be playing some role to explain these results.

Summarizing, the reputation of Grenache as a cultivar with higher leaf WUE, was confirmed. The analysis of the differential weight of water relations, [ABA] and K_h

on the regulation of g_s demonstrated that the strength of osmotic adjustment, and concomitantly leaf turgor, are key players in the regulation of g_s under water stress. Furthermore, in this Thesis shows that differences in this adjustment between varieties could lead to substantial differentiation in stomatal regulation and leaf water use efficiency.

2.- Modeling stomatal conductance and photosynthesis with process based models to understand their regulation.

The second broad objective of this thesis was **to introduce the use of mechanistic models to better understand the responses of grapevine leaves responses to water stress, particularly stomatal conductance and photosynthesis.**

As stated above, g_s is a key physiological parameter to understand plant carbon gain and water use. Therefore process based models can improve our understanding of g_s regulation. This Thesis applies some of the most used models for g_s (Ball et al., 1987 (BWB); Leuning, 1995 (BWB-L)) and also a simplification of the process-based model proposed by Buckley et al., 2003 (BMF). The original version of this model was simplified down to only three physiological parameters needed to be adjusted, while the rest of inputs corresponded to environmental variables. The parameters needed to be fitted were the main regulators of stomatal conductance as it has been discussed above such as; osmotic potential (π), hydraulic conductance (K_h) and a parameter related to chemical signals (n) such as ABA. The model could effectively predict g_s under both water stress and well water conditions. Given that the parameters of the BMF model have full physiological meaning, it is possible to measure some of these parameters and to use them as inputs. So, when $\Psi_{\pi,TLP}$ was used as a proxy of π, the K_h fitted and predicted by the model match well with the K_h calculated from Ohm´s law. The model predicted a) a decrease of osmotic potential (π) as it was observed in grapevines (Patakas et al., 2002; Martorell et al., 2014b), b) a decrease of hydraulic conductance throughout the season in well water conditions due to leaf age (Martorell et al., 2014b), more pronounced in water stress conditions (Lovisolo et al., 2008; Choat et al., 2010; Martorell et al., 2014b), and c) it was also able to predict a change of sensitivity of g_s to ABA xyl (Chapter 3.3). Finally, when the model was coupled with the mechanistic model of photosynthesis by Farquhar et al., 1980 (FvCB hereafter), it predicted photosynthesis nicely.

Although grapevine photosynthesis has been widely studied (Flexas et al., 1998; Bota et al., 2001; Medrano et al., 2003; Escalona et al., 2003; Tomàs et al., 2012), no literature was found considering a finite mesophyll conductance (g_m) to estimate the temperature response of the FvCB parameters to model photosynthesis. Several works had performed temperature responses of FvCB parameters to temperature in grapevine (Shultz, 2003; Greer and Weedon 2012) but all of them considering g_m as infinite. Recently, it has been highlighted that g_m has species-specific responses to temperature (Evans and von Caemmerer 2014; Flexas and Diaz-Espejo, 2014). Moreover, this Thesis shows that this response in the case of grapevine can be variety/cultivar dependent (Chapter 4.1). In consequence, cell wall effective path length and aquaporins in a narrow relationship with g_m are the main candidates to explain the differential temperature response between varieties. The anatomical characteristics of leaves in both cultivars might be playing a role in the observed response. The effective path lengths for liquid diffusion are influenced by the magnitude of the surface of chloroplasts respect to their mesophyll surface in the intercellular spaces, and also by the porosity of the cell wall. The later is difficult to measure and it is expected to change with the composition of the cell wall. On the other hand, the membrane permeability to CO_2 is affected by the composition of the membrane, e.g. the CO_2 permeability of lipid bilayers could be decreased by increasing the cholesterol content of the membrane (Itel, Al-Samir, Öberg et al., 2012). Aquaporins have been reported as main candidates to explain g_m variations and its response to environmental variables (Flexas et al. 2012; Pou et al., 2013; Moshelion et al., 2014). Evans and von Caemmerer (2014) concluded with the application of their simplified model, that high membrane permeability to CO_2 by inclusion of a large number of aquaporins would render the membrane g_m rather insensitive to temperature. The results of this Thesis seems to be in agreement with this possibility, especially in the case of Grenache where its temperature response appears to be fairly flat, similar to the woody plants shown in Evans and von Caemmerer (2014). All these possibilities need to be tested and knowledge about them is needed to understand the mechanistic basis of the control of g_m to temperature.

Using the new analysis proposed by Buckley and Diaz-Espejo 2014 the contribution of each variable to photosynthesis rate at different temperatures were quantified. This analysis showed that the biochemical component was the most important at the different temperatures studied, especially at low temperatures. The results counterpose previous studies that presented diffusional limitation as the most important (Grassi and Magnani

2005, Flexas et al., 2009, Gallé et al., 2009). However, in the present case we compared measurements under well water conditions were compared and also at a wide range of temperatures.

On the other hand diffusional contributions are the main difference between both cultivars with g_m playing a more modest role than g_s.

3. Scaling up from leaves to the canopy.

The last broad objective of this thesis was **to explore the usefulness of modeling to scale up from leaf to whole plant gaining a new perspective for whole grapevine behavior.**

There is an important gap to scale up from leaf to whole plant physiology which is not easy to solve as recently argued by different authors (Buckley et al., 2002; Niinemets, 2012; Peltoniemi et al., 2012; Buckley and Warren, 2014) showing that more detailed information is needed to perform such scaling up.

To introduce more detailed data, scaling up from the leaf to the whole grapevine canopy was tried taking into account the different leaf positions inside the canopy and the interactions of leaf-microclimate conditions for each one of them in a series of fourteen locations in the canopy. It is shown that A_N behaves clearly different among leaf locations being the east/west face positions a source of clear differences in the measured parameters. However, the carboxylation capacity for each side of the canopy was similar indicating that both sides should have had a similar potential assimilation rates, and therefore suggesting that other constrains were driving the actual photosynthesis rate values.

The application of the contribution analysis proposed by Buckley & Diaz-Espejo (2014) to those data showed that diffusional contributions were the highest limiting component of photosynthesis in the west side of the canopy in accordance with Warren and Buckley (2014) which predicted that irrespective of leaf position, CO_2 diffusion is needed to be optimized to enhance photosynthesis. The partitioning of diffusional contributions between g_s and g_m was useful to identify the principal regulator of A_{Nmax} between both sides. Thus, g_m contributions were lower than g_s and seemed not to be the major contributor of the changes in $A_{N,max}$ while g_s was observed to be the general contributor differentiating east and west side.

On the other side, the BMF model permits to extract the physiological parameters related to the control of stomata leading to infer the main constraints limiting g_s. BMF

model was able to reproduce K and also ABA behavior with the data measured (Diaz-Espejo et al., 2012; Rodriguez-Dominguez in press, Chapter 4.1). Using the BMF model and the cumulative radiation received for each leaf, a clear differentiation between west and east side of the canopy was observed thus K variations seemed to be determinant for g_s. These results are in coincidence with the recent report by Peltoniemi et al., (2012), that concluded that carbon gain should be optimized with hydraulic conductance. There are also evidences that K vary between light regimes and that it can be different for different daily accumulated light conditions changing along the canopy (Sack et al., 2003; Brodribb and Jordan 2011; Nardini et al., 2012) thus being largely dependent on the specific micro-environmental conditions.

In order to evaluate the limitations working on stomatal conductance an analysis to quantify how stomatal conductance is limited by the hydraulic component and chemical signals was performed following Rodríguez-Domínguez et al., (personal communication). This analysis shows differential regulation of both components suggesting that hydraulic constraints are the main limiting factor for g_s in both parts of the canopy and they become higher when maximum light intensity is received. This analysis reveals that K_h distribution around the canopy can result in an important limiting factor for g_s and also for A_N since a good relationship has been always observed between plant architecture and maximum photosynthesis (Brodribb et al., 2007). These findings open new frontiers in the study of the variability of hydraulic conductance along the canopy as a constraint to explain the distribution of stomatal conductance.

Another method to scale up is applying the optimization theory. This theory attempted to deduce g_s from the hypothesis that stomatal behavior tends to maximize carbon gain (A) for any given water loss (E) (Cowan and Farquhar, 1977). In the present Thesis, this theory is tested to explain spatial variations of A_N trough a grapevine crown considering mesophyll and boundary layer conductances. Results obtained suggest that neither the spatial aspect of the theory nor its assumption of negative curvature hold in grapevine canopies under hot, dry, sunny and calm conditions typical of Mediterranean summers. A suboptimal pattern of water use was found with some regions of the crown using more water while others using less water than the optimum. Under low boundary layer conditions a positive curvature in A_N versus E curves was observed in 40% of the cases. It is possible for stomata to be unable to detect the shift between carboxylation and regeneration limited photosynthesis

as it has been observed that stomatal responses to short term changes in atmospheric CO_2 were approximately optimal under regeneration-limited but not under carboxylation-limited conditions (Medlyn et al. 2011, 2013). The spatial distribution of nitrogen may also have contributed to these deviations. It was observed that the carboxylation capacity was not proportional to local irrandiance, as stated above (Chapter 5.1) and contrary to the predictions of the optimization theory for distribution of photosynthetic nitrogen (Evans 1993; Hirose &Werger 1994; Hollinger 1996; Makino et al. 1997; de Pury & Farquhar 1997; Bond et al. 1999; Friend 2001; Frak et al. 2002; Kull 2002; Lloyd et al. 2010; Buckley & Schymanski, 2014). The requirement of $\partial A/\partial E$ to be spatially invariant within the crown assumes that water loss can be arbitrarily allocated among leaves and over time within the crown. However, hydraulic constraints may make it impossible for leaves in the some crown positions to achieve optimal transpiration while also maintaining water potential above thresholds for catastrophic loss of hydraulic conductivity. Although this could be remedied by increasing hydraulic conductance in such leaves by re-allocating carbon, such re-allocation may itself be suboptimal, for two reasons. One is that stem carbon serves other functions, including mechanical support. Another is that hydraulic limitations to water loss may only be manifested during brief periods in the growing season, in which case the large carbon investment needed to achieve optimal distribution of water loss may outweigh any resulting gains in crown WUE. Thus, each leaf may, in fact, require a different target value for $\partial A/\partial E$ to reflect the realities of its light and water supply constraints. A full exploration of these ideas requires more intensive theoretical analysis and experimental data.

7.GENERAL CONCLUSIONS

7.1. CONCLUSIONS OF THE PRESENT THESIS

1- Turgor loss point is well related with stomata closure and P_{50} stem hydraulic conductance indicating that the Turgor Loss Point plays a key role in the response to water stress.

2- Leaf vulnerability to hydraulic dysfunction acclimates to seasonal drought within a single species indicating that leaf hydraulic conductance has a plastic response. This response is shown to be well related to osmotic adjustment.

3- Tempranillo and Grenache differ in terms of water use efficiency and these differences are related to different hydraulic conductance, ABA concentration and osmotic adjustment. The dynamics of the three parameters in response to water stress explain the cultivars differences in water use efficiency.

4- The process based model of Buckley *et al*. (2003) is able to satisfactorily predict stomatal conductance variations along the season both under water stress and well watered conditions.

5- The model of photosynthesis by Farquhar *et al.* (1980) can be improved by including the respose of mesophyll conductance to temperature as has been demonstrated for Grenache.

6- Stomatal conductance and photosynthesis showed important variations with canopy location. These variations can be predicted applying the BMF model. The two limitation analyses applied highlighted that the canopy variations in hydraulic limitations were the main constrain to stomatal conductance.

7- The optimization theory was not able to predict total carbon gain around the canopy showing that there is not a real optimization of photosynthesis vs. transpiration for all positions of the leaves in the canopy. The results suggest that such a lack of optimization might be related to the canopy variations in the hydraulic conductance.

8- The application of the different process-based models emerges as a powerful tool which will help to identify the most relevant physiological variables involved in the stomatal conductance and photosynthesis variations under water stress.

GENERAL REFERENCES

Abrams M.D., Kubiske M.E. & Steiner K.C. (1990) Drought adaptations and responses in five genotypes of Fraxinus pennsylvanica Marsh.: photosynthesis, water relations and leaf morphology. *Tree physiology*, **6**, 305-315.

Acock B. & Grange R.I. (1981) Equilibrium models of leaf water relations.*Mathematics and plant physiology*.

Aschmann H. (1973) Distribution and peculiarity of Mediterranean Ecosystems. In: *Mediterranean Type Ecosistems: Origin and structure* (eds Di Castri, F. and Mooney, H. A.), pp. 405. SpringerVerlag, New York

Baldocchi D. (1994) A comparative study of mass and energy exchange rates over a closed C3(wheat) and an open C4corn crop: II. CO_2 exchange and water use efficiency. *Agricultural and Forest Meteorology*, **67**, 291-321.

Ball J.T., Woodrow I.E. & Berry J.A. (1987) A model predicting stomatal conductance and its contribution to the control of photosynthesis under different environmental conditions. In *Progress in photosynthesis research.* Springer Netherlands.

Baltzer J.L., Davies S.J., Bunyavejchewin S. & Noor N.S.M. (2008) The role of desiccation tolerance in determining tree species distributions along the Malay–Thai Peninsula. *Functional Ecology*, **22**, 221-231.

Bartlett M.K., Scoffoni C. & Sack L. (2012) The determinants of leaf turgor loss point and prediction of drought tolerance of species and biomes: a global meta‐analysis. *Ecology Letters*, **15**, 393-405.

Bartlett M.K., Zhang Y., Kreidler N., Sun S., Ardy R., Cao K. & Sack L. (2014) Global analysis of plasticity in turgor loss point, a key drought tolerance trait. *Ecology letters*.

Blackman C.J., Brodribb T.J. & Jordan G.J. (2010) Leaf hydraulic vulnerability is related to conduit dimensions and drought resistance across a diverse range of woody angiosperms. *New Phytologist*, **188,** 1113-1123

Bond B.J., Farnsworth B.T., Coulombe R.A. & Winner W.E. (1999) Foliage physiology and biochemistry in response to light gradients in conifers with varying shade tolerance. *Oecologia*, **120**, 183-192.

Bongi G. & Loreto F. (1989) Gas-exchange properties of salt-stressed olive (Olea europea L.) leaves. *Plant physiology*, **90**, 1408-1416.

Bota B.J., Flexas J. & Medrano H. (2001) Genetic variability of photosynthesis and water use in Balearic grapevine cultivars. *Annals of Applied Biology*, **138**, 353-361.

Boyer, J. S. (1982). Plant productivity and environment. *Science*, *218*(4571), 443-448.

Brodersen C.R., McElrone A.J., Choat B., Lee E.F., Shackel K.A. & Matthews M.A. (2013) In vivo visualizations of drought-induced embolism spread in Vitis vinifera. *Plant physiology*, **161**, 1820-1829.

Brodribb T.J. & Holbrook N.M. (2004) Diurnal depression of leaf hydraulic conductance in a tropical tree species. *Plant, Cell & Environment*, **27**, 820-827.

Brodribb T.J. & Holbrook N.M. (2005) Water stress deforms tracheids peripheral to the leaf vein of a tropical conifer. *Plant Physiology*, **137**, 1139-1146.

Brodribb T.J. & Jordan G.J. (2011) Water supply and demand remain balanced during leaf acclimation of Nothofagus cunninghamii trees. *New Phytologist*, **192**, 437-448.

Brodribb T.J. & McAdam S.A. (2011) Passive origins of stomatal control in vascular plants. *Science*, **331**, 582-585.

Brodribb T.J., & Cochard H. (2009) Hydraulic failure defines the recovery and point of death in water-stressed conifers. *Plant Physiology*, **149**, 575-584.

Brodribb T.J., & Holbrook N.M. (2003) Stomatal closure during leaf dehydration, correlation with other leaf physiological traits. *Plant Physiology*,**132,** 2166-2173.

Brodribb T.J., Feild T.S. & Jordan G.J. (2007) Leaf maximum photosynthetic rate and venation are linked by hydraulics. *Plant Physiology*, **144**, 1890-1898.

Brodribb T.J., Holbrook N.M., Zwieniecki M.A. & Palma B. (2005) Leaf hydraulic capacity in ferns, conifers and angiosperms: impacts on photosynthetic maxima. *New phytologist*, **165**, 839-846.

Bucci S.J., Scholz, F.G., Campanello, P.I., Montti, L., Jimenez-Castillo, M., Rockwell, F. A. & Goldstein, G. (2012). Hydraulic differences along the water transport system of South American Nothofagus species: do leaves protect the stem functionality?. *Tree physiology*, **32**, 880-893.

Buckley T.N. & Diaz-Espejo A. (2014) Partitioning changes in photosynthetic rate into contributions from different variables. *Plant, Cell & Environment.* Doi: 10.1111/pce.12459

Buckley T.N. & Mott K.A. (2013) Modelling stomatal conductance in response to environmental factors. *Plant, Cell & Environment*, **36**, 1691-1699.

Buckley T.N. & Schymanski S.J. (2014) Stomatal optimisation in relation to atmospheric CO_2. *New Phytologist*, **201**, 372-377..

Buckley T.N. & Warren C.R. (2014) The role of mesophyll conductance in the economics of nitrogen and water use in photosynthesis. *Photosynthesis research*, **119**, 77-88.

Buckley T.N. (2005) The control of stomata by water balance. *New Phytologist*, **168**, 275-292.

Buckley T.N., Cescatti A. & Farquhar G.D. (2013) What does optimization theory actually predict about crown profiles of photosynthetic capacity when models incorporate greater realism?. *Plant, Cell & Environment*, **36**, 1547-1563.

Buckley T.N., Miller J.M. & Farquhar G.D. (2002) The mathematics of linked optimisation for water and nitrogen use in a canopy. *Silva Fennica*, **36**, 639-669.

Buckley T.N., Mott K.A. & Farquhar G.D. (2003) A hydromechanical and biochemical model of stomatal conductance. *Plant, Cell & Environment*, **26**, 1767-1785.

Caemmerer S. & Evans J.R. (2014) Temperature responses of mesophyll conductance differ greatly between species. *Plant, Cell & Environment*. Doi: 10.1111/pce.12449

Carswell F.E., Meir P., Wandelli E.V., Bonates L.C.M., Kruijt B., Barbosa E.M. & Jarvis P.G. (2000) Photosynthetic capacity in a central Amazonian rain forest. *Tree Physiology*, **20**, 179-186.

Charra-Vaskou, K., Badel, E., Burlett, R., Cochard, H., Delzon, S., & Mayr, S. (2012). Hydraulic efficiency and safety of vascular and non-vascular components in Pinus pinaster leaves. *Tree physiology*,

Chaves M.M., Flexas J. & Pinheiro C. (2009) Photosynthesis under drought and salt stress: regulation mechanisms from whole plant to cell. *Annals of Botany*, **103**, 551-560.

Chaves M.M., Santos T.P., Souza C.R.D., Ortuño M.F., Rodrigues M.L., Lopes, C. M., Maroco J.P. & Pereira, J. S. (2007) Deficit irrigation in grapevine improves water-use efficiency while controlling vigour and production quality. *Annals of Applied Biology*, **150**, 237-252.

Chaves M.M., Zarrouk O., Francisco R., Costa J.M., Santos T., Regalado A.P. & Lopes C.M. (2010). Grapevine under deficit irrigation: hints from physiological and molecular data. *Annals of botany*, **105**, 661-676.

Chaves, M.M., Maroco J.P. & Pereira J.S. (2003) Understanding plant responses to drought—from genes to the whole plant. *Functional Plant Biology*, **30**, 239-264.

Choat B., Drayton W.M., Brodersen C., Matthews M.A., Shackel K.A., Wada H. & McElrone A.J. (2010) Measurement of vulnerability to water stress‐induced cavitation in grapevine: a comparison of four techniques applied to a long‐vesseled species. *Plant Cell & Environment*, **33**, 1502-1512

Choat B., Gambetta G.A., Wada H., Shackel K.A. & Matthews M.A. (2009) The effects of Pierce's disease on leaf and petiole hydraulic conductance in *Vitis vinifera cv. Chardonnay*. *Physiologia plantarum*, **136**, 384-394.

Choat B., Jansen S., Brodribb T. J., *et al*. (2012) Global convergence in the vulnerability of forests to drought. *Nature* **491**, 752–755

Choat, B. (2013). Predicting thresholds of drought-induced mortality in woody plant species. *Tree physiology*, tpt046.

Choat, B., Cobb, A. R., & Jansen, S. (2008). Structure and function of bordered pits: new discoveries and impacts on whole-plant hydraulic function. *New Phytologist*, **177**, 608-626.

Cifre J., Bota J., Escalona J.M., Medrano H. & Flexas J. (2005) Physiological tools for irrigation scheduling in grapevine *Vitis vinifera* L. An open gate to improve water-use efficiency?. *Agriculture, Ecosystems & Environment*, **106**, 159-170.

Cochard H., Venisse J.S., Barigah T.S., Brunel N., Herbette S., Guilliot A., Tyree M.T. & Sakr S. (2007) Putative role of aquaporins in variable hydraulic conductance of leaves in response to light. *Plant Physiology*, **143**, 122-133

Cowan I.R. & Farquhar G.D. (1977) Stomatal function in relation to leaf metabolism and environment. *Symposia of the Soeiety for Experimental Biology,* **31**, 471-505.

Damour G., Simonneau T., Cochard H. & Urban L. (2010) An overview of models of stomatal conductance at the leaf level. *Plant, Cell & Environment*, **33**, 1419-1438.

Dang Q.L., Margolis H.A., Sy M., Coyea M.R., Collatz G.J. & Walthall C.L. (1997) Profiles of photosynthetically active radiation, nitrogen and photosynthetic capacity in the boreal forest: Implications for scaling from leaf to canopy. *Journal of Geophysical Research: Atmospheres,* **102**, 28845-28859.

de Souza C.R., Maroco J.P., dos Santos T.P., Rodrigues M.L., Lopes C. M., Pereira J. S. & Chaves M.M. (2003) Partial rootzone drying: regulation of stomatal aperture and carbon assimilation in field-grown grapevines (*Vitis vinifera cv. Moscatel*). *Functional Plant Biology*, **30**, 653-662.

Dewar R.C. (1995) Interpretation of an empirical model for stomatal conductance in terms of guard cell function. *Plant, Cell & Environment*, **18**, 365-372.

Di Marco G., Manes F., Tricoli D. & Vitale, E. (1990) Fluorescence Parameters Measured Concurrently with Net Photosynthesis to Investigate Chloroplastic CO_2 Concentration in Leaves of *Quercus ilex* L. *Journal of Plant Physiology*, **136**, 538-543.

Diaz-Espejo A. (2013) New challenges in modelling photosynthesis: temperature dependencies of Rubisco kinetics. *Plant, Cell & Environment*, **36**, 2104-2107.

Diaz-Espejo A., Buckley T.N., Sperry J.S. *et al.* (2012) Steps toward an improvement in process-based models of water use by fruit trees: a case study in olive. *Agricultural Water Management*, **114**, 37-49.

Diaz-Espejo A., Nicolas E., & Fernandez J.E. (2007) Seasonal evolution of diffusional limitations and photosynthetic capacity in olive under drought. *Plant, Cell & Environment*, **30**, 922-933.

Dixon H.H., & Joly J. (1894). On the ascent of sap. *Proceedings of the Royal Society of London*, **57**, 3-5.

Dodd I.C. (2005) Root-to-shoot signalling: assessing the roles of 'up' in the up and down world of long-distance signalling in planta. In *Root Physiology: from Gene to Function*. Springer Netherlands.

Domec J.C. & Johnson D. M. (2012) Does homeostasis or disturbance of homeostasis in minimum leaf water potential explain the isohydric versus anisohydric behavior of Vitis vinifera L. cultivars? *Tree Physiology*, **32**, 245-248.

Egea G., González-Real M.M., Baille A., Nortes P.A. & Diaz-Espejo A. (2011) Disentangling the contributions of ontogeny and water stress to photosynthetic limitations in almond trees. *Plant, Cell & Environment*, **34**, 962-979.

Ellsworth D.S. & Reich P.B. (1993) Canopy structure and vertical patterns of photosynthesis and related leaf traits in a deciduous forest. *Oecologia*, **96**, 169-178.

Engelbrecht B.M.J., Comita L.S., Condit R., Kursar T.A., Tyree M.T., Turner B.L. & Hubbell S.P. (2007) Drought sensitivity shapes species distribution patterns in tropical forests. *Nature* **447**, 80-82.

Escalona J.M., Flexas J., Bota J. & Medrano H. (2003) Distribution of leaf photosynthesis and transpiration within grapevine canopies under different drought conditions. *Vitis*, **42**, 57-64.

Evans J.R. & Von Caemmerer S. (2013) Temperature response of carbon isotope discrimination and mesophyll conductance in tobacco. *Plant, Cell & Environment*, **36**, 745-756.

Evans J.R. (1989) Photosynthesis and nitrogen relationships in leaves of C3 plants. *Oecologia*, **78**, 9-19.

Evans J.R. (1993) Photosynthetic acclimation and nitrogen partitioning within a lucerne canopy II. Stability through time and comparison with a theoretical optimum. *Functional Plant Biology*, **20**, 69-82.

Farquhar G.D. & Sharkey T.D. (1982) Stomatal conductance and photosynthesis. *Annual review of plant physiology*, **33**, 317-345.

Farquhar G.D., von Caemmerer, S. & Berry J.A. (1980) A biochemical model of photosynthetic CO_2 assimilation in leaves of C3 species. *Planta*, **149**, 78-90.

Fereres E., & Soriano M.A. (2007) Deficit irrigation for reducing agricultural water use. *Journal of Experimental Botany*, **58**, 147-159.

Field C.H. & Mooney H.A. (1986) photosynthesis--nitrogen relationship in wild plants. In *On the economy of plant form and function: proceedings of the Sixth Maria Moors Cabot Symposium," Evolutionary Constraints on Primary Productivity, Adaptive Patterns of Energy Capture in Plants," Harvard Forest, August 1983*.

Flexas J. & Diaz-Espejo A. (2014) Interspecific differences in temperature response of mesophyll conductance: food for thought on its origin and regulation. *Plant, Cell & Environment*, doi: 10.1111/pce.12476

Flexas J., Barbour M.M., Brendel O. *et al.* (2012) Mesophyll diffusion conductance to CO_2 An unappreciated central player in photosynthesis. *Plant Science*, **193**, 70-84.

Flexas J., Barón M., Bota J. *et al.* (2009). Photosynthesis limitations during water stress acclimation and recovery in the drought-adapted Vitis hybrid Richter-110 (V. berlandieri × V. rupestris). *Journal of Experimental Botany*, **60**, 2361-2377.

Flexas J., Escalona J.M. & Medrano H. (1998) Down-regulation of photosynthesis by drought under field conditions in grapevine leaves. *Functional Plant Biology*, **25**, 893-900.

Flexas J., Galmés J., Gallé A., Gulias J., Pou A., Ribas-Carbó M., Tomàs M. & Medrano H. (2010) Improving water use efficiency in grapevines: potential physiological targets for biotechnological improvement. *Australian Journal of Grape & Wine Research* **16**, 106-121

Flexas, J., Bota, J., Escalona, J. M., Sampol, B., & Medrano, H. (2002). Effects of drought on photosynthesis in grapevines under field conditions: an evaluation of stomatal and mesophyll limitations. *Functional Plant Biology*, *29*(4), 461-471.

Frak E., Le Roux X., Millard P., Adam B., Dreyer E., Escuit C., Sinoquet H., Vandame M. & 706 Varlet-Grancher C. (2002) Spatial distribution of leaf nitrogen and photosynthetic 707 capacity within the foliage of individual trees: disentangling the effects of local light 708 quality, leaf irradiance, and transpiration. *Journal of Experimental Botany*, **53**, 2207-2216.

Franks P.J., Drake P.L. & Froend R.H. (2007) Anisohydric but isohydrodynamic: seasonally constant plant water potential gradient explained by a stomatal control mechanism incorporating variable plant hydraulic conductance. *Plant, Cell & Environment* **30**, 19-30

Friedlingstein P., Cox P., Betts R., Bopp L., Von Bloh W., Brovkin V. & Zeng N. (2006). Climate-carbon cycle feedback analysis: Results from the C4MIP model intercomparison. *Journal of Climate*, **19**, 3337-3353.

Friend A.D. (2001) Modelling canopy CO_2 fluxes: are 'big-leaf' simplifications justified? *Global Ecology and Biogeography*, **10**, 603-619.

Gaastra P. (1959) *Photosynthesis of crop plants as influenced by light, carbon dioxide, temperature, and stomatal diffusion resistance*. H. Veenman en Zonen N. v..

Galle A., Florez-Sarasa I., Tomas M., Pou A., Medrano H., Ribas-Carbo M., & Flexas, J. (2009) The role of mesophyll conductance during water stress and recovery in tobacco (Nicotiana sylvestris): acclimation or limitation? *Journal of Experimental Botany*, **60**, 2379-2390.

Gao Q., Zhao P., Zeng X., Cai X. & Shen W. (2002) A model of stomatal conductance to quantify the relationship between leaf transpiration, microclimate and soil water stress. *Plant, Cell & Environment*, **25**, 1373-1381.

Gaudillère J.P., Van Leeuwen C. & Ollat N. (2002) Carbon isotope composition of sugars in grapevine, an integrated indicator of vineyard water status. *Journal of Experimental Botany*, **53**, 757-763.

Grassi G. & Magnani F. (2005) Stomatal, mesophyll conductance and biochemical limitations to photosynthesis as affected by drought and leaf ontogeny in ash and oak trees. *Plant, Cell & Environment*, **28**, 834-849.

Greer D.H. & Weedon M.M. (2012) Modelling photosynthetic responses to temperature of grapevine (Vitis vinifera cv. Semillon) leaves on vines grown in a hot climate. *Plant, Cell & Environment*, **35**, 1050-1064.

Guijarro, J. A. (1986). Contribución a la bioclimatología de Baleares. *Ph D Thesis. Universitat de les Illes Balears. Palma de Mallorca*.

Guyot G., Scoffoni C., & Sack L. (2012). Combined impacts of irradiance and dehydration on leaf hydraulic conductance: insights into vulnerability and stomatal control. *Plant, Cell & Environment*, **35**(5), 857-871.

Hendrickson L., Bal, M.C. Wood J.T., Chow W.S. & Furbank R.T. (2004) Low temperature effects on photosynthesis and growth of grapevine. *Plant, Cell & Environment*, **27**, 795-809.

Hetherington A.M. & Woodward F.I. (2003) The role of stomata in sensing and driving environmental change. *Nature*, **424**, 901-908.

Hightower M. & Pierce, S.A. (2008) The energy challenge. *Nature*, **452**, 285-286.

Hirose T. & Werger M.J.A. (1994) Photosynthetic capacity and nitrogen partitioning among species in the canopy of a herbaceous plant community. *Oecologia*, **100**, 203-212.

Hollinger D.Y. (1996) Optimality and nitrogen allocation in a tree canopy. *Tree Physiology*, **16**, 627-634.

Hubbard R.M., Ryan M.G., Stiller V. & Sperry J.S. (2001) Stomatal conductance and photosynthesis vary linearly with plant hydraulic conductance in ponderosa pine. *Plant, Cell & Environment*, **24**, 113-121.

IPCC, 2013. Stocker, T. F., Dahe, Q., Plattner, G. K., 2013. Climate Change 2013: The Physical Science Basis. Working Group I Contribution to the Fifth Assessment Report of the Intergovernmental Panel on Climate Change. Summary for Policymakers

Itel F., Al-Samir S., Öberg *et al.* (2012) CO_2 permeability of cell membranes is regulated by membrane cholesterol and protein gas channels. *The FASEB Journal*, **26**, 5182-5191.

Johnson D.M., McCulloh K.A. Meinzer F.C., Woodruff D.R. & Eissenstat D.M. (2011) Hydraulic patterns and safety margins, from stem to stomata, in three eastern US tree species. *Tree Physiology*

Johnson D.M., McCulloh K.A., Woodruff D.R. & Meinzer F.C. (2012) Evidence for xylem embolism as a primary factor in dehydration-induced declines in leaf hydraulic conductance. *Plant, Cell & Environment*, **35**, 760-769.

Johnson D.M., Meinzer F.C., Woodruff D.R. & McCulloh K.A. (2009) Leaf xylem embolism, detected acoustically and by cryo-SEM, corresponds to decreases in leaf hydraulic conductance in four evergreen species. *Plant, Cell & Environment*, **32**, 828-836.

Jones G., 2006. Climate and terroir: Impacts of climate variability and change on wine. Fine Wine and Terroir—The Geoscience Perspective. Geoscience Canada, eds Macqueen

RW, Meinert LD (Geological Association of Canada, St John's, Newfoundland), pp 1–14.

Jones H.G. & Sutherland R.A. (1991) Stomatal control of xylem embolism. *Plant, Cell & Environment* **14**, 607-612.

Jones M.M. & Rawson H.M. (1979). Influence of rate of development of leaf water deficits upon photosynthesis, leaf conductance, water use efficiency, and osmotic potential in sorghum. *Physiologia Plantarum*, **45**, 103-111.

Jones, H. G. (2013). *Plants and microclimate: a quantitative approach to environmental plant physiology*. Cambridge University Press.

Katsuhara M., Hanba Y.T., Shiratake K. & Maeshima M. (2008) Expanding roles of plant aquaporins in plasma membranes and cell organelles. *Functional Plant Biology* **35**, 1-14.

Kim Y.X. & Steudle E. (2007) Light and turgor affect the water permeability (aquaporins) of parenchyma cells in the midrib of leaves of *Zea mays*. *Journal of Experimental Botany*, **58**, 4119-4129

Kramer P. J. 1980. Drought stress and the origin of adaptations. - In: TURNER N. C. &

Kramer P.J. & Boyer J. S. (1995) *Water relations of plants and soils*. Academic press. New York

Kramer P.J. & Boyer J.S. (1995) Water relations of plants and soils. Elservier Science.

Kubiske M.E. & Abrams M.D. (1990) Pressure-volume relationships in non-rehydrated tissue at various water deficits. *Plant Cell & Environment*, **13**, 995-1000.

Kull O. (2002) Acclimation of photosynthesis in canopies: models and limitations. *Oecologia*, 731 **133**, 267-279.

Kursar T.A., Engelbrecht B.M.J., Burke A., Tyree M.T., EI Omari B. & Giraldo J.P. (2009) Tolerance to low leaf water status of tropical tree seedlings is related to drought performance and distribution. *Functional Ecology* **23**, 93-102.

Lens F., Tixier A., Cochard H., Sperry J.S., Jansen S. & Herbette S. (2013). Embolism resistance as a key mechanism to understand adaptive plant strategies. *Current Opinion in Plant Biology*, **16**, 287-292.

Leuning R. (1990) Modelling stomatal behaviour and and photosynthesis of Eucalyptus grandis. *Functional Plant Biology*, **17**, 159-175.

Leuning R. (1995) A critical appraisal of a combined stomatal-photosynthesis model for C3 plants. *Plant, Cell & Environment*, **18**, 339-355.

Lloyd J., Patino S., Paiva R.Q., Nadrdoto G.B., Quesada C.A., Santos A.J.B., Baker T.R., Brand 741 W.A., Hilke I., Gielmann H., Raessler M., Luizao F.J., Martinelli L.A. & Mercado L.M. 742 (2010) Optimisation of photosynthetic carbon gain and within-canopy gradients of 743 associated foliar traits for Amazon forest trees. *Biogeosciences*, **7**, 1833-1859.

Lloyd J., Patino S., Paiva R.Q., Nardoto G.B., Quesada C.A., Santos A.J.B. & Mercado L.M. (2010) Optimisation of photosynthetic carbon gain and within-canopy gradients of associated foliar traits for Amazon forest trees.*Biogeosciences*, **7**, 1833-1859.

Long S.P. & Bernacchi C.J. (2003) Gas exchange measurements, what can they tell us about the underlying limitations to photosynthesis? Procedures and sources of error. *Journal of Experimental Botany*, **54**, 2393-2401.

Lovisolo C., Perrone I., Hartung W. & Schubert A. (2008). An abscisic acid-related reduced transpiration promotes gradual embolism repair when grapevines are rehydrated after drought. *New Phytologist.* **180**, 642-651.

Maherali H., Pockman W.T. & Jackson, R.B. (2004) Adaptive variation in the vulnerability of woody plants to xylem cavitation. *Ecology*, **85**, 2184-2199.

Makino A., Shimada T., Takumi S. *et al.* (1997). Does decrease in ribulose-1, 5-bisphosphate carboxylase by antisense RbcS lead to a higher N-use efficiency of photosynthesis under conditions of saturating CO_2 and light in rice plants?. *Plant physiology*, **114**, 483-491.

Martorell S., Diaz-Espejo A., Medrano H., Ball M.C. & Choat B. (2014) Rapid hydraulic recovery in *Eucalyptus pauciflora* after drought: linkages between stem hydraulics and leaf gas exchange. *Plant Cell & Environment*, **37**, 617-626.

Martorell S., Medrano H., Tomàs M., Escalona J.M., Flexas J. & Diaz-Espejo A. (2014) Plasticity of vulnerability to leaf hydraulic dysfunction during acclimation to drought in grapevines: an osmotic-mediated process. *Physiologia plantarum*. Doi: 10.1111/ppl.12253

Maurel C., Verdoucq L., Luu D.T. & Santoni V. (2008). Plant aquaporins: membrane channels with multiple integrated functions. *Annual Review of Plant Biology*, **59**, 595-624.

McDowell N.G. (2011) Mechanisms linking drought, hydraulics, carbon metabolism, and vegetation mortality. *Plant physiology*, **155**, 1051-1059.

McElrone A.J., Brodersen C.R., Alsina M.M., Drayton W.M., Matthews M.A., Shackel K. A. & Choat, B. (2012). Centrifuge technique consistently overestimates vulnerability to water stress-induced cavitation in grapevines as confirmed with high-resolution computed tomography. *New Phytologist*, **196**, 661-665.

McElrone A.J., Pockman W.T., Martínez-Vilalta J. & Jackson R.B. (2004) Variation in xylem structure and function in stems and roots of trees to 20 m depth. *New Phytologist*, **163**, 507-517.

Medlyn B.E., Duursma R.A., De Kauwe M.G. & Prentice I.C. (2013) The optimal stomatal response to atmospheric CO_2 concentration: Alternative solutions, alternative interpretations. *Agricultural and Forest Meteorology*, **182**, 200-203.

Medlyn B.E., Duursma R.A., Eamus D., Ellsworth D.S., Prentice I.C., Barton C.V., Crous K.Y., De Angelis P., Freeman M. & Wingate, L. (2011) Reconciling the optimal and empirical approaches to modelling stomatal conductance. *Global Change Biology*, **17**, 2134-2144.

Medrano H., Escalona J.M., Bota J., Gulias J. & Flexas J. (2002) Regulation of photosynthesis of C3 plants in response to progressive drought: stomatal conductance as a reference parameter. *Annals of Botany*, **89**, 895-905.

Medrano H., Escalona J.M., Cifre J., Bota J. & Flexas J. (2003) A ten-year study on the physiology of two Spanish grapevine cultivars under field conditions: effects of water availability from leaf photosynthesis to grape yield and quality. *Functional Plant Biology*, **30**, 607-619.

Meir P., Kruijt B., Broadmeadow M., Barbosa E., Kull O., Carswell F. & Jarvis P.G. (2002). Acclimation of photosynthetic capacity to irradiance in tree canopies in relation to leaf nitrogen concentration and leaf mass per unit area. *Plant, Cell & Environment*, **25**, 343-357.

Mitchell P.J., Veneklaas E.J., Lambers H. & Burgess S.S. (2008) Leaf water relations during summer water deficit: differential responses in turgor maintenance and variation in leaf structure among different plant communities in south-western Australia. *Plant, Cell & Environment*, **31**, 1791-1802.

Morison J.I.L., Baker N.R., Mullineaux P.M. & Davies, W.J. (2008) Improving water use in crop production. *Philosophical Transactions of the Royal Society of London*, **363**, 639–658.

Moshelion M., Halperin O., Wallach R., Oren R. & Way D.A. (2014) Role of aquaporins in determining transpiration and photosynthesis in water-stressed plants: crop water-use efficiency, growth and yield. *Plant, Cell & Environment*. Doi: 10.1111/pce.12410

Mullins, M. G., Bouquet, A., & Williams, L. E. (1992). *Biology of the grapevine*. Cambridge University Press.

Munns R. (1988). Why measure osmotic adjustment?. *Functional Plant Biology*, **15**, 717-726.

Nahal I. (1981) Mediterranean climate from a biological viewpoint. *Ecosystems of the World*.

Nardini A. & Salleo S. (2000) Limitation of stomatal conductance by hydraulic traits: sensing or preventing xylem cavitation? Trees, Structure and Function **15**, 14-24

Nardini A., Pedà G. & Rocca N.L. (2012) Trade-offs between leaf hydraulic capacity and drought vulnerability: morpho-anatomical bases, carbon costs and ecological consequences. *New Phytologist*, **196**, 788-798

Nardini A., Pedá G. & Salleo S. (2012) Alternative methods for scaling leaf hydraulic conductance offer new insights into the structure–function relationships of sun and shade leaves. *Functional Plant Biology*, **39**, 394-401.

Nardini, A., Gortan, E., & Salleo, S. (2005). Hydraulic efficiency of the leaf venation system in sun-and shade-adapted species. *Functional Plant Biology*, *32*(10), 953-961.

Nardini, A., Lo Gullo, M. A., Trifilò, P., & Salleo, S. (2014). The challenge of the Mediterranean climate to plant hydraulics: responses and adaptations. *Environmental and Experimental Botany*, **103**, 68-79.

Niinemets Ü. (2012) Optimization of foliage photosynthetic capacity in tree canopies: towards identifying missing constraints. *Tree physiology*, **32**, 505-509.

Nilsen E.T., & Orcutt, D.M. (1996). Physiology of plants under stress. Abiotic factors. *Physiology of plants under stress. Abiotic factors.*

Nilson S.E., & Assmann S.M. (2007) The control of transpiration. Insights from Arabidopsis. *Plant physiology*, *143*(1), 19-27.

Patakas A. & Noitsakis B. (1999) Osmotic adjustment and partitioning of turgor responses to drought in grapevines leaves. *American journal of enology and viticulture*, **50**, 76-80.

Patakas A. & Noitsakis B. (2001) Leaf age effects on solute accumulation in water-stressed grapevines. *Journal of plant physiology*, **158,** 63-69.

Patakas A., Nikolaou N., Zioziou E., Radoglou K. & Noitsakis, B. (2002) The role of organic solute and ion accumulation in osmotic adjustment in drought-stressed grapevines. *Plant Science*, **163**, 361-367.

Peltoniemi M.S., Duursma R.A. & Medlyn B.E. (2012) Co-optimal distribution of leaf nitrogen and hydraulic conductance in plant canopies. *Tree Physiology*, **32**, 510–519.

Pou A., Flexas J., Alsina M.M. *et al.* (2008) Adjustments of water use efficiency by stomatal regulation during drought and recovery in the drought-adapted Vitis hybrid Richter-110 (V. berlandieri× V. rupestris). *Physiologia Plantarum*, **134**, 313-323.

Pou A., Medrano H., Flexas J. & Tyerman S.D. (2013) A putative role for TIP and PIP aquaporins in dynamics of leaf hydraulic and stomatal conductances in grapevine under water stress and re-watering. *Plant Cell & Environment*, **36**, 828-843

Pou, A., Medrano, H., Tomàs, M., Martorell, S., Ribas-Carbó, M., & Flexas, J. (2012). Anisohydric behaviour in grapevines results in better performance under moderate water stress and recovery than isohydric behaviour. *Plant and soil*, *359*(1-2), 335-349.

pp. 7-20. - John Willey & Sons, New York.

Prieto J.A., Louarn G., Perez Pena J., Ojeda H., Simonneau T. & Lebon E. (2012) A leaf gas exchange model that accounts for intra-canopy variability by considering leaf nitrogen content and local acclimation to radiation in grapevine (Vitis vinifera L.). *Plant, Cell & Environment*, **35**, 1313-1328.

Pury D.D. & Farquhar G.D. (1997) Simple scaling of photosynthesis from leaves to canopies without the errors of big-leaf models. *Plant, Cell & Environment*, **20**, 537-557.

Rodrigues M.L., Chaves M.M., Wendler R., David M.M., Quick W.P., Leegood R.C. & Pereira J.S. (1993) Osmotic adjustment in water stressed grapevine leaves in relation to carbon assimilation. *Functional Plant Biology*, **20**, 309-321.

Romero, P., Dodd, I. C., & Martinez-Cutillas, A. (2012). Contrasting physiological effects of partial root zone drying in field-grown grapevine (Vitis vinifera L. cv. Monastrell) according to total soil water availability. *Journal of experimental botany*,

Sack L. & Holbrook N.M. (2006) Leaf hydraulics. *Annual Reviews of Plant Biology*, **57**, 361-381

Sack L., & Tyree M.T. (2005). Leaf hydraulics and its implications in plant structure and function. *Vascular transport in plants*, 93-114.

Sack L., Cowan P.D. Jaikumar N. & Holbrook N. M. (2003) The 'hydrology'of leaves: co-ordination of structure and function in temperate woody species. *Plant Cell & Environment*, **26**, 1343-1356.

Sack L., Cowan P.D., Jaikumar N. & Holbrook N.M. (2003) The 'hydrology'of leaves: co-ordination of structure and function in temperate woody species. *Plant, Cell & Environment*, **26**, 1343-1356.

Sack L., Melcher P.J., Zwieniecki M.A. & Holbrook N.M. (2002) The hydraulic conductance of the angiosperm leaf lamina: a comparison of three measurement methods. *Journal of Experimental Botany*, **53**, 2177-2184.

Sack L., Streeter C.M. & Holbrook N.M. (2004) Hydraulic analysis of water flow through leaves of sugar maple and red oak. *Plant Physiology*, **134**, 1824-1833.

Saliendra N.Z., & Meinzer F.C. (1991) Symplast Volume, Turgor, Stomatal Conductance and Growth in Relation to Osmotic and Elastic Adjustment in Droughted Sugarcane1. *Journal of Experimental Botany*, **42**, 1251-1259.

Salleo S., Gullo L., Raimondo F., & Nardini A. (2001) Vulnerability to cavitation of leaf minor veins: any impact on leaf gas exchange?. *Plant, Cell & Environment*, **24**, 851-859.

Sancho-Knapik D., Álvarez-Arenas T.G., Peguero-Pina J.J., Fernández V. & Gil-Pelegrín E. (2011) Relationship between ultrasonic properties and structural changes in the mesophyll during leaf dehydration. *Journal of Experimental Botany*, **62**, 3637-3645

Sands P.J. (1995) Modelling canopy production. I. Optimal distribution of photosynthetic resources. *Functional Plant Biology*, **22**, 593-601.

Schultz H. R. (2003). Differences in hydraulic architecture account for near-isohydric and anisohydric behaviour of two field-grown Vitis vinifera L. cultivars during drought. *Plant, Cell & Environment*, **26**, 1393-1405.

Schultz H.R. (2003) Extension of a Farquhar model for limitations of leaf photosynthesis induced by light environment, phenology and leaf age in grapevines (Vitis vinifera L. cvv. White Riesling and Zinfandel). *Functional Plant Biology*, **30**, 673-687.

Schultz H.R., & Stoll M. (2010) Some critical issues in environmental physiology of grapevines: future challenges and current limitations. *Australian Journal of Grape and Wine Research*, **16**, 4-24.

Schulze E.D., Kelliher F. M., Korner C., Lloyd J., & Leuning R. (1994) Relationships among maximum stomatal conductance, ecosystem surface conductance, carbon assimilation rate, and plant nitrogen nutrition: a global ecology scaling exercise. *Annual Review of Ecology and Systematics*, **25**, 629-660.

Scoffoni C., McKown A.D., Rawls M. & Sack L. (2012) Dynamics of leaf hydraulic conductance with water status: quantification and analysis of species differences under steady state. *Journal of Experimental Botany* **63**, 643-658

Scoffoni C., Vuong C., Diep S., Cochard H. & Sack L. (2014) Leaf shrinkage with dehydration: coordination with hydraulic vulnerability and drought tolerance. *Plant Physiology*, **164**,1772-1788.

Scoffoni, C., Rawls, M., McKown, A., Cochard, H., & Sack, L. (2011). Decline of leaf hydraulic conductance with dehydration: relationship to leaf size and venation architecture. *Plant Physiology*, **156**, 832-843.

Sellers P.J., Dickinson R.E., Randall D.A., Betts A.K., Hall F.G., Berry J.A. & Henderson-Sellers A. (1997) Modeling the exchanges of energy, water, and carbon between continents and the atmosphere. *Science*,**275**, 502-509.

Sellin A. & Kupper P. (2007) Temperature, light and leaf hydraulic conductance of little-leaf linden (Tilia cordata) in a mixed forest canopy. *Tree Physiology*, **27**, 679-688.

Somerville C. & Briscoe J. (2001) Genetic engineering and water. *Science (New York, NY)*, ***292,*** (5525), 2217.

Sparks, J.P. & Black R.A. (1999) Regulation of water loss in populations of *Populus trichocarpa*: the role of stomatal control in preventing xylem cavitation. *Tree Physiology* **19**, 453-459.

Sperry J.S., Hacke U.G., Oren R. & Comstock J.P. (2002) Water deficits and hydraulic limits to leaf water supply. *Plant, Cell & Environment*, **25**, 251-263.

Tardieu F. & Simonneau T. (1998) Variability among species of stomatal control under fluctuating soil water status and evaporative demand: modelling isohydric and anisohydric behaviours. *Journal of Experimental Botany*, **49**, 419-432.

Tardieu F. & Simonneau T. (1998) Variability among species of stomatal control under fluctuating soil water status and evaporative demand: modelling isohydric and anisohydric behaviours. *Journal of Experimental Botany*, **49**, 419-432.

Tomás M., Medrano H., Escalona J.M., Martorell S., Pou A., Ribas-Carbó M. & Flexas J. (2014) Variability of water use efficiency in grapevines. *Environmental and Experimental Botany*, **103**, 148-157.

Tomás M., Medrano H., Pou A., Escalona J.M., Martorell S., Ribas-Carbó M. & Flexas J. (2012) Water-use efficiency in grapevine cultivars grown under controlled conditions: effects of water stress at the leaf and whole-plant level. *Australian Journal of Grape & Wine Research*, **18**, 164-172.

Tomás M., Medrano H., Pou A., Escalona J.M., Martorell S., Ribas-carbó M. & Flexas, J. (2012). Water-use efficiency in grapevine cultivars grown under controlled conditions: effects of water stress at the leaf and whole-plant level. *Australian Journal of Grape and Wine Research*, **18**, 164-172.

Torres-Ruiz J.M., Diaz-Espejo A., Morales-Sillero A., Martín-Palomo M.J., Mayr S., Beikircher B. & Fernández J.E. (2013) Shoot hydraulic characteristics, plant water status and stomatal response in olive trees under different soil water conditions. *Plant and soil*, **373**, 77-87.

Tramontini S., Döring J., Vitali M., Ferrandino A., Stoll M. & Lovisolo C. (2014) Soil water-holding capacity mediates hydraulic and hormonal signals of near-isohydric and near-anisohydric *Vitis* cultivars in potted grapevines. *Functional Plant Biology,* doi.org/10.1071/FP13263

Tyerman S.D., Bohnert H.J., Maurel C., Steudle E. & Smith J.A.C. (1999) Plant aquaporins: their molecular biology, biophysics and significance for plant water relations. *Journal of Experimental Botany*, **50**, 1055-1071.

Tyree M.T. & Dixon M.A. (1986) Water stress induced cavitation and embolism in some woody plants. *Physiologia Plantarum*, **66,** 397-405.

Tyree M.T. & Sperry J.S. (1989). Vulnerability of xylem to cavitation and embolism. *Annual review of plant biology*, **40**, 19-36.

Tyree M.T., Yang S., Cruiziat P. & Sinclair B. (1994) Novel methods of measuring hydraulic conductivity of tree root systems and interpretation using AMAIZED (A maize-root dynamic model for water and solute transport). *Plant Physiology*, **104**, 189-199.

Van Leeuwen C. & Seguin G. (1994) Incidences de l'alimentation en eau de la vigne, appréciée par l'état hydrique du feuillage, sur le développement de l'appareil végétatif et la maturation du raisin (Vitis vinifera variété Cabernet franc, Saint-Emilion, 1990). *J. Int. Sci. Vigne Vin*, **28**, 81-110.

Van Leeuwen C., Schultz H.R., de Cortazar-Atauri I.G., *et al.* (2013) Why climate change will not dramatically decrease viticultural suitability in main wine-producing areas by 2050. *Procedings of the National Academy of Sciences* **110**, E3051-E3052.

Voicu M.C., Zwiazek J.J. & Tyree M.T. (2008) Light response of hydraulic conductance in bur oak (Quercus macrocarpa) leaves. *Tree Physiology*, **28**, 1007-1015.

Walker B., Ariza L.S., Kaines S., Badger M.R. & Cousins A.B. (2013) Temperature response of in vivo Rubisco kinetics and mesophyll conductance in Arabidopsis thaliana: comparisons to Nicotiana tabacum. *Plant, Cell & Environment*, **36**, 2108-2119.

Warren C.R. & Dreyer E. (2006) Temperature response of photosynthesis and internal conductance to CO_2: results from two independent approaches. *Journal of Experimental Botany*, **57**, 3057-3067.

Warren C.R. (2008) Stand aside stomata, another actor deserves centre stage: the forgotten role of the internal conductance to CO_2 transfer. *Journal of Experimental Botany*, **59**, 1475-1487.

Xu Z. & Zhou G. (2008) Responses of leaf stomatal density to water status and its relationship with photosynthesis in a grass. *Journal of experimental botany*, **59**, 3317-3325.

Yamori W., Noguchi K., Hanba Y.T. & Terashima I. (2006) Effects of internal conductance on the temperature dependence of the photosynthetic rate in spinach leaves from contrasting growth temperatures. *Plant & Cell Physiology*, **47**, 1069-1080.

Zimmermann, M. H. (1983). *Xylem structure and the ascent of sap*. Springer-Verlag.